Phenological advance in the South African Namaqualand Daisy Bloom over the past decades

Pascal Ludwig Snyman

MSc Geography Dissertation

Final Submission

December 2020

Supervisor: Prof Jennifer Fitchett

DECLARATION

I declare that this dissertation is my own, unaided work, except where otherwise acknowledged. It is being submitted for the Degree of Master of Science at the University of the Witwatersrand, Johannesburg. It has not been submitted before for any degree or examination at this or any other university.

___________ ____________________________

Pascal Ludwig Snyman

_______3th_________day of_______December_______2020___________at___09:15________

ABSTRACT

Climate change is driving changes in environmental suitability, competitive dynamics and phenological cycles of plants and animals. Through the analysis of the timing of phenological events the impact of climate change on plant and animal species can be measured and assessed effectively. In this study the impact of climate change on the timing of bloom of Namaqualand daisies is explored. Although the Namaqualand is described as a desolate and arid region during the summer months, the region is transformed into a wonderland of colours during the springtime flowering. Using documentary sources including newspaper archives from The Rand daily Mail, Volksblad and Die Burger as well as social media records from Flickr and iNaturalist, a phenological dataset spanning 1935-2018, including first flowering, full bloom and end of bloom dates for the Namaqualand daisies was compiled. First flowering and full bloom phenology of the Namaqualand daisies are advancing significantly at rates of 2.6d.decade^{-1} and 2.1d.decade^{-1}. Climatic data, collectively spanning 1959-2018, from seven Namaqualand weather stations were individually correlated to the three flowering datasets. Calculations reveal that temperatures are increasing significantly in Namaqualand. The overall increase in temperature, from 1959-2018, for all seven assessed weather stations in Namaqualand is calculated at 1.18°C. Although no significant changes in precipitation were calculated, five out of the seven weather stations demonstrate slight decreases in precipitation over time ranging between 0.05-9.32mm from 1959-2018. The timing and amount of precipitation in the Namaqualand region is highly variable over time. For the periods spanned by both climate and phenology data, the relationships between the two were explored. Increasing temperatures are driving the calculated advances of the daisy flowering dates at statistically significant rates of change ranging from 0.01-0.11d.°C^{-1}. The main climate drivers of Namaqualand daisy flowering phenology are winter and spring temperatures, the onset of the winter rainy season during April and May, and total winter precipitation. The rates of advance and climate drivers are broadly consistent with global phenological meta-analyses and records for the Southern Hemisphere. The advances in the timing of Namaqualand daisy flowering will have a significant impact on the tourism sector in the region, as flower viewing tours need to be prearranged months in advance.

ACKNOWLEDGEMENTS

Firstly, I would like to thank my supervisor Prof Jennifer Fitchett. Before I started my MSc, I was unsure about my topic, however, with her guidance I found a research topic in a field that I was interested in. Thank you for your continuous support, guidance and wisdom not only throughout my MSc from 2019-2020, but since I walked into your second-year class in 2016. Thank you for always challenging and encouraging me. You taught me to think more critically about my work and pushed me to improve my research and writing skills. Thank you for all the unscheduled meetings where I would just burst into your office. Thanks for giving me peace of mind and helping me to break things up into smaller and more manageable workloads. Thank you for being my supervisor and for helping me to produce this dissertation.

Secondly, I would like to thank Marike Kluyts for her writing assistance and helping me to develop and plan my work efficiently. Thank you also for being willing to proofread my work even though it is a sizeable dissertation.

Thank you to all my friends and family who supported me throughout this journey. It was tough having to put in all those late nights and having to miss out on social events and even just missing watching a movie with you all. Thanks for always being willing to listen to me, and help me plan my work even though some of the things did not always make sense to you. Thanks for also reminding me that I should not work all the time and for occasionally taking my mind off the work.

Thanks to my fellow Geography students and friends who were always keen to proofread or listen to ideas and for helping me work though the whole process of writing a dissertation.

TABLE OF CONTENTS

LIST OF FIGURES

LIST OF TABLES

LIST OF ACRONYMS

AAO: Antarctic Oscillation

AVHRR: Advanced Very High Resolution Radiometer

BBCH*: Biologische Bundesanstalt, Bundessortenamt and Chemical Industry*

DRP: Digital Repeat Photography

ENSO: El Niño Southern Oscillation

FFD: First Flowering Date (Julian Dates)

IPCC: Intergovernmental Panel for Climate Change

ITCZ: Intertropical Convergence Zone

MAP: Mean Annual Precipitation (mm)

MJO: Madden-Julian Oscillation

MODIS: Moderate Resolution Imaging Spectroradiometer

NDVI: Normalised Difference Vegetation Index

R^2: Coefficient of Variation

SAM: Southern Annular Mode

SAWS: South African Weather Service

SPI: Standardized Precipitation Index

SST: Sea Surface Temperature (°C)

T_{max}: Maximum Temperature (°C)

T_{mean}: Mean temperature (°C)

T_{min}: Minimum Temperature (°C)

WMO: World Meteorological Organisation

WRZ: Winter Rainfall Zone

LIST OF UNITS

°C.yr^{-1}: change in degree Celsius per year

mm.yr^{-1}: change in millimetre per year

d.yr^{-1}: day change per year

d.°C^{-1}: day change per degree Celsius change (changes in flowering timing due to temperature)

d.mm^{-1}: day change per millimetre change (changes in flowering timing due to precipitation)

$d.d_{OR}^{-1}$: day change per day changes in onset of rainy season

$d.d_{ER}^{-1}$: day change per day changes in end of rainy season

d.SPI^{-1}: day changes per SPI changes

fe.yr^{-1}: frost events per year (frost after first flowering)

fd.yr^{-1}: frost days per year (frost days in a specific year)

$d.F_{N}^{-1}$: day changes per number of frost events

$d.F_{LD}^{-1}$: day changes per last frost date change

$d.F_{AF}^{-1}$: day changes per frost events after first flowering.

CHAPTER 1: INTRODUCTION

[1]

1.1 Phenology

Phenology involves “the study of the timing of recurrent biological events, the causes of their timing with regard to biotic and abiotic forces, and the interrelationship among phases of the same or different species’’ (Lieth, 1974: 4). The analysis of the timing of phenological events can be used assess the impacts of climate change on plant and animal species (Badeck *et al.,* 2004; Fitchett *et al.,* 2015). Phenological research also explores the causal factors, both biotic and abiotic, that drive the changes in the timing of these events (Wolf *et al.,* 2017; Wright *et al.,* 2019). Plant phenological studies can include analyses of the timing of budburst, flowering, leaf unfolding, leaf fall and harvest of flora, whereas animal phenological studies focus on hibernation, egg laying, hatching, migrations (departure and arrival dates) and birdsong (Wolf *et al.,* 2017).

Since the 1980s, an increasing amount of studies assessed the effects of climate change on phenology (Fitchett *et al.,* 2015; Donnelly & Yu, 2017). This growth in the discipline can be attributed in part to the awareness of anthropogenically induced climate variability and change, and the impact on plant productivity, interactions and competition (Langvall & Löfvenius, 2019; Menzel *et al.,* 2020). Phenological shifts are easily observable and sensitive to climate (Badeck *et al.,* 2004).

Phenological shifts directly influence the duration of the growing season of a plant and can affect other processes such as seed dispersal and pollination (Dreyer *et al.,* 2006; Doi, 2007; Hegland *et al.,* 2009; Cossani *et al.,* 2017). Although a range of global phenological studies have been conducted, comparatively little research has been conducted in South Africa, and none yet for wildflowers (Table 2.1; Grab & Craparo, 2011; Fitchett *et al.,* 2015; Fitchett & Fani, 2018). To address the gap, this research project explores the flowering phenology of the Namaqualand Daisies (family: Asteraceae) under a changing climate using historical newspaper records and social media records.

1.2 The Namaqualand

The Namaqualand landscape is desolate during summer, autumn and winter (Le Roux, 2005; Cowling, 2015). However, during springtime (approximately two to three months from August to mid-October), the Namaqualand region turns into a field of orange, white and yellow flowers (Le Roux, 2005; Davis *et al.,* 2016; Kemp *et al.,* 2018; Figure 1.1). The flowering season in the Namaqualand region is driven by climatic conditions (Le Roux, 2005; Cowling, 2015). According to Le Roux (2005) a good flowering season is determined by quality rainfall during autumn (April to May), followed by consistent winter rainfall. The timing of daisy flowering has been attributed to the first successful rainfall of the season, “the sooner the rains come the earlier the flowering season starts” (Le Roux, 2005: 13). The complete transformation of the region during spring flowering makes the Namaqualand region unique and provides one of the few tourist attractions for the region (Le Roux, 2005; Kruger *et al.,* 2013; Cowling, 2015). There has been an increase in tourism activity within South Africa over the past decade (Saayman & Saayman, 2008), which needs to be sustained for both the Namaqualand region and South Africa for the economic benefits (Binns & Nel, 2002; James *et al.,* 2007; Kruger *et al.,* 2013).

Figure 1.1: An orange field filled with Namaqualand daisies (de Waal, 2016)

1.3 Global Climate Change

The impact of climate change can potentially cause economic problems within the agricultural sector (IPCC, 2018). This is due to ecosystem responses that can change the regions of productive crops cultivations, disrupt the functioning of ecosystem services, and potentially cause species mismatches and extirpations (Visser & Holleman, 2001; Craparo *et al.,* 2015; Pecl *et al.,* 2017). With the current rate of anthropogenic warming (approximately 3.2°C), as projected by the United Nations, it is projected that more than 50% of animal geographic ranges will be lost, and 26% of vertebrates, 49% of insects, and 44% of plants (Warren *et al.,* 2018). Other factors that contribute to the increased extinction risk are climate variability, environmental suitability changes, phenological mismatches and competitive dynamic changes (Visser & Both, 2005; Faisal, 2008; Renner & Zohner, 2018). It is therefore crucial to study the impacts and effects of climate change in various locations on diverse animal and plant species (Ladneva *et al.,* 2004; Chmielewski *et al.,* 2005; Zhang *et al.,* 2018). Phenological shifts are easily observable and extremely responsive to climate change and variability (Pau *et al.,* 2011; CaraDonna *et al.,* 2014). Therefore, phenological studies act as reliable bioindicators of current climate variability as they accurately track the impact of changing temperature and precipitation frequencies on plants and animals (Melaas *et al.,* 2018; Zhang *et al.,* 2018; Menzel *et al.,* 2020).

1.4 Rationale

Phenological assessments in previously neglected regions, such as the Southern Hemisphere, together with innovative phenological data collection methods are essential to contribute to global phenological literature (Grab & Craparo, 2011; Fitchett & Fani, 2018). Regional to global phenological investigations are essential to refine the understanding of the influences of climate change and variability on phenology (Schwartz & Reed, 1999). Phenological studies are also pivotal for developing phenological concepts, understanding shifts and processes, and contributing to synthesised phenological datasets in ecological and climate models (Schwartz & Reed, 1999; Stöckli & Vidale, 2004; Pettorelli *et al.,* 2005; Cleland *et al.,* 2007; Moore *et al*., 2016). Changing climatic conditions that affect phenological timing can lead to unpredictable flowering events, shorter or longer flowering seasons and frost threats to flowers (Hegland *et al.,* 2009; Fitchett *et al.,* 2014b). The influence of climate change on the Namaqualand daisies is explored in this study. The Namaqualand daisies are endemic to the Northern and Western Cape and evolved to thrive in harsh climatic conditions (Le Roux, 2005; Mucina & Rutherford*,* 2006). Slight climate changes therefore have the potential to influence the plant species unfavourably because of their evolutionary characteristics (Le Roux, 2005; Cowling, 2015). Literature projects an increase in climatic variability and significant temperature increases across Southern Africa (Engelbrecht *et al.,* 2013; Davis *et al.,* 2016; Midgley *et al.,* 2016). The Namaqualand region needs to be studied and the effects of climate change on these regions assessed to ensure the survival and protection of these regions for future generations and to ensure economic growth through tourism activities. This the first assessment of the Namaqualand daisies' phenological phase responses to changing climatic conditions.

1.5 Aims and Objectives

The primary aim of this project is to reconstruct the phenological shifts in the Namaqualand daisies using phenological records compiled from documentary sources to determine the impact of local climate change. This will be achieved through the following objectives:

- To determine the annual flowering dates of the Namaqualand daisies from historical newspaper and social media records.
- To calculate the rate of change and statistical significance of any changes in flowering dates over the full study period.

- To determine the rate of change and statistical significance of annual daily rainfall and temperature records in the study region during the same timeline as the flowering data.
- To statistically assess the relationship between any phenological shifts and climate variability for the region.

1.6 Overview of Chapters

This dissertation comprises seven chapters, including this introduction. Chapter two assesses global and local literature and provides detail on phenology and changing climatic conditions in South Africa. The third chapter elaborates on the study region of Namaqualand and the significance of the region. Chapter four provides the methodology used for this study. It also outlines how the phenological dataset was curated and deals with the statistical analysis of the phenological and climate data. Chapter five presents the results of the study focussing first on climate and phenological changes in the region, and then describing the correlations and significant drivers of the calculated phenological changes and further elaborates on the collected local perceptions of Namaqualand daisy phenology. In Chapter six, the calculated results are discussed and compared to local and global phenological literature and the limitations of the study is also discussed. Chapter seven provides a summary of the study, the significance thereof, future avenues of studies and finally recommendations.

CHAPTER 2: LITERATURE REVIEW

[2]

2.1 Phenology

2.1.1 Phenological Overview

Plants and animals adapt to certain environmental conditions that meet their survival prerequisites (Hegland *et al.,* 2009; Pecl *et al.,* 2017). Throughout the evolutionary history of the earth, plant and animal species have responded to climatic variations and changes (Root *et al.,* 2003; Pecl *et al.,* 2017). However, the rapid rate at which climate is currently changing is of great concern (Warren *et al*., 2018). Rapid climate change influences the suitability of habitats for specific species of plants and animals (Parmesan & Yohe, 2003; Pecl *et al.,* 2017). The effects of rapid temperature rise places stress on, and influences, the relationship within species communities, and can ultimately cause extinctions or extirpations (Wiens *et al.,* 2016; Warren *et al.,* 2018). Responses of plants and animals to climate change includes changes in population numbers, location and ranges, and the timing of their life cycle events, termed phenological shifts (Alo & Wang, 2008; Calinger *et al.,* 2013; Pecl *et al.,* 2017). Meta-analyses (Parmesan & Yohe, 2003; Doi, 2007; Munguía-Rosas *et al.,* 2011; Calinger *et al.,* 2013; Ge *et al.,* 2015; Usui *et al.,* 2017; Cohen *et al.,* 2018) have demonstrated a mean global advance of approximately 2.3 days per decade in plant phenological phases. Spring events in many regions are occurring progressively earlier (Thackeray *et al.,* 2016; Cohen *et al.,* 2018), although phenological phase advances are not the exclusive response to climate change and delays are possible and potentially underrepresented (Menzel, 2002).

Flowering phenological phases are influenced by temperature increases above a critical threshold, fulfilment of chilling requirements, phylogenetic constraints, life traits of plant species, soil moisture and germination conditions, together with a range of other climate variables such as wind, precipitation, humidity, sunshine hours and atmospheric circulation (De Melo-Abreu *et al.,* 2004; Wang *et al.,* 2014; Shi *et al.,* 2017). The extent and magnitude of phenological shifts is therefore species and location specific (Faisal, 2008; Calinger *et al.,* 2013; Fitchett *et al.,* 2015; Colautti *et al.,* 2017). The most important driver of plant development and ultimately plant phenological phases is temperature (Ellwood *et al.,* 2013; Menzel *et al.,* 2020). Temperature controls the onset and duration of the growing season for perennial and annual species and controls the phenological phase shift from dormancy to reproductive phases (Guédon & Legave, 2008; Shi *et al.,* 2017; Menzel *et al.,* 2020). Phenological phases can influence the timing and success of other processes such as seed dispersal and pollination (Hegland *et al.,* 2009; Forrest, 2015).

In this literature review, phenological data collection and approaches, the location and species specificity of phenological cycles, phenological applications and South African phenological studies will be discussed. Global daisy and wildflower phenology literature is explored, and finally climate change in South Africa.

2.1.2 Phenological Data Collection and Study Approaches

To quantify the effects of climate change on phenological phase shifts, long temporal records are necessary (Davis *et al.,* 2015; Fitchett *et al.,* 2015; Morellato *et al.,* 2018). The World Meteorological Organisation (WMO) requires that datasets span at least three decades for climate change inferences (Langvall & Löfvenius, 2019). Meteorological variables used for climate change and phenological assessments include atmospheric pressure, relative humidity, air temperature, precipitation, and wind (Langvall & Löfvenius, 2019). Long phenological records enable researchers to accurately assess the impacts of climate on phenology (Parmesan, 2007).

Three primary methods are used to obtain phenological information and datasets (Fitchett *et al.,* 2015). The first and most recent phenological data collection method is through Digital Repeat Photography (DRP), also known as Near Surface Remote Sensing (Alberton *et al.,* 2017). Remote sensing, through the Advanced Very High Resolution Radiometer (AVHRR), Moderate Resolution Imaging Spectroradiometer (MODIS) and Normalised Difference Vegetation Index (NDVI) measures are used to collect phenological data for broader regions (Franch *et al.,* 2017). Detailed reviews have been published on the applications of DRP (Peichl *et al.,* 2015; Toomey *et al.,* 2015; Linkosalmi *et al.,* 2016; Moore *et al.,* 2016; Alberton *et al.,* 2017; Luo *et al.,* 2018; Chianucci, 2020) and Remote Sensing (Liu *et al.,* 2013; Palmer *et al.,* 2015; Gamon *et al.,* 2016; Davis *et al.,* 2017; Franch *et al.,* 2017). The most species-specific method for obtaining phenological information entails collecting ground-based observations of specific plants or animals (Fitchett *et al.,* 2015; Smith & Ramsay, 2020).

Phenological ground observations are deliberate recordings of phenological timing events for specific species, at a given locality and a specific time (Keatley *et al.,* 2013; Fitchett *et al.,* 2015; Fitchett & Fani, 2018). Ground observations are either collected systematically over time by scientists, naturalists and the public or alternatively during formal research projects (Fenech *et al.,* 2005; Wilson *et al.,* 2017; Bison *et al.,* 2019). Ground-based phenological research is recorded in sources such as; logbooks, historical studies, diaries, newspapers and letters (Keatley *et al.,* 2013; Aono, 2015). Ground level observations analyse and describe phenological phases at the individual level, i.e. individual plants are studied at high resolution (Badeck *et al.,* 2004; Denny *et al.,* 2014). Not all ground observations are made with the purpose of documenting phenological events as the main focus might be on something else, for example a newspaper article that speaks about the beauty of the Namaqualand flowering season, and therefore compromising the precision and reliability of the data (Fitchett *et al.,* 2015; Fitchett & Fani, 2018). This brings about limitations to consider within phenological studies that utilise innovative and unconventional phenological datasets (*for more information regarding the limitations of ground observations taken from* *historical sources please see section 6.3.1*). Different plant species and different locations can be assessed depending on the nature of the research (Badeck *et al.,* 2004). Historical ground observations of phenological events date back to the 9th century AD, in records of the Japanese cherry festival (Aono, 2015; Shi *et al.,* 2017). Later in Europe, scientists established phenological gardens (Menzel, 2000; Richardson *et al.,* 2017), to track and analyse phenological changes over time. Few phenological gardens have been established in the Southern Hemisphere (Chambers *et al.,* 2017).

To ensure reliable and accurate ground based phenological datasets, the selected species must be monitored frequently (Menzel, 2002; Miller-Rushing *et al.,* 2008a; Smith & Ramsay, 2020). Such strict standards are difficult to maintain, as it is not always possible to observe the investigated species on a daily basis (Fitchett *et al.,* 2015; Langvall & Löfvenius, 2019; Smith & Ramsay, 2020). Records obtained from naturalists are problematic because those records are the result of an individual's hobby and are not subject to strict quality control measures (Ledneva *et al.,* 2004; Fitchett *et al.,* 2015). Long-term ground observation datasets can contain irregularities due to possibly more than one observer of the species that use variable yardsticks to compare phenological phases and variable observational frequencies (MacKenzie *et al.,* 2017; Feldman *et al.,* 2018). Assessing phenological records documented by naturalists and diary records are therefore more subjective than the other ground-based phenological data collection methods (Ledneva *et al.,* 2004; Smith & Ramsay, 2020). The success of ground observations depends on the definition of the phenological event that is being monitored (Menzel, 2002; Feldman *et al.,* 2018). Ground observations can assess single phenological events such as flowering and leaf colouration but cannot study for example 50% bloom or 40% leaf fall at a high confidence level (Miller-Rushing *et al.,* 2008a; Feldman *et al.,* 2018). As a consequence of the limitations of this method, researchers use species specific datasets from various spatial locations to eliminate observational inconsistencies (Feldman *et al.,* 2018; Smith & Ramsay*,* 2020).

Recently, researchers have created citizen science projects to gather and capture phenological records (Leocadio *et al.,* 2018; Feldman *et al.,* 2018; Bison *et al.,* 2019). Volunteers taking part in citizen science programs can make phenological observations at any time and location, which leads to faster phenological data collection (MacKenzie *et al.,* 2017; Soroye *et al.,* 2018). With the advent of smartphones, mobile applications that can automatically georeference photographs of plants and animals and identify the species and its current phenological phase can also be used (Graham *et al.,* 2011; Criscuola *et al.,* 2018). Citizen science projects increases the size of distributional areas that can be assessed, increases the temporal resolutions of studies, and enhances research capacity when used in conjunction with professional phenological assessments (Soroye *et al.,* 2018; Langvall & Löfvenius, 2019). However, the quality, reliability and the temporal length of the gathered citizen science information is of concern since scientific integrity cannot be assured (MacKenzie *et al.,* 2017; Langvall & Löfvenius, 2019).

Newspaper archives can be used as a source for phenological information (Keatley *et al.,* 2013; Fitchett *et al.,* 2019). Local historical newspaper records have the potential to provide long and rich phenological records of significant local phenological events that occur annually (Futter, 2003; Fitchett *et al.,* 2019). Recently, phenological information can be collected from both print and social media records (Fitchett & Fani, 2018; Capinha, 2019). Biological records are constantly being created and stored publicly on social media platforms (Capinha, 2019). Posts on Twitter, Instagram, Facebook and TripAdvisor that clearly state observations of specific plant and animal phenological phases can be used to create a phenological dataset (Fitchett & Fani, 2018, Barnett, 2019; Capinha, 2019). Social media posts usually include the date and location of variable phenological observations, which increases the temporal and spatial resolution of the phenological dataset (Fitchett & Fani, 2018; Capinha, 2019).

2.1.3 Location and Species Specificity of Phenological Shifts

There is a bias towards studying spring phenological phases that occurs during the spring including flowering, bud burst and leaf unfolding instead of autumn phenological phases which include leaf colouring, and fruit and leaf fall (Cook *et al.,* 2012; Jiang *et al.,* 2016; Norman *et al.,* 2017). Spring phenological phases are commonly controlled by two temperature factors: chilling requirement fulfilment, to break the dormancy period, and warming requirement fulfilment, to induce the new ontogenetic stage (Wang *et al.,* 2014; Fu *et al.,* 2015; Benmoussa *et al.,* 2018). Spring phenological phases mark the onset of the growing season and the end of dormancy (Nordli *et al.,* 2008; Fu *et al.,* 2015). Autumn phenological phases can be influenced by a combination of external factors, which include changes in photosynthetic activity, delayed phenological phases, variable mineral levels and water stress (Badeck *et al.,* 2004; Chmielewski *et al.,* 2004; Gill *et al.,* 2015).

In the literature assessment of this study, spanning 1986-2019, 60 global phenological studies were identified that directly correlated phenological shifts to changing temperature variables (Table 2.1). Only three of these studies were conducted in the Southern Hemisphere (two in Australia and one in South Africa), and one study was a global phenological meta-analysis (Table 2.1). The most common climate variable related to phenological shifts is temperature (Fitchett *et al.,* 2014b). Temperature was found to drive 52% of terrestrial phenological phases in a phenological meta-analysis in the Southern Hemisphere (Chambers *et al.,* 2013). Most of the identified studies found advances in phenological flowering timing over time with a calculated overall average advance of 5.13d.°C^{-1} (Table 2.1). The most extensive spring flowering research comes from Europe, with an average phenological advance of 5.31d.°C^{-1}, displaying the greatest advances in spring flowering phenology (Table 2.1). Extensive phenological flowering research has also been conducted in North America and Asia with average spring advances of 3.39d.°C^{-1} and 3.8d.°C^{-1} respectively (Table 2.1). The individual studies in Table 2.1 that have correlated phenological advances to increasing temperature conditions corresponds with global phenological meta-analysis studies (Root *et al.,* 2003; Thackeray *et al.,* 2010; Chambers *et al.,* 2013; Menzel *et al.,* 2020).

Table 2.1: Publications linking flowering phenological shifts to climate change from 1986 to 2019 (adapted from Fitchett, 2015: 10-11). The calculated average phenological advance from 1986 to 2019 is 5.13d/°C.

Author	Year	Time Period	Location	Taxon	Phenological Advances
Cannel & Smith	1986	1921-1950	England	Apple	7-9 d/°C
Fitter *et al.*	1995	1954-1989	Central England	267 species	4-6 d/°C
Sparks & Carey	1995	1736-1925	England	Multi-species	4 d/°C
Kramer	1996		Europe	*Fagus sylvatica*	3.6 d/°C
Walkovszky	1998	1851-1930; 1952-1981; 1983-1994	Hungary	Locust Tree	5-10 d/°C
Bradley *et al.*	1999	1963-1947; 1976-1998	Wisconsin, USA	Multiple Species	2.7 d/°C
Sparks *et al.*	2000	1985-1947	British Isles	11 plant species	2-10 d/°C
Chmielewski & Rötzer	2001	1969-1998	Europe	White Birch, Sweet Cherry, Mountain Ash, Alpine Currant	5 d/°C
Chmielewski	2002	1961-2000	Europe; Germany	Multi Species; Apple and Cherry	6.7 d/°C; 5 d/°C
Chmielewski & Rötzer	2002	1969-1998	Europe	Multi species	10 d/°C
Keatley *et al.*	2002	1940-1962	Australia	*Eucalyptus sp.*	41.1 d/°C
Wielgolaski	2003	1995-1997	Norway	Multi species	4-6 d/°C
Chmielewski *et al.*	2004	1961-2000	Germany	Apple; Cherry	4.6 d/°C; 4.7 d/°C
De Melo-Abreu *et al.*	2004	Modelled	Portugal	Olives	5.2-7.4 d/°C
Ledneva *et al.*	2004	1970-2002	Southern Massachusetts, USA	Goldthread; Spice Bush; Wood Anemone	3 d/°C; 0.45 d/°C; 1.13 d/°C
Sparks *et al.*	2005	1980-2000	England	Agricultural plants	4-12 d/°C
Črepinšek and Kajfež-Bogataj	2006	1955-2000	Slovenia	Hazel; Apple and Plum	8 d/°C; 4-6 d/°C
Lu *et al.*	2006	1950-2004	Beijing, China	Peach; Almond; Lilac; Acacia sp.	2.88 d/°C; 2.19 d/°C; 2.43 d/°C
Menzel *et al.*	2006	1971-2000	Europe	542 plants	2.5 d/°C
Tao *et al.*	2006	1981-2000	China	Wheat	2.98 d/°C
Estrella *et al.*	2007	1951-2004	Germany	20 agricultural plants	4.31 d/°C
Doi	2007	1953-2005	Japan	Apricots	6 d/°C
Miller-Rushing *et al.*	2007	1981-2005	Japan	Cherry	2-9 d/°C
Guedon & Lagave	2008	1973-2002	France, Switzerland	Apple and Pear	6-8 d/°C
Miller-Rushing & Primack	2008a	1852-1858; 1978-1902; 1963-1993; 2003-2006	Massachusetts, USA	43 species	3.4 d/°C
Wang *et al.*	2008	1983-2004	Northern China	Wheat; Cotton	3.4 d/°C; 0.66 d/°C
Gordo & Sanz	2009	1943-2003	Spain	21 species	8.21 d/°C; 7.62 d/°C
Kalbarczyk	2009	1966-2004	Poland	Ground Cucumber	2.4 d/°C; 3.68 d/°C
Miller-Rushing & Inouye	2009	1973-2006	Colorado, USA	Delphinium sp.	6.1-7.1 d/°C

Primack *et al.*	2009b	800-2007	Japan	Cherry	3-5 d/°C
Primack *et al.*	2009a	1953-2005	Japan, Korea	*Prunus, Taraxacum, Camellia sp.*	4 d/°C
Amano *et al.*	2010	1891-1947 (1753-2010 modelled)	Central England	405 plant species	5 d/°C
Lambert *et al.*	2010	1975-2008	Colorado, USA	Glacier Lily	0.5 d/day change snowmelt - 1.2 d/cm precipitation
Lesica and Kittelson	2010	1995-2008	Rocky Mountains, USA	32 spring wildflowers	1.5d/°C
Beaubien & Hamann	2011	1936-2006	Alberta, Canada	7 plant species	1.5-5.3 d/°C
Grab & Craparo	2011	1973-2009	South Africa	Golden Delicious Apple; Granny Smith Apple	4.2 d/°C; 2.4 d/°C
Chen & Xu	2012	1986-2005	China	Siberian Elm	2.8 d/°C
Liu & Hu	2012	2000-2009	Tibetan Plateau	Meadow species; Steppe species	8.17 d/°C; 5.69 d/°C
Panchen *et al.*	2012	1840-2010	Greater Philadelphia, USA	28 Piedmont species	2.7 d/°C
Darbyshire *et al.*	2013	1963-2009	Australia	Apple and pear	2.8-7.5 d/°C
Guo *et al.*	2013	1963-2008	Beijing, China	Chestnut	2.4 d/°C
Grewling *et al.*	2014	1996-2011	Pomzan, Poland	Oak	1.9 d/°C
Bock *et al.*	2014	1985-2011	Guernsey	232 plant species	1.7 d/°C
Ellwood *et al*.	2014	1981-2011	Massachusetts, USA	Cranberry	2-2.7 d/°C
Fitchett *et al.*	2014b	1960-2010	Kerman and Shiraz, Iran	Citrus	0.1-6.6 d/°C
Polgar *et al.*	2014	1852-1860; 2009-2013	Massachusetts, USA	43 woody plant species	5 d/°C
Wang *et al.*	2014	1951-2000	30 European countries	50 species	3.8 d/°C
Bertin	2015	1855-2015 (discontinuous)	Massachusetts, USA	Multi-species	2.5-6.3 d/°C
Massetti *et al.*	2015	2012	Italy	*Tilia×europaea*	7 d/°C
Park & Schwartz	2015	1951-2009	Southeast USA	>1700 species	3.4 d/°C
Zhang *et al.*	2015	1963–1988	China	220 species	3.7 d/°C
Iler *et al.*	2017	1973-2013; 1996-2013	USA; Greenland	80 species	6.57 d/°C; 3.19 d/°C
Munson & Long	2017	1895–2013	Western North America	C3 and C4 grasses	5.65 d/°C; 24.45 d/°C (delay)
Wang *et al.*	2017	1989-2016	Beijing, China	Chinese wild peach, tree peony, and Yoshino cherry	3.73-4.75 d/°C
Cohen *et al.*	2018	1950-2018	Globally	Multi-species	3.08 d/°C
Drkenda *et al.*	2018	1963-2018	Europe	Golden Delicious Apple, Early Cherry	7.05 d/°C; 2.65 d/°C
Howard	2018	2011-2016	USA	Common Milkweed	3.93 d/°C
Huang & Hao	2018	1990-2015	China	Cotton	3.41 d/°C
Jin *et al.*	2019	2000-2016	Northeastern Europe	Multi-species	2.47 d/°C
Pearson	2019	1842-2019	Southeast USA	Sunflower family (*Asteraceae*)	1.8-2.3 d/°C

2.1.3.1 Plant Phenological Events

In addition to phenological shifts, plants can react to climatic changes in in the following ways: they can become extinct, change their ranges or adapt *in situ* (Hassal *et al.,* 2007; Cohen *et al.,* 2018). Plant migration and range changes depend on the seed dispersal range and are only possible for propagules (Durant *et al.,* 2007; Colautti *et al.,* 2017). The extent to which plant phenological phases change due to climate variability and change are species and location specific (White & Uller, 2014;

Fitchett *et al.,* 2015; Richardson *et al.,* 2017). Variations in phenological timing for species and inter-species responses to climate change are influenced by genetic variation, phenotypic plasticity (i.e. organism behaviour - where a specific genotype has the ability to produce different phenotypes due to exposure to variable environments) and the specific environment (Colautti *et al.,* 2017; Richardson *et al.,* 2017). The location specificity is highly dependent on the region's total precipitation and rainfall regime (Fitchett *et al.,* 2015). Species specificity can be demonstrated when exploring the example of apple blossom dates across the world (Table 2.2).

Table 2.2: Apple phenological responses to climate change in five different locations over the world

Author	**Plant Species Assessed**	**Location**	**Phenological Response**	**Study Period**
Cannell & Smith (1986)	Cox's Apple	England	9-12 days/°C	1936-1982
Chmielewski *et al.* (2004)	Apple (*Malus domestica*)	Germany	4.6 days/°C	1961-2000
Guédon & Legave (2008)	Golden Delicious Apple	Switzerland and France	6-8 days/°C	1963-2006
Fujisawa & Kobayashi (2010)	Apple (*Malus domestica*)	Japan	3.8-4.6 days/°C	1977-2004
Grab & Craparo, (2011)	○ Golden Delicious Apple ○ Granny Smith Apple	South Africa	○ 4.2 days/°C ○ 2.4 days/°C	1973-2009

Deciduous trees' leaf unfolding phenological phases are controlled by environmental conditions and internal mechanisms such as water availability and carbohydrate deficits (Zhang *et al.,* 2003; Dahlin *et al.,* 2015; Dalmolin *et al.,* 2015; Wu *et al.,* 2016). Although leaf unfolding phenological phase events are governed by external climate factors and intrinsic mechanisms, it can effectively be used to assess green wave phenological shifts through the use of remote sensing and ground-based observations (Schwartz *et al.,* 2006; Polgar & Primack, 2013; Toda & Richardson, 2018). Plant flowering timing, on the other hand, is more tightly controlled by climate (Fitter *et al.,* 1995; Park and Schwartz, 2015). Intrinsic controls on flowering are weak, whereas the climatic controls are more influential (Arora & Boer, 2005; McCormack *et al.,* 2014; König *et al.,* 2018).

An important factor to consider within phenological research is the difference between investigating annual and perennial plant species, and their responses to changes in climate, especially for agricultural plants (Fitchett, 2013). Global staples consist of oats, wheat, rice, millet and corn, which are all annual crops, and therefore extremely important concerning food security and the economic sector within the world's ever-changing climate regime (Blanc, 2012; Bai *et al.,* 2019). Phenological studies assessing shifts in staple crop growth as a response to climate change are imperative to ensure effective food production (Bolton & Friedl, 2013; Xiao *et al.,* 2016). Phenological shifts for annual crops can be compensated for by changing sowing dates, the growing location and by adding supplementary irrigation (Gholiphoor & Sinclair, 2011; Craparo *et al.,* 2015). Such adaptations by farmers are beneficial but will cause historical phenological records to display inconsistent phenological responses over the temporal record (Araujo *et al.,* 2016).

The climate effects on perennial plant phenological phases are stronger because perennial agricultural plants can require between two to ten years to reach full growth and to produce fruits, after which its phenological phases occur on an annual basis (Chapman *et al.,* 2005; Vander Mijnsbrugge & Janssens, 2019). Farmers can account for drought periods by using irrigation for the perennial plants, but changes and fluctuations in photoperiod length and temperature will be most influential on phenological cycles (Araujo *et al.,* 2016; Vander Mijnsbrugge & Janssens, 2019). Shifts in plant phenological phases to changing climates are therefore the most perceptible response of perennial plants (Wolfe *et al.,* 2005; Williams *et al.,* 2015). The genetic variation of perennial plants determines how the plant's phenological phases will respond to changing climatic conditions (Firmat *et al.,* 2017; Vander Mijnsbrugge & Janssens, 2019).

Depending on research requirements and scales, bloom measurements tend to include first flowering, 50%, 75%, and peak bloom (Fitchett *et al.,* 2015). The bloom measurement of first flowering date (FFD) relates to identifying the first open and visible flower (Bock *et al.,* 2015; Wang *et al*., 2017). This is a relatively straightforward measurement seeing that it cannot be biased by human error and judgement (Miller-Rushing *et al.,* 2008b; Amano *et al.,* 2010). Errors can, however, occur during data collection, especially when first flowering events occur when no observations are made and/or if flowering is situated out of sight (Bertin, 2015; Wilson *et al.,* 2017). Flowering events are therefore more likely to be noticed when it occurs in a visible region (Fitchett *et al.,* 2015). Limitations and errors that arise with single event recording is that it reduces the sample number and biases the phenological record, seeing that first flowering and peak bloom can occur later or earlier depending on inter-annual variation (Amano *et al.,* 2010; Fitchett *et al.,* 2015). Recording single phenological events instead of percentage floral events can therefore result in intrinsic errors (Fitchett *et al.,* 2015). First flowering can be activated by short periods of favourable climatic conditions that are good enough to ensure that buds open, but early flowering plants are vulnerable to later frost events that can therefore lead to a reduction in the number of flowers (Inouye, 2008; CaraDonna & Bain, 2016; König *et al.,* 2018).

Some plant species are dependent on animals as pollinators and therefore any changes in the reproductive patterns, location or timing of migrations can negatively influence plant reproductive success, seedling and fruit yields (Cohen *et al.*, 2018). Animal populations are important members within ecosystems. Their phenological responses are crucial to fully understand ecosystem responses to climate change (Visser *et al.,* 2006; Sheridan *et al.,* 2018).

2.1.3.2 Animal Phenological Events

Animals have different responses to climate change and variation; migration, *in situ* adaptation or extinction (Hassal *et al.,* 2007; Doi *et al.,* 2017). Another animal phenological response to rapid climate change includes variations in breeding patterns which also includes a reduction in reproductive outputs (Cohen *et al.,* 2018). Animal phenological phase responses, such as egg hatching and breeding, are assessed as secondary responses to climate variability and change (Parmesan & Yohe, 2003; Abarca *et al.,* 2018; Fitchett *et al.,* 2019). Studies that assess animal responses to changing climates therefore focus on documenting range and location fluctuations together with phenological phase shifts (Stevenson & Bryant, 2000; Gibbs & Breisch, 2001; Chuine & Régnière, 2017; Fitchett *et al.,* 2019). Migratory animal phenological studies focus on the climate change impacts on the species' departure and arrival dates, flight time and duration of visits (Miller-Rushing *et al.,* 2008c; Altwegg *et al.,* 2012; Fitchett *et al.,* 2019).

2.1.3.3 Species Mismatch

The periodic timing of phenological events is extremely important in space and time for the presence of pollinators during flowering, predator and prey overlaps and for species that rely on cross pollination (Miller-Struttmann *et al.,* 2015; Hutchings *et al.* 2018). Phenological mismatches occur when the recurring life events of interacting species change at variable rates in response to changing climatic conditions (Renner & Zohner, 2018; Heberling *et al.,* 2019). Phenological mismatches lead to unsynchronised phenological events together with weaker species interactions (Kharouba *et al.* 2018; Renner & Zohner, 2018). Phenological mismatches can serve as a benchmark to assess the extent and impact of climate change on plant survival (Stenseth & Mysterud, 2002; Visser & Both, 2005; Renner & Zohner, 2018). Phenological mismatches between flowering plants and their pollinators can negatively affect plant pollination which can lead to a decrease in the size and quality of fruit yields and seeds (Thomson, 2010; Langowska *et al.,* 2017).

2.1.3.4 Phenological Controls in Different Regional Locations

There is a strong correlation between phenological shifts and climate change in mid-latitude regions due to the temperature climatic environments and marked seasonality (Schwartz & Reiter, 2000; Haselhorst *et al.,* 2017). The most complex climatic variable that must be included in statistical analysis for mid-latitude regions is frost risks (Fitchett *et al.,* 2014b). As warmer temperatures induce spring phenological advances, last frost dates do not always change at the same rate as plant phenological phases, therefore resulting in increased frost risks (Polgar & Primack, 2013; Fitchett *et al.,* 2014b). Assessing the impacts of frost influence on phenological timing is still easier to account for than snowmelt due to frost being a function of daily minimum temperature (Rigby & Porporato, 2008; Ma *et al.,* 2019).

Phenological drivers are more variable in tropical regions (Sakai & Kitajima, 2018). Tropical regions predominantly comprise evergreen forests with very weak seasonality (Fitchett *et al.,* 2015; Moore *et al.,* 2016), making it unsuitable for assessing phenological shifts with remote sensing technology (White *et al.,* 2009; Richardson *et al.,* 2018). Tropical regions experience variable precipitation regimes throughout the year, but the incoming solar radiation and temperatures remain relatively constant (Corlett & Lafrankie, 1998; Souza *et al.,* 2018). All over the world, precipitation has notable influence on phenological timing (Grab & Craparo, 2011; Cleland *et al.,* 2012; Fitchett *et al.,* 2015), but in tropical regions with weak seasonality, changes in cloud cover can influence light intensity and/or effective photoperiod which also has a major influence on phenological timing (Körner & Basler, 2010; Wright & Calderón, 2018).

Another regional controlling factor is the relative position of the study site to urban areas and/or major water bodies (Lu *et al.,* 2006; Zipper *et al.,* 2016). Plants situated in close proximity to urban regions experience variable phenological shifts as a result of the urban heat island effect together with unnatural water availability (Rötzer *et al.,* 2000; Zipper *et al.,* 2016; Villalobos-Jiménez & Hassall, 2017). Changes in sea surface temperatures (SST) influence global and regional climate regimes and therefore phenological reactions (Beaubien & Freeland, 2000; Lavigne *et al.,* 2018).

Temperature, precipitation and photoperiod within the regional environment therefore mainly controls phenological shifts (Ruml *et al.,* 2011; Drake & Martin, 2018). The rate of warming at the poles is significantly faster than at equatorial regions which leads to variable responses of oceanic and atmospheric circulation systems causing variable responses in regional climates all over the world (Walther *et al.,* 2002; Høye *et al.,* 2007; IPCC, 2018). Phenological shifts are therefore location and species specific because different species are dependent and influenced by different climate variables and different species are found in regions where the extent and magnitude of climatic changes differ (Diez *et al.,* 2012; Colautti *et al.,* 2017; Theobald *et al.,* 2017; Vitasse *et al.,* 2017; Wang *et al.,* 2018).

2.1.4 Applications of Phenological Research

2.1.4.1 Agricultural Management

Climate change threatens environmental, economic and social factors (Blanc, 2012; Pecl *et al.,* 2017). Understanding agricultural crop responses to changes in climate provides farmers with the necessary knowledge to make crucial decisions based on when and where to plant crops, what areas are best suited for specific crop growth, when and how much irrigation is needed, and what crop yields to expect per season (Cossani *et al.,* 2017; da Silva Angelo *et al.,* 2019).

The timing of phenological phases within agricultural practices influences a range of production factors including the length of the growing season, potential yield, exposure to the number of frost days, disease and pest control, harvesting and irrigation (Viña *et al.,* 2004; Xiao *et al.,* 2016; Ahmad *et al*., 2017). Phenological shifts of field crops and fruit trees can have considerable effects on the crop's fruiting and ultimately the final yield (Grab & Craparo, 2011; Ahmad *et al*., 2017). Therefore, changes in phenological phases are extremely important within the food sector and for the economy (Chmielewski *et al.,* 2004; Valdivia-Mares *et al.,* 2016; Ahmad *et al*., 2017). Non-climatic factors such as irrigation, windbreaks, previous year's yields, pesticides and fertilizer quality, also control crop yields (Fitchett et al., 2016a). It is therefore difficult to distinguish the impact of climatic and non-climatic factors on changes in crop yields (Fitchett *et al.,* 2016a; Ahmad *et al*., 2017). Understanding agricultural crop responses to climate change and variability is essential in regions with low adaptation responses due to insufficient infrastructure, water availability and capital (Croitoru *et al.,* 2012; Valdivia-Mares *et al.,* 2016; Ahmad *et al*., 2017).

2.1.4.2 Biodiversity Indices

Growing concerns related to loss of global biodiversity leads to an increase in demand for assessing biodiversity indices (Amano *et al.,* 2010; Viña *et al.,* 2016). Global biodiversity indices facilitate monitoring and managing ecosystem health (Viña *et al.,* 2016; Ouchi-Melo *et al.,* 2018). Phenological assessments form critical components of ecosystem assessments under climate change because phenological phase studies indicate the level of animal and plant responses to changes in climate (Kramer *et al.,* 2000; Amano *et al.,* 2010; Dawson *et al.,* 2011; Browing *et al.,* 2018).

Animal and plant range, location and phenological shifts can be understood in terms of their responses to climate change and are included in regional and global biodiversity indices (Viña *et al.,* 2016; Fitchett & Ebhuoma, 2018). The phenological assessment of an individual plant or animal species that is highly influenced by climate variability and change can be used within biodiversity indices because all species contribute to ecosystem functioning (Hegland *et al.,* 2009; Dawson *et al.,* 2011; Viña *et al.,* 2012). Polgar *et al.* (2014) suggest that invasive species respond faster to global warming, which allows invasive plant's phenological responses to be more tolerant to climate change. Such species-specific phenological responses are important to include in ecosystem assessments and biodiversity indices (Polgar *et al.,* 2014). When assessing an individual species, significant changes in phenological responses to climate change may be detected, which could directly influence the survival of other co-dependent species, threatening the region's biodiversity (Cleland *et al.,* 2012).

2.1.4.3 Climate Models

Combining historical climate, phenological and herbarium records allows researchers to assess phenological timing and trends before the influence of anthropogenically induced climate change (Cleland *et al.,* 2007; Morisette *et al.,* 2009; Calinger *et al*., 2013; Zhu *et al.,* 2019). In Kyoto, Japan, phenological data on cherry tree blossoming was kept and used as a proxy to infer the springtime (February and March) temperatures (Aono & Kazui, 2008; Aono, 2015).

Phenological studies and information can be integrated into global and regional climate models (Chuine *et al.,* 2004; Richardson *et al.,* 2017). Although climate change and variability are the main drivers of phenological shifts, these shifts also influence future climate change and variability through their atmospheric feedback responses (Czernecki *et al.,* 2018; Pearson, 2019). Leaf senescence, flush, fall and growth phenology has a significant influence on regional water balance, surface albedo, canopy surface roughness, carbon intake and biogenic volatile organic compounds, i.e. impacting regional and local climate regimes (Richardson *et al.,* 2013; Keenan *et al.,* 2014; Ise *et al.,* 2018; Piao *et al.,* 2019). Phenological feedback responses are only understood qualitatively in terms of the mediated link between vegetation phenology and the resulting climate responses (Richardson *et al.,* 2013). Climate model projections therefore need to ensure that succeeding phenological responses and changes are quantified when considered within the modelling of climate projections (Hogg *et al.,* 2000; Piao *et al.,* 2019). The onset of leaf emergence for certain species are initiated by environmental conditions such as the carbon balance - where a plant will produce new leaves when the environmental conditions are favourable for the plant to increase its total carbon gains (Arora & Boer, 2005). This is an example of a functional relationship to consider within climate models between leaf phenology and regional atmospheric composition instead of only considering the geographical boundaries or the current climatic conditions (Arora & Boer, 2005; Richardson *et al.,* 2012). Long-term phenological studies can be used to reconstruct past climate conditions, which allows for increased accuracy in climate modelling (Chuine *et al.,* 2004; Meier *et al.,* 2007; Souriau & Yiou, 2012). However, more phenological research is required at far greater scales so that researchers can fully understand how plant development is influenced by climate change, in the past and future (Chmielewski *et al.,* 2005; Reyer *et al.,* 2013; Piao *et al.,* 2019).

2.1.4.4 Tourism Sustainability

Tourism activities in Namaqualand predominantly occurs during flowering periods and play an important role in regional and local economic growth (James *et al.,* 2007; Kruger *et al.,* 2013; Wang *et al*., 2017). Therefore, assessing and monitoring phenological shifts in Namaqualand's flower-viewing hotspots is essential for tourism activities that generate money from it in the region (Retief, 2006; Kruger *et al.,* 2013; Wang *et al*., 2017; Nagai *et al.,* 2019).

2.1.5 South African Phenological Studies

Thirty-eight phenological studies have been conducted in South Africa (Table 2.3). Some South African phenological studies focussed on the flowering and full bloom events of trees, while others explored regional to local vegetation populations (Table 2.3). Only four South African studies focussed on agricultural crop phenological responses to variable climatic conditions, while five assessed animal phenological characteristics (Table 2.3). The plant phenological studies conducted in South Africa generally focus on regional vegetation phenology, remote sensing applications for assessing phenology, flowering phenology, and finally experimental studies that assess growth in different environmental conditions (Table 2.3). Phenological studies that assess agricultural crops responses to climate change tend to focus on yield changes due to variable climatic conditions (Araujo *et al*., 2016; Cronje & Ratlapane, 2016).

Of the 38 South African phenological studies, 14 focussed on vegetation phenological patterns in the Western Cape floral and Namaqualand regions. In Namaqualand, the duration, timing of anthesis, and the number of flowers that are reproduced are governed by seasonal precipitation patterns and totals (Struck, 1994; Cowling *et al.,* 1999). The vegetation phenology of the succulent Karoo biome is strongly controlled by the timing of winter precipitation events and temperatures (Hoffman & Cowling, 1987; Dreyer *et al.,* 2006). Similarly, the onset of the regional growing season in the Western Cape starts after good autumn and winter rains and when there is a decrease in temperature (Van Rooyen *et al.,* 1979; Cowling *et al.,* 1999). Water stress can shorten the life span of plants considerably and lead to fewer flowers and reproductive organs (Steyn *et al.,* 1996). With the significant decrease in temperature during winter, the growth rates of regional vegetation decreases (Van Rooyen *et al.,* 1979). The increase in temperatures during spring leads to flowering before the region gets too dry (Van Rooyen *et al.,* 1979; Struck, 1994).

Remote sensing studies in Namaqualand found that NDVI values are significantly related to potential evapotranspiration and precipitation (Fox *et al.,* 2005; Davis *et al.,* 2017). Vegetation productivity varies along different precipitation gradients (Johnson, 1992; Davis *et al.,* 2017). In the western region of the Cape, flowering peaks during early spring (September-October) whereas in the eastern region of the Cape, flowering peaks occur during late spring/early summer (October-November; Johnson, 1992). The vegetation phenology of the Namaqualand region is advancing, with earlier start dates of the growing season and a longer growing season in general (Davis *et al.,* 2017). Drivers for the advances in vegetation phenological productivity include increased atmospheric carbon dioxide concentrations, increased temperatures and changes in land use (Davis *et al.,* 2017).

Grab and Craparo (2011) assessed the full bloom dates of apple trees in the southwestern Cape and confirmed that the observed shifts in flowering to earlier in the year are associated with increased regional early spring temperatures of approximately 0.45°C.decade^{-1} from 1973-2009. The study indicated that there was an advance of 2.4d.°C^{-1} in Granny Smith apple trees and that the most sensitive to climate change, Golden Delicious apples, had an advance of 4.2d.°C^{-1} (Grab & Craparo, 2011). Fitchett and Fani (2018) utilized a multi-method approach to gather flowering information of Jacarandas in Highveld cities of South Africa. The phenological dataset revealed an advance in flowering dates of 2.4d.decade^{-1} from 1924-2016 (Fitchett & Fani, 2018). These findings align with global phenological shifts observed in meta-analysis studies that revealed advances in phenological phases of approximately 2.3d.decade^{-1} (Ge *et al.,* 2015; Usui *et al.,* 2017; Cohen *et al.,* 2018). Similarly, spring phenological events are also advancing over time (Cohen *et al.,* 2018; Howard, 2018). In the context of these studies it is important to increase phenological research in South Africa to determine the extent of the phenological changes and the rates of changes for different species.

Table 2.3: South African phenological studies from 1979 to 2019.

Study	**Study Region and Context**	**Species Type**	**Phenological Event**	**Approach**
Van Rooyen *et al.,* 1979	Namaqualand	116 species	Vegetative growth, flowering, bud production, fruit development and mature fruit.	Field work 1974. Periodic visits from 1973-1977. Field observations every two weeks. General phenological conditions documented.
Milton & Moll, 1982	South-western Cape	Australian Acacias	Litter fall, growth, nectar and reproductive secretion phenology.	Ground observations monitoring shoot development, litter traps, nectar secretion phenology and destructive sampling (harvesting of shoots)
Steinke & Charles, 1984	Umgeni Estuary, Durban	*Avicennia marina* (Mangroves).	Productivity during different phenological phases.	Two-year study. Assessing litter and woody material production of mangroves. No climate data correlated.
Hoffman & Cowling, 1987	Karoo biome	*Regional vegetation*	General desktop study and overview of the regional ecosystem.	Regional phenological assessment conducted through assessing published literature.
Milton, 1987	Nylsvley, Limpopo	3 hook-thorn acacias, 2 straight-thorn acacias and 2 mixed-thorn acacias.	Shoot growth, shoot mortality and the abundance of fruit, flowers, and leaves.	Over 13 months, field observations made for ten Acacia trees. Four to six-week intervals. Phenological observations correlated to climatic conditions.
Steinke, 1988	Umgeni Estuary, Durban	*Bruguiera gymnorrhiza, Rhizophora mucronata* and *Avicennia marina*	Leaf emergence, abscission, propagules that are born, shoot development.	Floral phenological and vegetative observations over five years.
Tribe, 1991	South-western Cape	Red-haired pine bark beetle *(Hylurgus ligniperda)*	Phenological population.	Over five years, log traps were set out to capture beetles at two different sites.
Van Rooyen *et al.,* 1991	Namaqualand	*H. pendula, D. sinuata* and *U. calenduliflora*	Phenological development and flowering.	One-year experimental study. Three plants species all grown under various temperature, moisture and photoperiod regimes to assess development and flowering under different climatic conditions.
Johnson, 1992	Cape Floral Region	7075 Cape floral species	Flowering seasonality.	Based on mean and range data. Used descriptive catalogue of Cape flora with two other methods: (1) ranges methods and (2) means method. Related phenological data with rainfall seasonality.
Struck, 1994	North-western Cape, Goegap Nature reserve	112 succulent Karroo plant species	Flowering timing.	Three-year experimental study. Plants placed in permanent plots. Analyse flowering period of plants.
Rundel *et al.,* 1995	Richtersveld	*Pachypodium namaquanum* (*Apocynaceae*)	Growth phenology and leaf orientation	Field studies with morphometric measurements of phenological state, trunk thickness, trunk numbers, height and inclination.
Steyn *et al.,* 1996	Namaqualand	Five ephemeral species	General plant phenology.	Experimental study. Control plants with plants that were exposed to water stress. Two-week observation intervals. Document all phenological stages.
Cowling *et al.,* 1999	Namaqualand	Regional vegetation	General desktop study and overview of the regional ecosystem	Summarize literature relating to plant function, form, growth, phenology, reproduction, water use and carbon gain
Esler & Rundel, 1999	Succulent Karoo	Regional vegetation	Phenology and growth of regional vegetation.	Obtained phenological information from previous studies by (Van Rooyen *et al.,* 1979). Correlated the data with 64-year climate record for the region.
Shackleton, 1999	Mpumalanga and Limpopo (three identified sites)	Woody plants in the region.	(1) The onset and magnitude of leaf emergence, (2) the onset and duration of mature leaves, and finally (3) the proportion of leafless trees.	Field observations were carried oud during the first week of every month for 12 months. Transects randomly selected in top-land and lowland regions. Phenological information correlated to precipitation data.
Conradie *et al., 2002*	Stellenbosch and Durbanville	Sauvignon blanc Grapevines.	Budburst, ripening, growth, yield timing, chemical composition of yields.	Study the influence of climate and soil on wine quality. Seven-year study.

Shackleton, 2002	South African Lowveld	*Pterocarpus angolensis*	General phenology: Annual diameter increments, size class structure, morphometric relationships, and size of reproductive maturity.	Empirical literature analysis of *Pterocarpus angolensis* from existing studies for effective management of the threatened species.
Mosiane *et al.,* 2003	Gauteng	Diamondback moth (*Plutella xylostella*)	Seasonal phenology.	Sex-pheromone traps used to monitor the moths weekly for three years.
Hoare and Frost, 2004	South Africa	Southern African vegetation.	Phenological phenomena of vegetation in Southern Africa.	Derive a suite of phenological variables from NDVI data that accurately describes South African vegetation phenomena.
Jolly & Running, 2004	Kalahari region of South Africa	Drought deciduous plants.	Leaf flush, leaf senescence i.e. leaf dynamics.	BIOME-BGC ecosystem process model used to assess leaf flush and senescence timing. Leaf area index model projections compared to NDVI satellite derived information. The three-year study.
Knevel & Lubke, 2004	Coastal fore dunes of the Western Cape, Eastern Cape and KwaZulu-Natal	*Scaevola plumieri*	Reproductive phenology	Random selection. 11 squares identified. Six facing ocean and five facing land. From 1998-2001 stem reproductive structures, leaves, buds, seeds, and flowers were documented in four to eight-week intervals
Steyn, 2004	University of Pretoria	Five Namaqualand ephemerals	Climatic drivers of opening and closing of flowers	Experimental study conducted outdoors in $0.5m^3$ pots.
Fox *et al.,*2005	Namaqualand	Regional vegetation	General vegetation phenology.	Correlated NDVI values to different climatic variables.
Dreyer *et al.,* 2006	Cape floral region	*Oxalis L.*	Growth, flowering patterns, and seedling strategies.	Regional information collected in field (1999, 2003 and 2004). Supplemented by published literature. Local information collected in the field over weekly intervals. Phenological data was correlated to daily precipitation and temperature records.
Grab & Craparo, 2011	South-western Cape	Three apple species, *Malus domestica* (Golden Delicious, Sayaka, Granny Smith). One pear species, *Pyrus communis* (*Bon Chrétien*).	Full bloom date advancement in relation to climate change.	Phenological information from 1973-2009 was obtained from orchard networks. Temperature and precipitation records were correlated to the phenological data.
Wessels *et al., 2011*	South Africa	South African Vegetation.	Inter annual variability within vegetation phenology (start, end and length of the growing season).	AVHRR NDVI data from 1985 to 2000 was used to assess vegetation phenology to predict and describe different South African biomes.
Altwegg *et al.,* 2012	South Africa	Barn swallows (*Hirundo rustica*)	Migration phenology.	Analytical methods of assessing bird atlas data.
De Villiers *et al.,* 2013	36 different climatic regions in South Africa	*Ceratitis capitata, Ceratitis rosa*, and *Ceratitis cosyra* (*Diptera: Tephritidae*)	Seasonal phenology.	Three bucket traps placed above host plants for trapping flies. Climate data for 36 regions were correlated with fly totals in each region.
Bussière *et al.,* 2015	South Africa	Nine Palearctic and seven intra-African migratory bird species	Migration phenology.	Novel analytical methods used to assess phenological migratory information obtained from bird atlas data.
Araujo *et al.,* 2016	Western Cape, South Africa	Grapes	Yield assessment.	Standardized Precipitation Evapotranspiration Index (SPEI), i.e. climate data used to assess impacts of droughts on grape yields.
Cronje & Ratlapane, 2016	Malelane	Mauritius' litchi	Tree starch content, leaf N, flowering, shoot growth and yields.	Experimental study over one season. Different tests conducted regarding addition of nitrogen.
Whitecross *et al., 2016*	Nylsvley, Limpopo	Two broad leaved savannah trees (*Burkea africana* and *Terminalia sericea*).	Percentage of leaf age class i.e. new, fully expanded, or mature.	August 2012 to May 2014. Weekly observations made during green-up period and monthly observations made during rest of year. Linked soil moisture and precipitation to growth rate.
Davis *et al.,* 2017	South African West coast, Namaqualand	Regional vegetation	Temporal and spatial patterns of vegetation productivity.	AVHRR NDVI3g biweekly remotely sensed data used to assess regional vegetation phenology.
Whitecross *et al.,* 2017a	Seven sites along a latitudinal gradient from South Africa to Zambia.	Savannah broad leaved trees of which *Burkea africana* was the most common.	Early greening frequency across southern Africa.	NDVI data extracted from MODIS images from 2002-2014. Seasonal rainfall records and maximum temperature two weeks prior to flowering correlated with satellite images.

Whitecross *et al.,* 2017b	Nylsvley, Limpopo	Savannah broad leaved trees and between canopy grasses.	Greening events of trees and between-canopy grasses.	2012-2014. Assessed phenological responses with remotely sensed NDVI data to determine correlations with ground observations and if NDVI detects early green-up events accurately.
Fitchett & Fani, 2018	Gauteng (Johannesburg and Pretoria)	*Jacaranda mimosifolia*	Flowering and leaf colouring.	Utilised historical newspaper records and social media records to create phenological datasets from 1924-1954 and 2014-2016. Did not compare with climate records due to temporal gaps.
Mahlangu & Fitchett, 2019	South Africa	Wedding florals	Flowering phenology and its influence on wedding destinations and flower decorations.	Mixed method approach using phenological and wedding tourism literature's quantitative and qualitative information. Interviews were also conducted.
Fitchett *et al.* 2019	KwaZulu-Natal South Africa	Sardines	Migration timing.	Historical and local newspapers were used to create the phenological migration dataset from 1946 to 2012.

2.2 Global Daisy and Wildflower Phenology

Spring phenological advances for daisies and wildflowers have been associated with climate change in humid-temperate regions and semi-arid grasslands (Studer *et al.,* 2005; Torres & Galetto, 2011; Rosbakh & Poschlod, 2015). Most wildflowers bloom during spring and thereafter become more prevalent during summer (Lesica & Kittelson, 2010; Bailey & Kevan, 2017).

Asteraceae (daisy) is one of the largest flowering plant families in the world (Mitich, 2000). The family consists of 1,100 accepted genera and approximately 25,000 species (Heywood, 1993; Mitich, 2000). Daisy populations usually have a wide distribution and large species numbers (Schmidt-Lebuhn *et al.,* 2013). Characteristics of daisies that contribute to increased morphological diversity include diverse flower colours, unarmed and spiny species, wide array of life cycles and habitats and diverse forms and capitulum sizes (Schmidt-Lebuhn *et al.,* 2013). In the dry west coast of South Africa, including the arid Sandveld and succulent Karoo regions, there are massive displays of Asteraceae daisies during spring (Benjaminsen *et al.,* 2006; Scott *et al.,* 2006; James *et al.,* 2007).

2.2.1 Daisies and Wildflowers of Namaqualand

Water availability and threshold temperatures conditions determine the optimal growing conditions for most plants, particularly during spring and summer growing periods (Le Roux, 2005; Mucina &

Rutherford*,* 2006). The Namaqualand climate does not conform to this and places stressors on the natural environment (Le Roux, 2005). Namaqualand plants have evolved and adapted to survive in harsh, warm summer conditions and relatively cold and moist winters (Le Roux, 2005; Manning, 2013).

Namaqualand wildflower bloom normally occurs during July to the end of September, depending on the climatic conditions prior to, and during flowering (Manning, 2013; de Waal *et al.,* 2014, 2015, 2016). *Dimorphotheca* daisies grow all over the Namaqualand region in dense patches with an average of approximately 40 plants per square meter (Manning, 2013; de Waal *et al.,* 2015). A good flowering season is generally marked by the onset of early winter rains between April and May followed by frequent winter precipitation events (Wannenburgh & Dickson, 1984; Le Roux, 2005). There is a correlation between the timing of precipitation and Namaqualand daisy flowering events (Van Rooyen *et al.,* 1991; Le Roux, 2005). Berg winds, generally coming from an easterly direction in Namaqualand are one of the most influential climatic factors that determine the duration of the flowering season; one day of strong, warm berg winds can lead to the deaths of many of the wildflowers (Le Roux, 2005; Davis *et al.,* 2016).

The annual wildflowers of Namaqualand, the Namaqualand daisy (*Dimorphotheca sinuata*), have adapted to avoid the dry and warm summer periods by germinating, growing, flowering and producing seeds during the wet winter and spring months (Van Rooyen *et al.,* 1991; Cowling *et al.,* 1999; Le Roux, 2005). As with Namaqualand annual species, the individuals die during summer, but the population survives in the form of seeds until the next flowering season (Van Rooyen *et al.,* 1979; Struck, 1994; Le Roux, 2005; Manning, 2013). Namaqualand daisies produce two types of seeds; one comes from the disc florets and the other from the ray florets (Le Roux, 2005). Most Namaqualand annuals have dormant seeds that will not germinate after one precipitation event to ensure that there is always a practical amount of seeds stored in the soil (Van Rooyen *et al.,* 1991; Le Roux, 2005).

The timing and amount of precipitation is one of the most important regulating factors for the growth and flowering of the Namaqualand wildflowers (Van Rooyen *et al.,* 1979; Cowling *et al.,* 1999; Le Roux, 2005; Kruger *et al.,* 2013; Davis *et al.,* 2017). Annual average rainfall totals for the Namaqualand region are so low that certain definitions classify the region as a desert (Fox *et al.,* 2005; Le Roux, 2005; Davis *et al.,* 2017). However, the regional climate during the rainy season in the winter is so cold that almost no moisture is lost due to evaporation, which ensures enough moisture for the plants during the growing season (Le Roux, 2005). Seasonal precipitation timing is therefore essential for the growing season (Van Rooyen *et al.,* 1991; Le Roux, 2005; de Waal *et al.,* 2016). Regional annual rainfall is highly variable which leads to certain years being better flowering years than others (Le Roux, 2005; Kruger *et al*., 2013; de Waal *et al.,* 2016).

2.2.2 Controls on Flowering

All flowering plants have their own specific flowering periods, whether irregular, continuous or annual (Haggerty & Mazer, 2008). Flowering periods are variable depending on the plant species, location, population and climate (Colautti *et al.,* 2017; Theobald *et al.,* 2017). Flowering phenology is strongly related to temperature, precipitation, frost, species and local interactions, genetics, environmental factors, pollinators and photoperiod (Andersson, 2008; Rosbakh & Poschlod, 2015; Araujo *et al.,* 2016; Vander Mijnsbrugge & Janssens, 2019). All flowering plant species have distinctive flowering phenology, but every year variations in FFD occur for all species (Fitter *et al.,* 1995; CaraDonna *et al.,* 2014). Phenological flowering control assessments are difficult and intricate tasks due to the fact that flowering is controlled by a range of variables that influence phenological phase timing differently (Armbruster, 1995; Rosbakh & Poschlod, 2015; Araujo *et al.,* 2016; Petrauski *et al.,* 2019).

The three main abiotic factors that influence plant flowering phenology are temperature, precipitation and photoperiod (Torres & Galetto, 2011; Singh *et al.,* 2017). Temperature was found to be the main driving factor for daisy phenological flowering advances in a collection of Northern Hemisphere phenological assessments (Studer *et al.,* 2005; Hubálek, 2016; Bailey & Kevan, 2017; Petrauski *et al.,* 2019). In a wildflower flowering phenological assessment conducted in the Rocky Mountains, United States of America (USA), temperature variations in the month preceding the onset of phenological flowering caused 37% of the mean first flowering variation, with a flowering advance of 1.5d.°C^{-1} (Lesica & Kittelson, 2010). Menzel (2003) established that the relationship between phenology and temperature is even stronger when several mean monthly temperatures are assessed together. Petrauski *et al*. (2019) assessed spring wildflowers records over 111 years, in Central Appalachia (USA), and calculated flowering phenological advances of 3.18d.°C^{-1}.

Large-scale Northern Hemisphere phenological studies concluded that precipitation does not have a significant influence on phenological flowering phases (Cayan *et al.,* 2001; Buermann *et al.,* 2003; Studer *et al.,* 2005; CaraDonna *et al.,* 2014; Bailey & Kevan, 2017). The effects and influence of precipitation on phenological phases becomes more apparent when working within regional locations (Studer *et al.,* 2005). Lesica and Kittelson (2010) found that decreases in precipitation causes advances in flowering timing in the Rocky Mountains. However, in Namaqualand high moisture stress conditions causes delays in phenological flower initiation (Van Rooyen *et al.,* 1991).

Van Rooyen *et al.* (1991) assessed the effects of temperature, photoperiod and moisture stress on the phenological phases and development of Namaqualand ephemeral daisies (*Ursinia calenduliflora* and *Dimorphotheca sinuata* of the Asteraceae family and *Heliophila pendula* of the

Brassicaceae family). The daisies exhibited a facultative nature in their reactions to temperature and photoperiod variability which allowed them to flower over a wide temporal period during the flowering season as long as there was sufficient moisture available (Van Rooyen *et al.,* 1991). The daisies therefore have the ability to produce seeds and flower regardless of when the raining season starts (Van Rooyen *et al.,* 1991). Steyn *et al.* (1996) conducted a water stress experimental study on five ephemeral plant species within the Namaqualand region. Water stress caused the Namaqualand flowers to grow smaller plants with fewer reproductive organs and flowers (Steyn *et al.,* 1996). Water stress also had an adverse effect on the plants' life span (Steyn *et al.,* 1996). Plants that were sown out of season and subject to water stress experienced a delay in flowering timing, but plants sown in season and subject to water stress experienced an advance in flowering (Steyn *et al.,* 1996). In another experimental study, five Namaqualand daisy species were assessed to determine the influence of different climatic variables on the opening and closing of flowers (Steyn, 2004). The study concluded that for four out of the five assessed daisy species temperature was the main controlling factor that cues the opening and closing of daisies (Steyn, 2004).

Precipitation is an important climatic variable when working in regions where moisture is limited (Van Rooyen *et al.,* 1991; Studer *et al.,* 2005). The influence of precipitation on flowering phenology therefore becomes more significant when working in smaller regions with limited precipitation. Winter precipitation shares the same level of importance as spring temperatures for phenological flowering of wildflowers in semi-arid regions (Lesica & Kittelson, 2010).

The Namaqualand flowering phenological assessment by Van Rooyen *et al.* (1991) concluded that temperature significantly influenced phenological flowering timing. Van Rooyen *et al.* (1991) found that lower temperatures led to flowering advances, and that higher temperatures delayed flower initiation and decreased time between floral initiation and anthesis. These results are consistent with Pearson *et al.*'s (1995) findings but contradicts the findings of Studer *et al.* (2005) and Lesica and Kittelson (2010). Pearson *et al.* (1995) assessed the influence of photoperiod and temperature on the development of the Cape daisy (*Osteospermum jucundum*). This important experimental study found that *Osteospermum* daisies had chilling requirements that needed to be fulfilled before flowering can be initiated (Pearson *et al.,* 1995). The daisies that were kept in a 22°C growing environment were still in the vegetative stage after 120 days while daisies kept in a 12°C growing environment reached flowering after 81 days (Pearson *et al.,* 1995). Therefore, Van Rooyen *et al.* (1991) might have observed a delay in flowering timing at higher temperatures because the daisies did not experience the required chilling.

Phenological events for some plant species are constrained by photoperiods (Van Dijk & Hautekeete, 2007). Some plant species will only flower after a specific day-length is exceeded, or as soon as day-length becomes shorter (Fitter *et al.,* 1995; Tooke & Battey, 2010). In Van Rooyen's (1991) study in Namaqualand, photoperiods did not affect the selected species' phenological flowering timing (Van Rooyen *et al.,* 1991). However, in an experimental study of Cape daisies grown under glasshouse conditions, one group received 16 hours of sunlight a day while another group received eight hours per day (Pearson *et al*., 1995). The group that received double the amount of sunlight flowered 10 days earlier and grew twice as large as the group that only received 8 hours of sunlight per day (Pearson *et al.*, 1995).

Flowering phenological phase shifts are greater for early-flowering wild plant species than later-flowering species (Hubálek, 2016). Elevation variability also influences phenological flowering timing (Studer *et al.,* 2005; Petrauski *et al.,* 2019). Variability in response to climate change of different plant species in different regions suggest that a combination of climate factors initiate and influence flowering phenological phases (Lesica & Kittelson, 2010; Kaewthongrach *et al.,* 2019). Therefore, plant phenological flowering periods are strongly interconnected with climatic variables, taxonomic membership and plant characteristics (Haggerty & Mazer, 2008; Torres & Galetto, 2011).

Snowmelt timing influences phenological phases in high altitude and latitude regions (Inouye *et al.,* 2002; Forrest *et al.,* 2010; Fitchett *et al.,* 2014b). Frost damage as a result of snowmelt timing variation can lead to flower loss, which ultimately leads to a decrease in population fitness (Inouye, 2008; Torres & Galetto, 2011; Pardee *et al.,* 2018). A decrease in population fitness can in turn affect dependent herbivores, pollinators and seed predators (Inouye, 2008). Increased global temperatures have led to a decrease in winter precipitation and causes snow cover to melt away earlier (Feng & Hu, 2007; Forrest *et al.,* 2010; Pardee *et al.,* 2018). Advances in snowmelt increases frost risks (Inouye, 2008; Fitchett *et al.,* 2014b; Pardee *et al.,* 2018). The influence of snowmelt timing on flowering phenology is stronger and more severe for plant species that generally flower earlier (Dunne *et al.,* 2003; Pardee *et al.,* 2018). For certain flowering species, variations in snowmelt timing and snowpack does not only influence phenological timing events but also the duration and abundance of flowering (Forrest *et al.,* 2010; Pardee *et al.,* 2018).

Although pollination does not directly influence the timing of flowering, there is evidence that it impacts the plant community assemblage (Kraft *et al.,* 2015; Kemp *et al.,* 2018). Annual angiosperm species survival, fitness and persistence depend on successful fertilization through pollination (Ollerton *et al.,* 2011; Kemp *et al.,* 2018). Pollinator-plant interactions therefore play a crucial role in plant reproduction, ecological sorting and functional evolution (Kemp *et al.,* 2018).

2.2.3 Flowering Periods

The focal point for flowering phenological studies is FFD (Kemp *et al.,* 2018; Vilela *et al.,* 2018). Within phenological flower recording, it is essential to define ‘flowering’ (Tooke & Battey, 2010;

Stutz *et al.,* 2018). Researchers might define flowering as when anthers can be seen or as when stigmas and stamens can be observed without touching the flower (Fitter *et al.,* 1995; Last, 2001; Stutz *et al.,* 2018). Phenological flowering can be observed and recorded on variable levels; including individual flowers on a plant, flowering population groups, and individual plants in a population (Elzinga *et al.,* 2007; Tooke & Battey, 2010). Correlating climate records with flowering timing allows for the quantification of the total number of days advances/delays of flowering per climate unit increase/decrease in over a specific temporal period (Aono & Kazui, 2008; Petrauski *et al.,* 2019).

Phenological evaluations have revealed a strong relationship between warming spring temperatures and advances in flowering timing within temperate zones (Gordo & Sanz, 2005; König *et al.,* 2018). Flowering advances are very often related to warmer temperatures during the months that precede phenological flowering (Beaubien & Freeland, 2000; Miller-Rushing & Primack, 2008a; Petrauski *et al.,* 2019). In dryer regions, precipitation decreases are more important for explaining phenological flowering advances over time (Crimmins *et al.,* 2010; König *et al.,* 2018).

Wildflowers that generally flower early in spring display greater advances in flowering timing than late flowering wildflower species (Miller-Rushing & Primack, 2008b; Betrin, 2015). Earlier flowering spring wildflowers also demonstrate greater variability in FFD (Fitter *et al.,* 1995; Wolf *et al.,* 2017). In North America, there has been an increase in studies that have found similar evidence where early flowering species' phenological changes are greater than later flowering species (Pearse *et al.,* 2017), although such evidence is not apparent at every assessed study region (Miller-Rushing and Inouye, 2009).

Bailey and Kevan (2017) assessed the reproductive strategies of an endemic Asteraceae species *Erigeron Lemmonii A* (Lemmon's fleabane) in Arizona (USA). Bailey and Kevan (2017) observed two peak flowering stages, in early May and mid-August. Phenological transition for the study species from a tight bud to a flower takes approximately three days and is mainly controlled by precipitation and temperature variables (Bailey & Kevan, 2017). The Kachina Daisy (*Eigeron kachinensis*, Asteraceae), found in south-eastern Utah and south-western Colorado, however, has a longer flowering period from May to September (mid-spring to the end of summer; Allphin & Harper, 1997).

In a remote sensing study of the Namaqualand, observed phenological trends within the region reveal that the growing season is spatially clearly defined and relates to known precipitation and phenological trends (Davis *et al.,* 2017). Inter-annual variability observed within the growing periods within the Namaqualand region can be linked to annual rainfall and is therefore attributed to variability in the amount and timing of precipitation (Davis *et al.,* 2017). The flowering period for the Namaqualand daisies occurs from late winter to spring (July to September), depending on the influence of climatic factors (de Waal *et al.,* 2016; Davis *et al.,* 2017).

2.2.4 Phenological Shifts in Daisies and Wildflowers

Theobald *et al.* (2017) assessed the association between changing climatic conditions and the flowering phenology for 48 co-occurring wildflower species in a plot network across Mount Rainier (USA) from 2010-2015. The flowering phenology for the assessed species were influenced by several climate variables which include soil moisture, temperature, and snowmelt timing (Theobald *et al.,* 2017). A strong emerging trend that was observed was that increased temperatures led to earlier snowmelt timing and warmer growing conditions during spring which in turn led to advances in flowering phenology of the assessed wildflowers (Theobald *et al.,* 2017). A phenological study that assessed the first bloom dates of spring wildflowers in the semi-arid grasslands of the Rocky Mountains (USA), displayed flowering advances for 75% of the 32 analysed species (Lesica &

Kittelson, 2010). Only one species' phenological shifts suggested later flowering due to climate variation (Lesica & Kittelson, 2010). The mean phenological flowering advance from 1995-2008 was 0.61d.yr^{-1} (Lesica & Kittelson, 2010). Lesica and Kittelson (2010) further observed advances of FFD of 1.5d.°C^{-1} increase in spring (March) temperatures. Another study conducted in Arizona (USA) assessed the phenological patterns of Lemmon's fleabane, and found that prolonged flowering periods resulted from climate change influences on rainfall (Bailey & Kevan, 2017). Petrauski *et al.* (2019) observed a 3.18d.°C^{-1} advance in spring ephemerals in the USA mostly due to temperature increases and precipitation decreases.

The literature assessment conducted within this study revealed that the amount of global phenological studies that assess the impacts of climate change on wildflowers and daisies is limited. Studies that do in fact assess the influence of climate change on phenology generally rely on FFD, which in retrospect limits the understanding and assessment of ecological community response to changing climates (CaraDona *et al.,* 2014). There is therefore a need for more flowering phenological studies to be conducted that assesses more aspects of flowering phenology to account for changes that can occur in other levels of biological and ecological organisation (CaraDona *et al.,* 2014). Through understanding the impacts of climate change on plant's phenological phases and its reproductive biology, ensures effective management of the population by preserving its genetic diversity (Bailey & Kevan, 2017).

2.3 Climate Change in South Africa

Global winters are warming nearly twice as fast as global summers (Haggerty & Mazer, 2008; Allen *et al.,* 2018). Global warming is responsible for shorter winter periods, which leads to an earlier commencement of spring (Haggerty & Mazer, 2008; Altwegg *et al.,* 2012; IPCC, 2018). Global warming leads to longer growing seasons which in turn influences plant and animal phenological cycles (Root *et al.,* 2003; Badeck *et al.,* 2004; Haggerty & Mazer, 2008; Amano *et al.,* 2010; Gordo & Sanz, 2010; CaraDonna *et al.,* 2014; Colautti *et al*., 2017; IPCC, 2018).

It is projected that the African continent will become 2-6°C warmer within the next century (Dreyer *et al.,* 2006; Engelbrecht *et al.,* 2015). The South African agricultural sector and the population that depends on agriculture as a means of income and subsistence are extremely vulnerable to climate change due to the high risk-cropping environment that endures numerous droughts and extremely variable precipitation regimes (Deressa *et al.,* 2005; Fitchett *et al.,* 2016a; Rippke *et al.,* 2016).

Tourism success depends on regional climate conditions (Hernandez and Ryan, 2011; Fitchett *et al.,* 2016b; Hoogendoorn *et al.,* 2016; Fitchett & Hoogendoorn, 2019). Temperature, wind, cloud cover, and precipitation control the timing and length of the tourism season and the types of activities that tourists can partake in (Gössling *et al*., 2012; Fitchett *et al.,* 2016b; Hoogendoorn *et al.,* 2016). Climate change and global warming threatens the natural environment and seasonality and therefore indirectly the tourism sector (Gössling *et al*., 2012; Fitchett *et al.,* 2016b). Due to the mobile nature of tourists, seasons with unfavourable climate conditions can damage the attractiveness of a tourist destination and therefore essentially its long-term feasibility (Fitchett & Hoogendoorn, 2019). Within a globalised society, information regarding the climate conditions for tourism hot spots are easily accessible and tourists generally select destinations with suitable weather conditions (Saarinen *et al.,* 2012; Fitchett *et al.,* 2016b). South Africa is economically reliant on tourism (Hoogendoorn *et al.,* 2015, 2016). It is therefore essential to understand regional and local climate change and how it affects tourist destinations so that future changes can be anticipated and managed effectively (Fitchett *et al.,* 2016b; Fitchett & Hoogendoorn, 2019). Understanding how climate change affects the timing of daisy flowering can help tour guides establish the best periods in which to conduct tours of the Namaqualand daisies.

2.3.1 Climate Change in South Africa over Past Decades

2.3.1.1 Changes in Temperature Variables

Easterling *et al.* (1997) assessed South African temperature records from 1950-1993, reporting significant increases in annual daily mean maximum temperatures with frequent increases in annual daily mean minimum temperatures (Table 2.4). During this temporal period, diurnal temperature ranges for most regions in South Africa increased although global diurnal temperature ranges tended to decrease (Easterling *et al.,* 1997). However, Hulme *et al.* (2001) observed decreasing diurnal temperature ranges in South Africa from the 1950s-1960s, and cooling trends over coastal regions coinciding with warming trends over the central interior from 1901-1995 (Hulme *et al.,* 2001). Warming trends were found to be greater during the South African winter and spring than any other time of the year (Hulme *et al.,* 2001). From 1960-2003, Kruger and Shongwe (2004) found temperature increases over South Africa with the exceptions of decreases in a few regions. The strongest and most significant temperature increases were in autumn over the country's interior (Kruger & Shongwe, 2004). Diurnal temperature range assessments for the weather stations used in the study, produced mixed results with no significant regional patterns (Kruger & Shongwe, 2004). New *et al.* (2006) observed equivalent results for diurnal temperature ranges over a similar period (1961-2000); that minimum temperatures changed more significantly than maximum temperatures during cold periods, and that warm extreme events are increasing in South Africa. The average cold extreme days and nights decreased by 3.7 and 6.0d.decade^{-1}, respectively from 1961-2000 (New *et al.,* 2006). The average extreme warm day and night events increased by 8.2 and 8.6d.decade^{-1} respectively (New *et al.,* 2006). Kruger and Sekele (2013) assessed daily minimum and maximum temperature extremes for 28 weather stations across South Africa from 1962-2009, finding that across the country cold extreme events were decreasing and warm extremes increasing (Kruger & Sekele, 2013). The results vary regionally, but the general trends indicate strong increases in maximum temperature extremes for the north-eastern, eastern and westerns regions of the country, with decreases in minimum temperature extremes in all the remaining regions of South Africa (Kruger & Sekele, 2013). These results are consistent with South African thermal regimes, which are all vulnerable to temperature extremes (Kruger & Sekele, 2013).

An analysis of several weather stations' maximum and minimum temperatures from 1960-2010, found significant increases for maximum and minimum temperatures across South Africa (MacKellar *et al.,* 2014). Maximum temperature values are changing faster and more significantly than minimum temperature values (MacKellar *et al.,* 2014). In accordance with Hulme *et al.* (2001), seasonal temperature increases are also far greater during autumn and winter than any other season (MacKellar *et al.,* 2014). MacKellar *et al.* (2014) confirms the earlier results presented by Kruger and Shongwe (2004), and Kruger and Selele (2013). Kruger *et al.* (2019) assessed South African temperature trends, from 1951-2010. The study found that minimum temperatures have increased for most regions, and that maximum temperatures have significantly increased across the country (Kruger *et al.,* 2019). The greatest temperature increases occurred in the north-western interior of South Africa, ranging between 2-2.5°C (Kruger *et al.,* 2019). The study also found that the smallest temperature increases, ranging between 1-1.5°C, occurred in coastal regions, while temperature increases in the interior of the country ranged between 1.5-2°C (Kruger *et al.,* 2019).

Table 2.4: Synthesis of changes in South African temperature variables

Authors	Assessed Temporal Periods	Examined Variables	Key Findings
Easterling *et al.* (1997)	1950-1993	• Daily mean maximum temperature • Diurnal temperature ranges	• Increases in annual daily mean maximum and minimum temperatures • Increased diurnal temperature ranges most regions in South Africa
Hulme *et al.* (2001)	1901-1995	• Diurnal temperature ranges	• Diurnal temperature range decreases in South Africa (1950s-1960s) • Cooling trends over coastal regions • Warming trends over the central interior • South African winters and springs demonstrate the greatest warming trends
Kruger and Shongwe (2004)	1960-2003	• Daily mean maximum and minimum temperature • Diurnal temperature ranges	• Temperature increases over South Africa • Most significant temperature increases documented in autumn over the interior of the country
New *et al.* (2006)	1961-2000	• Diurnal temperature ranges • Extreme cold and warm days	• Minimum temperatures changing more significantly than maximum temperatures during cold periods • Warm extreme events are increasing • Average cold extreme days and nights decreased by 3.7 and 6.0d.decade^{-1} respectively • Average extreme warm day and night events increased by 8.2 and 8.6d.decade^{-1} respectively
Kruger and Sekele (2013)	1962-2009	• Maximum and minimum temperature extremes	• Cold extreme events are decreasing and warm extremes increasing
MacKellar *et al.* (2014)	1960-2010	• Maximum and minimum temperatures	• Significant increases for maximum and minimum temperatures across South Africa • Maximum temperature values are changing faster and more significantly • Seasonal temperature increases are greater during autumn and winter
Kruger *et al.* (2019)	1951-2010	• Maximum and minimum temperatures	• Minimum temperatures have increased for most South African regions • Maximum temperatures have significantly increased across the country • Greatest temperature increases occurred in the north-western interior of South Africa (2-2.5°C) • Smallest temperature increases, (1-1.5°C) occurred in coastal regions • Temperature increases in the interior of the country range between 1.5-2°C

Annual minimum and maximum temperatures, however, do not accurately reflect general temperature trends, therefore indicating that extreme temperature events cannot confidently be linked to distinguishable long-temporal climate change trends (Kruger & Sekele, 2013). The analysis of large temporal-scale temperature records suggest that warming trends accelerated in South Africa after the mid-1960s (Table 2.4; MacKellar *et al.,* 2014; SAWS, 2015; Midgley *et al.,* 2016).

2.3.1.2 Changes in Precipitation

Calculating precipitation trends (specifically in South Africa) is relatively difficult because of a paucity in dependable datasets due to research funds not being able to cover long temporal precipitation studies (Fauchereau *et al.,* 2003; Botai *et al.,* 2018). Factors to consider when studying precipitation trends include the beginning and end of the rainy season, rainfall seasonal distribution, the duration and frequency of heavy rainfall events, and dry and wet period duration (Midgley *et al.,* 2016). Due to South Africa's highly variable mean annual precipitation (MAP; Schulze, 2007), it is difficult to create and study long temporal and spatial, high quality datasets (Kruger, 2006; MacKellar *et al.,* 2014 Sousa *et al.,* 2018; Roffe *et al.,* 2019).

During the 20th century there has been a trend towards more frequent extreme rainfall events in the eastern and south-western regions of South Africa (Table 2.5; Easterling *et al.,* 2000; Engelbrecht *et al.,* 2013). A study by Groisman *et al.* (2005) confirms this trend after observing a statistically significant increase in annual extreme rainfall events from 1906-1997 in the eastern regions of South Africa. Mason *et al.* (1999) also observed increases in South African extreme precipitation events from 1961-1990. Kruger (2006) assessed daily precipitation trends in South Africa from 1910-2004 and found significant increases in extreme precipitation events in regions in the Eastern Cape and the southern Free State. These results confirm Donat *et al.*'s (2013) conclusion; global annual rainfall totals are increasing due to an increase in daily extreme rainfall events. In a South African extreme climate events assessment for 1961-2000, New *et al.* (2006) observed increases in extreme rainfall events, but not all the results were statistically significant. Nel (2009) assessed MAP for 11 weather stations in KwaZulu-Natal from 1955-2000 and observed no clear trend. Nel (2009) did, however, report an increase in summer rainfall and a decrease in autumn and winter rainfall, resulting in a shorter wet season and more distinct seasonal precipitation regime in the KwaZulu-Natal eastern escarpment of the Drakensberg region. Kruger (2006) observed a decrease in the duration of wet spells in the north-eastern parts of South Africa and some regions within the Eastern Cape from 1910-2004.

Table 2.5: Synthesis of changes in South African precipitation

Authors	Assessed Temporal Periods	Examined Variables	Key Findings
Mason *et al.* (1999)	1961-1990	• Extreme rainfall events	• Increases in South African extreme precipitation events
Groisman *et al.* (2005)	1906-1997	• Extreme rainfall events	• Increase in annual extreme rainfall in the eastern regions of South Africa
Kruger (2006)	1910-2004	• Daily precipitation trends	• Increases in extreme precipitation events in the Eastern Cape and the southern Free State • Decrease in the duration of wet spells in the north-eastern parts of South Africa and some regions within the Eastern Cape
New *et al.* (2006)	1961-2000	• Extreme climate events	• Increases in extreme rainfall events
Nel (2009)	1955-2000	• Mean annual precipitation	• No clear trends in MAP • Increase in summer rainfall and a decrease in autumn and winter rainfall in KwaZulu-Natal
DEA (2013)	1960-2010	• Annual rainfall trends • Extreme rainfall events	• Decrease in the total number of rainy days and precipitation totals • Increasing rainfall totals over the eastern regions of the country • During spring and summer there has been an increase in extreme rainfall events over the interior of the country • Reduction of extreme rainfall events during autumn is calculated
MacKellar *et al.* (2014)	1960-2010	• Seasonal and annual total rainfall • Number of rain days	
Kruger and Nxumalo (2017)	1921-2015	• Rainfall trends	• Increase in rainfall totals in the western regions of the country together with decreases in rainfall in the eastern regions

MacKellar *et al.* (2014) and DEA (2013) found few statistically significant trends in rainfall over South Africa, from 1960-2010. There is a trend towards a decrease in the total number of rainy days and precipitation totals, and evidence of increasing rainfall totals over the eastern regions of the country (DEA, 2013; MacKellar *et al.,* 2014). During spring and summer, over the interior of the country, there has been an increase in extreme rainfall events, and reduction of extreme events during autumn is calculated (DEA, 2013; MacKellar *et al.,* 2014). The results from these two studies align with previous findings (Warburton *et al*., 2005; Warburton & Schulze, 2005; Kruger, 2006). Kruger and Nxumalo (2017) assessed South African rainfall trends from 1921-2015. The primary finding was the increase in rainfall totals in the western regions of the country together with decreases in rainfall in the eastern regions (Kruger & Nxumalo, 2017). Overall, South African precipitation is decreasing over time (Botai *et al.,* 2018).

2.3.2 Climate Change Projections for the South African West Coast

Future GHG emission rates cannot be predicted accurately because there are variable emission scenarios, thus different climate scenario projections are calculated based on different emission levels (Hulme *et al.,* 2001; IPCC, 2018). Climate model outputs indicate that the northern and southern subtropical regions of Africa will experience large temperature increases (Engelbrecht *et al.,* 2015). In a low mitigation scenario provided in the Special Report on Emission Scenarios, 21st century temperature increases will range between 4-6°C in the African subtropical regions, and between 3-5°C in African tropical regions (Engelbrecht *et al.,* 2015). Despite the projections that some regions will experience increased precipitation, most regions in Africa will likely experience a decrease in soil-moisture availability due to the projected increase in evaporation levels (Engelbrecht *et al.,* 2015; IPCC, 2018).

The South African Country Study on Climate Change conducted during the 1990s by Midgely *et al.* (2005) revealed that the Western and Northern Cape provinces are at extremely high risk due to increased variation and change in temperature and precipitation variables. Midgley *et al.* (2016) composed an annual climate change report for South Africa, constructing climate trends for each province. A statistically significant decrease in total rainfall days is projected along the southern coastal regions of the Western Cape, yet rainfall totals do not show any significant trends (Midgley *et al.,* 2016). Rainfall decreases are also projected for the south-western Cape because of a pole-ward retreat of mid-latitude rain transporting cyclones (DEA, 2013; Engelbrecht *et al.,* 2013). SAWS (2017), however, suggests an increase in winter precipitation in the Western Cape from 1976-2005.

Minimum and maximum temperatures (T_{min} and T_{max}) have been increasing throughout all seasons at all the recording stations in the Western Cape (Midgley *et al.,* 2016). The total number of extremely cold nights are decreasing while the total number of extremely warm days are increasing significantly (Midgley *et al.,* 2016). The Northern Cape's station coverage is not representative; therefore, trends should be treated with caution (Engelbrecht *et al.,* 2013; Midgley *et al.,* 2016). The 90th percentile of daily rainfall has no significant trend, and no spatial patterns are visible (Midgley *et al.,* 2016). In the eastern part of the Northern Cape (outside the Namaqualand region), statistically significant increases are projected in the total number of rainfall days and increased rainfall totals (Midgley *et al.,* 2016). Temperature records are predominately from the western regions of the Northern Cape province and display significant increases in extremely hot days and increases in T_{max} (Midgley *et al.,* 2016), with a decade of above average temperatures (Midgely *et al.,* 2005). T_{min} in the province is also increasing (Midgley *et al.,* 2016). The temperature range in the Northern and Western Cape is therefore increasing (Midgley *et al.,* 2016).

Thus far, only four studies have assessed Namaqualand's historical climate records and trends (Kelso & Vogel, 2007; MacKellar *et al.,* 2007; Hoffman *et al.,* 2009; Davis *et al.,* 2016). Kelso and Vogel (2007) reconstructed the 19th century climate record for Namaqualand from archival and historical records. Seven drought periods linked to El Niño SouthernOscillation (ENSO) were identified (Kelso & Vogel, 2007). MacKellar *et al.* (2007) assessed interpolated weather station records for Namaqualand from 1950-1999, finding increased summer convective rainfall in the north-eastern regions of, with dry conditions along the coastal regions during early and mid-winters, which are linked to the poleward migration of mid-latitude cyclones (MacKellar *et al.,* 2007). Hoffman *et al.* (2009) assessed historical rainfall station data from 1900-2000 to determine drought frequency using the Standard Precipitation Index (SPI), reporting drying trends from 1900-1950, but no statistically significant observations on drought and rainfall trends from 1950-2000.

Davis *et al.* (2016) combined a high-resolution gridded data set (CRU TS 3.1) with data from five weather stations, observing an increase in the frequency of extremely hot days and mean temperature. Over the last 100 years, T_{max} and T_{min} has increased by 1.1°C and 1.4°C, respectively (Davis *et al.,* 2016). Two of the five weather stations analyzed displayed statistically significant decreases in the total number of cool days (approximately $-3d.decade^{-1}$) and an increase in the duration of warm spells ($+5d.decade^{-1}$; Davis *et al.,* 2016). Spatially variable seasonal rainfall trends were observed, similar to the results of Midgley *et al.* (2016), yet no clear statistically significant trends in rainfall totals were observed (Davis *et al.,* 2016). An increase in evapotranspiration is calculated along the coastline during spring and summer (Davis *et al.,* 2016). The increasing trends in temperature and evapotranspiration rates pose threats to regional water availability but further research is still needed to assess its statistical significance (Davis *et al.,* 2016).

2.4 Conclusion

The paucity of phenological studies in the Southern Hemisphere hinders global assessments of phenological responses to climate changes. All phenological data must therefore be regarded as valuable, regardless of the method of collection. At minimum, phenological data provides insight into the possible effects of anthropogenic induced climate change and further provides a model for predicting future phenological phase shifts.

CHAPTER 3: STUDY SITE

[3]

3.1 Introduction

The Namaqualand region is situated in the north-western area of South Africa in the Northern and Western Cape Provinces (Davis *et al.,* 2016). The term 'Namaqualand' is derived from the indigenous Nama-Khoi people who originally occupied the landscape (Benjaminsen *et al.,* 2006). Namaqualand is bordered by the Orange River to the north, the Atlantic Ocean to the west, the Olifants River to the south and the Bushmanland plains towards the east (Figure 3.2; Cowling *et al.,* 1999; Benjaminsen *et al.,* 2006). Namaqualand covers approximately 50,000km² and extends 200-300km inland from the west coast (Davis *et al.,* 2016). The Namaqualand daisies (Figure 3.1) which are of interest in this study can be found as far south as the West Coast National Park, located 170km south of the Olifants river. Thus, for the purpose of this study, daisies further south of the Namaqualand region will also be included in the phenological assessment (Figure 3.2). The Namaqualand's Succulent Karoo forms part of one of the only two global desert environments that can be classified as biodiversity hotspots (Cowling *et al.,* 2003; James *et al.,* 2007; Sloan *et al.,* 2014; Davis *et al.,* 2017). The climate data used in this study is sourced from seven accredited South African Weather Service (SAWS) meteorological stations (Figure 3.2).

Figure 2.1: A single Namaqualand daisy (*Dimorphotheca sinuate*; Sobey, 2018)

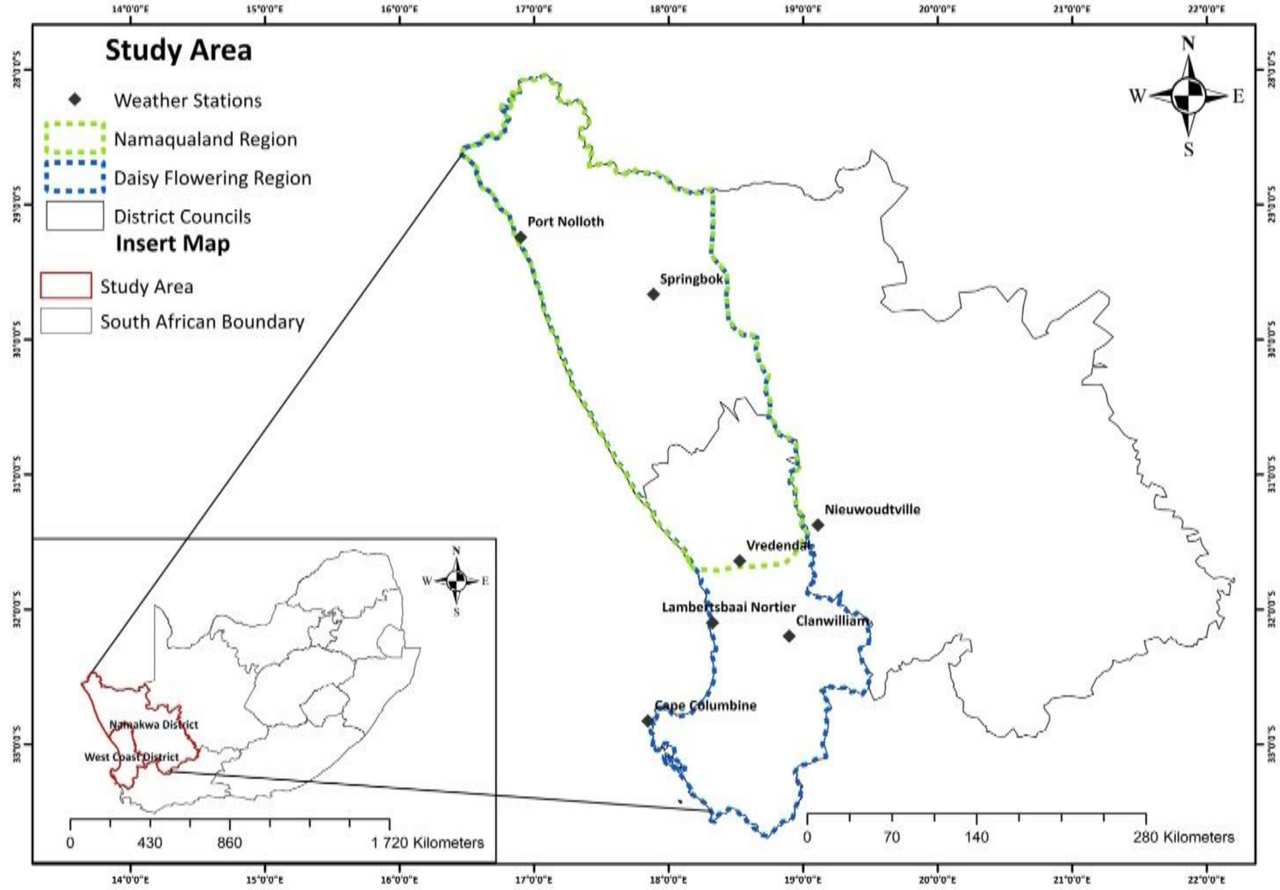

Figure 3.2: Outline of Namaqualand region (green) and the study region (blue). Assessed weather stations displayed on the map

3.2 Biogeographic Landscape

The Namaqualand region can be divided into four distinct biogeographic landscapes with similar topographic characteristics (Figure 3.3; Le Roux, 2005). First, the Namaqualand Klipkoppe (Figure 3.4A) is characterised by distinctive rocky, round, granite hills in between sandy plains (Le Roux, 2005; Mucina & Rutherford*,* 2006). These plains consist of brown and yellow-brown loamy sands (Mucina & Rutherford*,* 2006; Francis *et al.,* 2007). On top of the rocky hills are large, exposed, flat and sometimes rounded rock surfaces (Le Roux, 2005; Mucina & Rutherford*,* 2006). The region lies between the Bushmanland plateau and the Coastal Plain in an escarpment that is 50km wide (Le Roux, 2005). There is a distinct difference in vegetation height in this region, with vegetation on the rocky hills outstripping vegetation on the plains with 0.5-1m (Le Roux, 2005; Mucina & Rutherford*,* 2006). Kraalbos (*Galenia Africa*), a perennial dwarf shrub, can be found in extreme abundance in the pains of the Namaqualand Klipkoppe (Le Roux, 2005). Species that are dominant on the hilly regions include skaapbos (*Tripteris oppositifolia* and *T. sinuate*), kapokbos (*Eriocephalus microphyllus*), fluitjiesbos (*Lebeckia sericea*) and a selection of Aizoaceae species including members of the vyebosse family which comprise the species langbeen t'nouroebos (*Leipoldtia schulzei*) and swart t'nouroebos (*Ruschia robusta*; Le Roux, 2005; Mucina & Rutherford*,* 2006). Abundant ephemerals include what is termed The Namaqualand Daisy (*Dimorphotheca sinuata*), dassiegousblomme (*Tripteris amplectens*) and hongerblom (*Senecia arenarius*; Le Roux, 2005; Mucina & Rutherford*,* 2006).

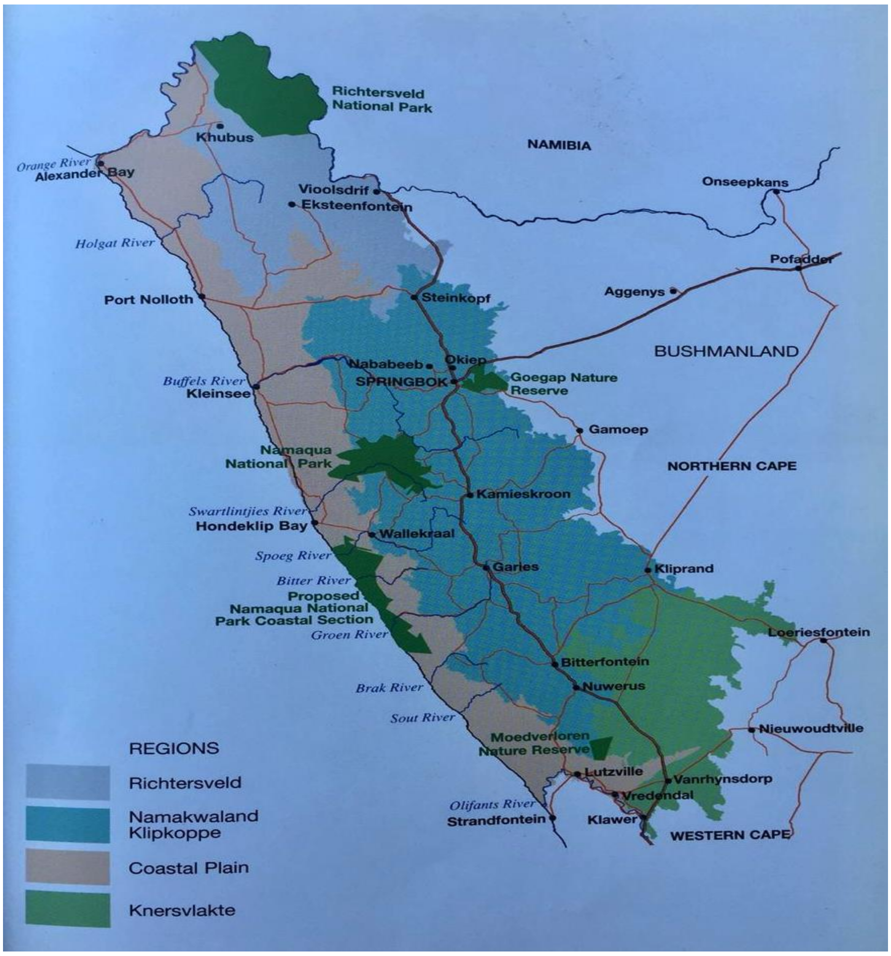

Figure 3.3: Topographic map displaying all four distinct regions within the Namaqualand landscape (Le Roux, 2005: 17).

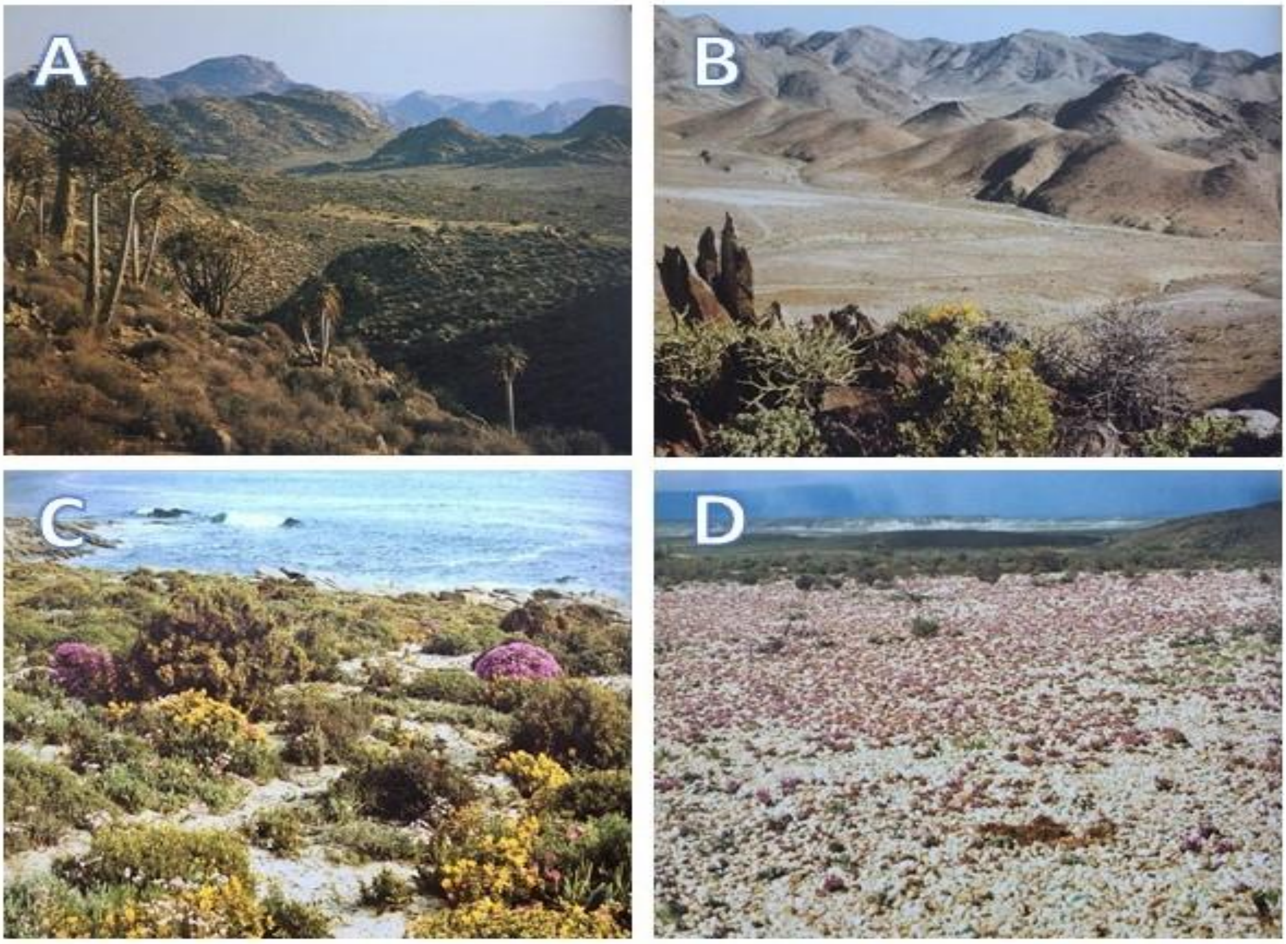

Figure 3.4: Namaqualand Klipkoppe (A), Richtersveld (B), Coastal plain (C), Knersvlakte (D) (Le Roux, 2005: 18-20)

The Richtersveld (Figure 3.4B) occupies the most northern part of Namaqualand (Wannenburgh & Dickson, 1984; Le Roux, 2005). This region is mountainous and hilly with a range of geological formations (Wannenburgh & Dickson, 1984; Le Roux, 2005; Mucina & Rutherford*,* 2006; Francis *et al.,* 2007). The Richtersveld consists of a range of meta-sediments and meta-volcanics composed of quartzite from the Stinkfontein Subgroup belonging to the Gariep Supergroup (Wannenburgh & Dickson, 1984; Mucina & Rutherford*,* 2006). Regional soils are sands, loamy sands, coarse silt and loams derived from granites with a pH of approximately 7-8 (Mucina & Rutherford*,* 2006; Francis *et al.,* 2007). The regional vegetation grows to an average height of less than 0.5m and is known for its diversity in species, shape and size (Le Roux, 2005; Mucina & Rutherford*,* 2006). The height and density of the vegetation increases with altitude (Mucina & Rutherford*,* 2006). The most common succulents belong to the crassula family (*Crassulaceae*), vygie family (*Aizoaceae*) and pelargonium family (*Geraniaceae*; Le Roux, 2005; Mucina & Rutherford*,* 2006).

Coastal Plains (Figure 3.4C), the third Namaqualand landscape, is also known as Sandveld (Cowling *et al.,* 1999; Le Roux, 2005). The Coastal Plain is 30km wide and extends along the full extent of the west coast region of Namaqualand from the Orange River to the Olifants River (Le Roux, 2005). Coastal Plain sands consists of aeolian deposits from the Quaternary period, located on top of Tertiary sediments that have marine origins (Francis *et al.,* 2007). Further inland from the Coastal Plain the soil changes from white sand to a more red, calcareous, loamy soil and the topography becomes more undulating (Le Roux, 2005). The coastal vegetation reaches an average height of 30cm and includes a range of *Drosanthemum* species, sjielingbos (*Zygophyllum cordifolium*) and melkbos (*Euphorbia karroensis*; Le Roux, 2005; Mucina & Rutherford*,* 2006). Further inland the vegetation grows up to an average of 1m and includes a range of species from the vygie family such as *Lampranthus suavissimus*, the skilpadbos (*Zygophyllum morgsana*) and ossierapuis (*Othonna cylindrica*; Le Roux, 2005; Mucina & Rutherford*,* 2006).

The fourth Namaqualand landscape, called Knersvlakte (Figure 3.4D) is found in southern Namaqualand near Nieuwoudtville and the Coastal Plain (Le Roux, 2005; Burge, 2013). The topography is characterised by small hills embedded with tiny white quarts pebbles (Patterson-Jones, 1998; Le Roux, 2005; Mucina & Rutherford*,* 2006; Burge, 2013). The geological composition of this region is underlain by the Vanrhynsdorp Group sediments, and moderately covered by Gariep Supergroup schists (Mucina & Rutherford*,* 2006). The regional soils are sandy, unstructured, red, aeolian and low in salinity (Francis *et al.,* 2007). The vegetation in the Knersvlakte region is typically low and ranges from 10-50 cm (Le Roux, 2005). Regional vegetation includes duim-en-vinger

(*Dactylopsis digitata*), *Leipoldtia*, krapogies (*Oophytum oviforme*), occasional Asteraceae shrubs and members of the mesem-family (Le Roux, 2005; Mucina & Rutherford*,* 2006).

A range of ephemeral rivers and streams flow from the mountainous regions to the coast (Figure 3.3; Benjaminsen *et al.,* 2006). The variation in biogeography reflects the varied regional vegetation, and includes Mountain Renosterveld, Succulent Karoo, Namaqualand Broken Veld and False Succulent Karoo (Benjaminsen *et al.,* 2006; Mucina & Rutherford*,* 2006). Approximately 1,940 of the 4,849 registered Succulent Karoo plant species are endemic to the Namaqualand region (Myers *et al.,* 2000; Benjaminsen *et al.,* 2006).

3.3 South African Climate Drivers

Weather patterns and trends do not conform to simple and clear linear cause-effect inter-connections (Schulze, 2007; Van Wilgen *et al.,* 2016; Roffe *et al.,* 2019). Weather systems form complex interrelated systems where a slight change in one region can result in an unpredictably large consequence in another (Schulze, 2007; Dieppois *et al.,* 2016; Collins *et al.,* 2018). Studies have revealed that temperature increases are more than 1.5 times greater in the central tropics and subtropics of Africa than the rest of the world due to the position of the African continent among the oceanic currents (Engelbrecht *et al.,* 2009; DEA, 2013; Engelbrecht *et al.,* 2015). Global and local climate regimes exhibit a wide range of variability within hemispheric and global circulation systems though inter-annual and inter-seasonal temporal scales (MacKellar *et al.,* 2014).

South African weather is governed by two mechanisms that operate and function at two different scales: daily regional climate regimes (Lennard & Hegerl, 2015), and teleconnective processes. Teleconnective processes include the Southern Annular Mode (SAM) and ENSO that influence weather over larger temporal and spatial scales, i.e. seasonal to monthly (Lennard & Hegerl, 2015).

There are four synoptic regimes that influence South African weather and climate, which divides the country into three distinct rainfall regimes: summer, winter and all-year rainfall regions (Roffe *et al.,* 2019). The first synoptic regime is located over the subtropical region of the country and forms part of the earthbound limb of the Ferrel and Hadley cells, creating a semi-permanent, high-pressure cell that is at its strongest during the winter season when it produces clear, cold and dry weather over the interior of the country (Lennard & Hegerl, 2015; Mahlobo *et al*., 2019). The second synoptic regime propagates in the mid-latitudes as westerly baroclinic disturbances that travel within the Rossby waves (Lennard and Hegerl, 2015). These mid-latitudinal disturbances influence the southern and south-western regions of the country (Taljaard, 1996; Favre *et al.,* 2012). During winter, the cold front arm of mid-latitude cyclones, which form part of the equator-ward displaced westerlies, bring heavy rainfall, cut-off lows and gale force winds to the southwestern Cape (Favre *et al.,* 2012; Roffe *et al.,* 2020). The third circulation system is a closed low-pressure, quasi-stationary, barotropic, sub-tropical easterly wave system that covers the South African interior (Lennard & Hegerl, 2015). During summer, this thermal low-pressure system can intercept mid-latitudinal cyclones from the southern regions of the country, producing tropical-temperate troughs or tropical-extratropical cloud bands (Hart *et al.,* 2010; Lennard & Hegerl, 2015). These systems induce convective rainfall over the South African interior that occurs as thunderstorm systems that range in size from single cell storms through to mesoscale systems (Blamey & Reason, 2009). The final circulation system is a mid-latitude anti-cyclone south of the country that is positioned eastwards from the southern Atlantic Ocean to the southern Indian Ocean (Lennard & Hegerl, 2015). During the summer, the high-pressure cell produces windy and dry weather over the southern and south-western regions of South Africa, but warm moist air associated with increased rainfall conditions over the eastern part of the country (Roffe *et al.,* 2020). Cold fronts are transported to the Eastern and Western Cape by this cell during the winter (Lennard and Hegerl, 2015; Roffe *et al.,* 2020).

Another climate driver that influences South African precipitation and convection at the intra-seasonal temporal scale is the Madden-Julian Oscillation (MJO; Pohl *et al.,* 2007). The MJO is a large-scale, eastward moving convective system from the tropics that operates within 30-60 days (Pohl *et al*., 2010; Midgley *et al.,* 2016). South African convection is highly influenced by MJO during warm tropical Indian Ocean temperatures and warm ENSO phases, which leads to a decrease in ENSO convection events and increased intra-seasonal variability (Pohl *et al.,* 2007).

The Antarctic Oscillation (AAO), also known as the Southern Annular Mode (SAM), is an additional low-frequency mode of variability within the mid-latitudinal regions (Reason & Rouault, 2005; Pohl *et al.,* 2010; Malherbe *et al.,* 2014). A positive AAO phase consists of a high-pressure system over the mid-latitudinal regions in the Southern Hemisphere and a low-pressure system over Antarctica (Pohl *et al.,* 2010). The positive AAO shifts the mid-latitude westerly winds and the subtropical upper-level jet south towards Antarctica (Gillett *et al.,* 2006; Pohl *et al.,* 2010). During a positive AAO phase, rainfall increases over central South Africa and this relationship is enhanced during La Niña phases (MacKellar *et al.,* 2014; Midgley *et al.,* 2016). During negative AAO phases the winter rainfall region of South Africa experiences increased precipitation due to westerly winds and upper-level subtropical jets that are shifted towards the equator (Reason & Rouault, 2005; Pohl *et al.,* 2010). Analysis over the past few decades has revealed that the AAO climatic driver significantly tends to a positive phase (Jones & Widmann, 2004; Pohl *et al.,* 2010).

SST within the eastern Pacific Ocean control ENSO variations and strength in two to seven-year intervals (Dore, 2005; MacKellar *et al.,* 2014). Southern African rainfall is influenced by ENSO through integrated weather teleconnections (Engelbrecht *et al*., 2011; Dieppois *et al.,* 2015;

Midgley *et al.,* 2016). Cold ENSO events, also known as La Niña, are linked to above-average rainfall within South Africa and warmer ENSO events are linked to below-average rainfall during South African rainfall periods (Midgley *et al.,* 2016; Crétat *et al.,* 2019). Research in South Africa has observed that summer droughts are related to warm ENSO conditions (Lindesay, 1988; Reason *et al.,* 2000; Dieppois *et al.,* 2015; Midgley *et al.,* 2016). Essentially, during El Niño periods, the dry regions in South Africa become drier and wet regions become wetter (Usman & Reason, 2004; Dieppois *et al.,* 2016). The strong relationship therefore allows for more accurate seasonal predictions of rainfall in South Africa (Midgely *et al.,* 2016). The relationship between South African rainfall and ENSO is extremely complex and cannot simply be described through a linear relationship due to various variables that influence and drive regional climate (Fauchereau *et al.,* 2008; MacKellar *et al.,* 2014; Dieppois *et al.,* 2015; Midgley *et al.,* 2016).

Decadal-scale climatic variations produce slow changing conditions around which the higher-frequency climatic modes fluctuate (MacKellar *et al.,* 2014; Malherbe *et al.,* 2016). Tyson *et al.* (2002) observed an 18-year succession within South African rainfall proxy records extending back 600 years. Although the oscillation and its occurrence is not fully understood, it is 'ENSO-like' with a multi-decadal variation pattern (Reason & Rouault, 2002; Midgley *et al.,* 2016). Inter-annual and multi-decadal climatic oscillations can operate together to alleviate or enhance regional climatic responses (Kruger, 1999; Reason & Rouault, 2002). Climate variation can also be induced by the influence of other climatic modes and their interactions with one another (MacKellar *et al.,* 2014).

3.4 Regional Climate

Namaqualand can be classified as a desert ecosystem with a unique and highly selective climate regime, comprising a moderate temperature regime throughout the year and a predictable annual rainfall regime (Van Rooyen *et al.,* 1990; Cousins *et al.,* 2007; de Waal *et al.,* 2016). The Koppen-Geiger classification for Namaqualand, ranges between BWh, BWk, BSh and BSk (Engelbrecht & Engelbrecht, 2016). Therefore, indicating that the Namaqualand region is arid and ranges from desert to steppe (unforested grasslands) regions (Engelbrecht & Engelbrecht, 2016). The Namaqualand region can be classified predominantly as a winter rainfall region receiving precipitation from May to September (Figure 3.5; Benjaminsen *et al.,* 2006; Davis *et al.,* 2016, 2017). The greatest rainfall occurs in the Garies region over the Kamiesberg Mountains with orographic blocking of moisture advected of the South Atlantic Ocean (Figure 3.5; Kelso & Vogel, 2007; Davis *et al.,* 2016). The topographic variation in the mountain landscape therefore causes significant variation within local rainfall (Figure 3.5; Benjaminsen *et al.,* 2006; MacKellar *et al.,* 2007).

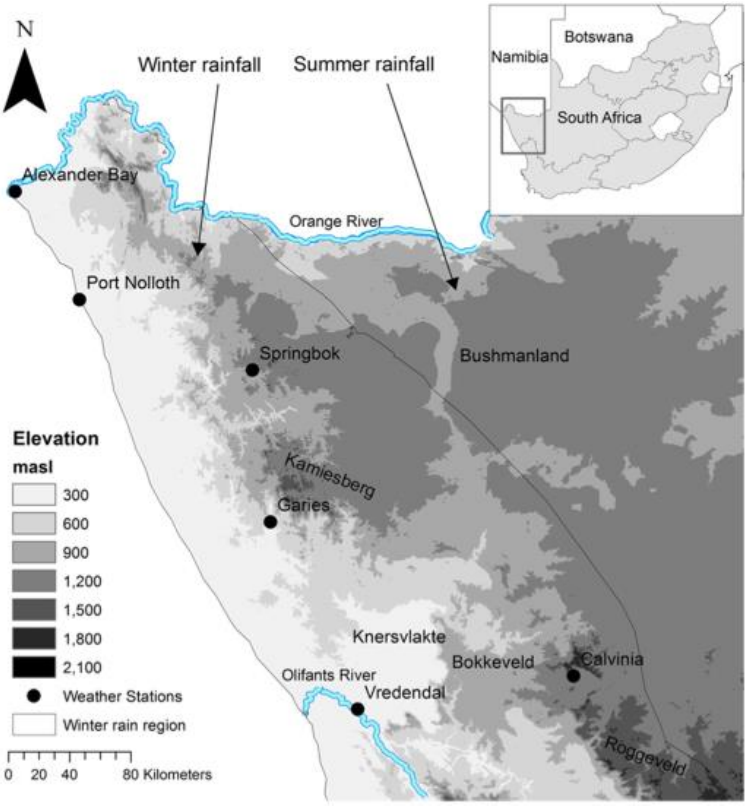

Figure 3.5: Greater Namaqualand region indicating the division between the winter and summer rainfall regions (Davis *et al.,* 2017: 77).

Namaqualand autumns can be classified as mild and relatively moist whereas the winters are moist and cold (Van Rooyen, 1979). During spring the Namaqualand climate is mild and relatively moist, and summer is classified as hot and dry (Van Rooyen, 1979). The Kamiesberg Mountains separate the summer and winter rainfall regions within Namaqualand (Figure 3.5; Kelso & Vogel, 2007; Davis *et al.,* 2017). The eastern Namaqualand plains receive inconsistent and irregular summer rains (Benjaminsen *et al.,* 2006). Winter rainfall comprises 60% of the annual rainfall due to the northward displacement of the Intertropical Convergence Zone (ITCZ) during winter (Davis *et al.,* 2016). Coastal cut-off lows are also a regular occurrence during the winter rainfall periods (MacKellar *et al.,* 2007; Davis *et al.,* 2016). Rainfall totals increases from western Namaqualand to eastern Namaqualand (Kelso & Vogel, 2007; de Waal *et al.,* 2015; Davis *et al.,* 2016), varying from approximately 50mm in the north-western region to 400mm in the central region (Cowling *et al.,* 1999; Davis *et al.,* 2017), with MAP of approximately 170mm (Mucina & Rutherford*,* 2006). Drought events occur frequently in the Namaqualand region (Kelso & Vogel, 2007). However, there have also been instances where a single rainfall event produces precipitation volumes greater than or equal to MAP totals (Kelso & Vogel, 2007).

Namaqualand climate regimes are controlled by a combination of atmospheric pressure systems (Kelso & Vogel, 2007). The regional climate is controlled by the mid-latitude westerly airstreams in winter and subtropical high-pressure systems in summer (Mucina & Rutherford*,* 2006; Davis *et al.,* 2016). The South Atlantic Anti-cyclone transports air and moisture from the Atlantic Ocean into the Namaqualand region (Kelso & Vogel, 2007). The cold Benguela current and the escarpment influences regional-scale moisture conditions (Kelso & Vogel, 2007; MacKellar *et al.,* 2007; Davis *et al.,* 2016). Cold ocean currents and high-pressure systems are responsible for the desert and arid climates of the South African West Coast and Namaqualand region (Kelso & Vogel, 2007). Northern

Cape and West Coast winter rain is produced by the advection of mid-latitude cyclone systems together with the resulting cold fronts moving inland from the south west coast (Kelso & Vogel, 2007). Frequent coastal fog and mist is extremely important for the coastal region's moisture balance as the region experiences approximately 75 fog days per year (Mucina & Rutherford, 2006; Cousins *et al.,* 2007; Davis *et al.,* 2016). Coastal fog forms when humid southerly winds (with humidity between 70% and 100%) blow over the cold Benguela current (Dewar, 2007).

Namaqualand mean annual T_{max} and T_{min} during the day are 30°C and 5°C, respectively (Mucina & Rutherford, 2006). The cold Benguela current to the west in the Atlantic Ocean causes relatively mild annual mean temperatures (T_{mean}) between 13°C in winter and 21°C in summer (Desmet, 2007; Dewar, 2007; Davis *et al.,* 2016). Namaqualand therefore experiences large diurnal and annual temperature ranges (Kelso & Vogel, 2007; Davis *et al.,* 2016). Moving northwards and inland, increases in the annual T_{mean} is experienced (Davis *et al.,* 2016). Extreme T_{max} occur because of berg winds caused by coastal low-pressure systems (Davis *et al.,* 2016). Evaporation rates increase during these conditions and in low-lying coastal regions temperatures can exceed 44°C for several days, which can devastate regional vegetation (Cowling *et al.,* 1999; Mucina & Rutherford, 2006; Davis *et al.,* 2016). The incidence of frost events in the Namaqualand region depends on altitude and distance from the ocean seeing as the west coast regions rarely experience frost events (Mucina & Rutherford, 2006). The occurrence of frost events varies annually, and the region experiences an average of 13 frost days per annum (Mucina & Rutherford, 2006). Namaqualand frost occurs because of thermal inversion in higher altitude areas on the central plateau and the escarpment (Cowling *et al.,* 1999; Davis *et al.,* 2016). The moderate temperature regime together with the highly predictable rainfall regime of Namaqualand allows the distinctive ecological and plant features found within the regional landscape to thrive (Cowling *et al.,* 1999, 2003).

3.5 The Significance of Namaqualand

Primary land use in Namaqualand consists of mining, large-and-small-scale livestock, irrigated farming, conservation and tourism (Benjaminsen *et al.,* 2006; Hoffman & Rohde, 2007; Davis *et al.,* 2016; Bourne *et al.,* 2017). The Western and Northern Cape regions are in urgent need of socio-economic development, which is not possible due to water scarcity (Midgely *et al.,* 2005). Due to low regional economic growth a trend towards urbanisation exists (Midgely *et al.,* 2005).

3.5.1 Farming

Approximately 50% of Namaqualand comprises roughly 412 private commercial farms (Benjaminsen *et al.,* 2006). There are six 'communal areas'; Steinkopf, Concordia, Richtersveld, Pella, Leliefontein and Komaggas (Rohde *et al.,* 2001; Benjaminsen *et al.,* 2006; Benjaminsen *et al.,* 2008). After apartheid, farmlands were redistributed which lead to 30% of Namaqualand land being used for communal farming; which supports 45% of the region's population (Benjaminsen *et al.,* 2006; Davis *et al.,* 2016). Ninety percent of the farmland is used for livestock grazing (Rohde *et al.,* 2001; Mucina & Rutherford*,* 2006; Bourne *et al.,* 2017; Davis *et al.,* 2017). The communal lands support more than 12,000 households (Rohde *et al.,* 2001); and due to land shortage and overcrowding, the farmers struggle to expand farming activities. Thus, they need to supplement their income by working on commercial farms and mines (Benjaminsen *et al.,* 2006). Approximately 41% of these households rely on monthly welfare grants for survival (Rhode *et al.,* 2001; Berzborn, 2007). Farming is predominantly subsistent and does not contribute to the economic activities of Namaqualand (Berzborn, 2007).

3.5.2 Mining

Mining companies own 7% of the land in Namaqualand, leading to extensive land degradation (Rohde *et al.,* 2001; Carrick & Krüger, 2007; Benjaminsen *et al.,* 2008). Throughout the 400km Namaqualand coastline are sporadic sites either being mined or prospected (Carrick & Krüger, 2007). Mining operations in Namaqualand cause severe and long-lasting damage to the natural environment (Cousins *et al*., 2007). Over more than a century of mining copper, gypsum, heavy metals and diamonds have contributed to Namaqualand land degradation (Carrick & Kruger, 2007). Furthermore, water from the Olifants River catchment is over-exploited, and groundwater in the Sandveld region is over-exploited due to unsustainable mining practices (Midgely *et al.,* 2005). Recent legislation compels mines to restore mined land to either economically viable land or to its natural state (Cousins *et al*., 2007). Some of the short-term restoration initiatives have shown limited assurance but rainfall determines the level of restoration success (Cousins *et al*., 2007).

3.5.3 Tourism

The arid Namaqualand region is famously transformed into a colourful wonderland during the spring daisy flower display (Van Rooyen *et al.,* 1991; Patterson-Jones, 1998; Le Roux, 2005; Davis *et al.,* 2016; Kemp *et al.,* 2018), which provides a major tourist attraction (Le Roux, 2005; Mucina & Rutherford*,* 2006). The community benefits economically from the increased tourist visitation during the daisy flowering period (Binns & Nel, 2002; James *et al.,* 2007; Kruger *et al.,* 2013). Although 'flower-viewing tourism' is not an official term, it forms part of nature-based tourism activities with tourists travelling to a specific location for its floral magnificence (Turpie & Joubert, 2004; Andereck, 2009; Nagai *et al.,* 2019). Flower-viewing tourism forms part of a restricted tourism activity seeing that it occurs in specific biome regions and evokes a niche market (Kruger *et al.,* 2013). Nature-based tourism and especially 'flower viewing' tourism are the primary attractions within Namaqualand (James *et al.,* 2007; Kruger *et al.,* 2013). The value of flower viewing tourism in the Namaqua National Park has been estimated at 50,000 USD (approximately R360,000 at the time; James *et al.,* 2007). Because this study was conducted over a decade ago, one can assume that the economic value of flower viewing in the Namaqualand region is currently far greater. SANParks (2012a, 2012b) estimated that during the 2012/2013 flowering season, the Namaqua National Park, and West Coast National Park, both of high relevance to wildflower tourism, were worth R15 million and R22 million, respectively. These figures do not include expenditure outside the National Parks (Kruger *et al.,* 2013). When considering the economic value of flower viewing in Namaqualand together with the positive impacts thereof on the community (job creation), it is clear that it is extremely significant to local and international visitors (James *et al.,* 2007; Kruger *et al.,* 2013). Wildflower tourism can also aid the protection of regional plant biodiversity (Turpie & Joubert, 2004; Hall *et al.,* 2011).

3.5.4 Conservation

Conservation areas make up 5% of Namaqualand (Rohde *et al.,* 2001). Future climate projections for Namaqualand suggest a decrease in regional rainfall and an increase in temperature (Cousins *et al.,* 2007; Engelbrecht *et al.,* 2013; Davis *et al.,* 2016; Midgley *et al.,* 2016), which will ultimately lead to a reduction in livestock production (Cousins *et al*., 2007). Through extensive mining operations and overexploitation of rangelands by ploughing and livestock, the Namaqualand landscape has suffered extensive land degradation (Bourne *et al.,* 2017). Land degradation influences ecosystem health and functioning and agricultural productivity (Bourne *et al.,* 2017). Conservation will therefore become even more important within Namaqualand to protect and effectively manage regional biodiversity seeing that flower viewing tourism will become an even more important economic stimulant for the region (Cousins *et al*., 2007). Policy makers must therefore find a balance between conserving biodiversity and ensuring socio-economic growth. Cost-effective and efficient ecological restoration activities have been implemented in the broader Karoo to diminish and reverse land degradation (Bourne *et al.,* 2017). The ecological restoration programs have focused on promoting water infiltration through micro-catchments, mulching and brush packing; supporting and securing agricultural productivity; re-introducing lost biodiversity through planting seeds; and erosion control to stabilise soils (Carrick & Kruger 2007; Carrick *et al.,* 2015; Bourne *et al.,* 2017).

CHAPTER 4: METHODOLOGY

[4]

4.1 Introduction

This dissertation is the first to explore the regional climatic influence on the phenology of *Dimorphotheca sinuata* on the South African West coast. This study involved the analysis of meteorological and phenological data. The study assesses change and continuity in the climate data, with all its different variables, together with the collected phenological responses and its changes over time. The relationships between the climate and phenological data are explored. This chapter outlines the acquisition and analysis of the data.

4.2 Data Collection

Ground-based and historical records are the principal method used to obtain phenological data of annually recurrent events for a specific species within a specific location (Fitchett *et al.,* 2015). This study utilised established methodology developed by Futter (2003), Fitchett and Fani (2018) and Fitchett *et al.* (2019). The methodology used for this study relied on standard approaches in phenological research, structured around statistical analysis of flowering dates and climate variables over the established temporal period (Fitchett *et al.,* 2014a).

4.2.1 Climate Data

The climate data for this project was obtained from the South African weather Service (SAWS). Commonly, the climate data required for phenological studies includes T_{max}, T_{min} and precipitation records that are preferably three decades long (Grab & Craparo, 2011; Fitchett & Fani, 2018). The Namaqualand daisy region spans from the West Coast National Park in Langebaan to Port Nolloth in the north. Seven weather stations were identified and assessed. Each of the selected weather stations had climate data for daily maximum temperature (T_{max}) and minimum temperature (T_{min})

and precipitation. The location, length of the climate record as well as missing climate data for all the assessed weather stations are detailed in Table 4.1.

Table 4.1: Namaqualand weather station locations, dataset ranges and missing data

Weather Station	**Latitude**	**Longitude**	**Length of Climate Record**	**Missing Data**
Cape Columbine	32°49'32"S	17°50'42"E	1959-2018	
Vredendal	31°40'05"S	18°30'04"E	1959-2018	
Nieuwoudtville	31°22'35"S	19°06'43"E	2003-2018	January-March 2003
Springbok	29°39'51"S	17°53'11"E	1988-2018	• Temperature: January-April 1988 and June-December 1989 • Precipitation: only starts August 1993
Port Nolloth	29°15'06"S	16°52'10"E	1960-2018	July 1979-June 1983
Lambertsbaai Nortier	32°05'48"S	18°18'30"E	1989-2018	Temperature: • January-September 1989 • December 1989 • January-April 1990 • June, October and November 1991 • April, August, November-December 1992 • The entire 1993 • January-October 1994 Precipitation: • January 1989-October 1994
Clanwilliam	32°10'54"S	18°53'31"E	2000-2018	During 2000 the first readings are only documented from November onwards.

The selected weather stations within the Namaqualand region are spatially distributed. Some weather stations are close to the coast (Port Nolloth, Lambertsbaai Nortier and Cape Culumbine) while others are inland (Springbok, Vredendal, Nieuwoudtville and Clanwilliam). The protocol followed for dealing with years or months that had missing climate records, are discussed in sections 6.3.1 and 6.3.2 (*Data and Statistical Limitations*).

4.2.2 Phenological Data

A mixed-method approach was used to acquire phenological data from a range of documentary evidence and sources (Fitchett & Fani, 2018). Multiple methods of data acquisition were utilised to allow for triangulation (Parmesan & Yohe, 2003). Evidence on the flowering dates were obtained from digitized newspaper records and social media platforms. For numerical analysis of the climate and phenological data, all flowering dates were converted to Julian Dates to facilitate quantitative and statistical analysis (Nordli *et al.,* 2008; Luedeling & Gassner, 2012; Fitchett *et al.,* 2019).

4.2.2.1 Newspaper Records

The Rand Daily Mail newspaper closed in 1985 due to its controversial views and opposition to the government of the time. Despite the controversy, there are digitized records of this newspaper from 1902-1985. ‘Die Burger’, an Afrikaans newspaper, that circulates in the Western and Eastern Cape, and ‘Volksblad’, a daily Afrikaans newspaper, that circulates in the Free State and the Northern Cape, are both available in digitized formats from the media house, Media24. The digitized records from ‘Die Burger’ and ‘Volksblad’ span from 1985 to present. As Namaqualand daisy flowering events are notable social, natural and economic events, the recorded dates are accurate (Fitchett *et al.,* 2019). Combined, all the newspaper records can therefore help to create a long temporal dataset (Table 4.2).

The methodology set out by Futter (2003) and Fitchett and Fani (2018) were followed to ensure accurate and consistent documentation of flowering events. Online digitized platforms allow one to search for key words and phrases. The location and date of every article, picture or headline that mentioned the Namaqualand daisies were documented (Futter, 2003; Fitchett & Fani, 2018; Stockigt *et al.,* 2018). The search terms used for the English newspaper, The Rand Daily Mail included: ‘Namaqualand daisies’, ‘Namaqualand flowers’, ‘Namaqualand wildflowers’, ‘Namaqualand full bloom’ and finally ‘Namaqualand’. A total of 74 records relating to the Namaqualand daisy flowering periods, spanning 1935-1985, were collected from The Rand Daily Mail. For the Afrikaans newspapers, the search terms included: ‘Namakwaland daisy’, ‘Namakwaland madeliefies’, and ’Namakwaland blomme’. A total of 456 records were obtained from ‘Die Burger’ and ‘Volksblad’ spanning 1986-2017. For the disclosure of the limitations related to the collected newspaper records please refer to section *6.3.1 Data Limitations*.

4.2.2.2 Social Media

Social media records span a relatively short period of approximately 10, years due to the recent advent of these platforms (Amaral *et al.,* 2014). When using social media records for phenological research, netnographic data collection approaches are employed, which entail gathering scientific information from unstructured, daily, self-reported individual accounts (Miguéns *et al.,* 2008; Jeacle & Carter, 2011). Photographs posted on the social media platforms Flickr and iNaturalist were documented, together with dates and locations (where specified) to gain insight into recent flowering periods from 2001-2018 (Miguéns *et al.,* 2008; Graham *et al.,* 2011; Fitchett & Fani, 2018; Table 4.2).

On Flickr, a video and photography hosting social media platform, people can share, explore and discuss photos. Flickr is an online media-sharing platform used by professional and amateur photographers. One of the benefits of using Flickr as a data source is the additional information that users can upload about the location and date where the image was taken. This strengthens the phenological data record of this study and increases the resolution of the flowering phenology dataset. The key words and search terms that were used to locate accurate flowering dates included 'Namaqualand' and 'Namaqualand daisies' (Fitchett & Fani, 2018). Photos that display clear pictures of Namaqualand daisies in bloom were documented. Photos or posts that displayed the date when the picture was taken, instead of the date of when the picture was uploaded, were ultimately documented (Table 4.2). The date, location and phenological comment was recorded and integrated into the phenological dataset (Fitchett & Fani, 2018). Some profiles had a whole cluster of photos of daisies taken on the same day. Such posts were documented as a single phenological event, unless different locations were provided. A total of 103 phenological dates and entries were collected from Flickr.

The other social media platform utilized in this study was iNaturalist. iNaturalist is an online social network used for citizen science projects (Graham *et al.,* 2011). Like all citizen science projects, the main aim of iNaturalist is to share, observe and map biodiversity all over the world (Graham *et al.,* 2011; MacKenzie *et al.,* 2017; Leocadio *et al.,* 2018). On the iNaturalist website, the search term *Dimorphotheca sinuata* (Namaqualand daisy) was entered with South Africa as the location, which provided 30 sightings on the site. The dates together with the locations of the sightings were documented and added to the phenological dataset (Table 4.2).

Table 4.2: Table describing and showing the integration of the gathered phenological data within this study.

Source	Type of Data	Phenological Information	Application in Study
Newspaper Records	○ Qualitative information related to the scenic nature of the daisies in different regions. ○ Dates of articles. ○ Focus on captions and mentions of ‘flowering’, ‘daisies’, ‘end of season’, ‘start of flowering’ and ‘colourful’. ○ Information relating to what regions are busy flowering and what sites would be the best to visit.	○ Insight into local perceptions of changes in daisy flowering timing. ○ Spatial and temporal insights to daisy flowering periods.	○ Analyse the spread of the data, start and end dates, peak flowering and changes over time.
Social Media	○ Comments made on the scenic nature of the daisies. ○ Focus on captions and mentions of ‘flowering’, ‘daisies’, ‘end of season’, ‘start of flowering’ and ‘colourful’. ○ Dates of entries/posts. ○ Linked to a specific location. ○ Photos posted online and on social media linked to daisy flowering.	○ Insight into spatial and temporal flowering periods. ○ Insight into local perceptions of changes in daisy flowering timing. ○ Extra phenological snippets of information here and there.	○ Analyse the spread of the data, start and end dates, peak flowering and changes over time.

A total of 663 phenological records, comprising 601 flowering dates and 62 qualitative data were documented. Some dates would indicate that ‘flowering has just started’ and others might have said that ‘full bloom has already been reached’ in specific regions. Therefore, due to the nature of the collected flowering dates, different growth and flowering stages were recognised using the *Biologische Bundesanstalt, Bundessortenamt and Chemical Industry scale* (Maan *et al.,* 2020).

4.2.2.3 Grouping of Phenological Data

Several government agencies have collaborated to create the *Biologische Bundesanstalt, Bundessortenamt and Chemical Industry scale* also known as the BBCH scale, which is a scale that quantifies and defines different phenological phases (Meier, 2001; Kalbarczyk, 2009; Morisette *et al.,* 2009; Fadón *et al.,* 2015; Flemmer *et al.,* 2015). The scale provides a standardised method and code for effective analysis and documentation of phenological phases of plant species (Morisette *et al.,* 2009; Polgar & Primack, 2011; Maan *et al.,* 2020). The BBCH code ascribes values from 1-100 that characterizes different phenological events and stages of growth for mono- and dicotyledonous plants (Hack *et al.,* 1992; Maan *et al.,* 2020). Plant developmental and growth cycles are subdivided into ten different developmental stages all in ascending order (Meier, 2001; Morisette *et al.,* 2009; Polgar & Primack, 2011). Flowering is the sixth principal growth stage in the BBCH scale. Secondary values or stages, ranging from 0-9, are used to describe developmental stages more accurately and in more detail (Meier, 2001; Flemmer *et al.,* 2015). For flowering, a two-digit BBCH code is ascribed (Maan *et al.,* 2020). Sorting phenological phases of plants into numerical codes therefore allows researchers to order and effectively assess plant phenological phases (Flemmer *et al.,* 2015; Ventura *et al.,* 2020).

The collected phenological comments ranged from explaining that 'first bloom has occurred', 'the daisies are in full bloom' or that 'the flowering season has come to an end'. Phenological comments were assigned to corresponding BBCH scale classifications (Figure 4.1). To account for human error and bias, similar BBCH codes were therefore grouped together for effective analysis of the collected flowering record. The collected phenological records of flowering dates of the Namaqualand daisies were divided into three main groups (Kalbarczyk, 2009). The three constructed flowering groups were created to capture the descriptions used by newspaper journalists, people posting on social media platforms and the comments and perceptions of local citizens. The first group comprises BBCH codes 60-61, termed first flowering/initial flowering (Figure 4.1). The second group, termed full bloom, relates 30-100% bloom with BBCH codes 63-65 (Figure 4.1). The last group comprises BBCH codes 67-69 and relates to the end of bloom or the end of the flowering period (Figure 4.1).

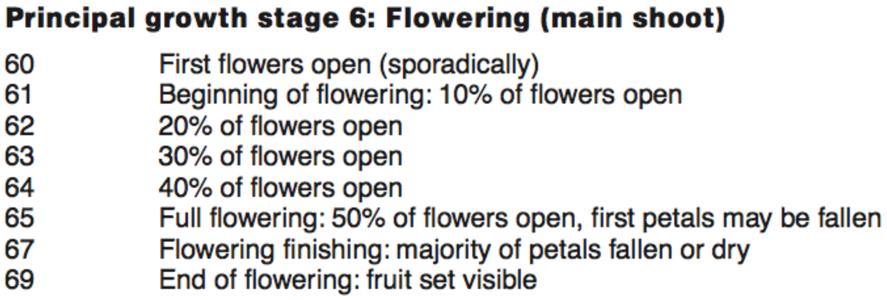

Principal growth stage 6: Flowering (main shoot)

60	First flowers open (sporadically)
61	Beginning of flowering: 10% of flowers open
62	20% of flowers open
63	30% of flowers open
64	40% of flowers open
65	Full flowering: 50% of flowers open, first petals may be fallen
67	Flowering finishing: majority of petals fallen or dry
69	End of flowering: fruit set visible

Figure 4.1: BBCH flowering code with descriptions (Meier, 2001: 12).

Due to the large phenological record obtained, some years had more than one Julian flowering date within each BBCH code group. Julian flowering dates for every year and for every BBCH group were therefore averaged to produce a single mean Julian flowering date (Fitchett & Fani, 2018). The initial flowering group (BBCH 60-61) had a total of 97 flowering dates. Full bloom (BBCH 63-65) flowering dates were the largest phenological group with a total of 469 flowering dates. End of bloom (BBCH 67-69) was the least documented phenological group with only 35 flowering dates.

4.3 Data Analysis

The climate data provided by the SAWS comprises daily climate records of T_{max}, T_{min} and precipitation for all the years available for the specific stations. T_{max} and T_{min} constitute the maximum and minimum recorded temperatures within a 24-hour period. For the daily temperature variables, the daily climate data was averaged to produce monthly T_{max} and T_{min} means for every year available. The monthly T_{max} and T_{min} for every year were then also averaged to produce annual average T_{max} and T_{min} values (Miller-Rushing & Primack, 2008a; Primack *et al.,* 2009b; Davis *et al.,* 2015). Mean temperature (T_{mean}) was also calculated from daily T_{max} and T_{min} (Fitchett *et al.,* 2014a; 2016a). Monthly and annual temperature averages for all seven weather stations and all three temperature variables were then plotted on separate timelines to efficiently analyse changes over time (Fitchett *et al.,* 2014a; 2016a). Precipitation records refer to the daily total rainfall, within a 24-hour period. Daily precipitation records were combined to produce monthly and annual precipitation totals for every year available. Monthly and annual precipitation totals were plotted per station (Fitchett *et al.,* 2014a, 2016a).

The preliminary data analysis involved calculating the average climatic conditions for all seven weather stations in the Namaqualand region and average flowering dates for the three constructed BBCH groups. The variability of all the datasets and the directions and magnitude of changes for every variable over time was also studied. Further climate data analysis for all the weather stations involved calculating the onset and end of the rainy season and assessing its change over time, conducting Standardized Precipitation Index (SPI) analysis, assessing winter and spring climate changes over time and documenting changes in frost event variables over time. The final data analysis that was conducted involved correlating observed changes in Namaqualand daisy phenological flowering timing with changes in the respective climate variables.

4.3.1 Changes in Climatic Variables and Phenological Flowering Dates

Linear regression analysis for each of the variables (T_{max}, T_{min}, T_{mean}, precipitation and Julian flowering dates) were calculated to assess the degree of change and variability over time and to assess if these trends were statistically significant over the specified temporal period (Badeck *et al.,* 2004; Fitchett *et al.,* 2016a). When conducting a linear regression analysis (time trend analysis), time acts as the independent variable (x-axis), against which the dependant variable (y-axis) is related to (Lu *et al.,* 2006; Nordli *et al.,* 2008; Nel, 2009).

In this study, changes in climate variables and phenological flowering dates over time were assessed; independently at first and then the relationship between the two variables were also assessed. Regression analysis can be used to quantify the changes of the different variables under question over time (Howard, 2018). The linear rates of changes of the respective variables over different temporal scales are quantified using a line of best fit (Lu *et al.,* 2006; Lomax, 2007; Manly, 2008). The line of best fit is calculated based on the following formula:

$$y = mx + c \qquad \text{(Lomax, 2007; Manly, 2008)}$$

In this formula, c is the y-intercept and m is the coefficient of x and both values are determined through the use of the following formulas:

$$c = \frac{\sum xy - \frac{\sum x \sum y}{n}}{\sum x^2 - \frac{(\sum x)^2}{n}}$$

$$m = \frac{\sum y - b \sum x}{n}$$

(Manly, 2008)

The m-value stipulates the rate of change brought about in the dependent variable when there are unit decreases or increases in the independent variable (Manly, 2008). Only the m-value from the line of best fit equation was reported on for this study. It is also referred to as the coefficient of x or the rate of change per year. When reporting on the calculated coefficients for the changes in flowering dates or climate changes over time, absolute values were used and the direction of the change over time was mentioned in-text. The rate of change per year varies depending on the variable under inspection. For temperature changes, the units reported will be degree Celsius change per year (°C.yr^{-1}). When assessing precipitation changes over time, the reported unit will be millimeter change per year (mm.yr^{-1}). Finally, for changes in flowering phenological Julian dates, the reported units will be day change per year (d.yr^{-1}) or per decade (d.decade^{-1}).

A Pearson Correlation Coefficient (r) calculation produces a value between -1 and +1. An r-value tending towards -1 or +1 indicates that the assessed variables are closely related and can be used to assess the strength, direction and magnitude of changes in variables over time (Nordli *et al.,* 2008; Burt *et al.,* 2009). The Pearson Correlation Coefficient was calculated using the following equation:

$$|r| = \left|\frac{\sum(x_i - \bar{x})(y_i - \bar{y})}{\sqrt{\sum(x_i - \bar{x})^2 \sum(y_i - \bar{y})^2}}\right|$$ (Manly, 2008; Underhill & Bradfield, 2009)

Correlation coefficient values of -1 and +1 indicate a strong relationship between the dependant and independent variables (Manly, 2008; Burt *et al.,* 2009). In this study, positive correlation coefficients indicate changes to warmer temperatures, increased precipitation, and later (delayed) flowering dates over time (Burt *et al.,* 2009). A negative correlation coefficient therefore indicates changes to cooler temperatures, decreased precipitation, or earlier flowering dates (advances) over time (Burt *et al.,* 2009). A correlation coefficient tending to 0 indicates a weak relationship between the dependant and independent variables and little to no change over time, or alternatively that there is no clear and observable pattern of change over time (Burt *et al.,* 2009). Within this study the absolute r-value was reported, i.e. the r-value will be between 0 and 1.

After assessing the relationship between two variables (trends and correlations) using the m and r-values, the p-value is used to assess the statistical significance between the variables under review (Chandler & Scott, 2011; Post *et al.,* 2018). Therefore, the p-value is used to determine the statistical significance of the relationship that is described by the r-value. The calculated p-value produces a value between 0 and 1 which indicates that trends are either accurate reflections of the data over the study temporal period, tending more towards 1, or occurring by chance and as a result of random sampling. i.e. tending more towards 0 (Burt *et al.,* 2009; Manly, 2008; Underhill & Bradfield, 2009). The calculation of a strong correlation in a large dataset reflects a more accurate existing relationship between a variable over time than a small dataset with a few consecutive values increasing or decreasing randomly over time. Therefore, large datasets with strong correlation coefficients are more likely to produce statistically significant results (Motulsky & Searle, 2003; Manly, 2008; Underhill & Bradfield, 2009).

The null hypothesis for the p-value states that there is no observable trend in the climate or phenological data over time (Manly, 2008; Underhill & Bradfield, 2009). All the potential fractions of results for scenarios where there is a relationship between the selected variable with time are defined by the p-value (Motulsky & Searle, 2003). A p-value of 0.05 indicates that there is a 5% chance of observing a specific calculated relationship of the same strength, if there is no real relationship between the variables over time (Motulsky & Searle, 2003). In this study, a calculated p-value of less than 0.05 rejects the null hypothesis and indicates that the observed trend is statistically significant (Burt *et al.,* 2009; Underhill & Bradfield, 2009; MacKellar *et al.,* 2014). Chapter 5 will present the results from the statistical tests in tabulated form. Statistically insignificant results can represent inaccurate relationships and therefore only trends and relationships that are statistically significant will be reported on in-text.

4.3.2. Relationships between Phenological Data and Climate Change

The phenological data collected within this study utilised data from different locations to create a 'Namaqualand' flowering timing dataset. The climate data for this study also has a wide spatial distribution, and the relationships between the phenological record and the climate data for the individual weather stations were therefore assessed independently (Post *et al.,* 2018). Seeing as there are considerable temporal and spatial variations in precipitation trends within different subregions, each weather station's precipitation dataset was also analyzed separately (MacKellar *et al.,* 2014; Kruger & Nxumalo, 2017).

After assessing all the changes over time for all identified variables, a general picture of temporal changes can be formed. The link between different climate variables and phenological flowering timing still needs to be assessed to identify correlations and causation between the datasets. A range of phenological studies use linear regression models to characterise the relationships between phenological shifts and changing climatic conditions (Hegland *et al.,* 2009; Grab & Craparo, 2011; Keatley & Hudson, 2012; Luedeling & Gassner, 2012; Fitchett *et al.,* 2014a; Davis *et al.,* 2015; Richardson *et al.,* 2017).

Correlation coefficient (r), regression analysis (line of best fit) and statistical significance (p-value) of the relationships between flowering phenology timing and the respective climate variables were calculated using the same methods described in section 4.3.1 (Manly, 2008; Underhill & Bradfield, 2009). For these tests, different climatic variables (independent variables plotted on the x-axis) were tested against the dependent variable, Julian flowering dates (y-axis; Leech *et al.,* 2005). The phenological flowering dates spanned 1935-2018. Monthly and annual climate variables for every year and for every weather station were placed on the same timeline for the analysis of correlations and significance with phenological flowering timing. The monthly temperature averages and precipitation totals together with annual averages and totals for the different weather stations were assessed to identify the months and seasons with the greatest influence on phenological flowering timing (Miller-Rushing & Primack, 2008a). It is important to note that the flowering timing datasets were split into three distinct phenological flowering groups and tests for correlations with respective climate variables therefore entailed testing the climate variables with all three of the identified phenological flowering groups.

As noted previously, linear regression is the primary method of analysis for studies that document phenological shifts resulting from climate change (Miller-Rushing & Primack, 2008a; Hegland *et al.,* 2009; Richardson *et al.,* 2017). As noted with the time trend analysis, the m-value quantitatively defines the rate of change of the dependant variable brought about by a unit change in the independent variable. The rate of change defines changes in flowering dates due to unit changes in the assessed climatic variables. The units of changes in flowering timing brought about by temperature and precipitation are measured in $d.°C^{-1}$ and $d.mm^{-1}$, respectively (Lambert *et al.,* 2010; Pearson, 2019). The direct analysis of phenological timing changes per climatic variable change allows the relationships between phenological timing shifts and the respective climate variables to be assessed and further allows different phenological responses to changing climatic conditions in variable locations to be compared to assess the magnitude of climate change for different species in different locations. Absolute m-values were reported and the direction of the relationships between the variables were provided in-text.

The correlation coefficients (r) obtained from the correlation between phenological flowering dates and the respective climate variables are interpreted similar to the linear regression (time trend) interpretation. Strong relationships are inferred by correlation coefficients tending towards 1 whereas weak correlations tend towards 0.

4.3.3 Assessing Precipitation Timing (Onset and End of the Rainy Season)

Diverse plant species respond to climate timing events, such as precipitation, differently (Parmesan & Yohe, 2003; Root *et al.,* 2003; Polgar & Primack, 2011). For certain plant species, flowering can be induced shortly after the onset of the rainy season (Bendix *et al.,* 2006). The onset and end of the rainy season is used to measure seasonal precipitation, which is an indicator of the start and end of plant phenological cycles (Amekudzi *et al.,* 2015; Roffe *et al.,* 2019).

A range of methods is used to calculate the onset and cessation of the rainy season. These methods were adapted from the literature (Moeletsi & Walker, 2012; Moeletsi *et al.,* 2013; Tongwane & Moeletsi, 2015; Bekele *et al.,* 2017) for the precipitation conditions of the South African West coast (Table 4.3). Although some criteria are region and crop-specific (Roffe *et al.,* 2020), they accurately identify wet periods, and rainy season start and end dates (Liebmann *et al.,* 2012).

Table 4.3: Criteria set out to assess the dates of the onset and end of the rainy season.

Precipitation Timing Event	**Formulated Criteria for Date Selection**
Onset of Rainy Season Date	The first day after April that has a total precipitation of 20mm.
	The last date after three consecutive precipitation days.
	The date as soon as consecutive precipitation days adds up to a total of 20mm of precipitation.
End of Rainy Season Date	The last precipitation event with a total of 20mm that takes place in the same calendar year as the onset of the rainy season.
	The last date after three consecutive precipitation days takes place in the same calendar year as the onset of the rainy season.
	The last date of consecutive rainy days that adds up to a total of 20mm precipitation that takes place in the same calendar year as the onset of the rainy season.

The precipitation records obtained from the SAWS recorded 0.1mm precipitation per day as the minimum measured rainfall value. Therefore, for the scope of this study, ‘one rain day’ is defined meteorologically as an accumulation of 0.1mm precipitation (Nandargi & Mulye, 2012; Burls *et al.,* 2019). The onset of the rainy season was documented from April onwards, to account for the autumn and winter rains within the South African winter rainfall zone (WRZ). Namaqualand forms part of the South African WRZ, and usually receives precipitation from April to September, thus the end of the rainy season falls in the same calendar year (Philippon *et al.*, 2012; Crétat *et al.,* 2012).

Months and years with missing precipitation records were dealt with as omitted records instead of interpolating precipitation totals, and rainy season onset and end dates. Occasionally during drought years, there was no clear rainy season onset or end, as it did not rain enough to meet the requisite criteria. During such years, the onset and/or end of the rainy season date was omitted to avoid skewing the data. All seven weather stations were assessed for the onset and end of the rainy season dates. Thereafter, the calculated rainy season onset and dates were converted to Julian dates for the purpose of quantitative analysis and to plot these events on a timeline.

Once again, time trend analysis (linear regression analysis), correlation coefficients (r) and the statistical significance (p-value) were calculated for every weather station's onset and end of rainy season datasets to assess changes over time (section 4.3.1). The units used for describing changes in rainy season onset and end dates were reported as $d.yr^{-1}$. Calculated coefficients and rates of changes were reported as absolute values and the direction of change was indicated in-text.

Analysis of the correlation and relationship between the onset and end of rainy season Julian dates and the documented Julian flowering dates were assessed. Every weather station's onsets and end of rainy season dates were correlated with the three identified BBCH flowering groups to test their correlation, and the statistical significance of these relationships (section 4.3.2). Precipitation timing dates (independent variable) were tested against the dependent variables, the flowering dates (Leech *et al.,* 2005). The units used to describe the changes in flowering timing brought about by changes in the onset and end of the rainy season are $d.d_{OR}^{-1}$ and $d.d_{ER}^{-1}$ respectively, which stands for: day change per onset/end of rainy season change, respectively. These units are not officially used in any assessed literature but are used for increased clarity within the analysis.

4.3.4 Standardized Precipitation Index

The Standardized Precipitation Index (SPI), developed by McKee *et al.* (1993), is a multi-scale drought index that assesses precipitation records to examine drought events (Blanc, 2012; Araujo *et al.,* 2016). SPI allows for the quantification of precipitation deficits on a range of different time scales (McKee *et al.,* 1993).

To calculate SPI values, a gamma probability density function has to be fitted over a precipitation frequency distribution (McKee *et al.,* 1993; Blanc, 2012). This determines cumulative probabilities of precipitation events for a selected temporal scale (McKee *et al.,* 1993; Blanc, 2012). The acquired values are then converted into a normal distribution that has a variance of 1 and a mean of 0. The SPI values are then articulated as standard deviations from the norm (McKee *et al.,* 1993; Blanc, 2012). Positive SPI values indicate normal or above average precipitation conditions and negative SPI values indicate below average precipitation conditions.

SPI analysis can assess precipitation conditions at variable temporal scales (Seiler *et al.,* 2002). Short-lived drought and wet periods are captured by a small scale 3-month SPI analysis. The 6-month SPI describes seasonal drought and wet conditions on a slightly larger scale. The 3- and 6-month SPI analysis therefore identifies meteorological drought conditions. Drought and wet periods are described on an annual basis when the 12-month SPI scale is utilised. The 24-month SPI calculation describes long lasting and severe drought events, also called agricultural drought events. The different monthly SPI scales can therefore be utilised to assess different kinds of precipitation variation over variable temporal scales (Seiler *et al.,* 2002; Blanc, 2012).

SPI was calculated for five of the seven Namaqualand weather stations for 3-, 6-, 12- and 24-month periods/scales. SPI could not be calculated for Nieuwoudtville and Port Nolloth because of a high frequency of omitted precipitation records. It is advised that precipitation datasets span 30 years to ensure accurate and reliable SPI calculations (McKee *et al.,* 1993). In this study, SPI was calculated regardless of the temporal length of the precipitation dataset.

Monthly SPI values were calculated for every year for the stations with sufficient precipitation data, and the calculated SPI values varied depending on the scale used (3-, 6-, 12- and 24-month). The monthly SPI values, for every selected SPI scale, were then averaged to calculate a mean SPI value for that specific year. Thereafter, the annual SPI means were plotted on a timeline. Every weather station therefore had four datasets or timelines with annual mean SPI values.

Each station's mean SPI value for each scale was calculated to assess the average drought index of each station. Linear regression analysis (time trend analysis), correlation coefficient (r) and statistical significance (p-value) were calculated for every station's four SPI scale datasets to assess drought index change over time (section 4.3.1). The SPI changes over time were reported as absolute values and the direction of change was indicated in-text. The relationship between the different SPI scale values for every weather station was also correlated with Julian flowering dates to assess the relationship between phenological flowering dates and SPI values (section 4.3.2). Every weather station therefore has four different sets of SPI values that were correlated to the three different BBCH flowering groups. The respective SPI values were used as the independent variables and tested against the dependent variables; the flowering dates (Leech *et al.,* 2005). The unit used for describing the calculated changes in flowering timing brought about by changes in SPI values are reported as $d.SPI^{-1}$ which indicates day changes per SPI changes.

4.3.5 Seasonal Assessment

Namaqualand daisies germinate when the winter rains start during April or May and vegetates until their flowering period commences in spring (Le Roux, 2005). Therefore, Namaqualand daisies have a seasonally structured life cycle (Lieth, 2013; Rudolf, 2019). Phenological literature suggest that there are strong correlations between winter and spring climate variables and plant phenological phases (Heikinheimo & Lappalainen, 1997; Ahas et al., 2002; Sparks *et al.,* 2000; Chmielewski & Rötzer, 2001; Menzel, 2003). Climate change is causing changes within seasonal climatic conditions such as seasonal fluctuations in precipitation and warmer T_{min} during winter (Williams & Middleton, 2008). This study therefore assessed the changes in seasonal climatic conditions and the impact of seasonality on the flowering phenology of Namaqualand daisies.

Winter and spring were therefore selected for the assessment of seasonal influence on Namaqualand daisy phenology. Winter months include June, July and August and the spring months include September, October and November. Average temperature conditions (T_{max}, T_{min} and T_{mean}) and total precipitation for all seven weather stations during both the winter and spring months were calculated for every year.

The mean climatic conditions spanning the temporal record of each weather station was assessed. To determine changes in the seasonal climatic conditions over time, linear regression analysis (m-value), correlation coefficient (r) and the statistical significance of the regression (p-value) were calculated for every weather station (section 4.3.1). Coefficients of change were indicated as absolute values and the direction of change was indicated in-text. Linear regression analysis (m-value), correlation coefficient (r) and the statistical significance (p-value), of the relationships between the seasonal climatic variables (independent variable) and flowering Julian dates (dependent variable), were assessed to determine the seasonal climatic influence of winter and summer on flowering timing of the Namaqualand daisies (section 4.3.2).

4.3.6 The Influence of Frost

Temperature plays a crucial role in plant development (Walck *et al.,* 2011; Rosbakh & Poschlod, 2015). Frost influences flowering, through influencing seed germination and damaging plant tissues when ice crystals are formed at freezing temperatures (Fitchett *et al.,* 2014b; Pardee *et al.,* 2018). This study used two frost temperature parameters: T_{min} ≤0°C and T_{min} ≤4°C. Although the one frost parameter is not below freezing, T_{min} ≤4°C would affect plants in low relative humidity conditions.

The assessed frost variables include the number of frost days, the last frost date (Julian days) and the number of frost events that occur after first flowering. The last frost date for every weather station was converted to Julian dates for analysis and comparison with collected flowering dates. The three frost variables were calculated for each station for every year. The collected frost data was plotted on a timeline. Linear regression analysis (m-value), correlation coefficient (r) and the statistical significance (p-value) were calculated for each set of frost variables for each weather station to assess changes over time (section 4.3.1). The coefficients of change were reported as absolute values and the direction of the change over time was indicated in-text. The unit used for changes in yearly frost days over time was $fd.yr^{-1}$ and the unit used for frost events that occur after first flowering was $fe.yr^{-1}$. These units are not official units used in literature but used for increased understanding within this study. Only weather stations that had more than 10 years of recorded frost dates were assessed in linear regression analysis.

Linear regression analysis was also conducted to assess the relationship between the different frost variables and the three identified Julian date flowering groups. The linear regression analysis could not be calculated for some of the weather stations for the three different flowering groups, seeing as BBCH 60-16 (first bloom) and BBCH 67-69 (end of bloom) did not have as many Julian dates compared to BBCH 63-65 (full bloom). Therefore, some of the regression analysis between frost for certain weather stations and flowering timing could not be assessed due to a lack of either flowering dates or frost events. The units that were used to describe the changes in flowering dates over time brought about by the frost variables include; $d.F_N^{-1}$ for days per number of frost events, $d.F_{LD}^{-1}$ for days per last frost event change and $d.F_{AF}^{-1}$ for days per frost events after first flowering. These are not official units but are used for ease of analysis.

No analysis on frost events influence on flowering can be calculated for Cape Columbine as only four frost events occurred during the period 1959-2018. Port Nolloth, Lambertsbaai Nortier and Clanwilliam similarly do not have enough data for frost events where $T_{min} \leq 0°C$ and comparisons of how frost ($T_{min} \leq 0°C$) has influenced any of the three BBCH flowering groups was therefore not calculated.

4.3.7 Multiple Regression Analysis

So far, this study has assessed the relationships between climate variables (independent variables) and phenological flowering dates (dependent variables). It allows for the assessment of the significant climatic factors that have an influence on flowering timing and how it has changed over time. However, phenological changes observed over time are likely due to a combination of climate variables operating collectively and are therefore all partly responsible for the observed changes in flowering timing (Richardson *et al.,* 2013; Fitchett *et al.,* 2015, 2016a). Multiple regression analysis should be conducted if there are more than one independent climate variable with a statistically significant relationship with flowering timing. Multiple regression analysis allows for the assessment of the relationships between different combinations of climate variables and flowering timing (Studer *et al.,* 2005; Davis *et al.,* 2017).

To increase the explanatory potential of statistical analysis of climate variables and their influence on flowering phenology, multiple regression analyses were completed to assess multiple climate variables at the same time to create a holistic model of phenological responses to changing climatic conditions (Leech *et al.,* 2005; Studer *et al.,* 2005; Gordo & Sanz, 2010; Fitchett *et al.,* 2016a). Multiple regression analysis was therefore used to assess the influence of different temperature variables and precipitation on phenological flowering timing of the Namaqualand daisies (Fitchett *et al.,* 2019). Multiple regression models are expressed in the following format:

$$y = \beta_0 + \beta_1 x_1 + \beta_2 x_2 + \beta_3 x_3 + \cdots \beta_n x_n + \in \qquad \text{(Manly, 2008; Fitchett } et\ al., \text{ 2019)}$$

The coefficient of variation (R^2) is used to define the strength of the multiple regression models and the percentage of predicted variability that the model can explain (Črepinšek & Kajfež-Bogataj, 2006; Lomax, 2007).

$$R^2 = \frac{\Sigma(y_{est} - \bar{y})^2}{\Sigma(y - \bar{y})} \qquad \text{(Leech } et\ al., \text{ 2005; Lomax, 2007)}$$

To produce the most accurate multiple regression model, the value of the coefficient of variation must be maximised (Leech *et al.,* 2005). The R^2-value can only be maximized through selecting the optimal combination of climate variables that all have statistically significant relationships with flowering timing. Therefore, creating a model that describes the holistic climate influences on flowering timing. The selection of variables for the multiple regression analysis could only be performed after the linear regression model tests between the respective climate variables and flowering timing were completed (Crepinsek & Kajfez-Bogataj, 2006). The excessive selection of climate variables had to be managed carefully to avoid multicollinearity (Leech *et al.,* 2005; Anderson *et al.,* 2012). Multicollinearity alludes to when the same change is captured in two variables (Leech *et al.,* 2005). To minimize the effect of multicollinearity, the R^2 value for the multiple regression analysis was assessed to determine the impact that different climate variables have on the multiple regression analysis formula (Huang and Hao, 2018). If a new variable is added to the multiple regression and the R^2 value changes slightly, then there is multicollinearity present. The multiple regression analysis was therefore conducted in a stepwise manner (variables were added individually) to be able to detect multicollinearity more accurately.

CHAPTER 5: RESULTS

[5]

5.1 Introduction

The structure of this results chapter follows that of published phenological studies, first exploring the climate and phenological trends independently, and thereafter the impact of climate on phenology. The climate data analysis involves T_{max}, T_{min}, T_{mean} and precipitation trends. Flowering dates are analysed for first, peak and end of flowering. Thereafter, the relationship between Namaqualand daisy phenology and climate is explored. Finally, a qualitative analysis of the local perceptions documented in newspaper records is presented. Statistically insignificant relationships are not reported in this chapter but are included in the supporting tables.

5.2 Climate Variability and Change in the Namaqualand Region

Clanwilliam has the warmest mean annual T_{max} (28.11°C; σ=1.05) of the seven Namaqualand weather stations (Table 5.1). Vredendal and Nieuwoudtville have similar mean T_{max} of 25.51°C (σ=0.95) and 25.12°C (σ=0.91), respectively. Springbok and Lambertsbaai Nortier also have similar mean T_{max} of 23.90°C (σ=0.96) and 22.06°C (σ=0.89), respectively. Port Nolloth and Cape Columbine have the lowest mean T_{max} in Namaqualand of 19.29°C (σ=0.75) and 19.14°C (σ=0.48), respectively. Nieuwoudtville has the lowest mean T_{min} in Namaqualand (8.65°C; σ=0.76). Vredendal, Port Nolloth and Lambertsbaai Nortier have similar mean T_{min} ranging from 11.01-11.26°C. Springbok is the subregion with the highest mean T_{min} in Namaqualand of 12.53°C (σ=0.78).

Table 5.1: Mean T_{max}, T_{mean} and T_{min} for the seven assessed weather stations in Namaqualand.

Weather Station	Mean Maximum Temperature (°C)	Mean Mean Temperature (°C)	Mean Minimum Temperature (°C)
Cape Columbine	19.14 (σ=0.48)	15.63 (σ=0.44)	12.12 (σ=0.45)
Vredendal	25.51 (σ=0.95)	18.89 (σ=0.64)	11.26 (σ=0.47)
Nieuwoudtville	25.12 (σ=0.91)	16.88 (σ=0.65)	8.65 (σ=0.76)
Springbok	23.90 (σ=0.96)	18.22 (σ=0.83)	12.53 (σ=0.78)
Port Nolloth	19.29 (σ=0.75)	15.15 (σ=0.59)	11.01 (σ=0.65)
Lambertsbaai Nortier	22.06 (σ=0.89)	16.64 (σ=0.91)	11.23 (σ=1.00)
Clanwilliam	28.11 (σ=1.05)	20.26 (σ=0.79)	12.41 (σ=0.65)

Although T_{max} increased for six of the seven weather stations, only three were statistically significant (Figure 5.1; Appendix A.1). From 1959-2018, Cape Columbine's annual T_{max} (r=0.54, p<0.0001), T_{min} (r=0.50, p<0.0001) and T_{mean} (r=0.54, p<0.0001) all increased at a statistically significant rate of 0.01°C.yr^{-1} (Figure 5.1; Appendix A.1). Annual Vredendal T_{max}, T_{min}, and T_{mean} increased at a statistically significant rates of 0.05°C.yr^{-1} (r=0.84, p<0.0001), 0.01°C.yr^{-1} (r=0.51, p<0.0001) and 0.03°C.yr^{-1} (r=0.82, p<0.0001) respectively (Figure 5.1; Appendix A.1). From 1960-2018, every assessed annual temperature variable for Port Nolloth increased at statistically significant rates of 0.03°C.yr^{-1} (r=0.64, p<0.0001) for T_{max}, 0.01°C.yr^{-1} (r=0.32, p=0.0147) for T_{min} and 0.02°C.yr^{-1} (r=0.49, p=0.0002) for T_{mean} (Figure 5.1; Appendix A.1).

T_{max} in Cape Columbine increased at statistically significant rates for six months of the year, including April, May and July, while statistically significant increases in T_{min} are calculated for 10 months of the year (Appendix A.1). For Vredendal, from 1959-2018, statistically significant increases in T_{mean} are calculated for 11 months of the year, and statistically significant increases in T_{min} are calculated for five months of the year (Appendix A.1). From 1988-2018, Springbok's annual T_{min} decreased at a statistically significant rate of 0.03°C.yr^{-1} (r=0.36, p=0.0447; Appendix A.1), the only statistically significant annual temperature variable in the subregion. Clanwilliam is the only weather station with a calculated decrease in T_{max}, T_{min} and T_{mean} over time, although none of these changes are statistically significant (Appendix A.1).

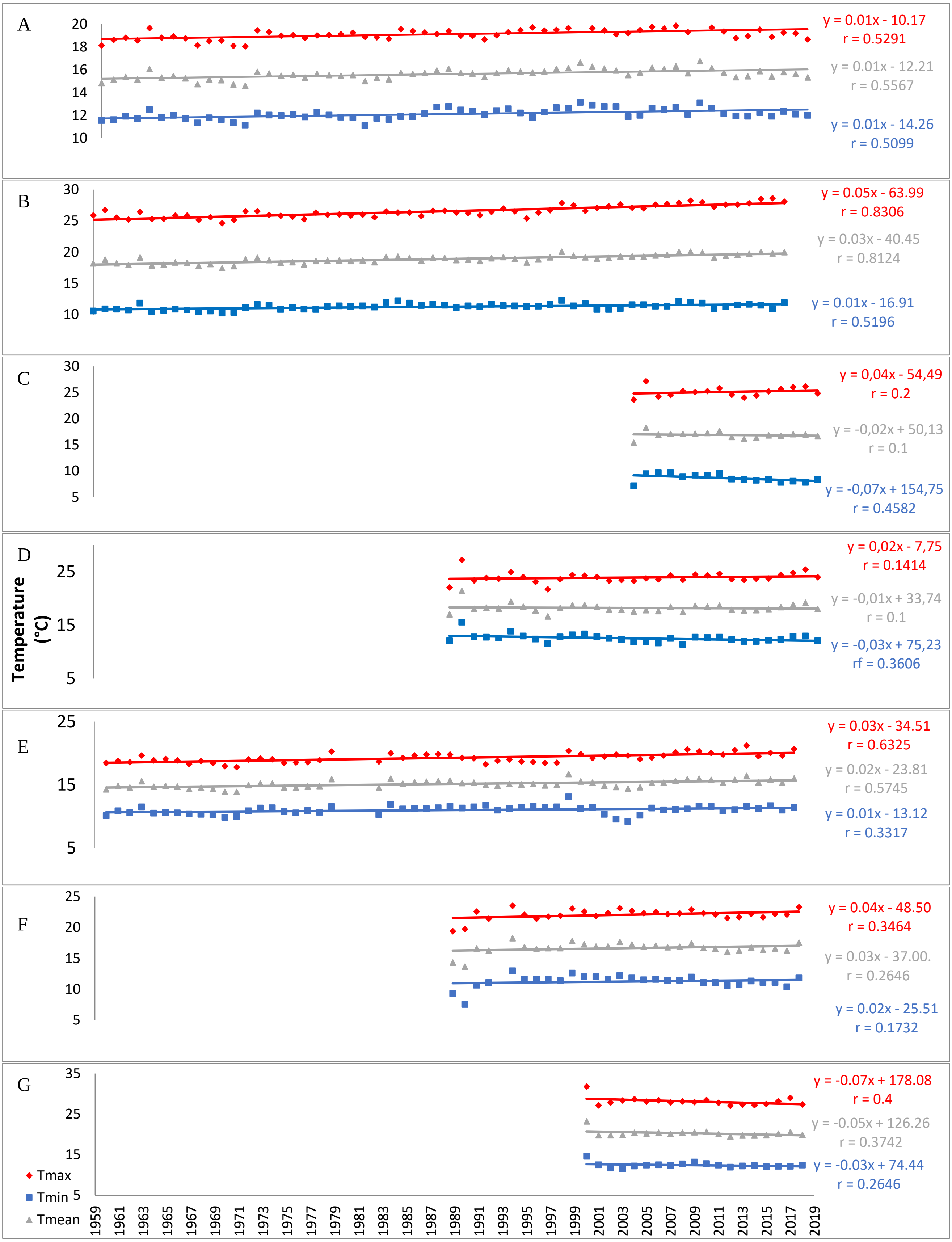

Figure 5.1: Temperature trends for the seven assessed weather stations in Namaqualand (A: Cape Columbine, B: Vredendal, C: Nieuwoudtville, D: Springbok, E: Port Nolloth, F: Lambertsbaai Nortier and G: Clanwilliam).

Nieuwoudtville receives the largest MAP in Namaqualand (379.63mm.yr^{-1}; σ=125.12). This is followed by Cape Columbine and Springbok, with MAP totals of 243.43mm.yr^{-1} (σ=57.54) and 207.01mm.yr^{-1} (σ=107.12), respectively. Clanwilliam, Vredendal and Lambertsbaai Nortier have similar MAP totals of 176.28mm.yr^{-1} (σ=68.72), 151.51mm.yr^{-1} (σ=53.83) and 147.0mm.yr^{-1} (σ=86.04), respectively. Port Nolloth has the lowest MAP in Namaqualand (61.94mm.yr^{-1}; σ=29.88). The large standard deviations indicate extremely variable precipitation in Namaqualand.

For every station except Lambertsbaai Nortier, the month of highest precipitation was June. For Lambertsbaai Nortier, the highest precipitation is recorded for July. All weather stations receive approximately 50% precipitation between May and August, therefore confirming that Namaqualand falls within the South African WRZ. None of the observed changes in precipitation for any of the seven selected weather stations in Namaqualand were changing statistically significantly over time (Figure 5.2; Appendix A.1). Five of the seven weather stations experienced tentative decreases in precipitation (Figure 5.2; Appendix A.1). Port Nolloth and Clanwilliam were the only two weather stations with increases in precipitation (Appendix A.1). The Clanwilliam record commences in 2000 and is therefore not comparable. Port Nolloth had four years of missing data in its record (July 1979-June 1983) which could have led to the calculated increase in its precipitation record.

For Vredendal, January was the only month with a statistically significant change in precipitation over time, at a rate of 0.06mm.yr^{-1} (r=0.27, p=0.0397; Appendix A.1). For Nieuwoudtville, precipitation during August decreased statistically significantly by 5.77mm.yr^{-1} (r=0.54, p=0.0299; Appendix A.1). June precipitation in Clanwilliam increased at a statistically significant rate of 2.67mm.yr^{-1} (r=0.59, p=0.0100; Appendix A.1). Overall, the changes in Namaqualand precipitation is insignificant (Appendix A.1).

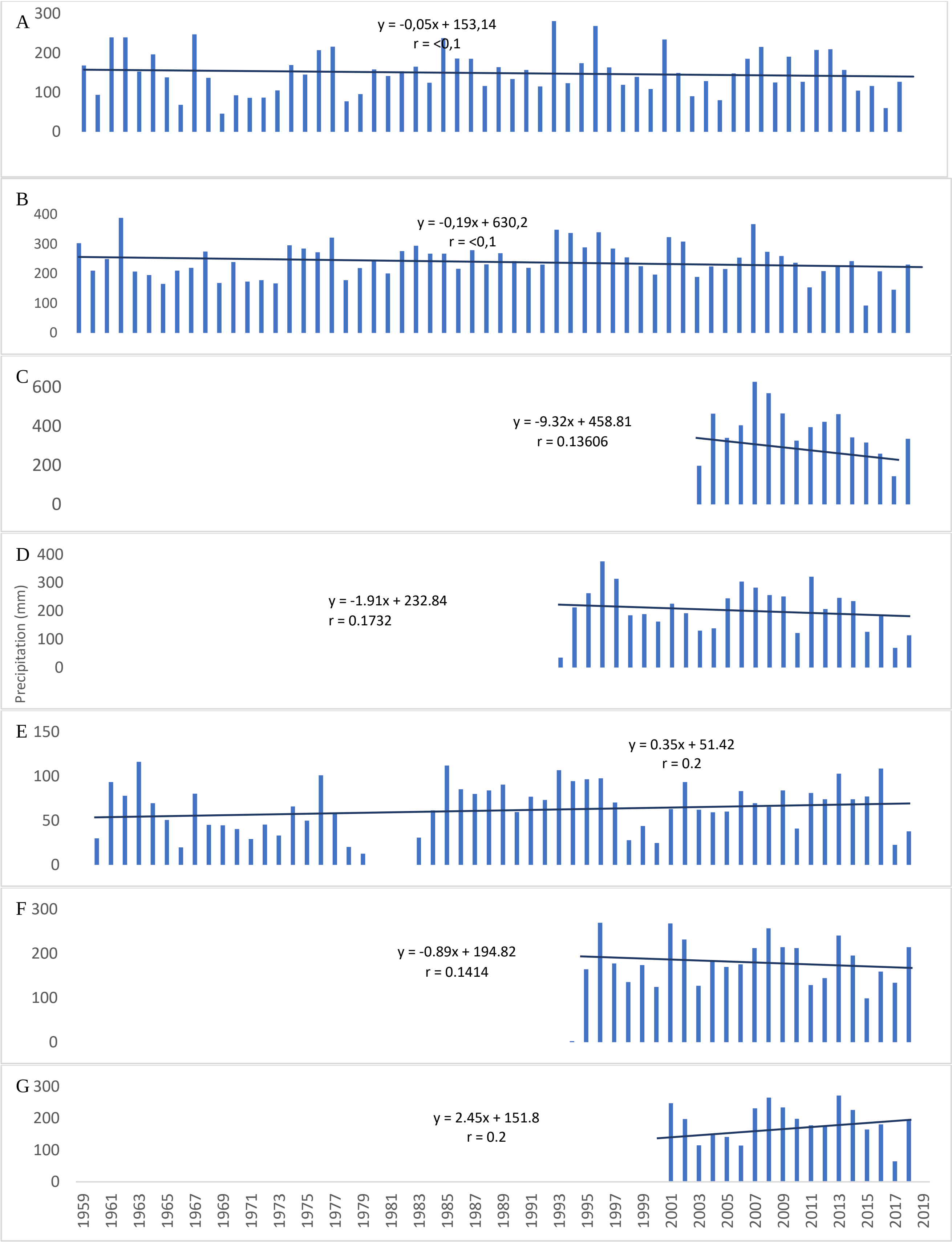

Figure 5.2: Precipitation trends for the seven assessed weather stations in Namaqualand (A: Cape Columbine, B: Vredendal, C: Nieuwoudtville, D: Springbok, E: Port Nolloth, F: Lambertsbaai Nortier and G: Clanwilliam).

5.3 Onset of Rain and the End of the Rainy Season

Nieuwoudtville has the longest rainfall season, with the earliest mean Julian date (127.88; 8 May) for the onset of the rainy season (Table 5.2), and the latest mean Julian date (301.63; 29 October) for the end of the rainy season. Port Nolloth has shortest rainfall season, with the latest mean onset date of the rainy season, 149.65 (30 May), and the earliest mean Julian date for the end of the rainy season, 261.81 (19 September; Table 5.2)

Table 5.2: Annual mean Julian Dates for onset and end of the rainy season.

Weather Station	Mean Onset of Rain Julian Date	Mean End of Rain Julian Date
Cape Columbine	131.58 (σ=30.40)	280.98 (σ=41.48)
Vredendal	144.64 (σ=39.18)	265.93 (σ=56.65)
Nieuwoudtville	127.88 (σ=39.07)	301.63 (σ=51.72)
Springbok	145.4 (σ=36.65)	291. 59 (σ=36.50)
Port Nolloth	149.65 (σ=43.93)	261.81 (σ=52.24)
Lambertsbaai Nortier	136.33 (σ=30.41)	273. 75 (σ=49.55)
Clanwilliam	137.61 (σ=31.15)	272.18 (σ=51.65)

None of the changes in the timing of onset or end of the rainy season were statistically significant (Table 5.3). However, considerable annual variability in the timing of the beginning and end of the rainy season Julian dates was evident for all the stations as reflected by the large standard deviations (Table 5.2). During some years, the onset of the rainy season took place in April and in other years the first significant rains only fell during mid-October. The rainy season can also continue until the next season, therefore having a late end of the rainy season, or no end at all in the case of a drought.

Table 5.3: Precipitation timing changes over time (rate of change, correlation and significance).

Weather Stations	**Onset of rain**	**End of rainy season**
Cape Columbine	m= -0.06 r= 0.05 p= 0.7837	m= 0.01 r= <0.01 p= 0.9799
Vredendal	m= -0.27 r= 0.12 p= 0.3660	m= 0.05 r= 0.02 p= 0.9004
Nieuwoudtville	m= 0.22 r= 0.03 p= 0.9223	m= 0.35 r= 0.03 p= 0.9065
Springbok	m= 0.19 r= 0.04 p= 0.8586	m= -1.46 r=0.30 p= 0.1756
Port Nolloth	m= -0.49 r= 0.20 p= 0.2104	m= 0.64 r= 0.24 p= 0.2289
Lambertsbaai Nortier	m= -0.01 r= <0.01 p= 0.9940	m= -2.03 r= 0.29 p= 0.1690
Clanwilliam	m= -0.20 r= 0.03 p= 0.8930	m= -0.88 r= 0.09 p= 0.7388

5.4 Standardized Precipitation Index

The SPI was calculated for five of the seven Namaqualand weather stations for 3-, 6-, 12- and 24-month periods. SPI could not be calculated for Nieuwoudtville and Port Nolloth. Time trend analysis was conducted with 3-, 6-, 12- and 24-month SPI records for the five weather stations. The average SPI values for the five assessed weather stations were small and tended towards zero (Table 5.4). The mean SPI values therefore indicate that the regions were more neutral precipitation zones instead of drought or wet regions. Clanwilliam has the largest mean SPI score of 0.01 and Lambertsbaai Nortier has the lowest mean SPI score of -0.001 (Table 5.4).

The SPI calculations for Springbok display the greatest change over time (Table 5.4). The 24- month SPI calculated for Springbok displays a negative change over time with a rate of change of 0.06 (r=0.43, p=0.0425) and is the only SPI analysis that is statistically significant (Table 5.4). The other Springbok monthly SPI calculations indicate tentative decreases over time, i.e. the subregion is becoming dry (Table 5.4). Cape Columbine and Lambertsbaai Nortier SPI calculations for all four of the selected monthly variables are decreasing (becoming dryer) over time at tentative negative rates ranging from <0.01-0.04 (Table 5.4). All the SPI calculations for Vredendal display increases over time (becoming wetter) at an insignificant rate of <0.01 per year (Table 5.4).

Table 5.4: First column: Mean SPI values for assessed weather stations. The rest of the columns: SPI of five out of the seven Namaqualand weather stations. Highlighted blocks indicate calculated statistically significant changes.

Weather Stations	**Mean SPI Value**	**3-month SPI**	**6-month SPI**	**12-month SPI**	**24-month SPI**
Cape Columbine	-0.002	m<-0.01 r= 0.06 p= 0.6484	m<-0.01 r= 0.05 p= 0.7225	m<-0.01 r= 0.05 p= 0.7117	m<-0.01 r= 0.05 p= 0.6935
Vredendal	0.002	m<0.01 r= 0.03 p= 0.8398	m<0.01 r= 0.01 p= 0.9220	m<0.01 r= 0.04 p= 0.7401	m<0.01 r= 0.04 p= 0.7533
Springbok	-0.01	m= -0.03 r= 0.35 p= 0.0852	m= -0.03 r= 0.34 p= 0.0932	m= -0.05 r= 0.40 p= 0.0531	m= -0.06 r= 0.43 p= 0.0425
Lambertsbaai Nortier	-0.001	m= -0.01 r= 0.17 p= 0.4310	m= -0.02 r= 0.16 p= 0.4479	m= -0.03 r= 0.24 p= 0.2717	m= -0.04 r= 0.28 p= 0.2110
Clanwilliam	0.01	m<0.01 r= 0.01 p= 0.9754	m<0.01 r= 0.07 p= 0.7819	m= -0.01 r= 0.04 p= 0.8673	m= 0.02 r= 0.08 p= 0.7551

Intra-annual variation in wet and dry periods is evident from the 3-month SPI scores across Namaqualand (Figure 5.3A, B). The drought and wet periods in Cape Columbine, generally lasted longer and were more severe compared to Vredendal, which had a dataset of the same length. The 6-month SPI analysis for Vredendal revealed a severe and long-lasting drought period persisting from October 1968 to October 1973 (Figure 5.3C). Over 20 drought periods are calculated for Vredendal (Figure 5.3C). The 6-month SPI analysis reveals seasonal drought conditions which demonstrates that the Namaqualand region is exposed to frequent drought periods. For every drought period in the 6-month SPI for Vredendal, the same number of wet periods are visible, but these wet periods are not strong or lengthy. The 24-month SPI displays reliable and long-lasting drought periods. The Namaqualand region has experienced seven severe and long-lasting drought periods from 1959-2018 and has not had a wet period since June 2011 (Figure 5.3D).

Figure 5.3: SPI analysis of two of the stations in Namaqualand (A: Cape Columbine 3-month SPI; B: Vredendal 3-month SPI; C: Vredendal 6-month SPI; D: Cape Columbine 24-month SPI)

5.5 Winter and Spring Climate Changes Over Time

The greatest mean winter T_{max} of 21.61°C, is calculated for Vredendal (Table 5.5). The lowest mean winter T_{max} of 16.61°C is calculated for Cape Columbine (Table 5.5). The subregion with the warmest mean T_{min} during winter is Cape Columbine (10.37°C; Table 5.5). Nieuwoudtville is the coldest subregion during the winter in Namaqualand with a mean T_{min} of 4.35°C (Table 5.5). The subregion that receives the most precipitation during winter in Namaqualand is Nieuwoudtville with mean precipitation of 205.79mm.yr^{-1} (Table 5.5). The driest winter subregion in Namaqualand is Port Nolloth with a mean winter precipitation of 27.56mm.yr^{-1} (Table 5.5).

Table 5.5: Winter and spring mean seasonal climate variables.

Weather Station	Season	T_{max} (°C)	T_{min} (°C)	T_{mean} (°C)	Precipitation (mm)
Cape Columbine	Winter	16.61 (σ= 0.93)	10.37 (σ= 0.82)	13.51 (σ= 0.84)	122.74 (σ= 42.12)
	Spring	18.82 (σ= 1.32)	11.65 (σ= 0.82)	15.22 (σ= 1.14)	41.76 (σ= 19.81)
Vredendal	Winter	21.61 (σ= 1.55)	7.22 (σ= 1.06)	14.42 (σ=1.02)	73.03 (σ= 34.73)
	Spring	26.21 (σ= 2.40)	10.92 (σ= 1.89)	18.56 (σ= 2.03)	26.49 (σ= 18.92)
Nieuwoudtville	Winter	18.41 (σ= 1.77)	4.35 (σ= 1.37)	11.38 (σ= 1.31)	205.79 (σ= 87.13)
	Spring	24.99 (σ= 3.13)	7.53 (σ= 2.27)	16.26 (σ= 2.59)	53.48 (σ= 19.10)
Springbok	Winter	17.40 (σ= 1.98)	8.24 (σ= 1.47)	12.91 (σ= 1.95)	94.70 (σ= 45.33)
	Spring	23.86 (σ= 2.74)	11.34 (σ= 2.03)	17.60 (σ= 2.34)	38.63 (σ= 29.35)
Port Nolloth	Winter	18.39 (σ= 1.68)	8.83 (σ= 1.17)	13.65 (σ= 1.44)	27.56 (σ= 17.88)
	Spring	18.60 (σ= 1.30)	10.61 (σ= 1.32)	14.62 (σ= 1.26)	11.20 (σ= 8.98
Lambertsbaai Nortier	Winter	18.98 (σ= 1.80)	8.70 (σ= 1.41)	13.84 (σ=1.52)	93.90 (σ= 30.66)
	Spring	21.71 (σ=1.95)	10.44 (σ= 1.61)	16.08 (σ= 1.66)	34.53 (σ= 15.51)
Clanwilliam	Winter	20.85 (σ= 1.67)	7.09 (σ= 1.16)	13.97 (σ= 0.92)	109.10 (σ= 44.21)
	Spring	27.67 (σ= 3.05)	11.56 (σ= 2.29)	19.61 (σ= 2.61)	23.82 (σ= 12.44)

Clanwilliam has a mean spring T_{max} of 27.67°C and is therefore the warmest Namaqualand spring subregion (Table 5.5). Port Nolloth has the coolest mean spring T_{max} of 18.60°C (Table 5.5). The subregion with the warmest spring T_{min} is Cape Columbine (11.65°C; Table 5.5). The coldest Namaqualand subregion during spring is Nieuwoudtville with a mean spring T_{min} of 7.53°C. (Table

5.5). The wettest subregion during spring is Nieuwoudtville with mean spring precipitation of 53.48mm.yr^{-1} (Table 5.5). Port Nolloth is the driest spring subregion, with mean spring precipitation of 11.20mm.yr^{-1}. During winter and spring Nieuwoudtville and Port Nolloth are the wettest and driest subregions in Namaqualand, respectively.

A statistically significant increase is calculated for Cape Columbine's temperature variables during winter and spring (Table 5.6). T_{max} and T_{mean} during winter and spring have both increased significantly at a rate of 0.01°C.yr^{-1} (winter T_{max}: r=0.33, p=0.0110; spring T_{max}: r=0.39, p=0.0021; winter T_{mean}: r=0.29, p=0.0267; spring T_{mean}: r=0.42, p=0.0008; Table 5.6). Spring T_{min} increased significantly at a rate of 0.02°C.yr^{-1} (r=0.44, p=0.0005), while winter T_{min} increased at a smaller rate of 0.01°C.yr^{-1} (r=0.32, p=0.0123; Table 5.6).

Table 5.6: Seasonal analysis of climate variable change over time (Winter: June July and August; Spring: September, October and November). Highlighted blocks indicate the statistically significant changes over time.

Weather Stations	**Winter Ave T_{max} (June, July, Aug)**	**Winter Ave T_{min} (June, July, Aug)**	**Winter Ave T_{mean} (June, July, Aug)**	**Winter Total Precip (June, July, Aug)**	**Spring Ave T_{max} (Sept, Oct, Nov)**	**Spring Ave T_{min} (Sept, Oct, Nov)**	**Spring Ave T_{mean} (Sept, Oct, Nov)**	**Spring Total Precip (Sept, Oct, Nov)**
Cape Columbine	m= 0.01 r= 0.33 p= 0.0110	m= 0.01 r= 0.32 p= 0.0123	m= 0.01 r= 0.29 p= 0.0267	m= 0.09 r= 0.04 p= 0.7873	m= 0.01 r= 0.39 p= 0.0021	m= 0.02 r= 0.44 p= 0.0005	m= 0.01 r= 0.42 p= 0.0008	m<-0.01 r= <0.01 p= 0.9743
Vredendal	m= 0.03 r= 0.50 p<0.0001	m<0.01 r= 0.04 p= 0.7352	m= 0.02 r= 0.40 p= 0.0016	m= 0.10 r= 0.05 p= 0.6990	m= 0.04 r= 0.58 p<0.0001	m= 0.01 r= 0.29 p= 0.0246	m= 0.03 r= 0.54 p<0.0001	m= -0.07 r= 0.07 p= 0.6124
Nieuwoudtville	m= 0.01 r= 0.03 p= 0.9136	m= -0.13 r= 0.59 p= 0.0165	m= -0.06 r= 0.33 p= 0.2080	m= -4.93 r= 0.27 p= 0.3131	m= 0.01 r= 0.06 p= 0.8255	m= -0.13 r= 0.70 p= 0.0024	m= -0.06 r= 0.34 p= 0.1967	m= -0.27 r= 0.07 p= 0.8010
Springbok	m= 0.01 r= 0.10 p= 0.6083	m= -0.03 r= 0.22 p= 0.2477	m= -0.02 r= 0.11 p= 0.5677	m= -0.54 r= 0.09 p= 0.6613	m= 0.02 r= 0.13 p= 0.4951	m= -0.04 r= 0.34 p= 0.0662	m= -0.01 r= 0.08 p= 0.6659	m= -1.44 r= 0.36 p= 0.0790
Port Nolloth	m= 0.02 r= 0.34 p= 0.0108	m<0.01 r= 0.02 p= 0.8901	m= 0.01 r= 0.19 p= 0.1659	m= 0.13 r= 0.12 p= 0.3621	m= 0.03 r= 0.60 p<0.0001	m= 0.01 r= 0.29 p= 0.0307	m= 0.02 r= 0.49 p= 0.0001	m= 0.06 r= 0.12 p= 0.3546
Lambertsbaai Nortier	m= 0.01 r= 0.04 p= 0.8622	m= -0.01 r= 0.11 p= 0.5711	m<-0.01 r= 0.04 p= 0.8559	m= 0.20 r= 0.05 p= 0.8339	m= 0.03 r= 0.25 p= 0.1838	m<0.01 r= 0.01 p= 0.9453	m= 0.02 r= 0.15 p= 0.4243	m= -0.25 r= 0.11 p= 0.5933
Clanwilliam	m= -0.03 r= 0.15 p= 0.5433	m= 0.02 r= 0.15 p= 0.5655	m<-0.01 r= 0.04 p= 0.8666	m= -0.12 r= 0.04 p= 0.9558	m= -0.02 r= 0.15 p= 0.5409	m= -0.02 r= 0.23 p= 0.3480	m= -0.02 r= 0.23 p= 0.3625	m= -0.45 r= 0.19 p= 0.4425

Vredendal winter T_{max} and T_{mean} both increased at statistically significant rates of 0.03°C.yr^{-1} (r=0.50, p<0.0001) and 0.02°C.yr^{-1} (r=0.40, p=0.0016) respectively (Table 5.6). Vredendal spring T_{max}, T_{min} and T_{mean} all increased significantly at rates of 0.04°C.yr^{-1} (r=0.58, p<0.0001), 0.01°C.yr^{-1} (r=0.29, p=0.0246) and 0.03°C.yr^{-1} (r=0.54, p<0.0001) respectively (Table 5.6).

Nieuwoudtville winter and spring T_{min} both decreased at a statistically significant rate of 0.13°C.yr^{-1} (winter: r=0.59, p=0.0165; spring: r=0.70, p=0.0024; Table 5.6). T_{max} during winter for Port Nolloth increased significantly at a rate of 0.02°C.yr^{-1} (r=0.34, p=0.0108; Table 5.6). Statistically significant increases in T_{max} and T_{min} during spring in Port Nolloth are calculated at rates of 0.03°C.yr^{-1} (r=0.60, p<0.0001) and 0.01°C.yr^{-1} (r=0.29, p=0.0307) respectively (Table 5.6).

All the statistically significant changes calculated during the winter and spring climate analysis reveal increasing T_{max}, T_{min} and T_{mean} values (for three weather stations) except for the calculated decrease in T_{min} in Nieuwoudtville (Table 5.6). It is possible that the locations that have not demonstrated statistically significant changes in their winter and spring temperature variables could be related to the lengths of their climate records. None of the calculated changes for total precipitation during winter or spring were statistically significant for any of the Namaqualand weather stations (Table 5.6).

5.6 Frost Events

Nieuwoudtville has the largest mean number of frost days for T_{min} ≤0°C of 11fd.yr^{-1} (Table 5.7). Nieuwoudtville is also the subregion that is exposed to frost events of T_{min} ≤0°C for the longest time every year because the subregion's mean last frost Julian day is 252.88 (10 September). Nieuwoudtville has the largest mean number of frost days per year for the threshold of T_{min} ≤4°C, which is 68.31fd.yr^{-1}, together with the latest mean last frost day of 306.25 or alternatively 2 November (Table 5.7).

Table 5.7: Mean values and standard deviation for frost variables.

Weather Station	Mean # of days with $T_{min} \leq 0°C$	Mean last JD with $T_{min} \leq 0°C$	Mean # of days with $T_{min} \leq 4°C$	Mean last JD with $T_{min} \leq 4°C$
Cape Columbine	Insufficient data	Insufficient data	Insufficient data	Insufficient data
Vredendal	1.22 (σ= 0.44)	197.44 (σ= 21.66)	19.67 (σ= 8.44)	246.27 (σ= 18.48)
Nieuwoudtville	11 (σ=7.79)	252.88 (σ=36.34)	68.31 (σ= 19.77)	306.25 (σ=24.10)
Springbok	1.33 (σ= 0.82)	234.83 (σ= 36.27)	17.72 (σ= 6.85)	268.28 (σ= 27.48)
Port Nolloth	Insufficient data	Insufficient data	3.91 (σ= 3.68)	207.47 (σ= 34.88)
Lambertsbaai Nortier	Insufficient data	Insufficient data	4.5 (σ= 4.52)	234.81 (σ= 37.15)
Clanwilliam	Insufficient data	Insufficient data	17.39 (σ= 7.01)	241.61 (σ= 18.20)

5.6.1 Change in Last Frost Dates

Only three weather stations are assessed for a change in last frost dates for the threshold of $T_{min} \leq 0°C$ (Table 5.8). None of the calculated changes over time in last frost dates ($T_{min} \leq 0°C$) were statistically significant. For the frost threshold of $T_{min} \leq 4°C$, three weather stations calculated advances in last frost Julian dates (earlier last frost dates) and three weather stations calculated delays in last frost Julian dates (Table 5.9). The only weather station with calculated statistically significant changes for last frost dates was Nieuwoudtville (Table 5.8, 5.9).

Table 5.8: Changes in number of frost days and last frost dates for the frost variable Tmin ≤0°Cover time. Highlighted blocks indicate statistically significant changes over time.

	$T_{min} \leq 0°C$	
Weather Stations	**Last Frost Date**	**Number of Frost days**
Cape Columbine	Insufficient data	Insufficient data
Vredendal	m= 0.18 r= 0.15 p= 0.6967	m<0.01 r= 0.14 p= 0.7291
Nieuwoudtville	m= 3.62 r= 0.48 p= 0.0630	m= 1.17 r= 0.72 p= 0.0018
Springbok	m= 1.58 r= 0.30 p= 0.5598	m= 0.04 r= 0.32 p= 0.5401
Port Nolloth	Insufficient data	Insufficient data
Lambertsbaai Nortier	Insufficient data	Insufficient data
Clanwilliam	Insufficient data	Insufficient data

Only four frost events, for T_{min} ≤4°C, were recorded in Cape Columbine from 1959-2018: occurring on 12 July 1977, 14 September 1981, 14 June 1991, and 6 July 2001. For Vredendal, nine years had frost temperatures of T_{min} ≤0°C (1965, 1967, 1969, 1971, 1972, 1975, 1995, 2003 and 2017). Frost analysis for T_{min} ≤0°C in Vredendal can therefore not be calculated due to insufficient frost dates (Table 5.8).

Table 5.9: Changes in number of frost days and last frost dates for the frost variable Tmin ≤4°C over time. Highlighted blocks indicate statistically significant changes over time.

	T_{min} ≤ 4°C	
Weather Stations	**Last frost Date**	**Number of Frost Days**
Cape Columbine	Insufficient data	Insufficient data
Vredendal	m= -0.11 r= 0.11 p= 0.4086	m= -0.11 r= 0.23 p= 0.0727
Nieuwoudtville	m= 2.82 r= 0.57 p= 0.0253	m= 2.35 r= 0.57 p= 0.0222
Springbok	m= -0.19 r= 0.06 p= 0.7657	m= 0.01 r= 0.01 p= 0.9472
Port Nolloth	m= -0.54 r= 0.26 p= 0.0939	m= -0.03 r= 0.13 p= 0.3971
Lambertsbaai Nortier	m= 0.22 r= 0.05 p= 0.8061	m= -0.08 r= 0.14 p= 0.4809
Clanwilliam	m= 0.17 r= 0.05 p= 0.8421	m= 0.04 r= 0.03 p= 0.8989

For Nieuwoudtville, frost events of T_{min} ≤0°C occurred earlier throughout the record when compared to frost events of Tmin ≤4°C. Calculated last frost events for T_{min} ≤4°C in Nieuwoudtville are delayed at a statistically significant rate of 2.82d.yr^{-1} (r=0.56, p=0.0253; Table 5.9). Last frost events in Nieuwoudtville, for T_{min} ≤0°C, were also delayed over time although this change was not statistically significant (Table 5.8).

For Springbok T_{min} ≤0°C has not been recorded once since 2007. The Port Nolloth climate record, from 1960-2018, has no years where T_{min} ≤0°C (Table 5.8). During 1990 there were two days where T_{min} ≤0°C in Lambertsbaai Nortier, with the last frost date occurring on 31 September. Since then, T_{min} ≤0°C has not occurred in Lambertsbaai Nortier again. For Clanwilliam, from 2001-2018, there were no days where T_{min} ≤0°C (Table 5.8).

5.6.2 Change in Number of Frost Days

An increase in the total number of frost days are calculated for the three weather stations that had sufficient frost days for T_{min} ≤0°C (Table 5.8). For Nieuwoudtville, the change in the number of frost days (T_{min} ≤0°C) was statistically significant (Table 5.8). Nieuwoudtville was the only subregion that had statistically significant changes is the number of frost days (T_{min} ≤4°C) per year (Table 5.9).

For Nieuwoudtville, the calculated total number of frost days for T_{min} ≤0°C are increasing at a statistically significant rate of 1.17fd.yr^{-1} (r=0.72, p=0.0018; Table 5.8). The calculated total number of frost days for T_{min} ≤4°C in Nieuwoudtville is also increasing at a statistically significant rate of 2.35fd.yr^{-1} (r=0.57, p=0.0222; Table 5.9). The significant increase in the number of frost events occurs concurrent to the observed decrease in Nieuwoudtville annual T_{min} over time (Figure 5.1C). Other than the statistically significant changes in frost variables calculated for Nieuwoudtville, none of the other stations had any significant changes in frost variables over time (Table 5.8, 5.9).

5.7 Phenological Shifts in Flowering Dates

A total of 663 records relating to flowering dates, flowering conditions and comments on climatic conditions were collected. These comprise 74 digitised records from the Rand Daily Mail newspaper, 456 records from the digital newspaper archives of Die Burger and Volksblad from Media 24, 103 records from Flickr and 30 records from iNaturalist. These combined records form the phenological flowering record for the Namaqualand daisies. The oldest record of timing for the Namaqualand daisies flowering dates to 1935, obtained from The Rand Daily Mail. Due to the nature of the sources used the flowering record is not continuous. Due to years with overlapping flowering dates a total of 600 flowering dates were averaged across the three different flowering datasets.

5.7.1 Flowering Records and Dates

5.7.1.1 First flowering (BBCH 60-61)

FFDs (BBCH 60-61) are found in 97 records, commencing from 1935. The earliest documented FFD per year was documented on 20 June 1987. The latest recorded FFD was documented on 29 September 1962. From 1935-2018, the discontinuous first flowering dataset reveals that the mean FFD is on the Julian date 211 (30th of July; σ=17.15). A statistically significant advance in the timing of first flowering is calculated at a rate of $0.26 d.yr^{-1}$ or $2.6 d.decade^{-1}$ (r=0.33, p=0.0326; Figure 5.4).

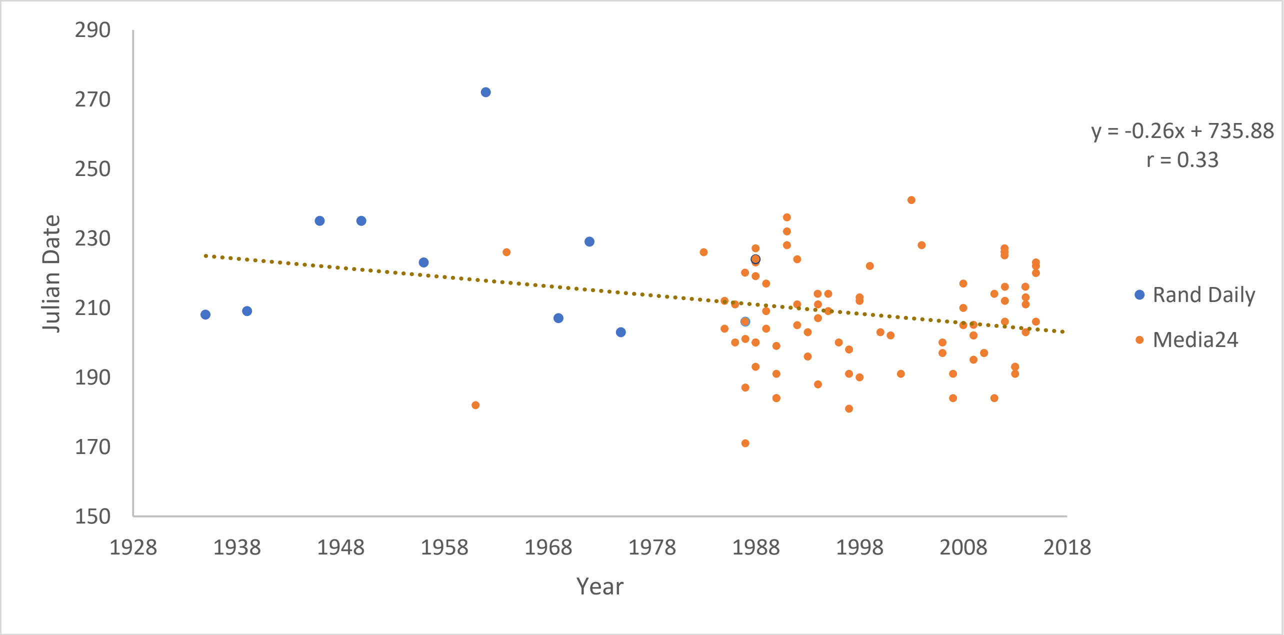

Figure 5.4: Time trends for the first flowering timing of the Namaqualand daisies, 1935-2018.

5.7.1.2 Full Bloom (BBCH 63-65)

The full bloom flowering dataset of the Namaqualand daisies has the most captured Julian flowering dates (Figure 5.5). From 1940, 469 full bloom flowering dates were documented. The earliest recorded date for full bloom flowering is 1 July 2012. The latest recorded full bloom date is 30 November 2010. The average full bloom flowering date between 1935-2018 is on the Julian date 243 (σ=14.82), therefore 31 August. A statistically significant advance is calculated for full bloom timing at a rate of 0.21d.yr^{-1} or 2.1d.decade^{-1} (r=0.32, p=0.0157; Figure 5.5).

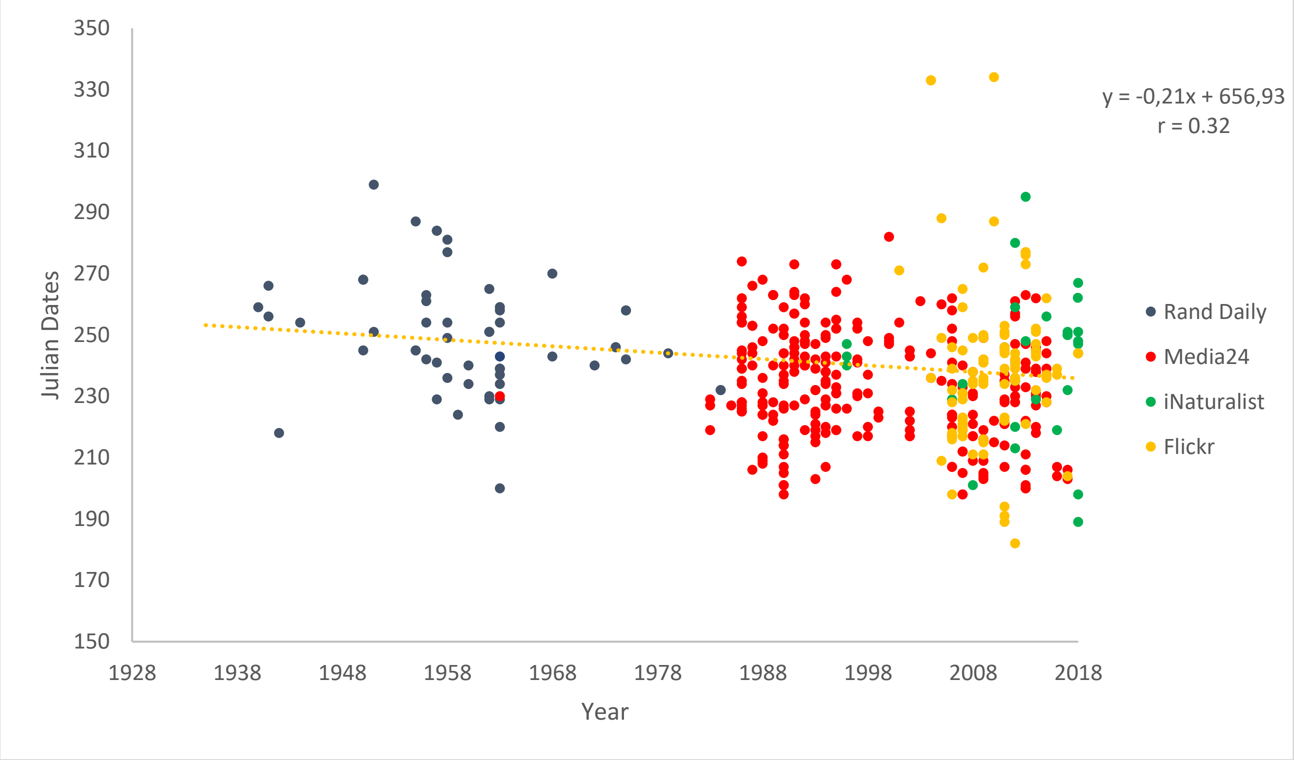

Figure 5.5: Time trend for full bloom timing of the Namaqualand daisies, 1940-2018.

5.7.1.3 End of Bloom (BBCH 67-69)

The end of bloom timing dataset is the smallest record of Namaqualand daisy flowering phenology (Figure 5.6). The end of bloom dataset consists of 35 flowering dates from 1938. The earliest recorded end of bloom date is 7 August 2007. The latest recorded end of bloom date is 20 October 1991. The average collected end of bloom flowering date is the Julian date 261 (18 September; σ=17.18). The rate of change in end of bloom timing is the greatest change out of all three created phenological flowering groups for the Namaqualand daisies (Figure 5.6). End of bloom flowering timing is, however, not changing at a statistically significant rate. A tentative advance is calculated for end of bloom at a rate of 0.28d.yr^{-1} or 2.8d.decade^{-1} (r=0.29, p=0.1875; Figure 5.6).

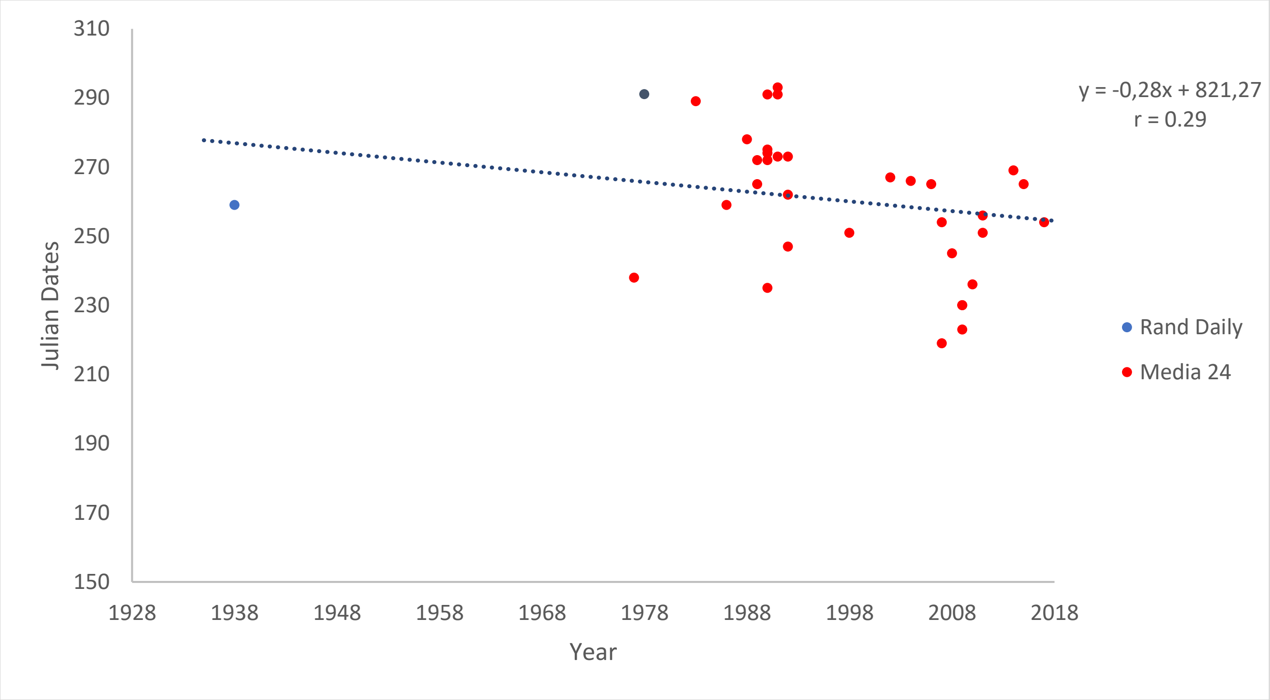

Figure 5.6: Time trend for end of bloom timing of the Namaqualand daisies, 1938-2018.

5.8 Flowering and Climate Change

5.8.1 Influence of Climate Variables on First Flowering (BBCH 60-61)

Statistically significant negative relationships are calculated between each annual T_{min} and T_{mean} and FFD for Cape Columbine, at rates of 0.01d.°C^{-1} each (T_{min}: r=0.43, p=0.0084; $T_{mean:}$ r=0.40, p=0.0133; Table 5.10). For Cape Columbine, temperatures during July, August and September have a statistically significantly relationship with first flowering timing (Table 5.10). All the significant relationships between temperatures from June to September in Cape Columbine were inverse relationships (Table 5.10). Cape Columbine annual T_{max}, T_{min} and T_{mean} were all increasing at significant rates over time (Appendix A.1). The overall increase in temperature in Cape Columbine has therefore contributed to first flowering timing advances over time.

For Vredendal, a significant negative relationship is calculated between first flowering timing and September T_{max} (0.02d.°C^{-1}; r=0.36, p=0.0290) and T_{mean} (0.03d.°C^{-1}; r=0.33, p=0.0447; Table 5.10). Annual T_{max} and T_{mean} in Vredendal have been increasing significantly over time (Appendix A.1).

September T_{max} and T_{mean} in Vredendal has also increased significantly (Appendix A.1). The increase in T_{max} and T_{mean} over time has therefore contributed to advances in first flowering timing in Namaqualand.

For Nieuwoudtville, a statistically significant positive relationship is calculated between first flowering and T_{max} during June (r=0.65, p=0.0216) and November (r=0.70, p=0.0110) with rates of change of 0.05d.°C^{-1} and 0.06d.°C^{-1}, respectively (Table 5.10). The only statistically significant relationship calculated between temperature for Springbok and the timing of first flowering is November T_{max} with a positive rate of change of 0.05d.°C^{-1} (r=0.40, p=0.0442; Table 5.10). No statistically significant relationship between temperature and first flowering timing could be established for Port Nolloth (Table 5.10).

Statistically significant positive relationships are calculated between first flowering timing and June T_{max} (r=0.62, p=0.0021), T_{min} (r=0.54, p=0.0089) and T_{mean} (r=0.61, p=0.0028) for Lambertsbaai Nortier, at rates of changes of 0.11d.°C^{-1}, 0.06d.°C^{-1} and 0.08d.°C^{-1}, respectively (Table 5.10). A significant positive relationship is also calculated between April T_{mean} and first flowering timing in Lambertsbaai Nortier at a rate of change of 0.03d.°C^{-1} (r=0.44, p=0.0482; Table 5.10).

Table 5.10: First Flowering (BBCH 60-61) linear regression analysis with climate data for all seven weather stations in Namaqualand. Coloured blocks indicate statistically significant correlations.

Weather Stations	**Climate Variable**	**Jan**	**Feb**	**Mar**	**Apr**	**May**	**Jun**	**Jul**	**Aug**	**Sept**	**Oct**	**Nov**	**Dec**	**Annual**
Cape Columbine	T_{max}	m= -0.01 r= 0.30 p= 0.0741	m= -0.01 r= 0.23 p= 0.7847	m= -0.01 r= 0.19 p= 0.2565	m= 0.01 r= 0.15 p= 0.3782	m= 0.01 r= 0.24 p= 0.1502	m= -0.01 r= 0.18 p= 0.2734	m= -0.02 r= 0.27 p= 0.1031	m= -0.02 r= 0.36 p= 0.0291	m= -0.01 r= 0.29 p= 0.0843	m<-0.01 r= 0.05 p= 0.7645	m<-0.01 r= 0.08 p= 0.6427	m= -0.01 r= 0.15 p= 0.3647	m= -0.01 r= 0.29 p= 0.0811
	T_{min}	m= -0.01 r= 0.35 p= 0.0326	m= -0.01 r= 0.21 p= 0.2095	m= -0.01 r= 0.15 p= 0.3787	m<0.01 r= 0.01 p= 0.9393	m<-0.01 r= 0.05 p= 0.7814	m= -0.01 r= 0.20 p= 0.2497	m= -0.01 r= 0.38 p= 0.0198	m= -0.02 r= 0.43 p= 0.0089	m= -0.02 r= 0.41 p= 0.0129	m= -0.01 r= 0.17 p= 0.3235	m= -0.01 r= 0.27 p= 0.1121	m= -0.01 r= 0.25 p= 0.1298	m= -0.01 r= 0.43 p= 0.0084
	T_{mean}	m= -0.01 r= 0.36 p= 0.0282	m= -0.01 r= 0.24 p= 0.1540	m= -0.01 r= 0.20 p= 0.2543	m<0.01 r= 0.11 p= 0.5096	m= 0.01 r= 0.12 p= 0.4655	m= -0.02 r= 0.31 p= 0.0599	m= -0.01 r= 0.35 p= 0.0322	m= -0.02 r= 0.43 p= 0.0089	m= -0.01 r= 0.26 p= 0.1176	m<-0.01 r= 0.11 p= 0.5144	m= -0.01 r= 0.18 p= 0.2987	m= -0.01 r= 0.21 p= 0.2088	m= -0.01 r= 0.40 p= 0.0133
	Precipitation	m= -0.05 r= 0.12 p= 0.4892	m= -0.04 r= 0.08 p= 0.6467	m= 0.07 r= 0.14 p= 0.4156	m= -0.27 r= 0.25 p= 0.1358	m= -0.32 r= 0.22 p= 0.1857	m= 0.18 r= 0.09 p= 0.5948	m= -0.04 r= 0.03 p= 0.8402	m= 0.12 r= 0.10 p= 0.5537	m= 0.05 r= 0.05 p= 0.7677	m= 0.16 r= 0.25 p= 0.1366	m= -0.07 r= 0.11 p= 0.5068	m= -0.09 r= 0.22 p= 0.1998	m= -0.32 r= 0.09 p= 0.6015
Vredendal	T_{max}	m= -0.01 r= 0.11 p= 0.5312	m= -0.03 r= 0.35 p= 0.0337	m= -0.02 r= 0.23 p= 0.1671	m<-0.01 r= 0.03 p= 0.8431	m= 0.03 r= 0.31 p= 0.0596	m<0.01 r= 0.04 p= 0.8206	m<-0.01 r= 0.001 p= 0.9926	m= -0.02 r= 0.25 p= 0.1400	m= -0.03 r= 0.33 p= 0.0447	m= -0.01 r= 0.13 p= 0.4367	m<-0.01 r= 0.03 p= 0.8701	m<-0.01 r= 0.02 p= 0.9119	m= -0.01 r= 0.18 p= 0.2951
	T_{min}	m= -0.02 r= 0.28 p= 0.0956	m= -0.01 r= 0.19 p= 0.2727	m= -0.01 r= 0.20 p= 0.2301	m= -0.01 r= 0.17 p= 0.3197	m= -0.01 r= 0.17 p= 0.3183	m<0.01 r= 0.07 p= 0.6880	m<-0.01 r= 0.06 p= 0.7228	m= -0.01 r= 0.23 p= 0.1780	m= -0.01 r= 0.26 p= 0.1186	m= 0.01 r= 0.20 p= 0.2428	m<0.01 r= 0.04 p= 0.8043	m= -0.01 r= 0.11 p= 0.5008	m= -0.01 r= 0.27 p= 0.1113
	T_{mean}	m= -0.01 r= 0.19 p= 0.2503	m= -0.02 r= 0.31 p= 0.0617	m= -0.02 r= 0.25 p= 0.1402	m= -0.01 r= 0.11 p= 0.5164	m= 0.01 r= 0.13 p= 0.4288	m<0.01 r= 0.08 p= 0.6515	m<-0.01 r= 0.03 p= 0.8480	m= -0.02 r= 0.27 p= 0.1021	m= -0.02 r= 0.36 p= 0.0290	m<-0.01 r= 0.004 p= 0.9766	m<-0.01 r= 0.0008 p= 0.9959	m<-0.01 r= 0.07 p= 0.6868	m= -0.01 r= 0.23 p= 0.1690
	Precipitation	m= 0.01 r= 0.06 p= 0.7031	m= -0.01 r= 0.07 p= 0.6787	m<0.01 r= 0.01 p= 0.9669	m= -0.34 r= 0.34 p= 0.0383	m= -0.40 r= 0.33 p= 0.0441	m= 0.28 r= 0.21 p= 0.2106	m= -0.14 r= 0.12 p= 0.4912	m= 0.14 r= 0.17 p= 0.3232	m= -0.02 r= 0.04 p= 0.8272	m= 0.11 r= 0.19 p= 0.2493	m= 0.15 r= 0.19 p= 0.2704	m= -0.14 r= 0.13 p= 0.4556	m= -0.37 r= 0.19 p= 0.4859
Nieuwoudtville	T_{max}	m= 0.05 r= 0.45 p= 0.1603	m= 0.01 r= 0.07 p= 0.8437	m= -0.02 r= 0.18 p= 0.5898	m= 0.02 r= 0.18 p= 0.5715	m= 0.06 r= 0.38 p= 0.2251	m= 0.05 r= 0.65 p= 0.0216	m<0.01 r= 0.01 p= 0.9791	m= -0.03 r= 0.22 p= 0.4994	m<0.01 r= 0.02 p= 0.9456	m= 0.02 r= 0.15 p= 0.6396	m= 0.06 r= 0.70 p= 0.0110	m= 0.05 r= 0.51 p= 0.0909	m<-0.01 r= 0.03 p= 0.9232
	T_{min}	m= 0.01 r= 0.07 p= 0.8353	m= -0.02 r= 0.18 p= 0.6065	m= -0.04 r= 0.40 p= 0.2170	m<0.01 r= 0.02 p= 0.9573	m= -0.02 r= 0.22 p= 0.5012	m= -0.01 r= 0.21 p= 0.5208	m= -0.01 r= 0.21 p= 0.5163	m= -0.02 r= 0.22 p= 0.4912	m= 0.02 r= 0.31 p= 0.3215	m= 0.01 r= 0.25 p= 0.4379	m= 0.01 r= 0.18 p= 0.5714	m<0.01 r= 0.01 p= 0.9839	m= -0.02 r= 0.48 p= 0.1169
	T_{mean}	m= 0.03 r= 0.35 p= 0.2849	m<-0.01 r= 0.07 p= 0.8354	m= -0.03 r= 0.32 p= 0.3423	m= 0.01 r= 0.12 p= 0.7025	m= 0.02 r= 0.22 p= 0.4990	m= 0.02 r= 0.36 p= 0.2463	m= -0.01 r= 0.09 p= 0.7710	m= -0.03 r= 0.23 p= 0.4769	m= 0.01 r= 0.16 p= 0.6270	m= 0.02 r= 0.22 p= 0.4995	m= 0.04 r= 0.52 p= 0.0839	m= 0.03 r= 0.33 p= 0.2882	m= -0.01 r= 0.26 p= 0.4090
	Precipitation	m= 0.21 r= 0.31 p= 0.3603	m= -0.29 r= 0.16 p= 0.6384	m= -0.12 r= 0.15 p= 0.6674	m= -0.43 r= 0.30 p= 0.3453	m= -2.18 r= 0.68 p= 0.0141	m= -1.44 r= 0.43 p= 0.1620	m= -0.81 r= 0.25 p= 0.4293	m= 1.77 r= 0.50 p= 0.0953	m<-0.01 r= 0.001 p= 0.9967	m= -0.08 r= 0.10 p= 0.7477	m= -0.17 r= 0.15 p= 0.6486	m= -0.22 r= 0.13 p= 0.6962	m= -4.06 r= 0.55 p= 0.0616
Springbok	T_{max}	m= -0.01 r= 0.12 p= 0.5542	m= 0.02 r= 0.11 p= 0.5963	m= -0.03 r= 0.33 p= 0.0981	m= 0.02 r= 0.19 p= 0.3432	m= 0.04 r= 0.30 p= 0.1228	m= 0.03 r= 0.24 p= 0.2328	m= -0.002 r= 0.02 p= 0.9394	m= -0.03 r= 0.20 p= 0.3319	m= -0.04 r= 0.21 p= 0.2791	m= -0.02 r= 0.15 p= 0.4585	m= 0.05 r= 0.40 p= 0.0442	m<0.01 r= 0.01 p= 0.9514	m<0.01 r= 0.01 p= 0.9426
	T_{min}	m= -0.001 r= 0.02 p= 0.9202	m= -0.02 r= 0.19 p= 0.3503	m= -0.03 r= 0.24 p= 0.2340	m= 0.01 r= 0.15 p= 0.4489	m= 0.02 r= 0.25 p= 0.2080	m= 0.02 r= 0.26 p= 0.2013	m<0.01 r= 0.05 p= 0.8077	m= -0.03 r= 0.24 p= 0.2389	m= -0.02 r= 0.16 p= 0.4315	m<-0.01 r= 0.001 p= 0.9805	m= 0.03 r= 0.32 p= 0.1117	m<-0.01 r= 0.01 p= 0.9789	m<-0.01 r= 0.03 p= 0.9008

	T_{mean}	m<-0.01 r= 0.08 p= 0.7079	m<-0.01 r= 0.02 p= 0.9151	m= -0.03 r= 0.29 p= 0.1472	m= 0.02 r= 0.18 p= 0.3751	m= 0.03 r= 0.29 p= 0.1387	m= 0.03 r= 0.25 p= 0.2094	m= -0.01 r= 0.06 p= 0.7794	m= -0.03 r= 0.22 p= 0.2766	m= -0.03 r= 0.19 p= 0.3419	m= -0.01 r= 0.09 p= 0.6535	m= 0.04 r= 0.38 p= 0.0584	m<0.01 r= <0.01 p= 0.9874	m<-0.01 r= 0.01 p= 0.9481
	Precipitation	m= -0.11 r= 0.12 p= 0.6072	m= -0.31 r= 0.29 p= 0.1981	m= -0.18 r= 0.12 p= 0.5939	m= -0.39 r= 0.42 p= 0.0609	m= -1.05 r= 0.46 p= 0.0340	m= -1.11 r= 0.46 p= 0.0363	m= -0.43 r= 0.21 p= 0.3611	m= 0.57 r= 0.31 p= 0.1590	m= 0.26 r= 0.17 p= 0.4381	m= 0.19 r= 0.28 p= 0.2083	m= -0.26 r= 0.23 p= 0.3030	m= 0.06 r= 0.14 p= 0.5338	m=-2.45 r= 0.41 p= 0.0601
Port Nolloth	T_{max}	m<-0.01 r= 0.05 p= 0.7799	m<0.01 r= 0.02 p= 0.9106	m<-0.01 r= 0.05 p= 0.7803	m= 0.01 r= 0.17 p= 0.3361	m= 0.01 r= 0.14 p= 0.4255	m= -0.01 r= 0.09 p= 0.5859	m= -0.01 r= 0.13 p= 0.4481	m= -0.02 r= 0.26 p= 0.1156	m<-0.01 r= 0.06 p= 0.7270	m<-0.01 r= 0.02 p= 0.9001	m= -0.01 r= 0.10 p= 0.5742	m<-0.01 r= 0.07 p= 0.6775	m<-0.01 r= 0.10 p= 0.5443
	T_{min}	m= -0.01 r= 0.16 p= 0.3558	m= -0.01 r= 0.11 p= 0.5343	m= -0.01 r= 0.15 p= 0.3712	m= -0.01 r= 0.18 p= 0.3092	m= -0.02 r= 0.31 p= 0.0694	m<-0.01 r= 0.02 p= 0.8851	m= -0.01 r= 0.22 p= 0.1831	m= -0.01 r= 0.19 p= 0.2576	m= -0.01 r= 0.16 p= 0.3568	m<0.01 r= 0.04 p= 0.7934	m= -0.01 r= 0.17 p= 0.3231	m= -0.02 r= 0.21 p= 0.2227	m= -0.01 r= 0.28 p= 0.0903
	T_{mean}	m= -0.01 r= 0.13 p= 0.4438	m<-0.01 r= 0.07 p= 0.6926	m= -0.01 r= 0.12 p= 0.4939	m<0.01 r= 0.03 p= 0.8590	m<-0.01 r= 0.05 p= 0.7606	m= -0.01 r= 0.07 p= 0.6785	m= -0.01 r= 0.11 p= 0.5231	m= -0.02 r= 0.30 p= 0.0756	m= -0.01 r= 0.09 p= 0.5953	m<0.01 r= 0.01 p= 0.9323	m= -0.01 r= 0.16 p= 0.3475	m= -0.01 r= 0.16 p= 0.3375	m= -0.01 r= 0.23 p= 0.1717
	Precipitation	m<-0.01 r= 0.002 p= 0.9862	m= -0.02 r= 0.10 p= 0.5498	m= -0.01 r= 0.04 p= 0.8022	m= -0.23 r= 0.34 p= 0.0424	m= -0.17 r= 0.37 p= 0.0255	m= -0.10 r= 0.14 p= 0.4168	m= -0.05 r= 0.11 p= 0.5112	m= 0.25 r= 0.46 p= 0.0043	m= 0.06 r= 0.16 p= 0.3440	m= 0.07 r= 0.25 p= 0.1429	m= 0.02 r= 0.07 p= 0.6980	m= -0.01 r= 0.05 p= 0.7832	m= -0.25 r= 0.20 p= 0.2430
Lambertsbaai Nortier	T_{max}	m= -0.01 r= 0.22 p= 0.3325	m= -0.01 r= 0.13 p= 0.5604	m= 0.01 r= 0.09 p= 0.6876	m= 0.03 r= 0.40 p= 0.0705	m= 0.04 r= 0.37 p= 0.0794	m= 0.11 r= 0.62 p= 0.0021	m= 0.03 r= 0.29 p= 0.1742	m<-0.01 r= 0.03 p= 0.8900	m<-0.01 r= 0.02 p= 0.9168	m= 0.02 r= 0.22 p= 0.3096	m= -0.01 r= 0.09 p= 0.6760	m<0.01 r= 0.06 p= 0.7989	m= 0.02 r= 0.29 p= 0.1573
	T_{min}	m= -0.01 r= 0.18 p= 0.4253	m<-0.01 r= 0.01 p= 0.9691	m= -0.01 r= 0.15 p= 0.5136	m= 0.02 r= 0.33 p= 0.1380	m= 0.02 r= 0.24 p= 0.2780	m= 0.06 r= 0.54 p= 0.0089	m= 0.02 r= 0.23 p= 0.2989	m= 0.01 r= 0.12 p= 0.5954	m= 0.01 r= 0.14 p= 0.5291	m= 0.03 r= 0.32 p= 0.1378	m= 0.02 r= 0.21 p= 0.3288	m= -0.003 r= 0.05 p= 0.8373	m= 0.02 r= 0.21 p= 0.3059
	T_{mean}	m= -0.01 r= 0.21 p= 0.3529	m= -0.01 r= 0.09 p= 0.7097	m<0.01 r= 0.01 p= 0.9754	m= 0.03 r= 0.44 p= 0.0482	m= 0.03 r= 0.32 p= 0.1431	m= 0.08 r= 0.61 p= 0.0028	m= 0.03 r= 0.28 p= 0.1953	m<0.01 r= 0.04 p= 0.8554	m<0.01 r= 0.06 p= 0.7876	m= 0.03 r= 0.27 p= 0.2069	m<0.01 r= 0.03 p= 0.8901	m<0.01 r= <0.01 p= 0.9845	m= 0.02 r= 0.26 p= 0.2101
	Precipitation	m= 0.17 r= 0.39 p= 0.0922	m= -0.13 r= 0.34 p= 0.1426	m= -0.06 r= 0.16 p= 0.4977	m= -0.10 r= 0.15 p= 0.5142	m= -0.82 r= 0.63 p= 0.0031	m= -0.51 r= 0.43 p= 0.0562	m= -0.30 r= 0.16 p= 0.4914	m= 0.27 r= 0.23 p= 0.3232	m= 0.03 r= 0.03 p= 0.9034	m= 0.20 r= 0.25 p= 0.2804	m= -0.27 r= 0.29 p= 0.2187	m= -0.11 r= 0.16 p= 0.4992	m= -1.63 r= 0.44 p= 0.0506
Clanwilliam	T_{max}	m<0.01 r= 0.02 p= 0.9550	m= -0.01 r= 0.11 p= 0.7019	m= -0.05 r= 0.52 p= 0.0576	m= -0.002 r= 0.04 p= 0.9024	m= 0.04 r= 0.46 p= 0.0986	m= 0.09 r= 0.65 p= 0.0111	m= 0.01 r= 0.17 p= 0.5654	m= -0.02 r= 0.21 p= 0.4680	m= -0.02 r= 0.18 p= 0.5425	m= 0.01 r= 0.20 p= 0.4932	m= 0.04 r= 0.50 p= 0.0605	m= -0.02 r= 0.18 p= 0.5259	m<0.01 r= 0.03 p= 0.9284
	T_{min}	m= -0.04 r= 0.06 p= 0.8347	m= -0.02 r= 0.23 p= 0.4275	m= -0.03 r= 0.42 p= 0.1338	m= 0.02 r= 0.23 p= 0.4377	m= -0.01 r= 0.17 p= 0.5535	m= -0.06 r= 0.57 p= 0.0351	m= -0.03 r= 0.51 p= 0.0648	m= -0.02 r= 0.42 p= 0.1378	m= -0.004 r= 0.08 p= 0.7823	m= 0.01 r= 0.19 p= 0.5136	m= 0.02 r= 0.24 p= 0.3960	m= -0.01 r= 0.18 p= 0.5233	m= -0.02 r= 0.32 p= 0.2513
	T_{mean}	m<-0.01 r= 0.02 p= 0.9543	m= -0.02 r= 0.17 p= 0.5609	m= -0.04 r= 0.50 p= 0.0683	m= 0.01 r= 0.13 p= 0.6602	m= 0.01 r= 0.27 p= 0.3528	m= 0.02 r= 0.38 p= 0.1749	m= -0.01 r= 0.17 p= 0.5543	m= -0.02 r= 0.32 p= 0.2618	m= -0.01 r= 0.16 p= 0.5736	m= 0.01 r= 0.25 p= 0.3974	m= 0.03 r= 0.43 p= 0.1075	m= -0.02 r= 0.19 p= 0.5046	m= -0.01 r= 0.11 p= 0.6852
	Precipitation	m= 0.15 r= 0.22 p= 0.4575	m= -0.10 r= 0.28 p= 0.3234	m= 0.12 r= 0.25 p= 0.3853	m= -0.10 r= 0.18 p= 0.5400	m= -0.91 r= 0.73 p= 0.0028	m= -0.34 r= 0.20 p= 0.4998	m= -0.47 r= 0.21 p= 0.4740	m= 0.24 r= 0.17 p= 0.5525	m= -0.05 r= 0.09 p= 0.7681	m= -0.13 r= 0.28 p= 0.3295	m= -0.11 r= 0.18 p= 0.5282	m= -0.07 r= 0.12 p= 0.6723	m= -1.55 r= 0.32 p= 0.2408

Statistically significant relationships are calculated between June T_{max} (r=0.65, p=0.0111) and T_{min} (r=0.57, p=0.0351) and first flowering timing for Clanwilliam, at rates of changes of $0.09d.°C^{-1}$ and $0.06d.°C^{-1}$, respectively (Table 5.10). The relationship between June T_{max} and first flowering timing is positive whereas the relationship between T_{min} and first flowering timing is inverse (Table 5.10).

Significantly inverse relationships are calculated between first flowering timing and precipitation for Vredendal, during April (r=0.34, p=0.0383) and May (r=0.33, p=0.0441) at negative rates of change of $0.34d.mm^{-1}$ and $0.40d.mm^{-1}$, respectively (Table 5.10). Statistically significant relationships are calculated between first flowering and rainfall for Springbok at a negative rate of $1.05d.mm^{-1}$ during May (r=0.46, p=0.0340) and $1.11d.mm^{-1}$ during June (r=0.46, p=0.0363; Table 5.10).

Significant inverse relationships are calculated between first flowering timing and precipitation for Port Nolloth during April (r=0.34, p=0.0424) and May (r=0.37, p=0.0255) at negative rates of $0.23d.mm^{-1}$ and $0.17d.mm^{-1}$, respectively (Table 5.10). A significant positive relationship is calculated between first flowering and precipitation for Port Nolloth during August at a rate of $0.25d.mm^{-1}$ (r=0.46, p=0.0043; Table 5.10).

Statistically significant inverse relationships are calculated between first flowering timing and precipitation during May for Clanwilliam, Nieuwoudtville and Lambertsbaai Nortier (Table 5.10). The significant inverse relationships have negative rates of changes of $0.91d.mm^{-1}$ (r=0.73, p=0.0028), $2.18d.mm^{-1}$ (r=0.68, p=0.0141) and $0.82d.mm^{-1}$ (r=0.63, p=0.0031), respectively (Table 5.10).

5.8.2 Influence of Climate Variables on Full Bloom (BBCH 63-65)

A significant inverse correlation is calculated between August T_{max} and full bloom timing for Cape Columbine with a negative rate of change of $0.02d.°C^{-1}$ (r=0.30, p=0.0484; Table 5.11). Statistically significant inverse relationships are calculated between Springbok full bloom timing and January T_{max}

(0.04d.°C^{-1}; r=0.52, p=0.0032), T_{min} (0.03d.°C^{-1}; r=0.45, p=0.0133) and T_{mean} (0.04d.°C^{-1}; r=0.50, p=0.0045; Table 5.11). Although temperatures during January are significantly related to full bloom timing in Springbok, climatic conditions during January are not temporally related to the germination, growth or flowering of the Namaqualand daisies.

A statistically significant inverse relationship is calculated between full bloom timing and annual T_{min} for Port Nolloth, at a negative rate of change of 0.02d.°C^{-1} (r=0.42, p=0.0048; Table 5.11). Statistically significant negative relationships are calculated between full bloom timing and T_{min} for six months of the year (January, March, May, August, November, December; Table 5.11). Port Nolloth annual T_{min} has been increasing significantly at a rate of 0.01°C.yr^{-1} (r=0.32, p=0.0147; Appendix A.1). The increase in T_{min} in Port Nolloth has therefore contributed to advances in full bloom timing.

The only calculated statistically significant relationship between temperature and full bloom timing for Lambertsbaai Nortier is for T_{min} during November with a rate of change of 0.03d.°C^{-1} (r=0.49, p=0.0095; Table 5.11). T_{min} during November cannot influence full bloom since most of the Namaqualand daisies have died by this time of the year.

Statistically significant positive correlations are calculated between full bloom timing and precipitation during October for four Namaqualand subregions (Table 5.11). The four subregions include; Cape Columbine (0.40d.mm^{-1}; r=0.45, p=0.0021), Vredendal (0.29d.mm^{-1}; r=0.41, p=0.0046), Port Nolloth (0.17d.mm^{-1}; r=0.45, p=0.0027) and Lambertsbaai Nortier (0.39d.mm^{-1}; r=0.62, p=0.0011; Table 5.11).

Table 5.11: Full bloom (BBCH 63-65) linear regression analysis with climate data for all seven weather stations in Namaqualand. Coloured blocks indicate statistically significant correlations.

Weather Stations	Climate Variable	Jan	Feb	Mar	Apr	May	Jun	Jul	Aug	Sept	Oct	Nov	Dec	Annual
Cape Columbine	T_{max}	m<0.01 r= 0.07 p= 0.6604	m<-0.01 r= 0.02 p= 0.8767	m= -0.01 r= 0.07 p= 0.6573	m= -0.01 r= 0.08 p= 0.5961	m= 0.02 r= 0.21 p= 0.1743	m= 0.01 r= 0.13 p= 0.3851	m= 0.01 r= 0.11 p= 0.4658	m= -0.02 r= 0.30 p= 0.0484	m<-0.01 r= 0.08 p= 0.6195	m= -0.01 r= 0.07 p= 0.6370	m<0.01 r= 0.03 p= 0.8290	m= -0.01 r= 0.12 p= 0.4239	m<-0.01 r= 0.05 p= 0.7402
	T_{min}	m<-0.01 r= 0.07 p= 0.6455	m<-0.01 r= 0.01 p= 0.9536	m= -0.003 r= 0.07 p= 0.6711	m= -0.01 r= 0.27 p= 0.0702	m<-0.01 r= 0.07 p= 0.9558	m<0.01 r= 0.01 p= 0.9630	m= -0.01 r= 0.11 p= 0.4904	m= -0.01 r= 0.18 p= 0.2314	m<-0.01 r= 0.06 p= 0.7082	m<-0.01 r= <0.01 p= 0.9800	m= 0.01 r= 0.19 p= 0.2162	m<-0.01 r= <0.01 p= 0.9966	m<-0.01 r= 0.09 p= 0.5460
	T_{mean}	m<0.01 r= 0.01 p= 0.9414	m<-0.01 r= 0.02 p= 0.9055	m<-0.01 r= 0.08 p= 0.6257	m= -0.01 r= 0.17 p= 0.2739	m= 0.01 r= 0.13 p= 0.3899	m<0.01 r= 0.08 p= 0.5813	m<0.01 r= 0.03 p= 0.8673	m= -0.01 r= 0.26 p= 0.0925	m<0.01 r= <0.01 p= 0.9844	m<-0.01 r= 0.05 p= 0.7570	m= 0.01 r= 0.11 p= 0.4655	m<-0.01 r= 0.07 p= 0.6557	m= -0.001 r= 0.06 p= 0.6905
	Precipitation	m= 0.11 r= 0.21 p= 0.1786	m= -0.10 r= 0.17 p= 0.2707	m= -0.06 r= 0.10 p= 0.5344	m= -0.25 r= 0.19 p= 0.2127	m= -0.37 r= 0.18 p= 0.2458	m= -0.13 r= 0.05 p= 0.7301	m= 0.01 r= 0.01 p= 0.9596	m= 0.22 r= 0.12 p= 0.4207	m= 0.07 r= 0.05 p= 0.7316	m= 0.40 r= 0.45 p= 0.0021	m= -0.14 r= 0.17 p= 0.2754	m= -0.07 r= 0.11 p= 0.4786	m= -0.32 r= 0.07 p= 0.6423
Vredendal	T_{max}	m= -0.02 r= 0.17 p= 0.2641	m= -0.02 r= 0.14 p= 0.3530	m= -0.02 r= 0.17 p= 0.2695	m<-0.01 r= 0.04 p= 0.8024	m= 0.03 r= 0.24 p= 0.1177	m= 0.02 r= 0.16 p= 0.2797	m= 0.01 r= 0.07 p= 0.6464	m= -0.03 r= 0.29 p= 0.0544	m= -0.01 r= 0.11 p= 0.4910	m= -0.01 r= 0.11 p= 0.4893	m= -0.01 r= 0.05 p= 0.7326	m= -0.02 r= 0.18 p= 0.2245	m= -0.01 r= 0.10 p= 0.5022
	T_{min}	m= -0.01 r= 0.09 p= 0.5604	m= -0.02 r= 0.29 p= 0.0552	m= -0.01 r= 0.19 p= 0.2125	m= -0.02 r= 0.19 p= 0.2238	m= -0.01 r= 0.14 p= 0.3556	m= -0.01 r= 0.13 p= 0.4076	m<-0.01 r= 0.05 p= 0.7508	m<0.01 r= 0.05 p= 0.7669	m<-0.01 r= 0.05 p= 0.7615	m<0.01 r= 0.01 p= 0.9539	m= 0.01 r= 0.10 p= 0.5094	m= -0.01 r= 0.13 p= 0.3774	m= -0.01 r= 0.23 p= 0.1257
	T_{mean}	m= -0.01 r= 0.15 p= 0.3379	m= -0.02 r= 0.22 p= 0.1506	m= -0.02 r= 0.20 p= 0.1895	m= -0.01 r= 0.12 p= 0.4438	m= 0.01 r= 0.14 p= 0.3737	m<0.01 r= 0.04 p= 0.8078	m<0.01 r= 0.04 p= 0.8111	m= -0.01 r= 0.20 p= 0.1796	m= -0.01 r= 0.10 p= 0.5083	m= -0.01 r= 0.07 p= 0.6523	m<0.01 r= 0.01 p= 0.9528	m= -0.02 r= 0.19 p= 0.2137	m= -0.01 r= 0.17 p= 0.2579
	Precipitation	m= 0.09 r= 0.28 p= 0.0589	m= -0.01 r= 0.07 p= 0.6570	m= -0.07 r= 0.19 p= 0.2041	m= -0.07 r= 0.08 p= 0.6133	m= -0.56 r= 0.36 p= 0.0161	m= -0.10 r= 0.06 p= 0.6813	m= 0.16 r= 0.11 p= 0.4803	m= 0.14 r= 0.13 p= 0.4095	m= 0.01 r= 0.01 p= 0.9575	m= 0.29 r= 0.41 p= 0.0046	m<0.01 r= <0.01 p= 0.9796	m= 0.05 r= 0.04 p= 0.8054	m= -0.07 r= 0.02 p= 0.951
Nieuwoudtville	T_{max}	m= 0.02 r= 0.26 p= 0.3465	m= 0.02 r= 0.31 p= 0.2532	m= 0.01 r= 0.07 p= 0.7934	m= 0.02 r= 0.22 p= 0.4078	m= 0.06 r= 0.41 p= 0.1103	m= 0.02 r= 0.33 p= 0.2157	m= 0.03 r= 0.35 p= 0.1888	m<-0.01 r= 0.01 p= 0.9709	m= 0.03 r= 0.30 p= 0.2544	m= -0.01 r= 0.07 p= 0.7861	m= 0.02 r= 0.31 p= 0.2354	m= 0.02 r= 0.23 p= 0.3928	m= 0.01 r= 0.23 p= 0.3979
	T_{min}	m= -0.01 r= 0.22 p= 0.4251	m<-0.01 r= 0.01 p= 0.9844	m<0.01 r= 0.05 p= 0.8530	m= 0.01 r= 0.14 p= 0.6014	m= 0.02 r= 0.26 p= 0.3254	m= 0.01 r= 0.11 p= 0.6884	m= 0.02 r= 0.23 p= 0.4003	m= 0.04 r= 0.38 p= 0.1429	m= 0.02 r= 0.31 p= 0.2421	m= 0.02 r= 0.29 p= 0.2838	m= 0.02 r= 0.40 p= 0.1282	m= 0.03 r= 0.35 p= 0.1833	m= 0.01 r= 0.16 p= 0.5561
	T_{mean}	m<0.01 r= 0.05 p= 0.8547	m= 0.01 r= 0.15 p= 0.5928	m= 0.01 r= 0.07 p= 0.8011	m= 0.01 r= 0.24 p= 0.3635	m= 0.04 r= 0.49 p= 0.0521	m= 0.01 r= 0.33 p= 0.2095	m= 0.02 r= 0.34 p= 0.1922	m= 0.02 r= 0.17 p= 0.5350	m= 0.03 r= 0.37 p= 0.1636	m= 0.01 r= 0.08 p= 0.7807	m= 0.02 r= 0.40 p= 0.1225	m= 0.02 r= 0.35 p= 0.1801	m= 0.01 r= 0.25 p= 0.3456
	Precipitation	m= 0.06 r= 0.07 p= 0.8126	m= -0.38 r= 0.32 p= 0.2472	m= -0.04 r= 0.06 p= 0.8209	m= 0.25 r= 0.19 p= 0.4811	m= -0.81 r= 0.31 p= 0.2504	m= -0.87 r= 0.30 p= 0.2611	m= -1.01 r= 0.38 p= 0.1428	m= 1.72 r= 0.59 p= 0.0162	m= 0.02 r= 0.02 p= 0.9407	m= 0.24 r= 0.38 p= 0.1519	m= -0.18 r= 0.19 p= 0.4863	m= 0.13 r= 0.09 p= 0.7415	m= -0.96 r= 0.13 p= 0.6224
Springbok	T_{max}	m= -0.04 r= 0.52 p= 0.0032	m= 0.01 r= 0.04 p= 0.8179	m= -0.03 r= 0.34 p= 0.0650	m= -0.02 r= 0.24 p= 0.1991	m= 0.04 r= 0.32 p= 0.0830	m= 0.01 r= 0.12 p= 0.5422	m<0.01 r= 0.02 p= 0.9317	m= -0.02 r= 0.16 p= 0.0462	m= -0.04 r= 0.27 p= 0.1522	m= -0.02 r= 0.13 p= 0.5061	m<-0.01 r= 0.05 p= 0.8103	m= -0.03 r= 0.27 p= 0.1461	m<-0.01 r= 0.07 p= 0.6982
	T_{min}	m= -0.03 r= 0.45 p= 0.0133	m= -0.02 r= 0.25 p= 0.1865	m= -0.04 r= 0.36 p= 0.0541	m= -0.02 r= 0.26 p= 0.1618	m= 0.03 r= 0.30 p= 0.1052	m<0.01 r= 0.01 p= 0.9661	m= 0.01 r= 0.19 p= 0.3389	m= -0.02 r= 0.18 p= 0.3438	m= -0.02 r= 0.19 p= 0.3261	m= -0.01 r= 0.05 p= 0.7902	m<0.01 r= 0.02 p= 0.9175	m= -0.03 r= 0.32 p= 0.0883	m= -0.01 r= 0.15 p= 0.4246

	T_{mean}	m= -0.04 r= 0.50 p= 0.0045	m= -0.01 r= 0.10 p= 0.6090	m= -0.04 r= 0.36 p= 0.0521	m= -0.02 r= 0.26 p= 0.1698	m= 0.03 r= 0.32 p= 0.0818	m= 0.01 r= 0.07 p= 0.7013	m= -0.01 r= 0.04 p= 0.8418	m= -0.02 r= 0.17 p= 0.3664	m= -0.03 r= 0.24 p= 0.2073	m= -0.01 r= 0.10 p= 0.6135	m<-0.01 r= 0.02 p= 0.9299	m= -0.03 r= 0.30 p= 0.1016	m= -0.01 r= 0.12 p= 0.5129
	Precipitation	m= -0.10 r= 0.10 p= 0.6511	m= -0.09 r= 0.10 p= 0.6203	m= -0.25 r= 0.21 p= 0.3084	m= -0.08 r= 0.09 p= 0.6787	m= -0.45 r= 0.24 p= 0.2387	m= -0.68 r= 0.34 p= 0.0947	m= 0.12 r= 0.07 p= 0.7334	m= 0.17 r= 0.11 p= 0.5959	m= 0.02 r= 0.02 p= 0.9316	m= 0.22 r= 0.32 p= 0.1081	m= -0.14 r= 0.15 p= 0.4504	m= -0.06 r= 0.16 p= 0.4314	m= -0.98 r= 0.19 p= 0.3620
Port Nolloth	T_{max}	m<-0.01 r= 0.03 p= 0.8726	m<-0.01 r= 0.04 p= 0.7894	m= -0.02 r= 0.20 p= 0.1951	m= -0.02 r= 0.14 p= 0.3720	m= -0.02 r= 0.15 p= 0.3218	m<0.01 r= 0.03 p= 0.8283	m= 0.02 r= 0.17 p= 0.2830	m= -0.03 r= 0.28 p= 0.0640	m<-0.01 r= 0.01 p= 0.9249	m= -0.01 r= 0.07 p= 0.6629	m<-0.01 r= 0.05 p= 0.7725	m= -0.01 r= 0.11 p= 0.4947	m<-0.01 r= 0.09 p= 0.5657
	T_{min}	m= -0.03 r= 0.35 p= 0.0220	m= -0.02 r= 0.22 p= 0.1557	m= -0.03 r= 0.32 p= 0.0394	m= -0.02 r= 0.27 p= 0.0887	m= -0.03 r= 0.37 p= 0.0169	m= -0.02 r= 0.20 p= 0.2120	m= -0.02 r= 0.17 p= 0.2727	m= -0.03 r= 0.37 p= 0.0171	m= -0.01 r= 0.17 p= 0.2913	m= -0.01 r= 0.14 p= 0.3741	m= -0.02 r= 0.35 p= 0.0234	m= -0.03 r= 0.31 p= 0.0409	m= -0.02 r= 0.42 p= 0.0048
	T_{mean}	m= -0.02 r= 0.24 p= 0.1265	m= -0.02 r= 0.20 p= 0.1974	m= -0.02 r= 0.30 p= 0.0542	m= -0.02 r= 0.21 p= 0.1751	m= -0.03 r= 0.26 p= 0.0913	m= -0.01 r= 0.11 p= 0.4703	m<0.01 r= 0.01 p= 0.9553	m= -0.03 r= 0.39 p= 0.0107	m<-0.01 r= 0.03 p= 0.8394	m= -0.01 r= 0.16 p= 0.3067	m= -0.01 r= 0.23 p= 0.1425	m= -0.02 r= 0.25 p= 0.1073	m= -0.01 r= 0.28 p= 0.0728
	Precipitation	m= -0.08 r= 0.16 p= 0.2918	m= -0.05 r= 0.26 p= 0.0942	m= -0.04 r= 0.12 p= 0.4376	m= -0.24 r= 0.28 p= 0.0698	m= -0.14 r= 0.26 p= 0.0926	m= -0.18 r= 0.20 p= 0.1972	m= -0.03 r= 0.05 p= 0.7428	m= 0.23 r= 0.31 p= 0.0407	m<0.01 r= <0.01 p= 0.9908	m= 0.17 r= 0.45 p= 0.0027	m= -0.05 r= 0.16 p= 0.3020	m= -0.07 r= 0.19 p= 0.2279	m= -0.42 r= 0.21 p= 0.1619
Lambertsbaai Nortier	T_{max}	m= -0.01 r= 0.10 p= 0.6373	m= -0.01 r= 0.14 p= 0.5097	m= -0.01 r= 0.08 p= 0.6838	m= -0.01 r= 0.11 p= 0.6165	m= 0.03 r= 0.32 p= 0.1034	m= 0.05 r= 0.32 p= 0.1071	m= 0.04 r= 0.31 p= 0.1137	m<-0.01 r= 0.05 p= 0.8251	m= 0.01 r= 0.09 p= 0.6474	m<-0.01 r= <0.01 p= 0.9859	m= -0.02 r= 0.17 p= 0.4013	m= -0.01 r= 0.10 p= 0.6225	m<0.01 r= 0.07 p= 0.7156
	T_{min}	m= -0.01 r= 0.07 p= 0.7254	m= -0.01 r= 0.11 p= 0.5943	m= -0.01 r= 0.16 p= 0.4420	m<-0.01 r= 0.01 p= 0.9601	m= 0.02 r= 0.23 p= 0.2535	m= 0.03 r= 0.30 p= 0.1384	m= 0.02 r= 0.24 p= 0.2268	m= 0.01 r= 0.20 p= 0.3303	m= 0.02 r= 0.30 p= 0.1271	m= 0.01 r= 0.15 p= 0.4402	m= 0.03 r= 0.49 p= 0.0095	m<-0.01 r= <0.01 p= 0.9805	m= 0.01 r= 0.17 p= 0.3825
	T_{mean}	m= -0.01 r= 0.09 p= 0.6678	m= -0.01 r= 0.13 p= 0.5202	m= -0.01 r= 0.12 p= 0.5431	m<-0.01 r= 0.06 p= 0.7664	m= 0.02 r= 0.29 p= 0.1466	m= 0.04 r= 0.32 p= 0.1071	m= 0.03 r= 0.29 p= 0.1357	m= 0.01 r= 0.07 p= 0.7208	m= 0.01 r= 0.21 p= 0.2882	m= 0.01 r= 0.07 p= 0.7276	m= 0.01 r= 0.11 p= 0.5872	m<-0.01 r= 0.05 p= 0.7912	m= 0.01 r= 0.13 p= 0.5062
	Precipitation	m= 0.16 r= 0.43 p= 0.0374	m= -0.03 r= 0.09 p= 0.6806	m= -0.02 r= 0.06 p= 0.7840	m= 0.09 r= 0.16 p= 0.4514	m= -0.19 r= 0.18 p= 0.4090	m= -0.39 r= 0.38 p= 0.0695	m= 0.01 r= 0.01 p= 0.9644	m= 0.15 r= 0.13 p= 0.5338	m<-0.01 r= <0.01 p= 0.9843	m= 0.39 r= 0.62 p= 0.0011	m= -0.18 r= 0.23 p= 0.2743	m= 0.10 r= 0.17 p= 0.4178	m= 0.10 r= 0.03 p= 0.8807
Clanwilliam	T_{max}	m= -0.02 r= 0.19 p= 0.4420	m<-0.01 r= 0.004 p= 0.9858	m= -0.02 r= 0.22 p= 0.3839	m= -0.02 r= 0.26 p= 0.3068	m= 0.03 r= 0.33 p= 0.1842	m= 0.04 r= 0.36 p= 0.1336	m= 0.03 r= 0.33 p= 0.1759	m= -0.01 r= 0.11 p= 0.6723	m= 0.01 r= 0.05 p= 0.8531	m= -0.01 r= 0.07 p= 0.7753	m= 0.02 r= 0.32 p= 0.1980	m= -0.01 r= 0.06 p= 0.8022	m<0.01 r= 0.12 p= 0.6264
	T_{min}	m= -0.02 r= 0.33 p= 0.1839	m= -0.01 r= 0.15 p= 0.5478	m= -0.01 r= 0.20 p= 0.4326	m= -0.01 r= 0.08 p= 0.7407	m= -0.01 r= 0.13 p= 0.6120	m= -0.02 r= 0.24 p= 0.3440	m= -0.01 r= 0.16 p= 0.5387	m<0.01 r= 0.10 p= 0.6791	m= 0.01 r= 0.19 p= 0.4604	m= 0.01 r= 0.24 p= 0.3311	m= 0.02 r= 0.38 p= 0.1183	m<0.01 r= 0.05 p= 0.8333	m<-0.01 r= 0.13 p= 0.6013
	T_{mean}	m= -0.02 r= 0.26 p= 0.2880	m= -0.01 r= 0.07 p= 0.7773	m= -0.02 r= 0.22 p= 0.3791	m= -0.01 r= 0.22 p= 0.3859	m= 0.01 r= 0.22 p= 0.3838	m= 0.01 r= 0.28 p= 0.2542	m= 0.01 r= 0.17 p= 0.4924	m<-0.01 r= 0.04 p= 0.8608	m= 0.01 r= 0.10 p= 0.7003	m<0.01 r= 0.07 p= 0.7963	m= 0.02 r= 0.40 p= 0.0991	m<-0.01 r= 0.01 p= 0.9564	m<0.01 r= 0.03 p= 0.9150
	Precipitation	m= 0.05 r= 0.08 p= 0.7559	m= 0.03 r= 0.12 p= 0.6419	m= 0.04 r= 0.11 p= 0.6705	m= 0.07 r= 0.13 p= 0.6081	m= -0.25 r= 0.23 p= 0.3565	m= -0.49 r= 0.35 p= 0.1540	m= -0.10 r= 0.05 p= 0.8327	m= 0.10 r= 0.09 p= 0.7301	m= 0.27 r= 0.51 p= 0.0300	m= -0.02 r= 0.06 p= 0.8225	m= -0.17 r= 0.34 p= 0.1640	m= 0.07 r= 0.16 p= 0.5391	m= 0.40 r= 0.12 p= 0.6268

Significant positive relationships are calculated between full bloom timing and precipitation during August for Nieuwoudtville and Port Nolloth, at rates of 1.72d.mm^{-1} (r=0.59, p=0.0162) and 0.23d.mm^{-1} (r=0.31, p=0.0407) respectively (Table 5.11). Nieuwoudtville precipitation totals during August have been decreasing at a statistically significant rate of 5.77mm.yr^{-1} (r=0.54, p=0.0299; Appendix A.1). The significant decrease in precipitation during August has therefore contributed to advances in full bloom timing of Namaqualand daisies in Nieuwoudtville.

A statistically significant inverse relationship is calculated between full bloom timing and precipitation for Vredendal during May, at a negative rate of change of 0.56d.mm^{-1} (r=0.36, p=0.0161; Table 5.11). A statistically significant positive relationship exists between precipitation during September (0.27d.mm^{-1}; r=0.51, p=0.0300) and full bloom timing for Clanwilliam (Table 5.11).

A statistically significant positive relationship is calculated between January precipitation and full bloom timing for Lambertsbaai Nortier, at a rate of change of 0.16d.mm^{-1} (r=0.43, p=0.0374; Table 5.11). Although January precipitation is statistically significantly related to full bloom timing, it cannot accurately influence full bloom timing seeing as it is temporally not related to the germination, growth or flowering timing of Namaqualand daisies.

5.8.3 Influence of Climate Variables on End of Bloom (BBCH 67-69)

Statistically significant inverse relationships are calculated between end of bloom timing and T_{max} for Cape Columbine, during March (r=0.56, p=0.0106), August (r=0.63, p=0.0031) and October (r=0.63, p=0.0021), with small negative rates of change ranging between 0.02-0.03d.°C^{-1} (Table 5.12). More statistically significant inverse relationships are calculated between T_{min} during June (r=0.63, p=0.0021) and October (r=0.47, p=0.0306) and end of bloom timing, with both negative rates of changes being 0.02d.°C^{-1} (Table 5.12). Statistically significant inverse relationships are calculated between end of bloom timing and T_{mean} for Cape Columbine during June (0.02d.°C^{-1}; r=0.47, p=0.0313), August (0.02d.°C^{-1}; r=0.57, p=0.0087) and October (0.03d.°C^{-1}; r=0.62, p=0.0030; Table 5.12). Calculations revealed that annual T_{max} (0.02d.°C^{-1}, r= 0.67, p= 0.0008), T_{min} (0.01d.°C^{-1}; r=0.51, p=0.0192) and T_{mean} (0.01d.°C^{-1}; r=0.63, p=0.0024) all demonstrate statistically significant inverse relationships with end of bloom timing for Cape Columbine (Table 5.12). Annual T_{max}, T_{min} and T_{mean} in Cape Columbine have been increasing significantly at a rate of 0.01°C.yr^{-1} (p<0.0001; Appendix A.1). The overall increase in temperature in Cape Columbine has therefore contributed to advances in end of bloom timing for the Namaqualand daisies.

Statistically significant inverse relationships are calculated between end of bloom timing and T_{max} and T_{mean} during February, March and August for Vredendal, at negative rates of change ranging between 0.02-0.05d.°C^{-1} (p<0.0500; Table 5.12). Significant inverse relationships are also calculated between annual T_{max} (r=0.44, p=0.0468) and T_{mean} (r=0.44, p=0.0468) and end of bloom timing with the same negative rate of change of 0.02d.°C^{-1} (Table 5.12). Vredendal T_{max} and T_{mean} have both been increasing significantly over time at rates of 0.05°C.yr^{-1} (r=0,84, p<0.0001) and 0.03°C.yr^{-1} (r=0.82, p<0.0001) respectively (Appendix A.1). Due to the inverse relationship between end of bloom timing and the respective temperature variables in Vredendal, increases in T_{max} and T_{mean} have therefore contributed to advances in end of bloom timing.

Table 5.12: End of bloom (BBCH 67-69) linear regression analysis with climate data for all seven weather stations in Namaqualand. Coloured blocks indicate statistically significant correlations.

Weather Stations	Climate Variable	Jan	Feb	Mar	Apr	May	Jun	Jul	Aug	Sept	Oct	Nov	Dec	Annual
Cape Columbine	T_{max}	m= -0.01 r= 0.34 p= 0.1287	m= -0.02 r= 0.38 p= 0.0865	m= -0.03 r= 0.56 p= 0.0106	m<0.01 r= 0.05 p= 0.8198	m= -0.01 r= 0.21 p= 0.3648	m= -0.02 r= 0.32 p= 0.1562	m= -0.02 r= 0.37 p= 0.1000	m= -0.02 r= 0.63 p= 0.0031	m<-0.01 r= 0.03 p= 0.9122	m= -0.03 r= 0.63 p= 0.0021	m= -0.01 r= 0.24 p= 0.2956	m= -0.01 r= 0.22 p= 0.3374	m= -0.02 r= 0.67 p= 0.0008
	T_{min}	m= -0.01 r= 0.36 p= 0.1120	m= -0.01 r= 0.30 p= 0.1802	m= -0.01 r= 0.13 p= 0.5719	m<0.01 r= 0.10 p= 0.6814	m= -0.01 r= 0.26 p= 0.2579	m= -0.02 r= 0.63 p= 0.0021	m<-0.01 r= 0.04 p= 0.8550	m= -0.01 r= 0.42 p= 0.0648	m= -0.01 r= 0.28 p= 0.2272	m= -0.02 r= 0.47 p= 0.0306	m= -0.02 r= 0.35 p= 0.1252	m<-0.01 r= 0.11 p= 0.6472	m= -0.01 r= 0.51 p= 0.0192
	T_{mean}	m= -0.01 r= 0.40 p= 0.0699	m= -0.02 r= 0.37 p= 0.1022	m= -0.02 r= 0.39 p= 0.0880	m<0.01 r= 0.08 p= 0.7360	m= -0.01 r= 0.24 p= 0.2874	m= -0.02 r= 0.47 p= 0.0313	m= -0.01 r= 0.28 p= 0.2105	m= -0.02 r= 0.57 p= 0.0087	m<0.01 r= 0.07 p= 0.7523	m= -0.03 r= 0.62 p= 0.0030	m= -0.01 r= 0.30 p= 0.1794	m= -0.01 r= 0.17 p= 0.4505	m= -0.01 r= 0.63 p= 0.0024
	Precipitation	m= 0.07 r= 0.15 p= 0.5262	m= -0.04 r= 0.09 p= 0.7128	m= 0.18 r= 0.34 p= 0.1312	m= 0.19 r= 0.15 p= 0.5067	m= -0.02 r= 0.01 p= 0.9497	m= -0.54 r= 0.43 p= 0.0489	m= -0.30 r= 0.25 p= 0.2701	m= -0.21 r= 0.23 p= 0.3164	m= 0.02 r= 0.03 p= 0.9022	m= 0.06 r= 0.09 p= 0.6989	m= -0.23 r= 0.41 p= 0.0624	m= -0.09 r= 0.22 p= 0.3408	m= -0.94 r= 0.27 p= 0.2409
Vredendal	T_{max}	m= -0.02 r= 0.22 p= 0.3463	m= -0.04 r= 0.45 p= 0.0478	m= -0.05 r= 0.54 p= 0.0115	m= -0.03 r= 0.35 p= 0.1247	m<-0.01 r= 0.01 p= 0.9768	m<-0.01 r= 0.03 p= 0.8915	m= -0.04 r= 0.39 p= 0.0821	m= -0.04 r= 0.54 p= 0.0120	m= -0.03 r= 0.36 p= 0.1056	m= -0.03 r= 0.35 p= 0.1247	m<-0.01 r= 0.06 p= 0.7880	m= -0.01 r= 0.19 p= 0.4165	m= -0.02 r= 0.44 p= 0.0468
	T_{min}	m= -0.02 r= 0.36 p= 0.1110	m= -0.03 r= 0.40 p= 0.0778	m= -0.01 r= 0.16 p= 0.4973	m= 0.01 r= 0.21 p= 0.3737	m= -0.02 r= 0.39 p= 0.0775	m= -0.02 r= 0.33 p= 0.1505	m<0.01 r= 0.07 p= 0.7553	m= -0.01 r= 0.14 p= 0.5517	m<0.01 r= 0.08 p= 0.7146	m= -0.01 r= 0.24 p= 0.3043	m= -0.01 r= 0.11 p= 0.6217	m= -0.01 r= 0.30 p= 0.1811	m= -0.01 r= 0.39 p= 0.0768
	T_{mean}	m= -0.02 r= 0.29 p= 0.2042	m= -0.03 r= 0.46 p= 0.0398	m= -0.03 r= 0.45 p= 0.0391	m= -0.01 r= 0.18 p= 0.4383	m= -0.01 r= 0.17 p= 0.4568	m= -0.01 r= 0.26 p= 0.2635	m= -0.02 r= 0.31 p= 0.1727	m= -0.02 r= 0.49 p= 0.0236	m= -0.01 r= 0.25 p= 0.2782	m= -0.02 r= 0.35 p= 0.1196	m<-0.01 r= 0.10 p= 0.6571	m= -0.01 r= 0.27 p= 0.2293	m= -0.02 r= 0.76 p= 0.0002
	Precipitation	m= 0.05 r= 0.16 p= 0.4869	m= -0.04 r= 0.30 p= 0.2027	m= 0.17 r= 0.50 p= 0.0217	m= 0.05 r= 0.09 p= 0.6970	m= -0.08 r= 0.06 p= 0.7864	m= -0.41 r= 0.42 p= 0.0601	m= -0.19 r= 0.18 p= 0.4455	m= -0.10 r= 0.18 p= 0.4431	m= 0.18 r= 0.38 p= 0.0915	m= 0.06 r= 0.11 p= 0.6202	m= -0.07 r= 0.20 p= 0.3887	m= -0.44 r= 0.42 p= 0.0598	m= -0.81 r= 0.35 p= 0.1204
Nieuwoudtville	T_{max}	m= 0.03 r= 0.30 p= 0.3968	m= 0.01 r= 0.06 p= 0.8613	m= -0.07 r= 0.71 p= 0.0207	m= -0.03 r= 0.29 p= 0.4127	m= 0.05 r= 0.24 p= 0.5113	m= 0.01 r= 0.18 p= 0.6210	m= -0.05 r= 0.49 p= 0.1541	m= -0.05 r= 0.41 p= 0.2453	m= 0.06 r= 0.53 p= 0.1133	m= 0.05 r= 0.46 p= 0.1829	m= 0.05 r= 0.55 p= 0.1023	m= 0.01 r= 0.13 p= 0.7170	m= 0.01 r= 0.13 p= 0.7152
	T_{min}	m= 0.02 r= 0.28 p= 0.4318	m= 0.01 r= 0.10 p= 0.7742	m= -0.06 r= 0.72 p= 0.0177	m= -0.02 r= 0.25 p= 0.4834	m= -0.02 r= 0.26 p= 0.4735	m= -0.01 r= 0.26 p= 0.4660	m= -0.05 r= 0.52 p= 0.1195	m= -0.02 r= 0.14 p= 0.6939	m= 0.01 r= 0.10 p= 0.7880	m<-0.01 r= 0.05 p= 0.8831	m= 0.01 r= 0.10 p= 0.7775	m= -0.02 r= 0.30 p= 0.3966	m= -0.01 r= 0.30 p= 0.4058
	T_{mean}	m= 0.03 r= 0.33 p= 0.3454	m= 0.01 r= 0.09 p= 0.7951	m= -0.07 r= 0.78 p= 0.0073	m= -0.02 r= 0.35 p= 0.3158	m= 0.01 r= 0.12 p= 0.7486	m<-0.01 r= 0.03 p= 0.9429	m= -0.05 r= 0.69 p= 0.0279	m= -0.03 r= 0.32 p= 0.3733	m= 0.04 r= 0.46 p= 0.1771	m= 0.02 r= 0.34 p= 0.3340	m= 0.03 r= 0.37 p= 0.2904	m= -0.01 r= 0.08 p= 0.8368	m<-0.01 r= 0.10 p= 0.7892
	Precipitation	m= 0.34 r= 0.56 p= 0.0950	m= -0.58 r= 0.37 p= 0.2995	m= -0.05 r= 0.12 p= 0.7471	m= 0.25 r= 0.19 p= 0.6003	m= -0.93 r= 0.25 p= 0.4787	m= -1.11 r= 0.34 p= 0.3417	m= -0.75 r= 0.20 p= 0.5714	m= 1.07 r= 0.27 p= 0.4530	m= -0.39 r= 0.29 p= 0.4169	m= -0.14 r= 0.17 p= 0.6319	m= -0.32 r= 0.25 p= 0.4915	m= -0.81 r= 0.53 p= 0.1176	m= -3.42 r= 0.37 p= 0.2938
Springbok	T_{max}	m= -0.01 r= 0.09 p= 0.7417	m= -0.06 r= 0.34 p= 0.2010	m= -0.06 r= 0.62 p= 0.0097	m= -0.02 r= 0.36 p= 0.1737	m= 0.04 r= 0.26 p= 0.3123	m= -0.03 r= 0.24 p= 0.3629	m= -0.06 r= 0.62 p= 0.0139	m= -0.04 r= 0.37 p= 0.1593	m= 0.03 r= 0.33 p= 0.2177	m= -0.02 r= 0.22 p= 0.4143	m= 0.04 r= 0.51 p= 0.0426	m= 0.02 r= 0.21 p= 0.4282	m= -0.01 r= 0.18 p= 0.4833

	T$_{min}$	m= 0.01 r= 0.10 p= 0.7212	m= -0.01 r= 0.09 p= 0.7459	m= -0.04 r= 0.42 p= 0.1095	m= -0.02 r= 0.20 p= 0.4516	m= 0.03 r= 0.31 p= 0.2280	m= -0.01 r= 0.32 p= 0.7057	m= -0.04 r= 0.56 p= 0.0307	m= -0.01 r= 0.08 p= 0.7546	m= 0.06 r= 0.68 p= 0.0037	m<0.01 r= 0.08 p= 0.7692	m= 0.04 r= 0.46 p= 0.0708	m= 0.01 r= 0.18 p= 0.5051	m= 0.01 r= 0.11 p= 0.6824
	T$_{mean}$	m<0.01 r= <0.01 p= 0.9922	m= -0.03 r= 0.30 p= 0.2646	m= -0.05 r= 0.53 p= 0.0340	m= -0.02 r= 0.28 p= 0.2900	m= 0.03 r= 0.29 p= 0.2670	m= -0.02 r= 0.19 p= 0.4751	m= -0.04 r= 0.61 p= 0.0148	m= -0.02 r= 0.25 p= 0.3523	m= 0.05 r= 0.53 p= 0.0361	m= -0.01 r= 0.12 p= 0.6576	m= 0.04 r= 0.51 p= 0.0460	m= 0.02 r= 0.20 p= 0.4606	m<-0.01 r= 0.05 p= 0.8363
	Precipitation	m= 0.37 r= 0.33 p= 0.2884	m= -0.31 r= 0.25 p= 0.4422	m= -0.15 r= 0.09 p= 0.7751	m= 0.08 r= 0.09 p= 0.7736	m= 0.04 r= 0.02 p= 0.9485	m= -0.75 r= 0.35 p= 0.2591	m<0.01 r= <0.01 p= 0.9925	m= -0.03 r= 0.03 p= 0.9279	m= 0.09 r= 0.14 p= 0.6622	m= 0.07 r= 0.12 p= 0.7167	m= -0.21 r= 0.22 p= 0.5003	m= -0.03 r= 0.16 p= 0.6095	m= -0.83 r= 0.15 p= 0.6522
Port Nolloth	T$_{max}$	m<-0.01 r= 0.07 p= 0.7593	m<-0.01 r= 0.08 p= 0.7497	m<-0.01 r= 0.03 p= 0.9030	m= 0.01 r= 0.13 p= 0.5953	m= -0.01 r= 0.12 p= 0.6041	m= 0.03 r= 0.28 p= 0.2363	m= -0.03 r= 0.30 p= 0.1888	m= -0.02 r= 0.31 p= 0.1735	m= -0.01 r= 0.08 p= 0.7241	m= -0.02 r= 0.32 p= 0.1553	m= -0.01 r= 0.20 p= 0.3838	m= -0.02 r= 0.38 p= 0.0934	m= -0.01 r= 0.29 p= 0.2094
	T$_{min}$	m= 0.01 r= 0.14 p= 0.5674	m= 0.02 r= 0.24 p= 0.3080	m<0.01 r= <0.01 p= 0.9939	m= 0.01 r= 0.19 p= 0.4302	m= -0.01 r= 0.22 p= 0.3551	m<0.01 r= 0.06 p= 0.8079	m= -0.01 r= 0.16 p= 0.4854	m= -0.01 r= 0.15 p= 0.5156	m<0.01 r= 0.11 p= 0.6220	m= -0.01 r= 0.21 p= 0.3647	m= -0.02 r= 0.36 p= 0.1141	m= -0.02 r= 0.42 p= 0.0581	m= -0.01 r= 0.21 p= 0.3718
	T$_{mean}$	m<0.01 r= 0.04 p= 0.8589	m= 0.01 r= 0.15 p= 0.5414	m<-0.01 r= 0.01 p= 0.9547	m= 0.01 r= 0.16 p= 0.5049	m= -0.01 r= 0.17 p= 0.4751	m= 0.01 r= 0.20 p= 0.3889	m= -0.02 r= 0.28 p= 0.2182	m= -0.02 r= 0.34 p= 0.1362	m<-0.01 r= 0.03 p= 0.9043	m= -0.02 r= 0.37 p= 0.0996	m= -0.01 r= 0.34 p= 0.1362	m= -0.02 r= 0.53 p= 0.0130	m= -0.01 r= 0.37 p= 0.1085
	Precipitation	m= 0.01 r= 0.06 p= 0.8047	m= -0.08 r= 0.50 p= 0.0263	m= 0.07 r= 0.32 p= 0.1677	m= 0.14 r= 0.22 p= 0.3556	m= -0.07 r= 0.17 p= 0.4837	m= -0.02 r= 0.03 p= 0.9040	m= 0.03 r= 0.08 p= 0.7382	m= 0.01 r= 0.02 p= 0.9160	m= 0.12 r= 0.45 p= 0.0385	m= 0.02 r= 0.06 p= 0.7878	m= -0.13 r= 0.60 p= 0.0053	m= -0.03 r= 0.21 p= 0.3683	m= -0.12 r= 0.09 p= 0.7133
Lambertsbaai Nortier	T$_{max}$	m= -0.03 r= 0.58 p= 0.0295	m= -0.03 r= 0.28 p= 0.3502	m= 0.01 r= 0.08 p= 0.7729	m= 0.03 r= 0.33 p= 0.2634	m= -0.01 r= 0.09 p= 0.7435	m= -0.01 r= 0.08 p= 0.7931	m= -0.04 r= 0.34 p= 0.2183	m= -0.04 r= 0.51 p= 0.0609	m= 0.02 r= 0.32 p= 0.2416	m= -0.02 r= 0.27 p= 0.3314	m= 0.04 r= 0.29 p= 0.3077	m= -0.02 r= 0.30 p= 0.2989	m= -0.02 r= 0.30 p= 0.2508
	T$_{min}$	m= -0.03 r= 0.43 p= 0.1245	m= -0.02 r= 0.27 p= 0.3740	m= -0.03 r= 0.48 p= 0.0794	m<0.01 r= 0.09 p= 0.7707	m= -0.04 r= 0.37 p= 0.1729	m= -0.03 r= 0.30 p= 0.3030	m= -0.01 r= 0.13 p= 0.6402	m= -0.01 r= 0.09 p= 0.7689	m= 0.01 r= 0.13 p= 0.6449	m= -0.02 r= 0.20 p= 0.4750	m= -0.01 r= 0.14 p= 0.6447	m= -0.02 r= 0.24 p= 0.4143	m= -0.03 r= 0.38 p= 0.1510
	T$_{mean}$	m= -0.03 r= 0.53 p= 0.0521	m= -0.03 r= 0.30 p= 0.3272	m= -0.01 r= 0.14 p= 0.6404	m= 0.02 r= 0.26 p= 0.3905	m= -0.02 r= 0.24 p= 0.3812	m= -0.02 r= 0.20 p= 0.4965	m= -0.02 r= 0.26 p= 0.3467	m= -0.02 r= 0.35 p= 0.2159	m= 0.01 r= 0.24 p= 0.3977	m= -0.02 r= 0.24 p= 0.3979	m= 0.02 r= 0.25 p= 0.3940	m= -0.02 r= 0.29 p= 0.3221	m= -0.02 r= 0.35 p= 0.1781
	Precipitation	m= 0.34 r= 0.63 p= 0.0279	m= 0.04 r= 0.10 p= 0.7557	m= 0.08 r= 0.27 p= 0.3888	m= -0.01 r= 0.05 p= 0.9581	m= -0.14 r= 0.10 p= 0.7527	m= -0.59 r= 0.67 p= 0.0173	m= -0.06 r= 0.03 p= 0.9199	m= -0.05 r= 0.09 p= 0.7764	m= -0.01 r= 0.02 p= 0.9511	m= 0.23 r= 0.27 p= 0.3997	m= -0.61 r= 0.56 p= 0.0569	m= -0.40 r= 0.53 p= 0.0786	m= -1.18 r= 0.35 p= 0.2690
Clanwilliam	T$_{max}$	m= -0.03 r= 0.24 p= 0.4713	m<0.01 r= 0.01 p= 0.9676	m= -0.06 r= 0.60 p= 0.0527	m= -0.03 r= 0.51 p= 0.1083	m= 0.03 r= 0.26 p= 0.4350	m<-0.01 r= 0.04 p= 0.9053	m= -0.05 r= 0.56 p= 0.0754	m= -0.03 r= 0.47 p= 0.1441	m= 0.05 r= 0.50 p= 0.1158	m= 0.02 r= 0.33 p= 0.3236	m= 0.03 r= 0.33 p= 0.3224	m<-0.01 r= 0.01 p= 0.9652	m= -0.01 r= 0.16 p= 0.6481
	T$_{min}$	m= -0.02 r= 0.25 p= 0.4644	m= -0.02 r= 0.17 p= 0.6156	m= -0.05 r= 0.58 p= 0.0610	m= -0.02 r= 0.28 p= 0.4051	m= -0.03 r= 0.51 p= 0.1094	m= -0.04 r= 0.72 p= 0.0129	m= -0.03 r= 0.52 p= 0.1007	m<-0.01 r= 0.02 p= 0.9622	m= 0.01 r= 0.23 p= 0.4872	m= -0.02 r= 0.55 p= 0.0799	m= -0.02 r= 0.26 p= 0.4329	m= -0.02 r= 0.30 p= 0.3736	m= -0.02 r= 0.80 p= 0.0034
	T$_{mean}$	m= -0.02 r= 0.25 p= 0.4601	m= -0.01 r= 0.07 p= 0.8375	m= -0.05 r= 0.62 p= 0.0408	m= -0.03 r= 0.45 p= 0.1654	m<-0.01 r= <0.01 p= 0.9896	m= -0.02 r= 0.50 p= 0.1209	m= -0.04 r= 0.75 p= 0.0081	m= -0.02 r= 0.38 p= 0.2427	m= 0.03 r= 0.44 p= 0.1745	m<-0.01 r= <0.01 p= 0.9940	m<0.01 r= 0.06 p= 0.8563	m= -0.01 r= 0.14 p= 0.6861	m= -0.01 r= 0.58 p= 0.0637
	Precipitation	m= 0.42 r= 0.51 p= 0.1065	m= -0.17 r= 0.45 p= 0.1598	m= 0.25 r= 0.46 p= 0.1544	m= 0.01 r= 0.01 p= 0.9777	m= -0.29 r= 0.21 p= 0.5400	m= -0.70 r= 0.49 p= 0.1240	m= -0.49 r= 0.23 p= 0.4884	m= -0.05 r= 0.05 p= 0.8858	m= 0.13 r= 0.24 p= 0.4821	m= -0.08 r= 0.19 p= 0.5825	m= -0.36 r= 0.52 p= 0.0977	m= -0.36 r= 0.57 p= 0.0696	m= -1.71 r= 0.43 p= 0.1853

Statistically significant inverse relationships are calculated between end of bloom timing and March T_{max} (r=0.71, p=0.0207), T_{min} (r=0.72, p=0.0177) and T_{mean} (r=0.78, p=0.0073) for Nieuwoudtville, all with negative rates of change ranging between 0.06-0.07d.°C^{-1} (Table 5.12). A statistically significant inverse relationship exists between end of bloom timing and T_{mean} during July, with a negative rate of change of 0.05d.°C^{-1} (r=0.69, p=0.0279; Table 5.12).

Significant inverse relationships are calculated between end of bloom timing and March and July, T_{max} (March: r=0.62, p=0.0097; July: r=0.62, p=0.0139) and T_{mean} (March: r=0.53, p=0.0340; July: r=0.61, p=00148) for Springbok, with rates of change that are both 0.06d.°C^{-1} for T_{max} and 0.05d.°C^{-1} and 0.04d.°C^{-1} for T_{mean}, respectively (Table 5.12). Statistically significant positive relationships are calculated between November T_{max} (r=0.51, p=0.0426) and T_{mean} (r= 0.51, p= 0.0460) and end of bloom timing for Springbok, with the same rate of change of 0.04d.°C^{-1} (Table 5.12). A significant inverse relationship is calculated between Springbok July T_{min} and end of bloom timing (similar to T_{max} and T_{mean} in July), with a rate of change of 0.04d.°C^{-1} (r=0.56, p=0.0307; Table 5.12). Statistically significant positive relationships are calculated between end of bloom timing and September T_{min} (0.06d.°C^{-1}; r=0.68, p=0.0037) and T_{mean} (0.05d.°C^{-1}; r=0.53, p=0.0361; Table 5.12). The statistically significant relationships between Springbok temperature variables and end of bloom timing that occur before August are all negative and the significant relationships that occur after September are all positive (Table 5.12). Annual T_{min} for Springbok has been decreasing significantly over time (r=0.36, p=0.0447; Appendix A.1). Decreases in T_{min} for Springbok between January and August have contributed to delays in end of bloom timing and decreases in T_{min} after September have contributed to advances in end of bloom timing in the Springbok subregion.

Significant relationships for Port Nolloth are calculated between end of bloom date and precipitation in September (r=0.45, p=0.0385) and November (r=0.60, p=0.0053; Table 5.12). For September, a positive rate of change of 0.12d.mm^{-1} is calculated, and for November an inverse rate of 0.13d.mm^{-1} (Table 5.12). Statistically significant relationships are calculated between precipitation during January (r=0.63, p=0.0279) and June (r=0.67, p=0.0173) and end of bloom timing for Lambertsbaai Nortier at rates of positive changes of 0.34d.mm^{-1} and inverse changes of 0.59d.mm^{-1}, respectively (Table 5.12).

A statistically significant inverse relationship is calculated between end of bloom timing and T_{min} during June (r=0.72, p=0.0129) for Clanwilliam, at a rate of change of 0.04d.°C^{-1} (Table 5.12). Another significant inverse relationship is calculated between annual T_{min} and end of bloom timing for Clanwilliam, at a rate of change of 0.02d.°C^{-1} (r=0.80, p=0.0034; Table 5.12). Statistically significant inverse relationships are calculated between end of bloom timing and T_{mean} during March (0.05d.°C^{-1}; r=0.62, p=0.0408) and July (0.04d.°C^{-1}; r=0.75, p=0.0081) for Clanwilliam (Table 5.12).

5.9 Multiple Regression Analysis

As mentioned in section 4.3.7, when conducting multiple regression analysis, issues related to multicollinearity needs to be considered. The use of the variable T_{mean} was avoided when T_{max} and T_{min} were already considered, seeing as the average temperature already contains traces of both mentioned variables. Another variable that was avoided was humidity, seeing as it is driven by temperature and precipitation, which were already considered within the multiple regression analysis. The multiple regression analysis was conducted in a stepwise manner, and when variables were added that only slightly changed the R^2 value, multicollinearity was identified and assessed accordingly (Huang and Hao, 2018).

Before the multiple regression analysis was performed, the climatic factors for months influencing flowering phenology of each station had to be assessed to establish the strongest correlations. The two weather stations that displayed statistically significant relationships and strong correlation values were Nieuwoudtville and Clanwilliam for first flowering phenology (BBCH 60-61). For Nieuwoudtville, calculations reveal that T_{max} during June (r=0.65) and November (r=0.70) together with total precipitation during the early winter month of May (r=0.68) have strong correlations that are statistically significant with first flowering phenology (Table 5.10). In Nieuwoudtville, 83.04% of the variability in FFD can be explained by this combination of climate variables in the following statistically significant model (p=0.0019).

$$\underline{\textit{Nieuwoudtville Flowering Date}} = 57.41 - 6.83(T_{max}, \textit{June}) + 1.35\ (T_{max}, \textit{Nov}) - 0.19(\textit{Precip, May})$$

For Clanwilliam, calculations reveal that T_{max} (r=0.65) and T_{min} (r=0.57) during June together with total precipitation during May (r=0.73) are all statistically significantly correlated to first flowering phenology (Table 5.10). For Clanwilliam, 69.48% of the variability in FFD can be explained by this statistically significant (p=0.0062) regression model that produced the following formula:

$$\underline{\textit{Clanwilliam Flowering Date}} = 180.7 - 0.45(\textit{Precip, May}) + 2.33(T_{max}, \textit{June}) - 1.47(T_{min}, \textit{June})$$

5.10 Influence of Precipitation Timing on Flowering Dates

5.10.1 Onset of Rain

Statistically significant positive correlations are calculated between first flowering (BBCH 60-61) and the onset of rain timing for six Namaqualand subregions (Table 5.13). Cape Columbine is the only location where no statistically significant relationship between onset of rain and first flowering is calculated (Table 5.13). The strongest relationship between first flowering timing (BBCH 60-61) and the onset of rain is calculated for Clanwilliam at $1.55d.d_{OR}^{-1}$ (r=0.76, p=0.0016; Table 5.13).

Table 5.13: Onset of Rain Julian dates correlation with three BBCH flowering groups. Highlighted blocks indicate statistically significant correlations.

Weather Stations	BBCH 60-61	BBCH 63-65	BBCH 67-69
Cape Columbine	m= 0.37 r= 0.21 p= 0.2181	m= 0.01 r= 0.01 p= 0.9699	m= 0.45 r= 0.27 p= 0.2285
Vredendal	m= 0.73 r= 0.35 p= 0.0351	m= 0.70 r= 0.33 p= 0.0265	m= 0.09 r= 0.07 p= 0.7479
Nieuwoudtville	m= 1.46 r= 0.62 p= 0.0316	m= -0.11 r= 0.05 p= 0.8549	m= 0.02 r= 0.02 p= 0.9667
Springbok	m= 1.59 r= 0.61 p= 0.0034	m<-0.01 r= 0.001 p= 0.9940	m= 0.24 r= 0.22 p= 0.5006
Port Nolloth	m= 0.97 r= 0.46 p= 0.0098	m= 1.24 r= 0.46 p= 0.0069	m= 0.70 r= 0.34 p= 0.1849
Lambertsbaai Nortier	m= 1.29 r= 0.57 p= 0.0086	m= 0.67 r= 0.35 p= 0.0935	m= 0.29 r= 0.28 p= 0.3853
Clanwilliam	m= 1.55 r= 0.76 p= 0.0016	m= 0.44 r= 0.24 p= 0.3345	m= 0.40 r= 0.30 p= 0.3663

Vredendal (0.70d.d_{OR}^{-1}; r=0.33, p=0.0265) and Port Nolloth (1.24d.d_{OR}^{-1}; r=0.46, p=0.0069) are the only two subregions with statistically significant positive relationships between full bloom timing (BBCH 63-65) and the onset of rain (Table 5.13). No statistically significant relationships are calculated between the end of bloom date (BBCH 67-69) and the timing of the onset of rain for any Namaqualand subregions (Table 5.13). Every relationship between end of bloom timing and onset of rain timing demonstrates a positive rate of change (Table 5.13). The overall positive relationship between flowering timing and the onset of the rainy season therefore indicates that if the onset of the rainy season is advanced, so too will the flowering season, and vice versa.

5.10.2 End of the Rainy Season

None of the calculations between first flowering timing (BBCH 60-61) and timing for the end of the rainy season are statistically significant (Table 5.14). For every subregion, besides Port Nolloth, a tentative inverse relationship between the timing of the end of the rainy season and first flowering timing is calculated (Table 5.14).

Table 5.14: End of rainy season Julian dates correlation with the three BBCH flowering groups

Weather Stations	**BBCH 60-61**	**BBCH 63-65**	**BBCH 67-69**
Cape Columbine	m= -0.44 r= 0.17 p= 0.3078	m= 0.33 r= 0.10 p= 0.5220	m= -0.78 r= 0.31 p= 0.1882
Vredendal	m= -0.03 r= 0.01 p= 0.9639	m= 0.24 r= 0.05 p= 0.7279	m= -0.63 r= 0.20 p= 0.4085
Nieuwoudtville	m= -0.80 r= 0.24 p= 0.4615	m= -0.06 r= 0.02 p= 0.9375	m= -1.46 r= 0.38 p= 0.2828
Springbok	m= -0.36 r= 0.14 p= 0.5904	m= 0.50 r= 0.21 p= 0.3529	m= -1.32 r= 0.50 p= 0.1448
Port Nolloth	m= 0.92 r= 0.37 p= 0.0994	m= 0.36 r= 0.08 p= 0.7203	m= -1.59 r= 0.48 p= 0.0995
Lambertsbaai Nortier	m= -0.18 r= 0.05 p= 0.8493	m= 1.13 r= 0.36 p= 0.0850	m= -1.42 r= 0.34 p= 0.2726
Clanwilliam	m= -0.35 r= 0.10 p= 0.7402	m= 0.08 r= 0.03 p= 0.9189	m= -2.41 r= 0.66 p= 0.0396

For every weather station besides Nieuwoudtville, a tentative positive relationship between end of the rainy season and full bloom timing is calculated (Table 5.14). None of the relationships between full bloom timing and the end of the rainy season timing are significant (Table 5.14).

An inverse relationship has been calculated between end of rainy season timing and end of bloom (BBCH 67-69) for every Namaqualand subregion (Table 5.14). The only statistically significant inverse relationship that exists is calculated for Clanwilliam (r=0.66, p=0.0369), at $2.41d.d_{ER}^{-1}$ (Table 5.14).

5.11 SPI and Flowering Phenology

Calculations of correlations between first flowering timing (BBCH 60-61) and the different monthly SPI values for all the weather stations reveal inverse relationships for 15 of the 20 tests, although only eight of the relationships are statistically significant (Table 5.15). The negative relationships between the monthly SPI averages and first flowering range from $<0.01\text{-}0.04d.SPI^{-1}$ (Table 5.15).

Table 5.15: Correlation between weather station SPI values (for the different scales of monthly assessments) and flowering timing. Highlighted blocks indicate calculated statistically significant correlations.

Weather Stations	SPI Analysis Scale	BBCH 60-61	BBCH 63-65	BBCH 67-69
Cape Columbine	3-Month	m<-0.01 r= 0.08 p= 0.6271	m= -0.01 r= 0.19 p= 0.2178	m<-0.01 r= 0.15 p= 0.5136
	6-Month	m<0.01 r= 0.01 p= 0.9591	m= -0.02 r= 0.20 p= 0.1796	m<0.01 r= 0.09 p= 0.7021
	12-Month	m<0.01 r= 0.02 p= 0.9137	m= -0.03 r= 0.19 p= 0.2270	m<0.01 r= <0.01 p= 0.9967
	24-Month	m<-0.01 r= 0.01 p= 0.9685	m= -0.05 r= 0.17 p= 0.2851	m= -0.01 r= 0.23 p= 0.3394
Vredendal	3-Month	m<-0.01 r= 0.01 p= 0.9509	m= -0.01 r= 0.18 p= 0.2244	m<0.01 r= 0.12 p= 0.6143
	6-Month	m<0.01 r= 0.10 p= 0.5404	m= -0.02 r= 0.21 p= 0.1683	m<0.01 r= 0.02 p= 0.9191
	12-Month	m= 0.01 r= 0.18 p= 0.2789	m= -0.03 r= 0.19 p= 0.2169	m<-0.01 r= 0.08 p= 0.7271
	24-Month	m<0.01 r= 0.09 p= 0.5843	m= -0.05 r= 0.18 p= 0.2358	m<0.01 r= 0.01 p= 0.9814
Springbok	3-Month	m= -0.02 r= 0.52 p= 0.0056	m= -0.01 r= 0.17 p= 0.4226	m= -0.01 r= 0.19 p= 0.5461
	6-Month	m= -0.03 r= 0.68 p= 0.0007	m= -0.01 r= 0.21 p= 0.3065	m= -0.01 r= 0.15 p= 0.6390
	12-Month	m= -0.04 r= 0.76 p= 0.0001	m= -0.01 r= 0.24 p= 0.2626	m= -0.01 r= 0.24 p= 0.4569
	24-Month	m= -0.03 r= 0.55 p= 0.0148	m= -0.02 r= 0.35 p= 0.1059	m= -0.02 r= 0.36 p= 0.2473
Lambertsbaai Nortier	3-Month	m= -0.02 r= 0.46 p= 0.0413	m<0.01 r= 0.05 p= 0.8061	m= -0.01 r= 0.28 p= 0.3849
	6-Month	m= -0.03 r= 0.50 p= 0.0256	m<0.01 r= 0.03 p= 0.8949	m= -0.01 r= 0.23 p= 0.4756
	12-Month	m= -0.04 r= 0.59 p= 0.0075	m<-0.01 r= 0.02 p= 0.9141	m= -0.01 r= 0.20 p= 0.5407
	24-Month	m= -0.02 r= 0.36 p= 0.1478	m<-0.01 r<0.01 p= 0.9854	m= -0.02 r= 0.29 p= 0.3664
Clanwilliam	3-Month	m= -0.02 r= 0.63 p= 0.0168	m<-0.01 r= 0.04 p= 0.8594	m= -0.01 r= 0.35 p= 0.2956
	6-Month	m= -0.02 r= 0.49 p= 0.0787	m<0.01 r= 0.02 p= 0.9320	m= -0.01 r= 0.26 p= 0.4406
	12-Month	m= -0.02 r= 0.45 p= 0.1213	m= -0.01 r= 0.15 p= 0.5580	m= -0.01 r= 0.24 p= 0.4728
	24-Month	m= -0.01 r= 0.12 p= 0.7124	m<-0.01 r= 0.08 p= 0.7749	m= -0.02 r= 0.27 p= 0.4503

Statistically significant inverse relationships are calculated between the 3-, 6-, 12- and 24-month SPI analysis and first flowering timing for Springbok, with p-values ranging from 0.0001-0.0148 and correlation coefficients between 0.52-0.76 (Table 5.15). For Lambertsbaai Nortier, statistically significant inverse relationships are calculated between 3-, 6- and 12-month SPI analysis and first flowering at negative rates of changes of 0.02d.SPI^{-1} (r=0.46, p=0.0413), 0.03d.SPI^{-1} (r=0.50, p=0.0256) and 0.04d.SPI^{-1} (r=0.59, p=0.0075) respectively (Table 5.15). A statistically significant inverse relationship is calculated between 3-month SPI and first flowering timing for Clanwilliam at a negative rate of change of 0.02d.SPI^{-1} (r=0.63, p=0.0168; Table 5.15). Therefore, if SPI values are increasing over time (subregions become wetter), first flowering timing will advance, and if SPI values are decreasing over time (subregions become drier), first flowering timing will be delayed. The 24-month SPI in Springbok has been decreasing at a statistically significant rate of 0.06 per year (r=0.43, p=0.0425; Table 5.4). The decrease in 24-month SPI has therefore contributed to delays in first flowering timing in the respective subregion.

Inverse relationships are calculated for 17 of the 20 tests for the correlations between full bloom timing (BBCH 63-65) and the different monthly SPI values but none of the correlations are statistically significant (Table 5.15). Similarly, inverse correlations are calculated for 15 of the 20 tests for the correlations between the different SPI values and end of bloom timing, and none of the correlations are statistically significant (Table 5.15).

5.12 Seasonal Influence on Flowering Phenology

The relationship between climate variables and end of bloom (BBCH 67-69) flowering timing demonstrates a pattern of significance over different seasons. Strong seasonal significance patterns during the winter months of June, July and August and during the spring months of September, October and November were observed (Table 5.12).

Table 5.16: End of flowering timing (BBCH 67-69) and seasonal linear regression analysis.

Weather Stations	**Winter Ave T_{max} (June, July, Aug)**	**Winter Ave T_{min} (June, July, Aug)**	**Winter Ave T_{mean} (June, July, Aug)**	**Winter Total Precip (June, July, Aug)**	**Spring Ave T_{max} (Sept, Oct, Nov)**	**Spring Ave T_{min} (Sept, Oct, Nov)**	**Spring Ave T_{mean} (Sept, Oct, Nov)**	**Spring Total Precip (Sept, Oct, Nov)**
Cape Columbine	m= -0.02 r= 0.53 p= 0.0141	m= -0.01 r= 0.51 p= 0.0186	m= -0.02 r= 0.55 p= 0.0095	m= -1.05 r= 0.49 p= 0.0226	m= -0.02 r= 0.48 p= 0.0270	m= -0.01 r= 0.50 p= 0.0220	m= -0.01 r= 0.41 p= 0.0619	m= -0.15 r= 0.15 p= 0.5059
Vredendal	m= -0.03 r= 0.44 p= 0.0455	m= -0.01 r= 0.21 p= 0.3678	m= -0.02 r= 0.46 p= 0.0349	m= -0.70 r= 0.36 p= 0.1124	m= -0.02 r= 0.37 p= 0.0995	m= -0.01 r= 0.15 p= 0.5094	m= -0.01 r= 0.35 p= 0.1211	m= 0.16 r= 0.23 p= 0.3097
Nieuwoudtville	m= -0.03 r= 0.40 p= 0.2472	m= -0.03 r= 0.36 p= 0.3004	m= -0.03 r= 0.48 p= 0.1649	m= -0.78 r= 0.12 p= 0.7503	m= 0.06 r= 0.73 p= 0.0167	m<0.01 r= 0.07 p= 0.8555	m= 0.03 r= 0.51 p= 0.1329	m= -0.85 r= 0.55 p= 0.0965
Springbok	m= -0.04 r= 0.49 p= 0.0555	m= -0.01 r= 0.20 p= 0.4479	m= -0.02 r= 0.38 p= 0.1476	m= -0.78 r= 0.22 p= 0.4855	m= 0.02 r= 0.41 p= 0.1189	m= 0.04 r= 0.76 p= 0.0007	m= 0.03 r= 0.67 p= 0.0043	m= -0.05 r= 0.05 p= 0.8842
Port Nolloth	m= -0.01 r= 0.19 p= 0.4190	m= -0.01 r= 0.12 p= 0.5696	m= -0.01 r= 0.20 p= 0.3756	m= -0.05 r= 0.06 p= 0.8119	m= -0.01 r= 0.27 p= 0.2301	m= -0.01 r= 0.23 p= 0.3092	m= -0.01 r= 0.37 p= 0.0964	m= 0.01 r= 0.02 p= 0.9184
Lambertsbaai Nortier	m= -0.03 r= 0.38 p= 0.1595	m= -0.01 r= 0.17 p= 0.5346	m= -0.02 r= 0.29 p= 0.2931	m= -0.70 r= 0.27 p= 0.3848	m<-0.01 r= 0.07 p= 0.8029	m= -0.02 r= 0.26 p= 0.3339	m= -0.01 r= 0.20 p= 0.4645	m= -0.40 r= 0.37 p= 0.2377
Clanwilliam	m= -0.03 r= 0.47 p= 0.1445	m= -0.02 r= 0.63 p= 0.0366	m= -0.03 r= 0.66 p= 0.0268	m= -1.24 r= 0.39 p= 0.2352	m= 0.04 r= 0.59 p= 0.0577	m= -0.01 r= 0.30 p= 0.3740	m= 0.01 r= 0.30 p= 0.3659	m= -0.32 r= 0.33 p= 0.3273

Statistically significant relationships were calculated between every climate variable during both winter and spring and end of bloom timing for Cape Columbine (Table 5.16). All the calculated relationships demonstrate inverse relationships between seasonal climate variables and end of bloom timing (Table 5.16). The greatest rate of change is calculated for total winter precipitation at a negative rate of change of 1.05d.mm^{-1} (r=0.49, p=0.0226; Table 5.16). The strongest correlation is calculated for winter average T_{mean} (r=0.55, p=0.0095; Table 5.16). Cape Columbine winter average T_{max}, T_{min} and T_{mean} have all been increasing at statistically significant rates over time (Table 5.6). The winter climate variables becoming warmer over time has therefore contributed to end of flowering timing being advanced by 0.01-0.02d.yr^{-1} (Table 5.16). The calculated inverse relationship between end of bloom timing and the spring climate variables in Cape Columbine, have rates of changes of 0.02d.°C^{-1} (T_{max}: r=0.48, p=0.0270), 0.01d.°C^{-1} (T_{min}: r=0.50, p=0.0220) and 0.01d.°C^{-1} (T_{mean}: r=0.41, p=0.0619; Table 5.16) respectively. Spring average T_{max}, T_{min} and T_{mean} in Cape Columbine have all also been increasing significantly over time (Table 5.6). The warmer spring temperatures have therefore contributed to advanced end of bloom dates. Overall, the calculated strengths of correlations between all the Cape Columbine climate variables during the winter months demonstrate stronger correlations when compared to the correlation strengths of the climate variables during spring (Table 5.16).

Inverse relationships are calculated between all the seasonal climate variables and end of flowering timing for Vredendal except for spring precipitation (Table 5.16). Statistically significant inverse relationships are calculated between winter average T_{max} and average T_{mean} with end of flowering timing, at negative rates of changes of 0.03d.°C^{-1} (r=0.44, p=0.0455) and 0.02d.°C^{-1} (r=0.46, p=0.0349) respectively (Table 5.16). Winter average T_{max} and T_{mean} in Vredendal have both been increasing at statistically significant positive rates of 0.03°C.yr^{-1} (r=0,50, p<0.0001) and 0.02°C.yr^{-1} (r=0.40 p=0.0016) respectively (Table 5.6). The increase in these two temperature variables over time has therefore contributed to significant advances in the end of flowering timing of Namaqualand daisies.

The calculated relationships between the seasonal climate variables and end of bloom timing for Nieuwoudtville demonstrates statistically insignificant inverse relationships for all the winter climate variables (Table 5.16). Positive relationships are calculated between spring temperature variables and end of bloom timing except for the inverse correlation that is calculated between total precipitation during spring and end of bloom timing (Table 5.16). The only calculated statistically significant correlation between end of bloom timing and the seasonal climate variables of Nieuwoudtville is average spring T_{max} (0.06d.°C^{-1}; r=0.73, p=0.0167; Table 5.16).

Inverse relationships are calculated between winter and spring climate variables and end of bloom timing for all the Springbok climate variables except for the temperature variables during spring

(Table 5.16). Statistically significant positive correlations are calculated between spring T_{min} and T_{mean} and end of bloom timing at rates of 0.04d.°C^{-1} (r=0.76, p=0.0007) and 0.03d.°C^{-1} (r=0.67, p=0.0043) respectively (Table 5.16).

No statistically significant relationships are calculated between winter and spring climate and end of bloom timing for Port Nolloth (Table 5.16). All the calculated correlations for the winter and spring climate variables are inverse except for spring precipitation (Table 5.16).

Calculations indicated that none of the seasonal climate variables for Lambertsbaai Nortier are statistically significantly related to end of bloom timing (Table 5.16). The seasonal analysis of the relationship between the climate variables in Lambertsbaai Nortier and end of bloom timing reveals inverse relationships for every climate variable during winter and spring (Table 5.16).

Statistically significant inverse relationships are calculated between winter T_{min} and T_{mean} and end of bloom timing for Clanwilliam. The significant relationships are changing at rates of 0.02d.°C^{-1} (r=0.63, p=0.0366) and 0.03d.°C^{-1} (r=0.66, p=0.0268), respectively (Table 5.16).

5.13 Frost Changes and the Influence on Daisy Phenological phases

5.13.1 Number of Frost Events After First Flowering

Nieuwoudtville has the largest ($\bar{x}$=4.33, σ=5.21) and Springbok the smallest ($\bar{x}$=0.33, σ=0.52) average number of frost events (T_{min} ≤0°C) occurring after first flowering (Table 5.17). Nieuwoudtville, with the average of 31.75 (σ=14.97), has the largest average number of frost events (T_{min} ≤4°C) occurring after first flowering (Table 5.17). Port Nolloth has the lowest average of 0.59 (σ=1.22) frost events occurring after first flowering (Table 5.17). Namaqualand daisies growing in the Nieuwoudtville subregion therefore has the greatest risk of frost damage. For many of the weather stations, the standard deviation for the number of frost events that are occurring after first flowering in the subregion is larger than the mean itself (Table 5.17).

Table 5.17: Average number and standard deviation of frost events that occur after first flowering events.

Weather Stations	**Average # of frost events after BBCH 60-61 (T_{min} ≤0°C)**	**Average # of frost events after BBCH60-61 (T_{min} ≤4°C)**
Cape Columbine	Insufficient Data	Insufficient Data
Vredendal	Insufficient Data	6.19 (σ= 4.27)
Nieuwoudtville	4.33 (σ= 5.21)	31.75 (σ= 14.97)
Springbok	0.33 (σ= 0.52)	9.28 (σ= 5.91)
Port Nolloth	Insufficient Data	0.59 (σ= 1.22)
Lambertsbaai Nortier	Insufficient Data	2.09 (σ= 3.37)
Clanwilliam	Insufficient Data	5.43 (σ= 4.07)

A statistically significant increase is calculated for the number of frost days (T_{min} ≤0°C) that occur after first flowering in Nieuwoudtville at a rate of 0.83fe.yr^{-1} (r=0.62, p=0.0328; Table 5.18). Statistically insignificant increases are calculated for the number of frost events that occur after first flowering in Springbok at a tentative rate of change of 0.01fe.yr^{-1} (r= 0.11, p= 0.8335; Table 5.18). It can therefore be concluded that frost events that have been occurring after first flowering, for T_{min} ≤0°C, for the two assessed weather stations, have been increasing over time.

Table 5.18: Average and standard deviation of frost events occurring after first flowering for T_{min} ≤0°C and T_{min} ≤4°C. Highlighted blocks indicate statistically significant correlations.

Weather Stations	**# of frost events after BBCH 60-61 (T_{min} ≤ 0°C)**	**# of frost events after BBCH 60-61 (T_{min} ≤ 4°C)**
Cape Columbine	Insufficient Data	Insufficient Data
Vredendal	Insufficient Data	m<-0.01 r= 0.01 p= 0.9480
Nieuwoudtville	m= 0.83 r= 0.62 p= 0.0328	m= 2.21 r= 0.57 p= 0.0524
Springbok	m= 0.01 r= 0.11 p= 0.8335	m= 0.06 r= 0.08 p= 0.7046
Port Nolloth	Insufficient Data	m<0.01 r= 0.01 p= 0.9426
Lambertsbaai Nortier	Insufficient Data	m= -0.10 r= 0.23 p= 0.3009
Clanwilliam	Insufficient Data	m= 0.11 r= 0.12 p= 0.6854

None of the calculated changes in the number of frost events (T_{min} ≤4°C) occurring after first flowering are statistically significant (Table 5.18). The greatest rate of change and strongest correlation with an increase in the number of frost events that occur after first flowering is calculated for Nieuwoudtville with an increase of 2.21fe.yr^{-1} (r=0.57, p=0.0524; Table 5.18).

5.13.2 Frost Risk for First Flowering

Frost risk, for the parameter T_{min} ≤0°C, could only be calculated for Vredendal, Springbok and Nieuwoudtville due to a lack of frost events occurring in the rest of Namaqualand. A statistically significant advance of 0.26d.yr^{-1} is calculated for first flowering (Figure 5.4). The calculated changes in last frost Julian dates (T_{min} ≤0°C) are not statistically significant (Table 5.8). However, according to Figure 5.7, last frost events (T_{min} ≤0°C) have been occurring after first flowering since 1985 in Springbok, 1998 in Nieuwoudtville and 2014 in Vredendal and are continuing to occur later in the year. Although not statistically significant, last frost events are occurring after first flowering and tentatively occurring later in the year, while first flowering is advancing, therefore indicating that frost risks of T_{min} ≤0°C are tentatively increasing in the respective Namaqualand subregions over time.

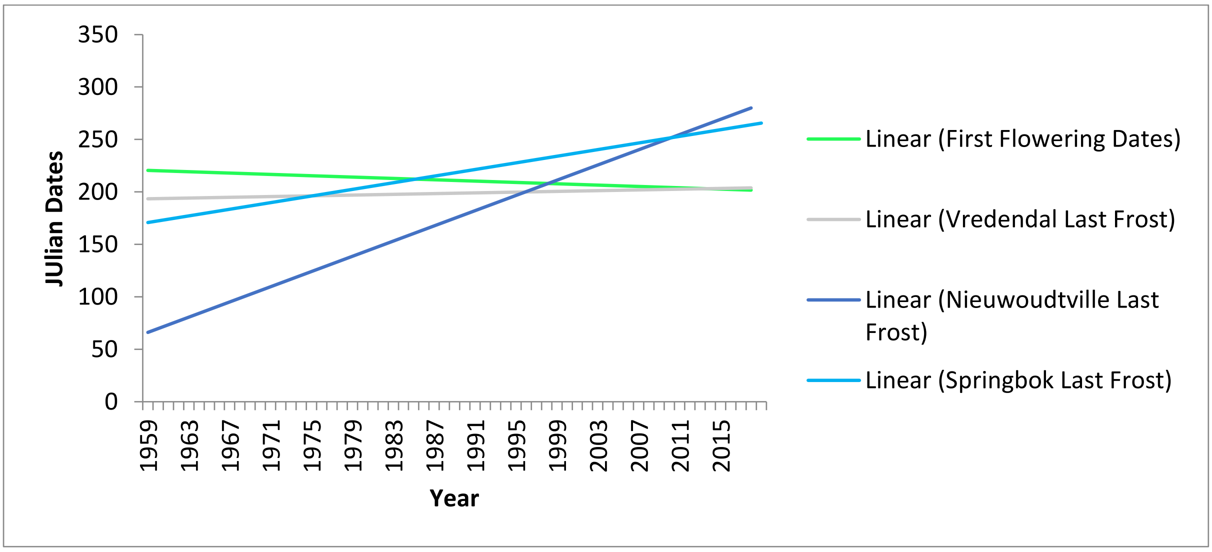

Figure 5.7: Trends in last frost dates for T_{min} ≤0°C and first flowering.

Last frost Julian dates (T_{min} ≤4°C) were increasing tentatively, i.e. becoming later in the year for Nieuwoudtville, Lambertsbaai Nortier and Clanwilliam, while last frost Julian dates (T_{min} ≤4°C) were decreasing tentatively, i.e. becoming earlier in the year for Vredendal, Springbok and Port Nolloth (Table 5.9). For Lambertsbaai Nortier and Clanwilliam, last frost Julian dates (T_{min} ≤4°C) were occurring after first flowering events and diverging from first flowering over time (Figure 5.8). Frost risks are therefore increasing in these subregions. Vredendal and Springbok last frost Julian dates were occurring after first flowering and converging over time (Figure 5.8). Although Vredendal and Springbok last frost Julian dates were advancing over time (Table 5.9), frost risk in these subregions are still increasing due to first flowering advancing at a greater rate than the advance in last frost Julian dates of Vredendal and Springbok (Table 5.9; Figure 5.4). Port Nolloth last frost Julian dates were occurring before first flowering and were diverging over time (Figure 5.8). Therefore, no frost risks are calculated for Port Nolloth. Last frost events in Nieuwoudtville have been occurring after first flowering since 1978, and these trends are diverging (Figure 5.8). A statistically significant increase in last frost Julian dates was calculated for Nieuwoudtville ($2.82d.yr^{-1}$; r=0.57, p=0.0253), i.e. last frost events are occurring later in the year (Table 5.9). A significant increase in frost risk is therefore calculated for Nieuwoudtville.

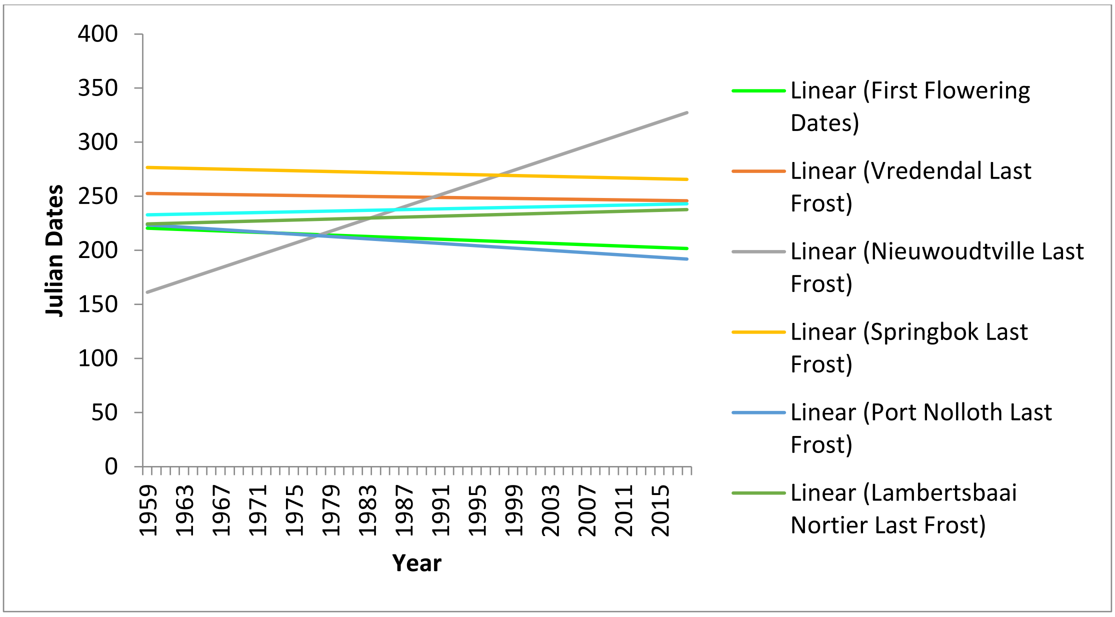

Figure 5.8: Trends in last frost dates for $T_{min} \leq 4°C$ and frst flowering.

A pattern regarding first flowering emerged from the data. Of 130 years of climate records that had frost events and FFD, 70 of those years demonstrated that first flowering occurs within four days of a frost event. A categorical statement cannot be made about this trend seeing that first flowering cannot be linked to first or last frost timing. This relationship is likely due to the plants' physiological reaction to frost events. However, if first flowering is linked to specific frost events, it cannot currently be determined.

5.13.3 Frost Influence on Full Bloom Timing

The number of frost days, where $T_{min} \leq 0°C$, and its influence on full bloom timing of Namaqualand daisies could only be calculated for Vredendal, Nieuwoudtville and Springbok, due to a lack of years where $T_{min} \leq 0°C$ (Table 5.19). No statistically significant relationships are calculated between full bloom timing and the number of frost days where $T_{min} \leq 0°C$ (Table 5.19).

Table 5.19: Number of Frost days, Last Frost Date and Number of Frost Events Occurring After First Flowering correlation with Full Bloom Timing (BBCH 63-65). Highlighted blocks indicate statistically significant correlations.

BBCH 63-65	**T_{min} ≤ 0°C**			**T_{min} ≤ 4°C**		
Weather Stations	**Number of Frost days**	**Last Frost Date**	**No. of Frost Events after First flowering**	**Number of Frost Days**	**Last Frost Date**	**No. of Frost Events after First flowering**
Cape Columbine	Insufficient Data	Insufficient Data	Insufficient Data	Insufficient Data	Insufficient Data	Insufficient Data
Vredendal	m= 0.03 r= 0.71 p= 0.1750	m= 0.08 r= 0.16 p= 0.7963	Insufficient Data	m= 0.10 r= 0.16 p= 0.2846	m= -0.07 r= 0.05 p= 0.7423	m= -0.06 r= 0.21 p= 0.2418
Nieuwoudtville	m= -0.07 r= 0.16 p= 0.5457	m= -0.28 r= 0.13 p= 0.6236	m= -0.06 r= 0.20 p= 0.5309	m= -0.28 r= 0.25 p= 0.3548	m= -0.09 r= 0.06 p= 0.8182	m= -0.46 r= 0.58 p= 0.0473
Springbok	m= 0.01 r= 0.25 p= 0.6316	m= -0.47 r= 0.28 p= 0.5934	m= -0.01 r= 0.54 p= 0.2643	m= 0.12 r= 0.26 p= 0.1734	m= 0.13 r= 0.07 p= 0.7263	m= -0.11 r= 0.30 p= 0.1499
Port Nolloth	Insufficient Data	Insufficient Data	Insufficient Data	m= 0.06 r= 0.24 p= 0.1859	m= 0.06 r= 0.03 p= 0.8907	m= -0.01 r= 0.11 p= 0.5924
Lambertsbaai Nortier	Insufficient Data	Insufficient Data	Insufficient Data	m= -0.06 r= 0.20 p= 0.3307	m= -1.01 r= 0.41 p= 0.0367	m= -0.08 r= 0.35 p= 0.1122
Clanwilliam	Insufficient Data	Insufficient Data	Insufficient Data	m= 0.05 r= 0.03 p= 0.9067	m= -0.23 r= 0.22 p= 0.3811	m= -0.13 r= 0.58 p= 0.0300

None of the calculated relationships between last frost Julian dates (T_{min} ≤0°C) and full bloom timing are statistically significant (Table 5.19). Statistically insignificant inverse correlations are calculated between the number of frost events (T_{min} ≤0°C) occurring after first flowering and full bloom timing in Nieuwoudtville and Springbok (Table 5.19).

None of the calculated relationships between the total number of frost days where T_{min} ≤4°C, and full bloom timing are statistically significant (Table 5.19). Positive relationships between the total number of frost days where T_{min} ≤4°C and full bloom timing are calculated for Vredendal, Springbok, Port Nolloth and Clanwilliam (Table 5.19). Inverse relationships between the number of frost days, for the frost parameter of T_{min} ≤4°C, and full bloom timing are calculated for Nieuwoudtville and Lambertsbaai Nortier (Table 5.19).

Inverse relationships between last frost (T_{min} ≤4°C) Julian dates and full bloom timing are calculated for Vredendal, Nieuwoudtville, Lambertsbaai Nortier and Clanwilliam (Table 5.19). The calculated relationship between last frost Julian dates and full bloom flowering timing for Lambertsbaai Nortier is statistically significant at a rate of change of 1.01d.F_{LD}^{-1} (r=0.41, p=0.0367; Table 5.19).

Inverse relationships are calculated between full bloom flowering timing and the number of frost events (T_{min} ≤4°C) occurring after first flowering for every weather station (Table 5.19). Statistically significant inverse relationships between full bloom flowering timing and the number of frost events occurring after first flowering timing are calculated for Nieuwoudtville and Clanwilliam at rates of changes of 0.46d.F_{AF}^{-1} (r=0.58, p=0.0473) and 0.13d.F_{AF}^{-1} (r=0.58, p=0.0300) respectively (Table 5.19).

5.13.4 Frost Influence on End of Bloom Timing

The Number of frost days, last frost Julian dates, and the number of frost events that occur after first flowering, for the frost threshold of T_{min} ≤0°C, can only be correlated with end of bloom Julian dates for Nieuwoudtville and Springbok (Table 5.20).

Table 5.20: Number of Frost days, Last Frost Date and Number of Frost Events Occurring After First Flowering correlation with End of Bloom Timing (BBCH 67-69). Highlighted blocks indicate statistically significant correlations.

BBCH 67-69	**T_{min} ≤ 0°C**			**T_{min} ≤ 4°C**		
Weather Stations	**Number of Frost days**	**Last Frost Date**	**No of Frost Events after First flowering**	**Number of Frost Days**	**Last Frost Date**	**No of Frost Events after First flowering**
Cape Columbine	Insufficient Data	Insufficient Data	Insufficient Data	Insufficient Data	Insufficient Data	Insufficient Data
Vredendal	Insufficient Data	Insufficient Data	Insufficient Data	m= 0.05 r= 0.13 p= 0.5831	m= 0.09 r= 0.07 p= 0.7641	m= -0.04 r= 0.18 p= 0.4668
Nieuwoudtville	m= 0.16 r= 0.32 p= 0.3730	m= 0.98 r= 0.34 p= 0.3292	m= 0.02 r= 0.10 p= 0.7979	m= 0.34 r= 0.27 p= 0.4514	m= -0.09 r= 0.05 p= 0.8885	m= -0.24 r= 0.33 p= 0.3917
Springbok	Insufficient Data	m= -1.14 r= 0.76 p= 0.2398	m= -0.02 r= 0.78 p= 0.2224	m= 0.04 r= 0.13 p= 0.6503	m= -0.11 r= 0.07 p= 0.8091	m= -0.04 r= 0.11 p= 0.7082
Port Nolloth	Insufficient Data	Insufficient Data	Insufficient Data	m= 0.01 r= 0.08 p= 0.7737	m= 1.15 r= 0.60 p= 0.0172	m= 0.02 r= 0.23 p= 0.4770
Lambertsbaai Nortier	Insufficient Data	Insufficient Data	Insufficient Data	m= 0.09 r= 0.24 p= 0.3793	m= -0.40 r= 0.26 p= 0.3547	m= 0.04 r= 0.15 p= 0.5972
Clanwilliam	Insufficient Data	Insufficient Data	Insufficient Data	m= 0.17 r= 0.44 p= 0.1748	m= 0.09 r= 0.07 p= 0.8463	m= -0.01 r= 0.04 p= 0.9142

No statistically significant relationships are calculated between last frost (T_{min} ≤0°C) Julian dates, end of bloom timing or the number of frost events (T_{min} ≤0°C) occurring after first flowering and end of bloom timing (Table 5.20). For the T_{min} ≤4°C frost parameter, the calculated relationships between the number of frost days and end of bloom timing are positive for all the analysed weather stations (Table 5.20). However, none of the calculated relationships are statistically significant (Table 5.20).

The calculated relationships between last frost (T_{min} ≤4°C) Julian dates and end of bloom timing are inverse and statistically insignificant for Nieuwoudtville, Springbok and Lambertsbaai Nortier (Table 5.20). Positive statistically insignificant relationships are calculated between last frost (T_{min} ≤4°C) Julian dates and end of bloom timing for Vredendal, Port Nolloth and Clanwilliam (Table 5.20). The calculated correlation between end of bloom timing and last frost Julian dates for Port Nolloth is statistically significant with a rate of change of $1.15d.F_{LD}^{-1}$ (r=0.60, p=0.0172; Table 5.20).

None of the calculated relationships between the number of frost (T_{min} ≤4°C) events occurring after first flowering and end of bloom timing are statistically significant for any of the assessed weather stations (Table 5.20).

5.14 Local Perceptions

Digitized newspaper and social media records were collected to compile the phenological flowering record. These accounts were generated by locals and non-specialists and reflects their perceptions of the flowers and the timing of flowering. Journalists often spoke to locals in the Namaqualand region and documented their insights into the flowering season and factors affecting flowering timing and conditions. The locals and longstanding citizens in the region provide insightful opinions into the flowering phenomenon, as they observe the flowering event annually and base their opinions and theories about factors contributing to good/bad flowering seasons on their observations. All local perceptions recorded in the digitized newspaper records of The Rand Daily Mail, Volksblad and Die Burger are documented and summarized below and should be regarded as perceptions and not necessarily as facts.

Although flowering timing varies annually, the ‘anticipated’ time for flowering of the Namaqualand daisies according to an article in Die Burger on 30 July 1986 is from late August to the end of September. The first subregions to flower in Namaqualand are the coastal areas which have greater moisture year-round. An article from the Volksblad on 4 August 2012 mentioned that first flowering in the coastal subregions are followed by flowering further inland, and then in the higher altitude subregions. Flowering is also perceived to occur first in the warmer subregions of Namaqualand. Nieuwoudtville is known to bloom later than the rest of Namaqualand because the subregion is cooler on average. The subregions that bloom later are also known to bloom longer into late spring and early summer.

One of the most important climatic factors, perceived by the Namaqualand locals, is precipitation. In an article in Die Burger on 22 July 2017, a local resident, Hendrik van Zijl is quoted saying “rainfall is the only factor that can determine the quality of the flowering season” [translated]. The amount and timing of precipitation is important for the development and flowering of the Namaqualand daisies. An article in Volksblad on 27 May 1993 stated that early winter rains result in early flowering in a particular season. If winter rains are delayed and only start in late July and onwards, it might be too late to ensure a quality flowering season. Precipitation quality (amount of rainfall) determines the abundance of the flowering daisy spectacle. An article written in Volksblad on 5 August 2002 confirms that the amount of precipitation received determines the abundance of the daisies by stating that 1997 was one of the best flowering years because the region received above average rainfall. Similarly, an article from Volksblad on 7 August 2007 also stated that plentiful winter precipitation will lead to a long and full flowering season. Different subregions in Namaqualand receive variable levels and quality of precipitation, and because flowering is so dependent on precipitation, some subregions might therefore have better flowering conditions compared to others on an annual scale.

Another important factor is follow up rains during late winter and early spring. Although the newspaper records refer to ‘follow up’ rains, the term ‘subsequent rains’ will be used from here on out for scientific accuracy. These later rainfalls provide enough moisture for effective growth during late winter leading to flowering during early spring. On 22 August 2006, an article in Die Burger mentioned that subsequent rains ensure that the flowers do not dry out too quickly and die once in bloom. Another article in Die Burger on 23 September 2006 stated that spring precipitation events could prolong the flowering season by up to three weeks due to the added moisture. Therefore, for a great flowering season, one needs sufficient autumn and winter rains, which are followed up by enough and frequent subsequent rain events from mid-July onwards.

El Niño events are perceived to influence the Namaqualand daisies negatively due to the resultant drought conditions. During drought years, one will only be able to observe small patches of flowers scattered across the landscape. During a drought year in 2003, an article on 19 June in Volksblad stated that drought conditions also lead to shorter flowering periods. An article written in Die Burger in 2003 on 26 August stated that the region received 50% less tourists during the flowering season because the drought resulted in less flowers. All the flower expos had to be cancelled in 2003 because of the drought. The newspaper records therefore confirm that flower abundance is controlled by precipitation totals.

Once the flowers have opened and are in bloom, berg winds (also referred to as August winds) can dry the flowers out in a matter of days. An article in Die Burger on 16 June 1989 mentioned that berg winds have the ability to kill all the flowering daisies and bring the flowering season to an abrupt end within a few days.

According to locals, cold conditions will lead to later and longer flowering periods. In 1991 on 21 September an article in Volksblad stated that cold fronts and light rain during the flowering season have the ability to prolong the flowering season, because these conditions provide extra moisture to the flowers. On 27 August 2013, however, an article in Volksblad stated that extreme cold conditions during flowering (frost events) can have detrimental effects on the daisies. The article further stated that snow during the winter months add to the moisture balance, which is advantageous for the daisies.

Flowers do not open on rainy and overcast days. One can therefore only admire the beauty of the Namaqualand daisies on sunny days. Tourists are constantly reminded in newspapers that flower viewing trips should not be planned for one day only seeing as they might miss the flowers on an overcast day. Furthermore, the Namaqualand region is also relatively large, and one can therefore not see all the flowers in all the subregions on one day. The best flowers are always seen on the roads less travelled and one therefore must take one’s time when viewing the Namaqualand daisies.

5.15 Synthesis

The results of the data analysis reveal that the calculated advances for first flowering and full bloom for the Namaqualand daisies are statistically significant. The strongest correlations, most significant influence and determining factor for first flowering timing are late autumn and early winter rainfall periods. The timing of the onset of the rainy season significantly drives the timing of first flowering. Full bloom timing of the Namaqualand daisies reacts more significantly to climate variables and factors occurring later in the year compared to first flowering timing. Precipitation is one of the key drivers for the timing of the onset of full bloom. Linear regression analysis indicates specifically that precipitation during late winter and early spring (from August to October) is statistically significantly correlated to full bloom timing. Temperature variables have the greatest and most significant influence on end of bloom timing.

CHAPTER 6: DISCUSSION

[6]

6.1 Introduction to Climate and Phenological Change in Namaqualand

The following chapter will discuss and compare the findings of the calculated results and the local perceptions documented in the assessed newspaper records with global and local phenological and climate change literature. The calculated changes in climate and phenology will first be discussed separately. Thereafter, the climate drivers that influence the observed phenological changes will be unpacked. An outlook for the Namaqualand daisy flowering timing will be presented based on future climate projections for the Namaqualand region. The finding of the study will then be compared to local, Southern Hemisphere, and global phenological studies and literature. Lastly this chapter will highlight some of the study limitations and how they were compensated for.

6.1.1 Climate Change

6.1.1.1 Temperature Changes

Although South African temperature trends are spatially variable, general warming trends have been calculated over recent decades (Easterling *et al.,* 1997; Kruger & Shongwe, 2004; Kruger & Sekele, 2013; MacKellar *et al.,* 2014; Davis *et al.,* 2016; Midgley *et al.,* 2016; Kruger & Nxumalo, 2017; Kruger *et al.,* 2019). MacKellar *et al.* (2014) observed that South African T_{max} has significantly increased throughout the whole country, from 1960-2010. The greatest increases in T_{max} is observed in the interior of the country with an approximate increase of 2°C during autumn, whereas the smallest calculated increase in temperature is 0.35°C, also in the interior of the country during summer (MacKellar *et al.,* 2014). Kruger *et al.* (2019) utilized point-based climate data for the period 1951-2005 from 22 locations in South Africa to calculate the country's temperature increases. In the north-eastern and southwestern parts of South Africa, temperatures are increasing at the largest rates of $0.20°C.decade^{-1}$ (Kruger *et al.,* 2019). Although T_{min} in South Africa is also increasing, its rate of change is considerably slower than that of T_{max} (Midgley *et al.,* 2016; Kruger *et al.,* 2019). In contrast to these findings, Van Wilgen *et al.* (2016) stated that calculated increases in T_{min} are greater than T_{max} in South African National parks, using point station meteorological data.

Davis *et al.* (2016) calculated the overall increase in Namaqualand T_{min} (1.4°C) as greater than the overall increase in T_{max} (1.1°C). In contrast to Davis *et al.* (2016) and Van Wilgen *et al.* (2016), this research project calculated greater and more significant increases in T_{max} compared to the calculated increases in T_{min} for the entire Namaqualand region (section 5.2; Appendix A.1). The overall increase in T_{max} for all of the assessed Namaqualand stations equates to $0.20°C.decade^{-1}$ or alternatively 1.18°C (section 5.2; Appendix A.1). The discrepancy in the results of this project and those of Davis *et al.* (2016) can be ascribed to the use of high resolution gridded climate datasets and point based climate data from 1901-2009 in the latter; whereas this research project utilized point based meteorological information from 1959-2018. The calculated increase in Namaqualand T_{max} from this study (1.18°C) is similar to the increase in T_{max} calculated by Davis *et al.* (2016) which is 1.1°C.

South African climate studies reveal that the greatest seasonal temperature changes occur during autumn and winter (MacKellar *et al.,* 2014; Midgley *et al.,* 2016). Hulme *et al.* (2001) used gridded climate datasets for the period 1900-2000 and found that South African winter and spring temperature warming trends are the greatest of all seasons. Although the results of these studies are different, they all found that winter temperatures increased the most (Hulme *et al.*, 2001; MacKellar *et al.,* 2014; Midgley *et al.,* 2016). Apart for the significant decrease in Nieuwoudtville T_{min} during both winter and spring, the seasonal climate analysis for Namaqualand reveals that all the significant calculated changes in temperatures are increasing over time (section 5.5). Therefore, the most significant temperature increases in the Namaqualand region are occurring during the growing period of the Namaqualand daisies (June-August).

Springbok and Nieuwoudtville are the only two weather stations that have statistically significant temperature decreases over time. These results contradict the observation of weak increases in T_{min} by Midgley *et al.* (2016) and Kruger *et al.* (2019). Both subregions are more than 100km inland from the South African west coast. Springbok and Nieuwoudtville are therefore both experiencing an increase in their diurnal temperature ranges over time, which relates to observed diurnal temperature range increases found by Easterling *et al.* (1997) from 1950-1993 using station metadata. Although the following studies that are going to be used for comparison with this Namaqualand study do not have data that spans similar temporal periods, as the climate records for Springbok and Nieuwoudtville do not extend to the 1960s, broad comparisons on rate of change can tentatively be made. The observed patterns within this Namaqualand study contradicts Hulme *et al.* (2001), who calculated decreases in diurnal temperature ranges in South Africa during the 1950s and 1960s. It therefore suggests that after the 1960s, diurnal temperature trends increased more significantly. This trend relates to large scale temporal temperature studies that observed increased rates of warming in South Africa after the mid-1960s (Kruger & Sekele, 2013; MacKellar *et al.,* 2014; SAWS, 2015; Midgley *et al.,* 2016).

Davis *et al.* (2016) observed significant decreases in the number of cool days or possible frost events in Namaqualand. Similarly, Midgley *et al.* (2016) found that the number of extreme cold nights in the Western Cape are decreasing. The analysis presented here (section 5.6.2), however, calculated significant increases in the number of frost days (for frost thresholds T_{min} ≤0°C and T_{min} ≤4°C) in Nieuwoudtville. Nieuwoudtville's only significant temperature changes were decreases in T_{min} over time; it is also the only subregion in Namaqualand with significant changes in frost variables (section 5.6). In Nieuwoudtville, last frost events (T_{min} ≤4°C) are progressively occurring later in the year (section 5.6.1).

From 1901-1995, Hulme *et al.* (2001) observed cooling trends in South African coastal regions through analysis of gridded climate data. Kruger *et al.* (2019) utilized point based climate data, and observed that the smallest temperature increases occur in coastal regions and range between 1-1.5°C. Contrary to these results, the current study found significant temperature increases for the two coastal subregions of Cape Columbine and Port Nolloth. Port Nolloth and Cape Columbine are also the most northern and southern subregions assessed, respectively.

6.1.1.2 Precipitation Changes

As a result of climate change, global precipitation patterns are becoming more variable (Dore, 2005; Botai *et al.,* 2018). Previous studies have noted that due to South Africa's variable precipitation regimes (Schulze, 2007; Midgeley *et al.,* 2016), trends in precipitation are seldom statistically significant (Kruger, 2006; MacKellar *et al.,* 2014). DEA (2013) and MacKellar *et al.* (2014) assessed South African precipitation patterns from 1960-2010 using point based meteorological records. Neither studies observed significant precipitation trends or changes over time. These two studies did, however, identify a decrease in the number of precipitation days per year (DEA, 2013; MacKellar *et al*., 2014). Botai *et al.* (2018) similarly found that South African precipitation is decreasing over time.

Several studies that assessed Namaqualand precipitation patterns over time revealed that changes over time are insignificant, inconsistent and non-directional (MacKellar *et al.,* 2014; Davis *et al.,* 2016; Midgley *et al.,* 2016). Consistent with the literature, this research project found that none of the calculated changes in precipitation in the Namaqualand region are significant over time (section 5.2). The calculated precipitation trends in the Namaqualand subregions are decreasing for five of the seven assessed weather stations (section 5.2). Variable trends in precipitation are due to stations starting their precipitation records at different times. Furthermore, temporal scales and location also need to be considered when assessing precipitation records (Fauchereau *et al.,* 2003; Botai *et al.,* 2018). The calculated decreasing precipitation trends for five of the seven weather stations in Namaqualand concurs with the results of Botai *et al.* (2019). The calculated insignificant precipitation decreases can also be linked to the observed decreases in the number of precipitation days in South Africa found by DEA (2013) and MacKellar *et al.* (2014). In contrast to the average observed precipitation decrease in Namaqualand, Van Wilgen *et al.* (2016) and Kruger and Nxumalo (2017) observed precipitation increases in the western regions of the country. The observed precipitation increases in the aforementioned studies can possibly be explained by the studies' data sources. Van Wilgen *et al.* (2016) quantified regional trends through creating climate clusters and Kruger and Nxumalo (2017) utilised point meteorological data to create average rainfall datasets for 94 districts in South Africa. The current study, however, utilised point based meteorological data (section 4.2.1).

Previous Namaqualand studies have indicated that precipitation in the region is highly variable, resulting in differences in annual flowering quality and quantity (Le Roux, 2005; Kruger *et al*., 2013; de Waal *et al.,* 2016; Davis *et al.,* 2017). Davis *et al.* (2017) attributed the calculated inter-annual variability in the growing season of Namaqualand to the observed variability in the timing and amount of precipitation received annually. The standard deviation for precipitation for the seven assessed weather stations range between 29.88 and 125.12, which indicates that annual precipitation in Namaqualand is highly variable (section 5.2). Dunning *et al*. (2016) observed large variability in the onset and cessation of the rainy season in South Africa through using satellite-based precipitation data for the entire African continent. Similarly, none of the changes in the timing of the onset and end of the rainy season in Namaqualand are significant over time (section 5.3).

Kelso and Vogel (2007) found that drought periods in Namaqualand are correlated to ENSO. Hoffman *et al.* (2009) assessed drought frequency in the South African WRZ and observed drying trends from

1900-1950, but no significant or drying trends from 1950-2000. The SPI drought index scores for five of the calculated weather stations indicate that the Namaqualand region is a neutral precipitation zone, rather than a wet or arid region (section 5.4). This concurs with the observations of Hoffman *et al.* (2009) who found no significant changes in the SPI indexes in Namaqualand after the 1950s (section 5.4). The only significant change in SPI over time, for the current study, was calculated in Springbok for the 24-month analysis (section 5.4). The significant decrease in 24-month SPI indicates that the Springbok subregion may become more drought-prone over time.

Namaqualand precipitation patterns from 1950-1999 were assessed by MacKellar *et al.* (2007) using gridded datasets. MacKellar *et al.* (2007) observed precipitation increases during the summer months in the north eastern regions of Namaqualand. MacKellar *et al.* (2007) further observed drying conditions during the winter along the west coast. Similar to the rest of the precipitation records from Namaqualand for this study, none of the calculated changes in winter and spring precipitation are significant over time (section 5.5). The three coastal subregions assessed during this study, which include Cape Columbine, Lambertsbaai Nortier and Port Nolloth, all display trends towards increasing precipitation during winter, which contradicts the results of MacKellar *et al*. (2007), although none of these trends are significant. A possible explanation for the contradictory findings between these studies, can be the use of a gridded dataset used by MacKellar *et al.* (2007), which interpolates precipitation patterns for a larger region (Zhang *et al.,* 2013).

6.1.2 Phenological Change

Although phenological phase studies have been conducted on Namaqualand daisies (Van Rooyen *et al.,* 1991; Cowling *et al.,* 1999; Manning, 2013; de Waal *et al.,* 2014, 2015, 2016; Davis *et al.,* 2017); neither phenological shifts over time, nor the relationship between observed shifts and changing climatic conditions have been conducted (Kelso & Vogel, 2007; MacKellar *et al.,* 2007; Hoffman *et al.,* 2009; Davis *et al.,* 2016, 2017). The current research is therefore imperative to better understand the influence of continuous climate change on the flowering timing of the Namaqualand daisies.

A global meta-analysis study, conducted by Parmesan and Yohe (2003), assessed 1,700 species covering a large geographic area. The study made use of at least 20 years of temporal data for each location, and found that spring phenological phases are advancing at a rate of 2.3d.decade^{-1}. Ge *et al.* (2015) conducted a meta-analysis in China that studied 112 plant and animal species, and calculated an average spring phenological advance of 2.75d.decade^{-1}. The assessment of the phenological changes in first flowering, full bloom and end of bloom timing of the Namaqualand daisies, calculated advancing trends for the daisies (section 5.7.1). However, only the calculated advances for first flowering and full bloom timing are statistically significant (section 5.7.1.1, 5.7.1.2). In accordance with global meta-analyses, first flowering and full bloom for the Namaqualand daisies are advancing at rates of 2.6d.decade^{-1} (section 5.7.1.1) and 2.1d.decade^{-1} (section 5.7.1.2) respectively.

Davis *et al.* (2017) assessed Namaqualand vegetation productivity and phenological spatial and temporal patterns from 1982-2011. The study found that the vegetation growing season in Namaqualand starts in autumn (March-April) and the growing season peaks during late winter (August) after the wet winter months (Davis *et al.,* 2017). The 30-year analysis indicated that regional vegetation phenology has advanced over time (Davis *et al.,* 2017). The calculated phenological flowering advances of the Namaqualand daisies relates to the work done by Davis *et al.* (2017). Phenological changes are directly related to the duration of the growing season, which ultimately influences all phenological phases of a plant (Hegland *et al.,* 2009; Butt *et al.,* 2015; Forrest, 2015). If the onset of the growing season is advancing (Davis *et al.,* 2017), then first flowering will also advance over time as the temporal period for daisy development has essentially advanced. The advance in first flowering cannot extend to earlier than the date of germination, and therefore while earlier germination will not cause earlier flowering, early germination dates are required to facilitate early season flowering.

Taking the average dates of the start of the phenological flowering record and the average dates of the end of the phenological flowering record for each of the three flowering groups, advances of 14.3 (first flowering), 16.9 (full bloom) and 11.7 (end of bloom) days are recorded, respectively, from 1935-2018. The recorded full bloom flowering timing advancement of 16.9 days is therefore the greatest of the three flowering groups.

The perceptions of flowering timing have also advanced since 1986. In an article from Die Burger on 30 July 1986, the general flowering period for the Namaqualand daisies was perceived to start in late August and end towards the end of September. When this perception is calculated in terms of Julian days, the flowering period for the Namaqualand daisies during 1986 was from 237-273 Julian days. The calculated average FFD for the last five years (2014-2018) is on 207.7 Julian days, and end of bloom timing is on 255.5 Julian days. Compared to local perceptions, there has therefore been a tentative advance in flowering timing from 1986-2018.

6.1.3 Drivers of Namaqualand Daisy Phenological Advances

Phenological research entails assessing phenological shifts over time (Fitchett *et al.,* 2015). By statistically assessing the relationship between phenological phase changes and climate variables, researchers can identify climate variables that drive phenological change (Keatley & Hudson, 2012; Fitchett & Fani, 2018). The magnitude and extent of a plant's phenological phase shifts depend on how influential climate drivers react to global warming (Cleland *et al.,* 2012; Thackeray *et al.,* 2016).

Regional climatic conditions drive and influence Namaqualand plant phenology (Van Rooyen *et al.,* 1979; Van Rooyen *et al.,* 1991; Struck, 1994). The Namaqualand climate is harsh and plants growing in this region have adapted to thrive under tremendous climatic stress (Le Roux, 2005). This section will highlight the newspaper record's representation of drivers of phenology, which will then be compared to the statistical findings of this study. Finally, a reflection of published literature from the region on drivers for Namaqualand daisies will be presented.

Assessed records from the digitized newspapers provided an assortment of perceptions relating to climatic drivers influencing the flowering phenological phases of Namaqualand daisies (section 5.14). In an article in Die Burger on 13 August 2002, the perceived climatic conditions that make for a good flowering season include early winter rains and sufficient subsequent rains. The article also indicated that flowering first occurs closer to the coastal regions, that cold conditions lead to later flowering, and that berg winds can threaten the flowering daisies significantly. The observations of the climate drivers influencing the flowering timing of the daisies are derived from longstanding residents in Namaqualand and some come from journalists who have researched the flowering spectacle. The reports on flowering climate drivers therefore have varied accuracy.

An article written in Volksblad on 8 June 1990 suggested that first flowering is expected to occur first in the warmer regions of Namaqualand. Throughout the assessed newspaper records there were only four mentions of warm conditions leading to advanced flowering timing. On 8 September 2011, an article in Volksblad suggested that warm spring and summer days lead to advanced end of bloom timing. Similarly, another article written in Volksblad on 19 August 2014 mentioned that cold conditions lead to later flowering timing. Throughout the assessed newspaper records there are 16 mentions of local perceptions suggesting that cold conditions generally lead to delays in flowering timing and longer flowering periods (section 5.14). An article published in Volksblad on 21 September

1991, stated that cold fronts during the growing season can prolong the flowering season (section 5.14). Contrastingly, on 23 August 2013 another article that appeared in Volksblad suggesting that cold fronts are detrimental for the daisies once they are in bloom. The negative impact of cold fronts on the daisies might suggest possible frost risks. The differences in perceptions can be the result of different journalists having different perceptions of the drivers of flowering. The opinions that cold conditions generally lead to longer flowering periods is motivated by the fact that during cold periods, moisture is retained better due to less evapotranspiration and the increased moisture therefore prolongs the flowering season (section 5.14). In 1986, on 19 September in Volksblad, a Namaqualand local was quoted, saying that the flowering season in Nieuwoudtville generally starts later and lasts longer than the rest of the Namaqualand subregions since it is situated on top of the escarpment, which makes the regional temperature conditions relatively cooler. Three other articles also suggested that daisy flowering in Nieuwoudtville occurs later than the rest of Namaqualand due to the subregion’s cooler conditions.

An article written on 27 May 1993 in Volksblad, stated that early winter precipitation events lead to earlier flowering events in that season (section 5.14). Throughout the assessed newspaper records there were 30 mentions of the importance of the onset of the rainy season significantly influencing first flowering timing. Based on the assessed newspaper records, precipitation timing significantly drives the phenological flowering timing of the Namaqualand daisies (section 5.14). The newspaper records suggest that if winter precipitation events are delayed and the onset of rain takes place during late July and onwards, these rains will be too late, and a good flowering season cannot be guaranteed (section 5.14). Similarly, an article written in the Rand Daily Mail on 29 August 1949, suggested that a late onset of the rainy season cannot save the prospects of a good flowering season.

The digitized newspaper records repeatedly mention that early winter rains needed to be accompanied by subsequent rains that fall during late winter and early spring (section 5.14). Subsequent rains significantly influence the flowering timing and the duration of flowering of the Namaqualand daisies (section 5.14). The perceived importance of subsequent precipitation events was mentioned in 90 of the assessed newspaper articles. An article from 1990 on 18 October stated that there are still daisies visible in the southern Namaqualand subregions due to in-season precipitation. On 23 September 2006, an article written in Die Burger suggested that precipitation events during spring can prolong the flowering season by up to three weeks due to the added moisture (section 5.14).

A driver of phenological flowering of the Namaqualand daisies related to moisture availability that has been mentioned in newspaper records, is that regions closer to the coast tend to flower before the inland regions (section 5.14). Another perception that stands out from the newspaper records is that generally if a region is wetter, first flowering will be advanced and drier regions tend to have flowering delays (section 5.14).

The observed newspaper records further suggest that El Niño periods also significantly influences Namaqualand daisy flowering periods negatively due to the resulting drought conditions that are brought about by ENSO (section 5.14). This research project did not assess the impact of ENSO on the flowering phenology of the Namaqualand daisies. However, warm ENSO events are linked to drought periods in South Africa with below-average rainfall in all regions of the country (Midgley *et al.,* 2016; Crétat *et al.,* 2019). During El Niño years, the dry regions of the country essentially become drier and the wet regions become wetter (Usman & Reason, 2004; Dieppois *et al.,* 2016). Seven articles mentioned the perceived negative impact that drought periods have on flowering phenology of the Namaqualand daisies. On 26 July 1969, the Rand Daily Mail suggested that during drought periods, only small patches of daisies can be observed across the landscape (section 5.14). According to an article published in Volksblad on 19 June 2003, drought conditions can lead to shorter flowering periods (section 5.14). On 23 September 2003, Volksblad reported that there are no flowers throughout the entire Namaqualand region due to the worst drought in 30 years.

The last perceived significant climate factor that can influence end of bloom timing of the Namaqualand daisies is berg winds (section 5.14). There were 15 articles in the newspaper records that perceived berg winds to negatively impact the end of bloom timing. On 25 July 1987, an article in Volksblad suggested that berg winds dry the stems of the daisies and therefore decreases the lifespan of the flowers significantly. On 16 June 1989, an article published in Die Burger suggested that berg winds blowing from an easterly direction can bring the flowering season to an abrupt end within a few days due to the associated dry and warm conditions (section 5.14).

Based on the perceptions from the collected newspaper records, first flowering and full bloom timing of the Namaqualand daisies is significantly driven by the timing of the onset of the rainy season and subsequent rains during winter and spring (section 5.14). The newspaper record perceptions further suggested that the end of the flowering season is mainly driven by subsequent rains during the flowering season, the timing of the end of the rainy season, spring and summer temperatures, and berg winds (section 5.14). The perceptions that drought periods also influence flowering phenology can be linked with a lack of precipitation and regional moisture availability.

The results of the current study suggest that temperatures from June to September (winter to early spring), drive first flowering timing in Namaqualand (section 5.8.1; Figure 6.1). Most of the significant correlations between the respective temperature variables and first flowering timing of Namaqualand daisies are inverse and range between 0.01-0.11d.°C^{-1} (section 5.8.1). Temperatures during August significantly drives full bloom flowering timing of the Namaqualand daisies with inverse correlations ranging between 0.01-0.04d.°C^{-1} (section 5.8.2; Figure 6.1). End of bloom flowering timing for the Namaqualand daisies are strongly driven by temperatures from June to October (section 5.8.3; Figure 6.1). All the correlations between temperatures and end of bloom are inverse with coefficients ranging between 0.02-0.06d.°C^{-1} (section 5.8.3). All the significant correlations between temperatures and flowering phenology of the Namaqualand daisies are inverse (section 5.8) which therefore indicates that increased temperatures will contribute to flowering advances. The findings of the current study are in accord with the assessed newspaper records that remarked that warmer temperatures contribute to advancing flowering timing (section 5.14).

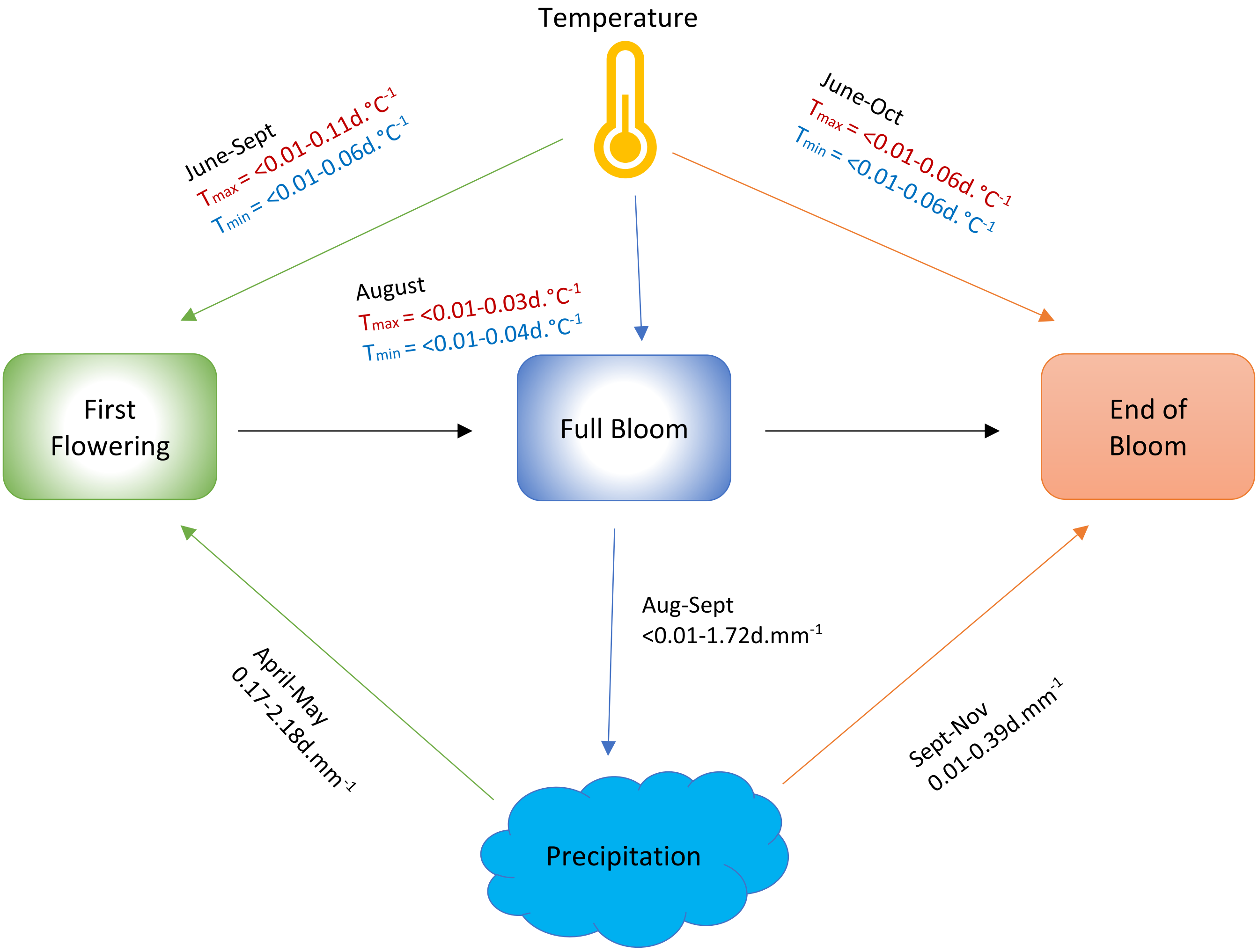

Figure 6.1: Diagram illustrating the significant climate drivers responsible for the calculated phenological flowering advances of the Namaqualand daisies. The rates of change for the precipitation correlations with flowering timing are significantly stronger that the temperature correlations

This research project further explored seasonal assessments based on research conducted by Struck (1994) and Cowling *et al.* (1999) in Namaqualand. These studies investigated seasonal climatic impacts on the vegetation of the region. Due to the pattern of significant correlations observed between temperatures during winter and spring and end of bloom timing, the seasonal influence of temperatures and precipitation on end of bloom timing were assessed (section 5.12). Calculations revealed that all the temperature variables during winter and spring, except for in Springbok and Nieuwoudtville, are significantly inversely related to end of bloom timing (section 5.12). The positive relationships calculated between end of bloom timing and spring T_{max} in Nieuwoudtville and spring T_{min} and T_{mean} in Springbok (section 5.12), serve to reduce the advancing effect that all the other significant correlations have produced. The correlation strengths for the winter temperature relationships are stronger than the spring correlation strengths (section 5.12). Winter temperature variables therefore drive end of bloom timing more significantly. A possible explanation for this is the fact that winter temperatures significantly drive first flowering timing and if first flowering timing is advanced by increased temperatures, end of bloom timing will also ultimately advance.

The temperature analysis conducted with the acquired climate data revealed that Nieuwoudtville is the coldest subregion in Namaqualand (section 5.2). Nieuwoudtville has the largest average number of frost events occurring after first flowering for both frost threshold temperatures of 0°C and 4°C. The number of frost days (T_{min} ≤0°C) that are occurring after first flowering in Nieuwoudtville is also increasing significantly over time (section 5.13.1). The present findings are in accord with the assessed newspaper record perceptions that proposed that flowering in Nieuwoudtville occurs last due to the subregion's cooler temperatures. In Nieuwoudtville, significant increases in the number of frost days (T_{min} ≤0°C; section 5.6.2), have contributed to delays in end of bloom timing due to calculated positive correlations between end of bloom timing and the number of frost events occurring in the subregion (section 5.13.4). These findings support the observed perceptions from the newspaper records that suggests that colder climatic conditions lead to flowering delays (section 5.14).

The number of frost events occurring after first flowering for the frost threshold of T_{min} ≤4°C, increased for four of the six analysed weather stations, although none of these changes are statistically significant (section 5.13.1). The increased number of frost events after first flowering can be attributed firstly to decreasing minimum temperatures in Nieuwoudtville, Springbok and Clanwiliam (section 5.2); and secondly, to the significant advancement of first flowering while last frost dates are not advancing significantly (section 5.6.1).

The frost risk analysis assessed first flowering advances over time together with changes in last frost Julian dates (section 5.13.2). Calculations therefore reveal that frost risks in Springbok, Nieuwoudtville, Vredendal, Lambertsbaai Nortier and Clanwilliam are all increasing over time (section 5.13.2). However, the number of frost days and the last frost date for the frost threshold of T_{min} ≤0°C has no calculated influence on first flowering and full bloom timing of the Namaqualand daisies (section 5.13). Furthermore, the number of frost days in a region for T_{min} ≤4°C has no calculated relationship with full bloom timing (section 5.13.3). The number of frost events (T_{min} ≤4°C) occurring after first flowering is also calculated to have no significant influence on end of bloom (section 5.13.4). These findings stand in contrast with the newspaper articles that suggested that cold climatic conditions lead to delays in flowering timing (section 5.14).

In Nieuwoudtville and Clanwilliam, significant inverse relationships are calculated between full bloom timing and the number of frost events (T_{min} ≤4°C) occurring after first flowering (section 5.13.4). In both subregions, frost events have been increasing (section 5.13.3). The increased incidence of frost has therefore contributed to full bloom timing advances in Nieuwoudtville and

Clanwilliam, which does not correspond with the assessed newspaper records that remarked that cold conditions lead to flowering delays (section 5.14).

In Port Nolloth, the calculated positive correlation between end of bloom timing and last frost Julian dates (T_{min} ≤4°C) is significant (section 5.13.4). Advances in last frost Julian dates in Port Nolloth have therefore contributed to advancing end of bloom dates (section 5.13.4). Significant increasing temperatures calculated in Port Nolloth (section 5.2) have led to advances in last frost Julian dates in the subregion which has therefore contributed to end of bloom timing advances. This finding once again therefore confirms with the perceptions from the assessed newspaper records that suggested that increasing temperatures drive flowering advances (section 5.14).

No significant relationships are calculated between the last frost (T_{min} ≤0°C) Julian date and end of bloom timing (section 5.13.4). However, the calculated relationship between last frost Julian dates and end of bloom timing for Nieuwoudtville is positive, which indicates that delays in last frost events contribute to end of bloom timing delays (section 5.13.4). The increase in frost incidence in Nieuwoudtville also leads to end of bloom timing delays due to the positive correlation between end of bloom and the number of frost events occurring after first flowering (section 5.13.4). Although not significant, all the calculated relationships between the number of frost events (T_{min} ≤4°C) and end of bloom timing are positive (section 5.13.4), therefore aligning with the observations and perceptions captured in the newspaper records (section 5.14).

In accordance with the observed newspaper records, first flowering timing of Namaqualand daisies is significantly impacted by precipitation events during April and May, which is the start of the winter rainfall season in Namaqualand (Roffe *et al.,* 2019; section 5.8.1; Figure 6.1). The bulk of the significant correlations between precipitation and first flowering timing are inverse and range between 0.17-2.18d.mm^{-1} (section 5.8.1). The strongest relationships between first flowering timing and climate variables in Namaqualand are calculated for precipitation (section 5.8.1). Furthermore, significant positive relationships are calculated between the onset of the rainy season and first flowering timing for every weather station besides Cape Columbine (section 5.10.1). Seeing as all the significant relationships between onset of the rainy season and first flowering are positive and range between 0.73-1.59d.d_{OR}^{-1} (section 5.10.1), it corresponds with the newspaper records that suggested an advanced rainy season leads to advanced first flowering (section 5.14). The large inter-annual variability calculated for the onset of the rainy season (section 5.3) therefore leads to high inter-annual variability in first flowering timing of the Namaqualand daisies.

Although early winter precipitation in May is significantly related to full bloom timing, precipitation later in the year during August and September have stronger relationships with full bloom timing with coefficients ranging between 0.23-1.72d.mm^{-1} (section 5.8.2; Figure 6.1). Therefore, full bloom flowering timing of the Namaqualand daisies are driven by late occurring precipitation events (August to September). These findings corroborate the perceptions observed in the newspaper records that suggested that subsequent rains during late winter and early spring significantly drives flowering timing of the Namaqualand daisies (section 5.14). Statistically significant positive relationships are calculated between the onset of the rainy season and full bloom timing for Vredendal and Port Nolloth, with rates of changes ranging between 0.70-1.24d.d_{OR}^{-1} (section 5.10.1). The calculated correlations are positive, which again indicates that if the onset of rain timing is advanced during early winter; first flowering advances will contribute to full bloom timing advancing.

None of the calculated relationships between the timing of the end of the rainy season and first flowering are significant (section 5.10.2). However, most of the relationships are inverse, which indicates that if the end of the rainy season is extended, first flowering will likely advance over time.

No significant relationships are calculated between full bloom timing of the Namaqualand daisies and end of the rainy season timing (section 5.10.2). Most of the insignificant correlations are positive. These correlations and results therefore need to be interpreted with caution.

Precipitation is not as strongly correlated to end of bloom timing as compared to first flowering and full bloom. Precipitation events that generally occur later in the flowering season significantly drives end of bloom timing (section 5.8.3; Figure 6.1). These findings support the perceptions documented in the newspaper records that suggest that subsequent rains and in-season precipitation events significantly drive end of bloom timing in the region (section 5.14). The seasonal assessment with end of bloom timing and winter and spring precipitation indicated an inverse relationship for 11 of the 14 calculations (section 5.12). The only significant relationships (also inverse) between end of bloom timing and seasonal precipitation was for Cape Columbine during winter and spring (section 5.12). If precipitation were to decrease during winter or spring, end of bloom timing will be delayed. The delay is due to less precipitation in winter, which leads to delays in first flowering timing which has a causal sequence effect for all other flowering timings.

The onset of the rainy season in Namaqualand has no significant influence on end of bloom timing (section 5.10.1). The calculated correlations between end of bloom and the onset of the rainy season are all positive, which indicates that if the onset of rain is advanced, the end of bloom will also advance, and vice versa (section 5.10.1). The onset of the rainy season is not supposed to drive the timing of the end of the flowering season. However, the positive correlation between onset of rain timing and end of bloom timings is due to the effect that rain timing has on FFD.

Inverse relationships are calculated between the end of the rainy season timing and end of bloom timing for every weather station assessed in Namaqualand (section 5.10.2). The correlation between end of the rainy season timing and end of bloom in Clanwilliam is statistically significant.

Therefore, as the end of the rainy season is advanced over time in Clanwilliam (section 5.3), end of bloom timing will be delayed. This result does not link with newspaper record observations that suggests in-season precipitation events can extend the duration of the flowering season (section 5.14) and serves to reduce the advancing effect that the statistically significant correlations indicate.

Every SPI calculation (3-, 6-, 12- and 24-months) of correlation with first flowering is significant for Springbok (section 5.11). Similarly, for Lambertsbaai Nortier, the 3-, 6- and 12-month SPI correlations with first flowering are also significant (section 5.11). The calculated inverse relationships indicate that if a region is generally wetter, flowering timing will be advanced and if the region is drier, flowering will be delayed. The SPI relationships with flowering timing results are consistent with remarks in the newspaper records related to the negative impact that drought periods have on flowering timing. Thus, leading to flowering delays, fewer flowers, and a shorter flowering season (section 5.14).

Much of the literature consider temperature as the most influential driver of plant development and phenological phase shifts (Struck, 1994; Steyn *et al.,* 2004; Ellwood *et al.,* 2013; Davis *et al.,* 2017; Menzel *et al.,* 2020). Prior studies conducted in Namaqualand have noted that temperature significantly drives regional vegetation phenological phases (Van Rooyen *et al*., 1979; Van Rooyen *et al*., 1991; Struck, 1994; Le Roux, 2005; Davis *et al*., 2017). Their results concur with the results of this research project, and with observations from the collected newspaper records.

Van Rooyen *et al.* (1991) conducted a one-year experimental study where three Namaqualand specimens, one of which was the Namaqualand daisy, were grown under different climatic conditions to assess the phenology and development of the plants. Struck (1994) conducted a three-year experimental study on six permanent plots in the Goegap Natrure reserve in Namaqualand where the flowering timing of the regional vegetation was analysed. Steyn *et al*. (1994) conducted a one-year experimental study that assessed the phenological cycles of five Namaqualand ephemerals, under various levels of water stress. The results from Struck (1994), Van Rooyen *et al.* (1979), the current project, and the observed newspaper records all observed that increased temperatures during spring significantly drives first flowering timing. Van Rooyen *et al*. (1979) also stated that regional vegetation growth rates slowed down in Namaqualand during the winter. The increase of winter temperatures in Namaqualand over time (section 5.2, 5.5) indicates increased growth rates during winter periods, which leads to advances in phenological flowering timing of the Namaqualand daisies.

Fox *et al*. (2005) and Davis *et al*. (2017) both assessed Namaqualand regional vegetation patterns and phenology through correlating NDVI data with climate data. Fox *et al*. (2005) used a dataset from 1985-2001 and Davis *et al.* (2017) used a longer dataset from 1982-2011. Fox *et al.* (2005) observed peak NDVI values for Namaqualand vegetation productivity during August, just before first flowering is supposed to occur. In agreement with the calculated results from this study, Davis *et al.* (2017) attributed advances in Namaqualand vegetation productivity to increased temperatures. Davis *et al*. (2017) further observed advances in the end of the vegetation growing season due to increased temperatures.

Throughout the phenological flowering record, approximately 54% of first flowering events occur within four days of a frost event for both frost threshold temperatures (section 5.13.3). First flowering timing cannot be related to first or last frost events (section 5.13). A possible explanation for this observation comes from an experimental study conducted under glasshouse conditions by Pearson *et al.* (1995), where the impacts of temperature and photoperiod were assessed on the phenology of the Cape daisy (*Osteospermum jucundum*). Pearson *et al.*'s (1995) study is of relevance to the current research project since the Cape daisy is an ephemeral daisy that grows in the same region as the Namaqualand daisies. Daisies grown under an average temperature of 22°C remained in their vegetative stages for 120 days, while daisies grown under an average of 12°C started flowering after 81 days (Pearson *et al.,* 1995). The study therefore revealed that the Cape daisy has chilling requirements that needs to be satisfied before flowering can be initiated (Pearson *et al.,* 1995). According to Pearson *et al.* (1995), increased exposure to cold conditions prior to flowering leads to quicker fulfilment of chilling requirements for daisies growing on the south-west coast of South Africa. Thus, cold conditions prior to flowering advances full bloom timing. These results contradict the current study's findings and the observations printed in the newspapers. The contradiction can be attributed to the glasshouse growing conditions (Pearson *et al.,* 1995). Further studies on daisy chilling requirements in Namaqualand has not been conducted, but the trend of first flowering events within four days of a frost event suggest that Namaqualand daisies may have chilling requirements.

Van Rooyen *et al.* (1991) confirms the local perceptions that decreased temperatures will lead to longer flowering periods. Colder periods reduce evapotranspiration during the day, which ensures that moisture is available to the daisies for a longer period (Le Roux, 2005). This supports the results of Fox *et al.* (2005) and Davis *et al.* (2017), that vegetation dynamics are driven by evapotranspiration through the direct influence on regional moisture availability.

The findings of the current study are consistent with those of previous studies conducted in Namaqualand that confirmed early precipitation during April and May as key drivers for a successful flowering year (Wannenburgh & Dickson, 1984; Van Rooyen *et al.,* 1979; Cowling *et al.,* 1999; Le Roux, 2005; Kruger *et al.,* 2013). Various authors also highlight the importance of the timing of seasonal precipitation (Van Rooyen *et al.,* 1979; Cowling *et al.,* 1999; Le Roux, 2005; Kruger *et al.,* 2013; de Waal *et al.,* 2016; Davis *et al.,* 2017). The current study's findings and the perceptions captured in newspaper articles align with their findings; the onset of the rainy season drives the timing of first flowering of the Namaqualand daisies. Similarly, Davis *et al.* (2017), using remote sensing applications, found that autumn and early winter precipitation drives the onset of the vegetation growing season in Namaqualand. To expand on the calculated results of this study and the assessed newspaper records, Van Rooyen *et al.* (1991) and Struck (1994) both concluded that the first significant temperature decreases during autumn indirectly drives the onset of the rainy season, which significantly drives the flowering timing of the Namaqualand daisies. In a vegetation assessment of Namaqualand, Le Roux (2005) stated that early flowering events are driven by early winter rains. The importance of early winter rains was also mentioned as a driver for early flowering in the assessed newspaper records (section 5.14), and the findings of the current study (section 5.10.1). Seasonal precipitation totals and patterns therefore significantly drives flowering timing, duration and the number of flowers during a flowering season in Namaqualand (Struck, 1994; Cowling *et al.,* 1999).

A phenological assessment conducted by Johnson (1992) studied the flowering seasonality of 7,075 Cape floral species. Johnson (1992) stated that the western regions of the Cape flower during spring, whereas the eastern regions flower closer to summer. The findings by Johnson (1992) aligns with the documented perceptions from the assessed newspaper records that suggested that Namaqualand regions closer to the coast flower before the inland regions due to greater moisture availability (section 5.14). Variability in the timing of first flowering events in different Namaqualand subregions can be explained by varying vegetation productivity along a precipitation gradient (Johnson, 1992; Davis *et al.,* 2017).

Le Roux (2005) stated that subsequent rains ensures that the Namaqualand daisies do not dry out and die once they are in bloom (Le Roux, 2005). Struck (1994) concluded that subsequent precipitation events and in-season precipitation significantly stimulates flowering and extends the length of the flowering season in Namaqualand. The remote sensing study by Fox *et al.* (2005) concluded that the vegetation dynamics of Namaqualand are driven by precipitation and evapotranspiration from June to August. The findings of these studies correspond with the perceptions from the digitized newspaper records (section 5.14), and the calculated results from the current study that revealed that precipitation events from early winter right up until the end of the rainy season are important for the flowering season and its duration (section 5.8; 5.10; Figure 6.1).

Malo and Nicholson (1990) stated that Namaqualand daisies tend rather to react to soil moisture levels than to direct precipitation events. During dryer periods, the Namaqualand daisies make use of soil moisture for survival (Malo & Nicholson, 1990). Le Roux (2005) confirmed that soil moisture is an important driver for flowering timing. According to Le Roux (2005) almost no moisture is lost in the Namaqualand region during the rainy winter months, due to low temperatures during winter, which allows the plants to benefit from the increased soil moisture levels during their vegetative growing periods. In the experimental greenhouse study, Van Rooyen *et al.* (1991) observed that the Namaqualand daisies can flower under a range of different temperature and photoperiod conditions as long as there is sufficient moisture available. In accordance with observed newspaper perceptions, various studies identified soil moisture availability as a driver for flowering timing of Namaqualand daisies; evidenced by larger moisture levels in coastal regions that tend to flower before the drier inland regions (Malo & Nicholson, 1990; Van Rooyen *et al.,* 1991; Fox *et al.,* 2005). Struck (1994) also stated that evapotranspiration and precipitation are the main climatic drivers of regional vegetation productivity in Namaqualand. Remote sensing studies similarly revealed that Namaqualand vegetation dynamics are driven by evapotranspiration rates and precipitation, which ultimately influences the potential moisture balance (Fox *et al.,* 2005; Davis *et al.,* 2017). These findings further support the observed newspaper perceptions of the Namaqualand daisies needing subsequent rains to ensure sufficient moisture for flowering (section 5.14).

An experimental study concluded that drought conditions lead to delays in first flowering timing of the Namaqualand daisies (Van Rooyen *et al.,* 1991). This finding is consistent with the current study's calculated significant inverse relationships between SPI and flowering timing for Springbok, Lambertsbaai Nortier and Clanwilliam (section 5.11). In the water stress experimental study on Namaqualand ephemerals, Steyn *et al.* (1996) was further able to demonstrate that water stress periods, or drought conditions, can significantly shorten the life span of Namaqualand daisies. Davis *et al.* (2016) observed that increased temperatures during summer leads to less available moisture, and the decreasing moisture levels add to advances in the end of bloom timing. These findings are consistent with earlier newspaper observations that also concluded that drought conditions lead to shorter flowering periods (section 5.14).

In an ecological and biogeographical overview of Namaqualand, Cowling *et al.* (1999) mentioned that berg winds bring about warm and dry conditions, thus increasing evapotranspiration rates (Davis *et al.,* 2016). Berg winds were not assessed in this research project, however, in the newspaper records it was identified as harmful to the daisies (section 5.14). The dry and warm conditions brought about by berg winds relates to the significant drivers of end of bloom timing of the Namaqualand daisies, since it can end the flowering season within a few days (Le Roux, 2005; Davis *et al.,* 2016).

6.1.4 Synthesis of Drivers of Flowering Phenology for the Namaqualand Daisies

A range of different climate drivers influence the timing of Namaqualand daisy phenological phases over time. Some of the possible drivers of phenological changes such as photoperiod, winds, land use practices and atmospheric CO_2, were not assessed during this research project. However, Van Rooyen *et al.* (1991) revealed that photoperiod does not significantly drive flowering timing of Namaqualand daisies. Contrastingly, Pearson *et al.* (1995) found that daisies receiving 16 hours of sunlight per day, flower 10 days earlier compared to daisies receiving eight hours of sunlight per day. Davis *et al.* (2017) attributes changes in vegetation productivity in Namaqualand to changes in land use practices. The removal of equines and goats from the landscape has also led to increases in vegetation productivity in Namaqualand (Hoffman, 2014; Van Rooyen *et al.,* 2015). Increased vegetation productivity can lead to flowering advances of certain plants. Another factor that can lead to flowering timing advances over time is increased atmospheric CO_2 (Kgope *et al.,* 2010; Buitenwerf *et al.,* 2012; Zhu *et al.,* 2016) which leads to increased biomass productivity through influencing the efficiency of a plant's water usage (Housman *et al.,* 2006). The increased atmospheric CO_2 therefore leads to increased vegetation productivity (Davis *et al*., 2017). With advances in vegetation productivity, flowering timing can be advanced over time.

According to the local perceptions documented in the newspaper records, a good flowering season is driven by autumn and early winter precipitation together with frequent subsequent precipitation events (section 5.14). Assessed literature confirms the importance of autumn/early winter precipitation driving flowering timing of the Namaqualand daisies; although precipitation is said to work in accordance with temperatures (Van Rooyen *et al.,* 1979; Hoffman & Cowling, 1987; Cowling *et al.,* 1999; Dreyer *et al.,* 2006; de Waal *et al.,* 2016). The calculated results of this study also concluded that precipitation events and temperature variables during different periods of the Namaqualand daisy growth period significantly drives flowering timing.

Multiple regression analysis indicated that 83.04% of the variability in first flowering in Nieuwoudtville is driven by T_{max} during June and November and precipitation during May (section 5.9). Another multiple regression analysis revealed that 69.48% of the observed variability in first flowering timing in Clanwilliam is driven by T_{max} and T_{min} during June together with precipitation during May (section 5.9). Thus, a combination of climate variables work concurrently to drive the observed flowering advances of the Namaqualand daisies. These calculated results are therefore in agreement with Crimmins' *et al*. (2010) findings that indicated that a combination of climate variables contribute to advance flowering timing.

As observed in the climate and newspaper records, the levels and timing of precipitation in Namaqualand varies considerably (section 5.2, 5.3, 5.14). Because precipitation timing and totals drive daisy flowering, inter-annual variability in flowering timing will occur. Each weather station in Namaqualand is responding to climate change differently (section 5.2). Different subregions in Namaqualand have different climate drivers influencing the timing of daisy phenological phases. The phenological flowering responses of the Namaqualand daisies are therefore location specific.

Temperature drivers were not mentioned frequently in the newspaper records compared to precipitation drivers (section 5.14) and are also not as strongly correlated to flowering timing compared to precipitation events (section 5.8). The results of this study and the newspaper perceptions agree with the literature from the region that suggests that increased temperatures contribute to advanced flowering dates (section 5.8; Davis *et al*., 2016, 2017). The assessed literature also explains that precipitation drivers are extremely important for flowering timing, but also includes moisture availability, droughts and berg winds as potential climate drivers of flowering phenology in Namaqualand, which confirms the documented newspaper perceptions (section 5.14).

The newspaper records indicate that dry conditions lead to delays in flowering timing whereas wetter conditions lead to advanced flowering timing. Flowering timing and SPI relationships are inverse for 47 of 60 tests (section 5.11). Although the SPI and flowering relationships indicate similar trends as the observed newspaper records, only eight of the 47 inverse relationships between flowering timing and SPI are statistically significant.

The documented perceptions from the newspaper records, the calculated correlations and results of this current study and the limited literature of regional phenology all agree that respective climate drivers influence the flowering phenology of the Namaqualand daisies. In conclusion, the timing and amount of precipitation that the Namaqualand region receives, drives the flowering timing of the Namaqualand daisies. The majority of the temperature relationships with flowering timing are inverse (section 6.1.3). Therefore, as temperature increases, flowering timing advances. Therefore, similar to the conclusion by Davis *et al.* (2017), the significant drivers of Namaqualand daisy flowering phenology work simultaneously within complex interrelationships to produce overall flowering advances over time.

6.1.5 Outlook for Namaqualand Daisies

South African climate change modelled projections predict that climate variability will increase dramatically (Davis, 2010; Midgley *et al.,* 2016). Precipitation frequency and intensity will change, temperatures may increase by up to 4°C by the end of the century, wind strength and direction will become more variable and sea levels will increase (Davis, 2010; Midgley *et al.,* 2016).

Midgely *et al.* (2005) conducted the South African Country Study on Climate Change during the 1990s, which revealed that the Northern and Western Cape regions are high-risk climate change regions. Precipitation and temperature variables are projected to increase in variability due to climate changes (Midgely *et al.,* 2005). Similarly, Wand *et al.* (2007) identified the South African Western Cape and the South African WRZ as a region that is highly vulnerable to globally changing climatic conditions. Within the next 30 years temperature is projected to increase by 1-2°C in the Western Cape (Wand *et al.,* 2007). However, Hewitson and Crane (2006) contrastingly projected minimal climate changes within the south-western Cape region. The conflicting findings of these studies can be as a result of Hewitson and Crane's use of self-organising maps together with a downscaling approach when they assessed their respective climate datasets. Using global circulation models, Engelbrecht *et al.* (2015) projected rapid temperature increases in the southern subtropical regions of Africa. Under a low-mitigation emission scenario Engelbrecht *et al.* (2015) projected that African subtropical regions will experience temperature increases ranging between 4-6°C during the 21st century. As stated in section 6.1.3; temperatures during winter and spring are one of the climate factors that significantly drives flowering advances of the Namaqualand daisies. The calculated results also confirm that temperatures in Namaqualand are increasing significantly (section 6.1.1.1). The projected increasing temperatures will therefore contribute to further flowering advances of the Namaqualand daisies.

In an assessment of the onset and end of the rainy season dates of the rainfall zones in South Africa from 1987-2016, Roffe *et al*. (2020) established that the winter rainfall periods in the south-western Cape regions tend to have a longer wet season compared to the winter rainfall periods along the West coast and further north in Namaqualand. Roffe *et al*. (2020) established that precipitation patterns and totals in Namaqualand are variable over time and space. Precipitation is projected to decrease in the South African WRZ (Hewitson & Crane, 2006; Wand *et al.,* 2007). Mid-latitude cyclones are projected to retreat pole-wards due to climate change, which leads to decreases in south-western Cape precipitation (DEA, 2013; Engelbrecht *et al.,* 2013). Midgely *et al.* (2005) stated that precipitation variability will increase due to global warming. Although south-western Cape precipitation is extremely variable over time, Midgley *et al.* (2016) projected significant decreases in the number of rainfall days in the region. The results from this research project calculated no significant changes in precipitation totals, onset and end of the rainy season dates (section 6.1.1.2). Although precipitation is calculated to be extremely variable over time, precipitation is decreasing tentatively for five of the seven assessed weather stations in Namaqualand (section 5.2). The calculated precipitation trends concur with the assessed literature (Midgely *et al.,* 2005; Hewitson & Crane, 2006; Wand *et al.,* 2007; Midgley *et al.,* 2016). Namaqualand daisies are significantly driven by precipitation timing and totals (section 6.1.3). Decreases in precipitation will therefore contribute to delays in flowering timing. If precipitation in the Namaqualand region is more variable over time, flowering timing will therefore also become more variable. Precipitation variability can therefore strengthen or weaken future phenological flowering advances.

As a result of the projected increasing temperatures and decreasing precipitation in the south-western Cape, evaporation levels are therefore also projected to increase over time (Engelbrecht *et al.,* 2015; IPCC, 2018). With increased evaporation levels, the soil moisture levels in Namaqualand will likely decrease. Soil moisture is essential for the Namaqualand daisies (section 6.1.3; Malo & Nicholson, 1990; Le Roux, 2005). If climate change causes increasing temperatures together with significant decreases in precipitation, it is difficult to predict if the Namaqualand daisies will be able to adapt to and survive a harsher climate. During drought periods, flowering timing is delayed (section 6.1.3). Namaqualand daisies can survive under a wide range of temperature conditions if there is sufficient soil moisture available (Van Rooyen *et al.,* 1991). If precipitation variability increases and the Namaqualand region still has sufficient moisture available, the flowering timing of Namaqualand daisies will essentially be advanced.

6.2 Namaqualand Daisies in the Global Context

Phenological studies are essential for a greater understanding of how climate change impacts biodiversity and ecosystems (Parmesan & Yohe, 2003; Colautti *et al.,* 2017; Donnelly & Yu, 2017; Pearson*,* 2019). The majority of global phenological studies assess spring phenological phase changes, such as bud burst and flowering together with changing climatic conditions (Cook *et al.,* 2012; Jiang *et al.,* 2016; Norman *et al.,* 2017). Different species are driven and influenced by fluctuating climate variables and their regions where the magnitude and extent of climate change differs (Diez *et al.,* 2012; Theobald *et al.,* 2017). Depending on a plant's intrinsic ability to adapt, different species' phenological responses to changing climatic conditions vary (White & Uller, 2014; Bussière *et al.,* 2015; Fitchett *et al.,* 2015; Richardson *et al.,* 2017).

6.2.1 Comparison with South African Phenological Studies

Similarities were identified when comparing the climate variables driving Namaqualand daisy phenological flowering to climate drivers influencing phenological phases from South African literature. This section will compare vastly different species due to the lack of phenological research in South Africa (Grab & Craparo, 2011; Fitchett & Fani, 2018).

Grab and Craparo (2011) assessed full bloom phenology of apple and pear trees in the south-western Cape from 1973-2009. Grab and Craparo's (2011) study is comparable to this research project since it deals with full bloom phenology in in the southwestern Cape. Grab and Craparo

(2011) observed significant advances in full bloom dates of apple trees in the south-western Cape due to increasing temperatures and slight decreases in precipitation. Similar to the Namaqualand daisies, apple trees' full bloom timing in the south-western Cape are significantly driven by maximum temperatures during August and September (Grab & Craparo, 2011). The calculated phenological full bloom advances of the apple trees that range between 2.4-4.2d.°C^{-1} (Grab & Craparo, 2011), are far greater than the full bloom advances calculated for the Namaqualand daisies that range between 0.01-0.03d.°C^{-1} (section 5.8.2). The phenological responses of apples to increasing temperatures are therefore far greater than that of Namaqualand daisies to increasing temperatures. Although regional precipitation changes in the south-western Cape are not significant, precipitation and temperature work concurrently to drive apple trees' phenological phases (Grab & Craparo, 2011). The drivers of apple tree phenological advances are therefore analogous to the drivers of Namaqualand daisy flowering phenology.

Fitchett and Fani (2018) and Fitchett *et al.* (2019) assessed Jacaranda flowering phenology (1924-2016) and sardine migration phenology (1946-2012), respectively. Similar to Namaqualand daisy flowering events, Jacaranda flowering and the sardine migration are significant natural and cultural events that occur annually in South Africa. Fitchett and Fani (2018) assessed historical newspaper and social media records, whereas Fitchett *et al.* (2019) only used historical newspaper records to reconstruct and create phenological datasets. It is therefore possible to create phenological records of significant natural events that have been documented in historical sources. The historical phenological dataset from 1924-2016, calculated a phenological flowering advance of 2.4d.decade^{-1} for Jacaranda trees (Fitchett & Fani, 2018). The average calculated phenological flowering advance for the Namaqualand daisies, from 1935-2018, 2.5d.decade^{-1} (section 5.7), is very similar to the calculated flowering advance of Jacaranda trees (Fitchett & Fani, 2018). In contrast to the results of this study and other South African phenological studies, Fitchett *et al.* (2019) observed delays of 1.3d.decade^{-1} in sardine migration to South Africa due to a southern advancement of the 21°C mean annual SST isotherm as a result of continuous climate change. The calculated results of this research project further agrees with Fitchett and Fani (2018) that found that due to phenological flowering advances being greater than the calculated advances in last frost dates in both regions (Namaqualand and the Highveld), both Jacarandas and Namaqualand daisies are becoming more threatened by increasing frost risks (Fitchett & Fani, 2018; section 6.1.3).

Altwegg *et al*. (2012) and Bussière *et al.* (2015) conducted two South African migratory bird phenological studies that assessed how climate change drives bird phenological phases in their non-breeding habitats. Similar to this research project that used a non-conventional method for collecting phenological information for a region that has no historical phenological data (section 4.2.2), both studies utilised novel methods for collecting their phenological datasets through the use of the South African Bird Atlas Projects (Altwegg *et al*., 2012; Bussière *et al.,* 2015). Although migratory phenological studies and plant phenological studies are not the same, it is interesting to note that both Altwegg *et al*. (2012) and Bussière *et al.* (2015) observed advances in migratory bird 'out of South Africa' phenological timing. Phenological advancing trends in South Africa are therefore not just observed for plants but also for certain animals.

Milton (1987) conducted a 13-month phenological study where seven Acacia species were assessed in Nylsvley, Limpopo. One year later, Steinke (1988) conducted a five-year vegetative and flowering phenological assessment of three mangrove species in the Umgeni Estuary, Durban. Both studies conducted in-situ observations of shoot growth and development, leaf emergence and abscission (Milton, 1987; Steinke, 1988). Milton (1987) and Steinke (1988) both observed that in two completely different regions, temperature and photoperiod significantly drives growth productivity of woody savanna plants and leaf emergence of mangroves, respectively. In accord with Milton (1987) and Steinke (1988) the calculated results of this study have identified temperature to significantly drive phenological flowering advances of the Namaqualand daisies (section 6.1.3), although photoperiod influences were not evaluated in this study. Pearson *et al.* (1995) revealed that, in an experimental study, Cape Daisies that received longer periods of sunlight flowered earlier than the daisies receiving less sunlight. It is therefore possible that the Namaqualand daisies might be influenced by photoperiod.

Numerous phenological studies conducted in the succulent karoo have found that vegetation and flowering phenology is driven by similar climatic drivers as the Namaqualand daisies (Hoffman & Cowling, 1987; Struck, 1994; Esler & Rundel, 1999; Hoare & Frost, 2004). Precipitation and moisture availability are critical drivers of flowering timing within the winter rainfall karoo biomes (Hoffman & Cowling, 1987; Struck, 1994; Esler & Rundel, 1999; Hoare & Frost, 2004). Hoffman and Cowling (1987) composed a synthesis on the vegetation of the karoo biome. Struck (1994) assessed the flowering phenology of the South African WRZ through conducting a three-year experimental study in permanent pots in the Goegap Nature reserve, Namaqualand. Esler and Rundel (1999) did a comparative literature study between the winter rainfall regions of the succulent karoo in South Africa and the Mojave Desert in the United States of America. Hoare and Frost (2004) utilised remote sensing NDVI datasets to assess and define the vegetation phenology across southern Africa. The findings of this research project are consistent with those of Struck (1994) who found that the onset of the rainy season and temperature increases during spring significantly drives first flowering timing in the karoo biome. Esler and Rundel (1999) similarly found that the onset of the rainy season significantly drives first flowering timing in the karoo. These findings support the calculated results and observed newspaper perceptions documented for this study (section 6.1.3). Hoffman and

Cowling (1987) and Struck (1994) further stated that precipitation during flowering seasons controls the duration of flowering and precipitation during early spring stimulates regional vegetation flowering and growth. These studies correspond with the observed newspaper records and the calculated results of this study that found that end of bloom timing of the Namaqualand daisies can be prolonged because of precipitation events during spring (section 6.1.3). Hoffman and Cowling (1987) and Esler and Rundel (1999) confirms that soil moisture availability is crucial for regional plant growth productivity and that winter temperatures ensures that vegetation can grow and develop sufficiently to flower during early spring. Hoffman and Cowling (1987) also states that coastal regions have increased moisture available due to coastal fog. Hoffman and Cowling (1987) therefore confirms that due to increased moisture levels Namaqualand daisy flowering occurs first in the coastal regions. The climate drivers of phenological phases in the karoo are therefore remarkably similar to the climate drivers influencing Namaqualand daisy flowering timing and should be similar seeing as Namaqualand forms part of the succulent karoo (Davis *et al.,* 2016).

Shackleton (2002) conducted a literature assessment of the phenological growth patterns of *Pterocarpus angolensis* in the South African lowveld savannas. Annual vegetation growth phenological phases in the lowveld savannas of South Africa are significantly related to precipitation (Shackleton, 2002). A remote sensing study by Wessels *et al*. (2011), from 1985-2000, assessed the growing season in all the different vegetative biomes of South Africa. Wessels *et al*. (2011) concluded that precipitation seasonality significantly drives the onset of vegetative phenological phases in all biomes of South Africa. The results of Shackleton (2002) and Wessels *et al.* (2011) are therefore consistent with the findings of this study that concluded that the onset of the rainy season is significantly correlated to flowering timing of the Namaqualand daisies. Precipitation timing and totals are therefore not only significant drivers of Namaqualand daisy flowering timing, but significant for vegetation productivity in all South African biomes (Wessels *et al.,* 2011).

The findings of this research project are consistent with those of Milton and Moll (1982), Shackleton (1999), and Jolly and Running (2004) that found that vegetation phenology in the south-western Cape, South African savannas and Kalahari regions are all driven by regional moisture availability. Milton and Moll (1982) studied four Acacia species in the south-western Cape and conducted in field phenological assessments. Shackleton (1999) conducted a one-year study in South African savannas where woody community phenology was assessed at three sites through transect recording methods. Jolly and Running (2004) assessed the impacts of soil moisture availability and precipitation on drought deciduous plant phenology in the Kalahari from 1989-1992. Assessing precipitation and potential evapotranspiration allows for a more complete phenological analysis seeing as water gains and losses in the system can be accounted for (Jolly & Running, 2004). The leaf area index of regional vegetation in the Kalahari was modelled and compared to NDVI data for three years (Jolly & Running, 2004). Milton and Moll (1982) found that similar to the Namaqualand daisies, the four assessed Australian Acacias in the south-western Cape, also flower during early spring. Shackleton (1999) found that the study sites that had increased moisture availability demonstrated advanced onset of leaf growth in South African savannas. This finding by Shackleton (1999) supports this research project's results and the observed newspaper perceptions that indicate that sufficient precipitation and moisture leads to earlier flowering events (section 6.1.3). In accordance with the results from this Namaqualand phenological study, Shackleton (1999) and Jolly and Running (2004) both found that evapotranspiration rates significantly drive plant phenological phases in their respective study regions.

Shackleton (1999) further stated that the onset of leaf growth and the duration of leaf growth in South African savannas varies along a precipitation gradient. In section 6.1.3 the calculated results of this study, the perceptions of local Namaqualand residents from newspaper records, and the assessed literature by Johnson (1992) and Davis *et al.* (2017) confirmed that phenological flowering timing of the Namaqualand daisies are driven along a precipitation gradient from west to east. The western areas of the Cape floral region flower during spring and the eastern regions flower during summer (Johnson, 1992). Plant phenological flowering or the onset of vegetative productivity in both the Cape floral region and South African savannas are therefore significantly driven along precipitation gradients (Johnson, 1992; Shackelton, 1999). These findings support the findings that the Namaqualand daisies tend to flower first along the western coastal region of Namaqualand and then later more inland, i.e. from west to east (section 6.1.3).

The studies by Whitecross *et al.* (2016, 2017a, b) explore the phenology of broad-leaved savanna trees and their immediate environment. Whitecross *et al.* (2016) assessed broad-leaved savanna tree phenology from 2012-2014. The study included an irrigation experiment during the dry season to assess if supplementary irrigation before the onset of the rainy season significantly impacts the leaf phenology of the trees (Whitecross *et al.,* 2016). Whitecross *et al.* (2017a) assessed the climate drivers of broad-leaved savanna trees' early greening phenology from 2002-2014 using remote sensing and NDVI values. Whitecross *et al.* (2017b) studied the phenological interactions between savanna trees and their surrounding grasses over three seasons from 2012-2014. Whitecross *et al.* (2016) observed that broad-leaved savanna trees can adapt their phenological green-up events based on environmental conditions that are suitable for the trees. Broad-leaved savanna trees also have the ability to que the onset of green-up events before the onset of the rainy season (Whitecross *et al.,* 2017a). Rainfall variability has the strongest correlation with early greening of broad-leaved savanna trees in South Africa (Whitecross *et al.,* 2017a). Broad-leaved savanna tree and Namaqualand daisy phenological phases are therefore not similar. Namaqualand daisies are more similar to savanna grasses growing around the broad-leaved trees, seeing as the green-up events and vegetative productivity of the grasses are closely related to precipitation and moisture availability (Whitecross *et al.,* 2017b). During periods with sufficient moisture and precipitation, grass growth is driven by light availability (Whitecross *et al.,* 2017b). Namaqualand daisies have a fixed life cycle of germinating shortly after the first winter rains, growing during the winter and flowering during early spring (section 6.1.3). Apart from underlying genetic differences within the Namaqualand daisy population, the Namaqualand daisies are less able to adapt the timing of their phenological cycles and are fully dependent on their regional environmental conditions (section 6.1.3). Regional climatic conditions, and especially precipitation, in Namaqualand is extremely variable (section 5.2). For that reason, flowering timing and quality varies from region to region in Namaqualand (section 5.14).

Araujo *et al.* (2016) related SPI calculations to grape yields in the Western Cape at regional and farm scales. Although yields are not directly impacted by phenological phases, climatic variables that influence grape phenology will ultimately impact the yields of the grapes. This study is useful for comparison to this research project seeing as it was also conducted in the Western Cape. Araujo *et al.* (2016) found that grape yields are significantly influenced by drought conditions. Droughts conditions during El Niño years bring about temperature increases together with decreases in precipitation which reduces the total grape yields in the region (Araujo *et al.,* 2016). This research project found that Namaqualand daisy first flowering timing in Springbok, Lambertsbaai Nortier and Clanwilliam are inversely correlated to SPI values (section 5.11), therefore indicating that drought years leads to delayed flowering timing. These results are therefore consistent with that of Araujo *et al.* (2016). Namaqualand daisies are more at risk to drought impacts than grapes grown at a commercial level since farmers can use supplementary irrigation during drought periods.

Conradie *et al.* (2002) also conducted a grape study in the Western Cape where the effects of environmental factors on the grapevines were assessed. The assessment by Conradie *et al.* (2002) is relevant for comparison to this Namaqualand study seeing as it helps to explore phenological sensitivity in the Western Cape as there are not yet any other South African wildflower phenological studies to compare to. Five commercial vineyards were studied for seven years (Conradie *et al.,* 2002). The study by Conradie *et al.* (2002) revealed that increased temperatures do not induce significant advances in first flowering rates, as in the case of the Namaqualand daisies. Conradie *et al.* (2002) did, however, perceive that increased temperatures lead to earlier ripening of the grapes which is similar to the results from the current study that found that increased temperatures leads to advanced flowering for all flowering stages of the Namaqualand daisies (section 5.8, 6.1.3).

Most phenological studies conducted in South Africa were conducted in the Western Cape regions. Thus, many of the phenological studies have similar climate drivers influencing phenological phases. As mentioned previously, precipitation is one of the most important climate drivers of phenological phases (Wessels *et al.,* 2011), although increasing temperatures significantly drive the observed phenological advances (Grab & Craparo, 2011; section 6.1.3).

6.2.2 Comparisons with Global Wildflower Phenological Studies

The findings of this study are consistent with a range of authors globally, who have reported advances in spring flowering for wildflowers and daisies due to climate change and global warming (Menzel & Fabian, 1999; Ahas *et al.,* 2002; Dose & Menzel, 2004; Studer *et al.,* 2005; Menzel *et al.,* 2006; Torres & Galetto, 2011; Rosbakh & Poschlod, 2015; Hubálek, 2016; Thackeray *et al.,* 2016;

Bailey & Kevan, 2017; Petrauski *et al.,* 2019). The drivers of Namaqualand daisy flowering advances are consistent with a collection of Northern Hemisphere phenological assessments that identified temperature as one of the main climatic variables driving advances in daisy and wildflower flowering phenology (Studer *et al.,* 2005; Lesica & Kittelson, 2010; Whittington *et al.,* 2015; Hubálek, 2016; Bailey & Kevan, 2017; Petrauski *et al.,* 2019).

Bailey and Kevan (2017) conducted a study in the USA that provides valuable comparison with the Namaqualand daisy flowering record. The study assessed Asteraceae wildflowers which belongs to the same family as the Namaqualand daisies (Bailey & Kevan, 2017). Bailey and Kevan (2017) observed that the onset of the growing season for *Erigeron lemmonii* is driven by increased temperatures during spring. The onset of the growing season for the Namaqualand daisies, however, is driven by the onset of the winter rainy season (section 5.14, 6.1.3) whereas during winter in Arizona, *Erigeron lemmonii* wildflowers are dormant (Bailey & Kevan, 2017). In contrast to the Namaqualand daisies, the wildflowers studied by Baily and Kevan (2017) have two peak flowering periods, one during May and the other during August. In accordance with the Namaqualand daisies, the flowering season for the Arizona wildflowers can be prolonged due to in-season precipitation events (Baily & Kevan, 2017).

Lesica and Kittelson (2010) conducted a phenological assessment of 32 common spring wildflowers in the Rocky Mountains of the USA, from 1995-2008. This study is useful for comparison with the phenological assessment of the Namaqualand daisies seeing as it assessed wildflowers in a semi-arid region (Lesica & Kittelson, 2010). Petrauski *et al.* (2019) assessed the flowering phenology of two wildflowers, *Cardamine concatenate* and *Erythronium americanum*, in West Virginia of the USA over 111 years. Furthermore, Petrauski *et al*. (2019) collected their phenological information from dated photographs and herbarium specimens which is also a form of historical records and is therefore a useful study for comparison with the Namaqualand record. Pearson (2019) assessed 10,000 herbarium specimens of wildflowers from the Asteraceae family from south-east USA, and this study is therefore also valuable to compare to the Namaqualand flowering phenological dataset. Lesica and Kittelson (2010) found that approximately 37% of the observed mean wildflower flowering variation is accounted for by the preceding month's temperatures. This study therefore confirms the calculated significant correlation between August temperatures and full bloom timing for the Namaqualand daisies (section 6.1.3). Both of the studied wildflowers by Petrauski *et al.* (2019) have advanced their flowering phenology over the past century with an average flowering advance of 0.91d.decade^{-1}. The Namaqualand daisy average flowering advance of 2.5d.decade^{-1} (section 5.7, 6.2.1) is greater than the flowering advance observed by Petrauski *et al.* (2019). These results indicate that temperature during spring is a strong driver of the phenological flowering advances in West Virginia (Petrauski *et al.,* 2019). The calculated flowering advances for the Namaqualand daisies that range between 0.01-0.11d.°C^{-1} (section 5.8) are smaller than the flowering advances of 1.5d.°C^{-1} calculated by Lesica and Kittelson (2010). Pearson (2019) observed Asteraceae spring flowering advances that range between 1.8-2.3d.°C^{-1}. For *Cardamine concatenate* and *Erythronium americanum*, flowering timing advanced by 2.91-3.44d.°C^{-1}, which therefore indicates that daisies and wildflowers from North America are more sensitive to temperature increases than Namaqualand daisies (Lesica & Kittelson, 2010; Pearson, 2019; Petrauski *et al.,* 2019).

Lesica and Kittelson (2010) and Petrauski *et al.* (2019) further observed spring wildflower flowering advances, due to decreasing winter precipitation and increased spring temperatures. In arid regions, phenological flowering advances are more significantly driven by precipitation decreases (Crimmins *et al.,* 2010; König *et al.,* 2018). König *et al.* (2018) conducted a meta-analysis literature assessment in the Northern Hemisphere where 562 species were studied across 18 study sites. A model created by König *et al*. (2018) revealed that increasing temperatures and decreasing precipitation and regional moisture are strongly related to first flowering advances. The onset of winter precipitation significantly drives first flowering timing for the Namaqualand daisies, subsequent precipitation events during late winter and early spring drives full bloom timing and precipitation during spring leads to longer flowering seasons for the Namaqualand daisies (section 6.1.3). Precipitation in Namaqualand has been decreasing while temperatures have been increasing over time (section 5.2). These precipitation decreases and temperature increases have been occurring concurrently with significant flowering timing advances (section 5.7, 6.1.2). These findings are therefore in agreement with the results from Lesica and Kittelson (2010) and Petrauski *et al.* (2019).

Pearson (2019) further stated that increased precipitation during spring led to flowering delays of Asteraceae wildflowers in south-east USA. Similarly, in Namaqualand, calculated relationships indicate that increased precipitation during spring contributed to end of flowering delays, i.e. a longer flowering season (section 5.8, 6.1.3).

Certain phenological studies conducted in the Northern Hemisphere revealed that precipitation does not significantly drive flowering phenology of wildflowers (Cayan *et al.,* 2001; Buermann *et al.,* 2003; Studer *et al.,* 2005; CaraDonna *et al.,* 2014; Bailey & Kevan, 2017). Flowering phenological phases of Namaqualand daisies on the other hand are significantly driven by precipitation from late autumn/early winter until the end of the flowering season (section 6.1.3). Studer *et al*. (2005) conducted a multi-species spring phenological assessment for 15 flowering plants, of which the Daisy (*Leucanthemum vulgare*) was one, in the Alps in Switzerland during the period 1965-2002. The 1.5d.decade^{-1} flowering advance calculated by Studer *et al.* (2005), which is smaller than the calculated flowering advance of the Namaqualand daisies, was argued to be significantly driven by winter and spring temperatures and that precipitation did not influence the phenological flowering timing of the plants at all. These contrasting results of Studer *et al.* (2005) can be attributed to the empirical orthogonal function analyses that was used to calculate an approximation of flowering trends for the region. Studer *et al.* (2005) did, however, state that precipitation can significantly drive flowering phenology at a regional scale. In this Namaqualand study, the calculated results confirmed, and the assessed newspaper records perceived, that regional precipitation and moisture balances drive flowering phenology (section, 6.13).

Some phenological flowering assessments have concluded that first flowering timing is related to snowmelt timing (Inouye, 2008; Miller-Rushing & Inouye, 2009). In the Northern Hemisphere, increased temperatures during spring leads to earlier snowmelt dates which therefore significantly drives advances in first flowering timing (Miller-Rushing & Inouye, 2009; Theobald *et al.,* 2017). Due to the advances in first flowering timing, wildflowers are exposed to increased frost risks since last frost dates might not be advancing at the same rate (Inouye, 2008). The Namaqualand region infrequently experience snowfall periods, and thus similar assessments cannot be made. Due to first flowering advances being greater than the calculated advances in last frost dates in the different Namaqualand subregions, frost risks are increasing in Namaqualand (section 6.1.3).

Previous studies have demonstrated that increased temperatures during the months that precede flowering, significantly drives advances in flowering timing (Beaubien & Freeland, 2000; Miller-Rushing & Primack, 2008a; Petrauski *et al.,* 2019). Winter and spring temperatures significantly drives flowering phenological timing of wildflowers in Switzerland (Studer *et al.,* 2005). Similarly, Torres and Galetto (2011) assessed 43 Asteraceae wildflowers in the Chaco Serrano forest, Argentina, and concluded that flowering phenology is significantly driven by seasonal variations in climate variables. For temperate regions, increasing temperatures during spring also significantly drive advances in wildflower flowering timing (Gordo & Sanz, 2005; König *et al.,* 2018). In

Namaqualand temperatures and precipitation from May (winter) until October (spring) significantly drive the observed flowering advances of the Namaqualand daisies (section 5.8, 6.1.3). These findings support the results of Studer *et al*. (2005) that stated that winter and spring temperatures drive phenological flowering timing of wildflowers; and the results by Torres and Galetto (2011) that stated that seasonal climate variations drive the flowering phenology of wildflowers.

Literature suggests that a combination of climate variables during different temporal periods work concurrently to drive flowering phenology (Crimmins *et al.,* 2010). To create a clearer and more comprehensive picture of the significant drivers of flowering phenological phases, multiple climate variables or drivers need to be assessed together (Menzel, 2003; Theobald *et al.,* 2017). The calculated multiple regression analysis conducted for the Namaqualand daisies during first flowering similarly reveals that temperature and precipitation variables work concurrently to significantly drive the observed phenological flowering advances (section 5.9, 6.1.3).

6.2.3 Comparison with Southern Hemisphere Phenological Studies

The majority of conducted global phenological studies were completed in the Northern Hemisphere (Chambers, 2009; Chambers *et al.,* 2013, 2017; Fitchett *et al.,* 2015). Within Southern Hemisphere phenological assessments, the observed phenological changes are location and species specific (Chambers, 2009; Chambers *et al.,* 2013). In accordance with the calculated flowering advances of the Namaqualand daisies, a range of phenological assessments conducted in Australia have revealed advances in phenological events due to increasing temperatures (Keatley *et al.,* 2002; Chambers, 2005; Beaumont *et al.,* 2006; Keatley & Hudson, 2007; Gallagher *et al.,* 2009; Hoffman and Rohde, 2010; Chambers *et al.,* 2013).

Although the following studies that are used for comparison with this Namaqualand study do not have datasets spanning similar temporal periods, broad comparisons on responses to increasing temperatures and rates of changes can tentatively be made. Gallagher *et al.* (2009) assessed 171 flowering plants from the Australian alps, from herbarium records due to a lack of phenological datasets in Australia. The study identified five plant species that demonstrated 'sensitive' phenological flowering responses to increasing temperatures from 1950-2007 (Gallagher *et al.,* 2009). As part of the five identified 'sensitive' species from the herbarium records, Gallagher *et al.* (2009) assessed an Asteraceae flowering plant, the alpine groundsel (*Senecio pectinatus*). The alpine groundsel has a calculated significant phenological flowering advance of 6.9d.decade^{-1} (Gallagher *et al.,* 2009) which is considerably larger than the calculated phenological flowering advance of 2.5d.decade^{-1} for the Namaqualand daisies (section 6.2.1). The calculated phenological changes for the other four 'sensitive' plant species were not statistically significant, although Gallagher *et al.* (2009) stated that future continuous temperature increases may lead to significant changes in these species' flowering timing. Darbyshire *et al.* (2013) conducted estimates of pome fruit spring phenology in Australia using eight existing datasets that are 24-43 years long. Pome fruit spring phenology estimates revealed that phenological phases were to advance between 4.1-7.7d.°C^{-1}, although only one dataset revealed significant advances over time (Darbyshire *et al.,* 2013). The phenological advances estimated by Darbyshire *et al.* (2013) are larger than the calculated phenological advances of the Namaqualand daisies (0.01-0.11d.°C^{-1}; section 6.1.3). The Namaqualand daisies are therefore less sensitive to changing climatic conditions as compared to the Australian plants assessed by Gallagher *et al.* (2009) and Darbyshire *et al.* (2013).

It is important to compare and contrast the results of this study with meta-analysis studies conducted in the Southern Hemisphere to assess if the calculated phenological advances and the significant climate drivers impacting the Namaqualand daisies are similar. Chambers *et al.* (2013) conducted a phenological meta-analysis that assessed Southern Hemisphere phenological studies that focussed on both animal and plant phenological phases. The meta-analysis revealed that, in accordance with the Namaqualand daisies, Southern Hemisphere spring phenological phases are advancing significantly over time (Chambers *et al.,* 2013). The calculations of the meta-analysis revealed that 42% of marine and 82% of terrestrial datasets confirmed significant phenological advances (Chambers *et al.,* 2013). In the meta-analysis conducted by Chambers *et al.* (2013), increasing temperatures were identified as the main driver for phenological advances. Precipitation also drives phenological changes but due to large inter-annual variability in precipitation, it cannot be attributed as a main driver of phenological change (Chambers *et al.,* 2013). In New Zealand, plant and animal phenological phases are also driven by temperature conditions (Primack, 1980; Irvin *et al.,* 1999; Verghis *et al.,* 1999). In agreement with Chambers *et al*. (2013) and phenological assessments conducted in New Zealand, the significantly increasing temperatures in Namaqualand drive the calculated advances of the Namaqualand daisies (section 6.1.3). However, precipitation timing and totals are also significantly driving the advanced flowering phenology of the Namaqualand daisies. Similar to what Chambers *et al*. (2013) observed, precipitation is extremely variable over time, thus the impact of precipitation on flowering timing is also variable (section 6.1.1).

Webb *et al*. (2007) led a phenological assessment of future phenological changes of wine grapes in Australia. The increased temperatures brought about by global warming were projected to significantly advance first flowering and end of bloom timing, together with contracting the overall flowering season (Webb *et al.,* 2007). With the projected increases in temperatures in the Western and Northern Cape, future flowering advances are also estimated for the Namaqualand daisies (section 6.1.5). The projected results of the Namaqualand study are therefore consistent with the projected phenological flowering advances calculated by Webb *et al.* (2007). Increased temperatures during the flowering season can also contribute to an earlier end to the flowering season, i.e. advancement of the end of bloom, and depending on precipitation variability and totals, possibly contribute to a shorter flowering season (section 6.1.3).

Namaqualand daisies are advancing their flowering timing due to increasing temperatures and decreasing precipitation (section 6.1.3). Bull and Burzacott (2002) have observed that the calculated advances in the pairing dates of Sleepy Lizards (*Tiliqua rugosa*), in Australia, are similarly driven by increased winter temperatures and general drier conditions. When phenological rates of changes and the accompanying driving climatic variables are similar, species mismatch risks are reduced (Bartomeus *et al.,* 2011). The alignment between these two southern hemisphere records is thus promising but would require targeted studies in both South Africa and Australia on symbiotic or predator-prey pairs to make accurate mismatch projections. Anwar *et al.* (2015) conducted a phenological assessment, in western and eastern Australia, of broadacre crops based on future projections from Global Climate Models from the Special Report on Emission Scenarios. The project entailed imputing downscaled climate data into an Agricultural Production Systems Simulator to model future crop yields (Anwar *et al.,* 2015). Similar to what is happening in Namaqualand, Anwar *et al.* (2015) calculated phenological advances brought about by the projected precipitation decreases together with increased temperatures. They projected a significant reduction in crop yields (Anwar *et al.,* 2015). Contrasting to precipitation decreases driving flowering advances, Keatley *et al.* (2002) observed that precipitation increases in south-eastern Australia have led to flowering advances of two Eucalypt plant species. Namaqualand daisy flowering phenology is more significantly driven by precipitation timing although increased precipitation would lead to a longer flowering season, i.e. delays in end of bloom timing (section 6.1.3). Furthermore, the assessed newspaper records perceived that increased winter precipitation would lead to flowering advances of the Namaqualand daisies (section 5.14).

Primack (1980) conducted a phenological flowering assessment of montane shrubs in the South Island, New Zealand. The study concluded that first flowering timing for high altitude shrubs are advanced due to increased temperatures. When temperatures are higher, the duration of the flowering season for high-altitude shrubs in New Zealand is shorter (Primack, 1980). The Namaqualand daisies, similarly, are driven by temperature conditions (section 6.1.3). The Namaqualand daisies first flowering timing is significantly advancing due to increased temperatures during winter and spring while the end of the flowering season is tentatively advanced due to increased spring temperatures (section 5.8, 6.1.3). Approximately 30% of migratory phenological changes observed in Australia are related to increases in T_{min} (Chambers, 2009). Similarly, increases in temperatures have led to advances in arrival dates for long distance migratory birds in south-eastern and western Australia (Chambers, 2005; Beaumont *et al.,* 2006). SST significantly drive the breeding phenology of Little Penguins (*Eudyptula minor*) on the Phillip Islands in Victoria, Australia (Chambers, 2004). The Namaqualand daisy study, in accordance with the assessed literature from the Southern Hemisphere, therefore, confirms that temperatures significantly drive plant and animal phenological phases (section 6.1.3).

In a phenological assessments conducted in Australia, it was observed that certain plant species can flower during any temporal period as long as there is sufficient moisture available (Kassas, 1966; Mott, 1972; Davies, 1976). The Namaqualand daisies also need sufficient moisture but can only flower during spring, after the winter rainfall period, and when temperatures begin to increase (section 6.1.3).

In an experimental phenological study conducted in Western Australia from 1969-1971, Mott and McComb (1975a, 1975b) assessed the influence of temperature and moisture stress on three annual plant species under glasshouse conditions. These two studies are useful for comparison to the Namaqualand study since the assessed plants come from an arid region. In agreement with the findings of this research project, Mott and McComb (1975a) found that flowering was delayed for one of the assessed species (*Aristida contorta*) when the annual winter plant was exposed to lower temperatures. The Namaqualand daisies flowering timing will also be delayed when exposed to lower temperatures (section 6.1.3). Mott and McComb (1975b) found that moisture stress conditions led to delays in flowering timing for two of the assessed winter ephemeral plants. In agreement with Mott and McComb (1975b), when the Namaqualand daisies are exposed to moisture stress conditions or general drought periods, first flowering will also be delayed (section 6.1.3). The flowering season in general will also be shorter due to end of bloom advancing because the daisies need moisture to survive for longer during the flowering season (section 6.1.3).

6.2.4 Namaqualand Daisy Phenological Flowering Advances within the Global Context

In accordance with the calculated flowering advances of the Namaqualand daisies, the majority of published global phenological literature advocates that in different regions all over the world, spring phenological phases have been advancing during recent decades (Chmielewski *et al.,* 2004; Doi, 2007; Miller-Rushing *et al.,* 2007; Nordli *et al.,* 2008; Primack *et al.,* 2009a; Munguía-Rosas *et al.,* 2011; Cook *et al.,* 2012; CaraDonna *et al.,* 2014; Ge *et al.,* 2015; Thackeray et al., 2016; Cohen *et al.,* 2018; Howard, 2018; König *et al.,* 2018). In the literature review a table (Table 2.1) documented past global phenological studies and related observed phenological changes to temperature changes. The identified studies (Table 2.1) indicate phenological advances over time with a calculated mean phenological advance of 5.13d.°C^{-1}. The significant flowering advances of this research project that range between 0.01-0.11d.°C^{-1}, are significantly smaller than the average phenological advance calculated from Table 2.1. This finding is supported by Davis *et al.*'s (2010) conclusion that plants from the Asteraceae family do not project changes in climatic conditions as successfully as plants from other families.

Global literature on phenological meta-analysis papers have demonstrated that phenological shifts for plants and animals are advancing at a global mean of approximately 2.3 d.$decade^{-1}$ (Parmesan & Yohe, 2003; Doi, 2007; Munguía-Rosas *et al.,* 2011; Ge *et al.,* 2015; Usui *et al.,* 2017; Cohen *et al.,* 2018). In line with this global meta-analysis of phenological advances, the overall mean advance of flowering timing for the Namaqualand daisies is calculated to be 2.5d.$decade^{-1}$ (section 5.7, 6.2.1). The overall mean flowering advance of the Namaqualand daisies is also consistent with that of Menzel *et al.* (2006), who conducted an European phenological meta-analysis from 1971-2000 and calculated a 2.5d.$decade^{-1}$ advance in spring and summer phenological phases.

The phenology of annual and perennial plant growth is significantly driven by temperatures (Guédon & Legave, 2008; Shi *et al.,* 2017; Menzel *et al.,* 2020). Temperatures drive the onset and duration of seasonal growth and therefore drives phenological shifts from dormancy to reproductive phenology of annual and perennial plants (Guédon & Legave, 2008; Shi *et al.,* 2017; Menzel *et al.,* 2020). Numerous global phenological studies have concluded that increasing air temperatures significantly drive phenological flowering advances (Araujo *et al.,* 2016; CaraDonna & Bain, 2016; Ahmad *et al*., 2017; Wang *et al.,* 2018). Every flowering stage of the Namaqualand daisies, from first flowering to end of bloom, is also driven by temperatures at different periods during the year (section 6.1.3). The results from this Namaqualand daisy study are consistent with the abovementioned literature; that increasing temperatures significantly drive the advances of Namaqualand daisy flowering phenology (section 6.1.3). Certain phenological studies have concluded that combinations of climatic variables concurrently drive plant phenological phases (Crimmins *et al.,* 2010; Polgar & Primack, 2011; Ruml *et al.,* 2011; Drake & Martin, 2018). Polgar and Primack (2011) assessed leaf-out phenology of temperate woody plants and concluded that photoperiods and temperatures significantly drive leaf-out phenology. Ruml *et al.* (2011) and Drake and Martin (2018) stated that regional precipitation and temperatures significantly drives phenological shifts observed for plums (*Požegača*) and cavity-nesting birds, respectively. In accordance with the presented literature, Namaqualand daisy flowering phenology is not only driven by increasing temperatures, but also by a combination of temperature and precipitation variables at different stages of the daisy growth period (section 6.1.3).

In another phenological meta-analysis of the Northern Hemisphere conducted by König *et al.* (2018), decreases in precipitation were found to be stronger drivers for phenological first flowering advances than increasing temperatures. These results are in accordance with the calculated results for the Namaqualand daisy study where both precipitation and temperature are significantly driving the observed flowering advances although, the calculated correlations between first flowering timing and precipitation timing are the strongest (section 5.15, 6.1.3). Wang *et al.* (2014) collected ground based phenological information of 20-50 years, which they related to matching climatic datasets. Wang *et al*. (2014) concluded that in regions where spring temperature variance is too large, plants occasionally suppress their responses to spring temperatures and rather rely on other climatic drivers of phenological phases such as photoperiod or chilling requirements. Therefore, spring phenology can be driven by chilling requirement fulfilment, photoperiods and warming requirements which breaks dormancy and induces the next ontogenetic stages (Wang *et al.,* 2014; Benmoussa *et al.,* 2018). Bud burst phenology during spring is also influenced by precipitation timing, winter chilling requirements, and increased temperatures (Nordli *et al.,* 2008; Fu *et al.,* 2015;

Bailey & Kevan, 2017). As discussed in section 6.1.3, all these climatic variables have been assessed in this Namaqualand study and, to a certain degree (not always significant), has some driving power over Namaqualand daisy flowering phenology. Precipitation totals and timing have the strongest calculated correlations with flowering timing. The calculated climatic drivers for the Namaqualand daisies produced results, which corroborate the findings of previous work in this field (section 6.1.3).

In high-altitude and -latitude regions, plant phenological phases are driven by temperature and precipitation seasonal variations, photoperiods and snowmelt timing (Körner, 2007; Wipf *et al.,* 2009; Ziello, 2009; Forrest *et al.,* 2010; Bjorkman *et al.,* 2015; Chen *et al.,* 2015; Filippa *et al.,* 2015; Colautti *et al.,* 2017; Vitasse *et al.,* 2017). Global phenological literature states that plant phenology in mid-latitudes are significantly driven by climate factors that influence regional seasonality (Schwartz & Reiter, 2000; Haselhorst *et al.,* 2017; Cohen *et al.,* 2018). Lesica and Kittelson (2010) similarly stated that winter precipitation and spring temperatures significantly drive wildflower phenology in semi-arid regions in the USA. In a meta-analysis, Cook *et al.* (2012) correlated growing degree day temperature datasets with FFD for 490 species in Europe and the USA. Cook *et al*. (2012) confirmed that climate variables during different seasons can have variable impacts on plant phenological phases. In accordance with the assessed global literature that indicates that seasonal climate variables drive phenology, the calculated results for this study indicate that winter and spring climate variables are the main drivers of advances for Namaqualand daisy flowering (section 6.1.3). The onset of the winter rains and increased temperatures during both winter and spring drives flowering phenology for the Namaqualand daisies (section 6.1.3).

Inouye (2008) assessed the influence that increased global temperatures have on snowmelt timing, which ultimately drives the growing season of montane wildflowers growing in experimental pots in the Rocky Mountains, USA. Due to increasing temperatures, snowmelt dates in the Rocky

Mountains are advanced which leads to an advancement of the growing season (Inouye, 2008). Advanced growing seasons for three assessed wildflowers exposes the flowers to more frequent frost events, ultimately increasing the overall frost risk for wildflowers in the region (Inouye, 2008). Some phenological studies suggests an increased frost risk in mid-latitudinal regions because increased temperatures during spring leads to significant flowering advances, leaving the flowers vulnerable to frost damage (Inouye, 2008; Polgar & Primack, 2013; Fitchett *et al.,* 2014b). Plants that flower during early spring are more at risk to frost damage, which can negatively affect full bloom flowering timing (Cannell & Smith, 1986; Inouye, 2008; CaraDonna & Bain, 2016; König *et al.,* 2018). The findings of the current study are agreement with the assessed literature. Frost risk is increasing for the Namaqualand daisies due to advancing flowering timing being greater than the advances of last frost dates (section 5.13.2, 6.1.3).

Advanced snowmelt timing, due to increased temperatures, further drives leafing and flowering phenology in highland regions (Walker *et al.,* 1995; Wang *et al.,* 2018). Spring temperatures influence snowmelt timing that ultimately influences soil moisture availability in arid regions (Walker *et al.,* 1995; Wang *et al.,* 2018). Wang *et al.* (2018) studied alpine vegetation growth phenology on the Tibetan Plateau using MODIS and NDVI satellite remote sensing datasets from 2000-2015. This study found a positive correlation between vegetation growth phenology and snowmelt dates. Therefore, if snow cover melts during early spring, the start of vegetative growth in the region will be advanced (Wang *et al.,* 2018). Although the Namaqualand region hardly experiences snowfall periods; the impact of snowmelt timing on soil moisture availability is comparable to precipitation timing. First flowering timing of the Namaqualand daisies is driven by precipitation timing (section 6.1.3). The soil moisture in Namaqualand is also influenced by subsequent precipitation events that also significantly drives full bloom and end of bloom timing (section 6.1.3), which is therefore, similar to snowmelt timing that impacts moisture availability and ultimately first flowering timing in the Northern Hemisphere (Walker *et al.,* 1995; Wang *et al.,* 2018).

Tropical regions predominantly exhibit weak seasonality and are evergreen regions (Fitchett *et al.,* 2015; Moore *et al.,* 2016). Sakai and Kitajima (2018) assessed the perspectives and advances of phenology in tropical regions. Due to the absence of a cool season, plant phenological phases are variable depending on the species (Sakai & Kitajima, 2018). Some species reproduce several times per year whereas others only reproduce once in several years (Sakai & Kitajima, 2018). Precipitation regimes in tropical regions are also variable (Corlett & Lafrankie, 1998; Souza *et al.,* 2018). Tropical regions have more variable climate variables that drive plant phenological phases compared to high-altitude and latitude regions (Sakai & Kitajima, 2018). Wright *et al*. (2019) created a phenological model that used 29 years of census data to predict flowering dates for two annual plants that flower multiple times per year in Panama, USA. The flowering timing for *Hybanthus prunifolius* and *Handroanthus guayacan* in the Neotropical forest in Panama can be triggered by precipitation events that produce more than 5mm of rain after an extended drought period (Wright *et al.,* 2019). Namaqualand daisy flowering cannot be triggered by a single precipitation event or even consecutive precipitation events (section 6.1.3). The first significant winter precipitation events in Namaqualand drives the onset of the growing season for the Namaqualand daisies throughout the winter season and ultimately the timing of first flowering in early spring (section 6.1.3). The results of this Namaqualand study are consistent with other tropical phenological studies that found that precipitation regimes in tropical regions significantly drives phenological phases such as anthesis, leaf fall and bud burst (Mendivelso *et al.,* 2016; Yun *et al.,* 2018). Due to weak seasonality in tropical regions, photoperiod variability, as a result of changes in cloud cover, also significantly drives phenological phases (Wright & van Schaik, 1994; Körner & Basler, 2010; Cortés-Flores *et al.,* 2017;

Wright & Calderón, 2018). Photoperiods were not assessed in this research project, however, Pearson *et al.* (1995) observed that the Cape daisy flowering timing is advanced under increased photoperiod conditions. These results suggest that further studies involving the effects of photoperiods on the Namaqualand daisies should be conducted.

6.3 Study Limitations

6.3.1 Data Limitations

The climate data used for this research was obtained from the SAWS, which is a WMO accredited organisation, administered by the South African government. The meteorological and climate data provided by the SAWS is subject to quality control to ensure and guarantee high accuracy data (SAWS, 2019; Roffe *et al,* 2019). The selected weather stations use robust electronic and manual recording methods. The consistency of the climate data can be impacted by mechanical faults, system changes, and human error when conducting manual recordings. Some of the weather stations' data records have months and years of missing data and some stations have short (less than 30 years) meteorological records. The gaps in the climate record can bias the analysis, compromise its reliability, and obscure the true climate changes in the region (Ledneva *et al.,* 2004; Nordli *et al.,* 2008). Years with missing climate data were omitted, instead of interpolating the climatic conditions.

The longest datasets (1959-2018 and 1960-2018) revealed significant changes in annual temperature variables. The shorter datasets (1989-2018, 2000-2018 and 2003-2018) showed no significant changes over time (section 5.2). The misalignment between result are due to the variability of assessed subregions and variable temporal periods (MacKellar *et al.,* 2014; Kruger & Nxumalo, 2017).

Although the Namaqualand daisy flowering phenological dataset covers a large geographic area (Figure 3.2), climate data from meteorological stations were used instead of gridded climate data. Park and Schwartz (2015) similarly assessed the flowering phenology of herbarium specimens in South Carolina, USA, and used the meteorological data from 13 weather stations to correlate to the observed phenological changes. A range of other phenological studies conducted in large geographic regions utilised point based meteorological or weather station data (Sparks *et al.,* 2000; Lu *et al.,* 2006; Doi, 2007; Zavalloni *et al.,* 2006; Amano *et al.,* 2010; Craparo *et al.,* 2015). A possible limitation of *in situ* meteorological climate data, which provides location specific information, is the fact that it does not provide information for a larger region (Schulze, 2007; Rana *et al.*, 2015). Namaqualand is a sparsely populated area, thus only a few meteorological stations are available for analysis. This limits spatial representativity. To overcome this limitation, this study utilised every weather station available. The fact that there are only a few meteorological stations in the region also limits the reliability of using gridded climate data. Gridded climate data is more spread out over a region and is interpolated, which means that data can be over or underestimated (Zhang *et al.,* 2013). Meteorological data serves as a true estimate of the climatic conditions in a specific area (Zhang *et al.,* 2013). It is impossible to avoid all the limitations associated with the type of climate data used. The use of meteorological point weather station data within phenological research in the Namaqualand region is more reliable and accurate because the data comes from the SAWS (accredited by the WMO).

The assessed newspaper records frequently mentioned the importance and significance of berg winds on end of bloom timing of the Namaqualand daisies (section 5.14). Climate data related to the wind speed and direction during flowering could increase the analytical accuracy of the study. SAWS collects wind speed and direction data for certain weather stations, thus it could have been included in the phenological assessment of the flowering timing of Namaqualand daisies. However, the main variables explored in existing phenological studies include temperature, precipitation, and photoperiod (Parmesan & Yohe, 2003; Fitchett *et al.,* 2015; Cortés-Flores *et al*., 2017; Cohen *et al.,* 2018). These three climate variables generally account for the observed changes in plant phenological phases (Badeck *et al.,* 2004; Polgar & Primack, 2013). The climate conditions brought about by berg winds in Namaqualand lead to increased temperatures and dry conditions (Le Roux, 2005). The influence of wind in phenological assessments usually assesses the impact of wind-pollination on plant phenology (Koenig *et al.,* 2012; Calinger *et al.,* 2013), or aerial species' phenological cycles (Irons *et al.,* 2017). Therefore, wind speed and direction were not included in this research project.

For a study to infer that climate change affects plants' phenological responses it is essential to have a phenological dataset that spans a minimum of 30 years (Menzel & Fabian, 1999; Fitchett & Fani, 2018; Langvall & Löfvenius, 2019). Obtaining such a long record was difficult, since first and last flowering events of the daisies in Namaqualand have not been documented. Tour guide operators and National Parks were contacted to find out if any records and dates of Namaqualand daisy flowering events exists. Most tour guide operators do not keep records of specific flowering events but kept the dates of past flower viewing tours. None of the National Parks in the Namaqualand region kept any records of FFD of the Namaqualand daisies.

Newspaper records and social media platforms were assessed to create a phenological flowering dataset of the Namaqualand daisies (section 4.2.2). Within the newspaper and social media records a great margin for inconsistency arises, seeing as human bias and judgement can influence the quality of the phenological information (Chmielewski & Rotzer, 2001; Menzel, 2002; Miller-Rushing & Primack, 2008a; Grab & Nash, 2010). The journalists writing the articles describing flowering conditions in Namaqualand and the people posting information of the Namaqualand daisies on social media are not trained phenological experts. Journalists and people posting pictures on social media do not create descriptive phenological records that are meant to be used for dating flowering timing and the records that they produce are not always scientifically accurate. Different journalists from different newspaper records will also judge and bias phenological information variably over time (Menzel, 2002; Miller-Rushing & Primack, 2008a). The newspaper records provided information relating to the flowering season throughout the season (from first flowering to the end of bloom) and one could therefore document or track the flowering season throughout the year. When newspapers stated that the flowering season has started, or is in full bloom, there is no further information relating to how many flowers are in bloom. Similarly, when the end of the flowering season was announced, it was not clear if the flowers are starting to die or if there are no flowers left at all. Some of the documented extracts from the newspapers did not always provide highly accurate information. For example, an article written on 21 July 2009 in Die Burger stated that there are "patches of flowers" in certain Namaqualand regions. There were a few extracts similar to this one, which are not a very clear or descriptive and the researcher used discretion and documented the date of the article as a 'first flowering' date, seeing as there are flowers scattered in the landscape although not in full bloom just yet. Another example from an article written on 23 September 2004 in Volksblad stated that "we are now nearing the end of the flowering season." With extracts similar to this, it is not clear if there are still enough flowers for the next two days or two weeks. For instances like this, the date of the article was documented as an 'end of bloom' date. Therefore, the researcher had to use discretion when documenting the phenological information and used pictures where possible to help identify the correct phenological phases. The use of the three different phenological flowering groups helped to group information that was not explicitly clear into the group that suits it best to ensure that as many dates were recorded within a phenological flowering dataset that has variable flowering phenological phases. Phenological records are limited, thus any phenological records needs to be assessed and examined in terms of responses to changing climatic conditions (Miller-Rushing *et al.,* 2008a; Fitchett *et al.,* 2015; Fitchett & Fani, 2018).

Single event phenological recording biases the phenological record and reduces the sample number (Amano *et al.,* 2010; Fitchett *et al.,* 2015). The creation of the three BBCH phenological groups (section 4.2.2.3) therefore decreased the probability of misidentification. Accurate identification of first bloom and end of bloom is considerably less difficult than identifying full bloom phenological phases (Miller-Rushing *et al.,* 2008a; Fitchett *et al.,* 2015). The use of three BBCH flowering groups (first flowering, full bloom and end of bloom) increased the accuracy of identification of different flowering periods.

Another possible limitation of this study is the fact that only one phenological flowering dataset for the entire Namaqualand region was correlated to seven different weather stations in Namaqualand. The collected phenological flowering dates of the Namaqualand daisies from newspapers and social media records was not detailed or large enough to have separate flowering records for each subregion. A phenological flowering record for the entire Namaqualand region was therefore created and assessed. The observed relationships between temperature variables and phenological datasets are not always linear and certain plants respond variably in different regions (Primack *et al.,* 2009b).

6.3.2 Statistical Limitations

The Namaqualand daisy flowering phenological dataset and the climate datasets for the seven assessed weather stations had missing data in. Missing data is inevitable in historic studies (Fitter *et* *al.,* 1995; Ahas *et al.*, 2002; Ledneva *et al.,* 2004). One of the main statistical limitations for this study is that missing data will skew and bias the statistical analysis, which compromises trends and patterns over time. For the phenological and climate records, years or months that have missing data would remain as 'omitted data'. Interpolating phenological flowering dates will bias the phenological record since inter-annual variability needs to be accounted for (Nordli *et al.,* 2008). Missing values lead to a reduction in the *n-values* of observations. When missing data is interpolated, the increased *n-values* can also potentially skew the statistical analysis of the data.

To account for the missing values that might influence the statistical analysis of the data trends and patterns, the *p-value* or statistical significance of the datasets were calculated (section 4.3). Assuming that that the null hypothesis is correct, the *p-value* explains the probability of obtaining results similar to the actual observed results. Alternatively, that the calculated relationships and trends can still be true within the dataset. A lower *n-value* leads to lower statistical significance values but ensures that the obtained *p-values* are valid, and the obtained results were not created by chance (due to not having interpolated values). Even though there are a lot of statistically significant results in this study, the missing values still need to be considered. Years with more than six months of missing data were omitted from the statistical analysis to preserve the statistical integrity of the data.

The SAWS provided datasets with variable temporal lengths for the different weather stations depending on the time that the SAWS started collecting data in the specific subregion. The longest datasets (1959-2018 and 1960-2018) revealed statistically significant changes in annual temperature variables (section 5.2). All the shorter datasets (1989-2018; 2000-2018 and 2003-2018) had no calculated significant changes over time (section 5.2). This might be a coincidence, although having datasets with the same temporal resolution can increase the level of statistical analysis and accuracy in the study.

The limitations of this study includes missing climate data, variable temporal lengths of the climate datasets, possible bias of the phenological dataset, the length of the phenological dataset and the fact that one phenological dataset was correlated to variable weather stations in Namaqualand. Although there were limitations related to the climate and phenological data from this study, all the limitations were dealt with and compensated for. There is a lack of phenological research in South Africa (Fitchett & Fani, 2018) as well in the Southern Hemisphere (Chambers *et al.,* 2017) and it is therefore crucial to use unconventional methods to assess changes in phenological cycles to better understand the impacts of global warming on Southern Hemisphere ecosystems. The data limitations mentioned in this section could have influenced the calculated results for this study although the data limitations did not impact the achievements of any of the study aims and objectives.

CHAPTER 7: CONCLUSION

[7]

7.1 Synthesis

The aim of this research project was to create a phenological flowering dataset for the Namaqualand daisies through unconventional data sources which includes historical and digitized newspaper and social media records. The calculated phenological flowering advances were correlated to corresponding climate records to identify the significant drivers of the phenological advances.

Annual temperatures for three of the seven assessed weather stations are increasing significantly over time. The greatest increase in T_{max} was calculated for Vredendal with 2.95°C from 1959-2018. The overall mean increase in temperature for all seven assessed weather stations in Namaqualand is calculated to 1.18°C. T_{max} is increasing more rapidly than any of the other temperature variables in Namaqualand. Although no significant change in precipitation was calculated for the Namaqualand region, five of the seven weather stations demonstrate slight decreases in precipitation over time. Precipitation totals and timing in the Namaqualand region is extremely variable over time.

The calculated advances of first flowering (2.6d.decade^{-1}) and full bloom (2.1d.decade^{-1}) of the Namaqualand daisies are statistically significant. Therefore, the phenological flowering timing of the Namaqualand daisies has been advancing and becoming earlier since 1935-2018.

The perceptions documented in newspaper records coincides with the calculated drivers of Namaqualand daisy flowering phenology. First flowering timing of the Namaqualand daisies is significantly driven by winter and early spring temperatures or alternatively temperatures from June to September. The strongest climate drivers influencing first flowering timing of the Namaqualand daisies is autumn and early winter precipitation events during April and May. The onset of the rainy season therefore significantly drives the timing of Namaqualand daisy first flowering.

Full bloom of the Namaqualand daisies is significantly driven by temperature conditions later in the growing season during August. Similarly, precipitation events occurring during August and September also influence full bloom flowering timing of the daisies. Climate conditions during August and September that significantly influence the vegetation productivity of the Namaqualand daisies therefore ultimately drive the full bloom flowering advances.

Moisture availability also significantly influences the timing of Namaqualand flowering phenology. The Namaqualand region's soil moisture conditions are significantly influenced by late winter and early spring precipitation events also referred to as subsequent rains. The strongest and most significant drivers of first flowering and full bloom phenology of the Namaqualand daisies are the onset of the rainy season, subsequent rains, therefore soil moisture conditions.

The end of the bloom or the end of the flowering season for the Namaqualand daisies is more significantly driven by temperature conditions from June to October. Precipitation is not as strongly correlated to end of bloom phenology of the Namaqualand daisies although precipitation events during the flowering season can prolong the flowering season. Berg winds, which bring about dry and warm conditions, have the ability to bring the flowering season to an abrupt end.

The coefficients ranging between 0.01-0.11d.°C^{-1} for all the significant relationships between temperature and flowering are relatively small. These indicate that Namaqualand daisies are not as sensitive to changes in temperature as compared to other species assessed in the literature (Gallagher *et al.,* 2009; Lesica & Kittelson, 2010; Grab & Craparo, 2011; Darbyshire *et al.,* 2013; Pearson, 2019; Petrauski *et al.,* 2019). The coefficients of correlation between precipitation and flowering timing range between 0.12-2.18d.mm^{-1}, therefore indicating that the Namaqualand daisies are more sensitive to changes in precipitation totals and timing.

Namaqualand regional precipitation is extremely variable over time and future climate projections predict that variability in precipitation will increase even more (section 6.1.4). Increased precipitation variability in Namaqualand will lead to variable flowering timing. With projected future temperature increases in Namaqualand (section 6.1.4), the phenological flowering timing of the Namaqualand daisies will continue to advance over time as long as sufficient moisture remains available. This study can conclude that changing climatic conditions are significantly advancing the flowering timing of the Namaqualand daisies.

7.2 Achievement of Study Aims

This research project had four research aims to be fulfilled, as stated in section 1.5. The following section will provide insight into the achievement of these study aims and where they are documented in the dissertation.

1. **To determine the annual flowering dates of the Namaqualand daisies from historical newspaper records and social media records.**

Since no previous long-term annual-resolution records of Namaqualand daisy flowering timing exist, this research project had to create a phenological flowering record for the Namaqualand daisies. This research project utilised a mixed method approach, adapted from Fitchett and Fani (2018), of obtaining phenological data from a range of different sources. A total of 663 individual flowering dates were collected (section 5.7). In the Methods chapter, under section 4.2.2, the process of obtaining the phenological flowering dates for the Namaqualand daisies from newspaper records and different social media platforms was explained. The collected flowering dates were divided into three BBCH flowering groups, from 1935-2018, as explained in section 4.2.2.3. For years that had more than one collected flowering date, the mean flowering date was calculated. The full bloom flowering phenological dataset had the most dates whereas the end of bloom flowering group had the least dates within its phenological dataset. These collected and documented phenological datasets allowed for the calculation of annual flowering dates for the Namaqualand daisies.

2. **To calculate the rate of change and statistical significance of any changes in flowering dates over the full study period.**

To calculate changes in the flowering dates from 1935-2018, linear correlation analysis was conducted as stated in section 4.3.1. Separate linear correlation analysis was conducted for each of the three BBCH flowering groups. The statistical significance of each flowering change was also calculated (section 4.3.1). The statistical analysis therefore produced m, r and p values that represent the coefficient of change, the correlation strength and the statistical significance, respectively. All three flowering groups had calculated advances in flowering timing over time although only first flowering and full bloom advances were statistically significant (section 5.7).

3. **To determine the rate of change and statistical significance of annual daily rainfall and temperature records in the study region during the same timeline as the flowering data.**

Similar to the second aim of this study, linear correlation analysis was conducted for every climate variable for every weather station in Namaqualand as stated in section 4.3.1. The meteorological data provided by the SAWS for each weather station in Namaqualand does not have the exact same timeline as the collected phenological flowering dates for the Namaqualand daisies. The phenological flowering record spans 1935-2018 whereas the two longest meteorological records (Cape Columbine and Vredendal) span 1959-2018 (section 4.2.1). The shortest meteorological record spans 2003-2018 (section 4.2.1). From the provided climate records, other climatic variables were also identified and documented. These climate variables include the onset and end of the rainy season and frost variables (number of frost events per year and last frost date per year). Once again, the statistical analysis produced coefficients of change, correlation strength and statistical significance values. Temperatures in Namaqualand are increasing over time (section 5.2), although not all the changes are significant over time. Precipitation totals and timing in Namaqualand are not changing significantly and are extremely variable over time (section 5.2).

4. **To statistically assess the relationship between any phenological shifts and climate variability for the region.**

The relationships between the three created flowering groups and the respective climate variables were assessed through linear regression and correlation analysis as stated in section 4.3.2. The climate variables were represented as the independent variables on the x-axis and the Julian flowering dates were represented as the dependent variables on the y-axis (Leech *et al.,* 2005). The calculated relationships between the climate variables and the collected flowering dates are presented in the Results chapter from section 5.8-5.13. The statistical analysis of the relationships produced coefficients of change (m-values), correlation strengths (r-values) and statistical significance (p-values).

Significant relationships between temperatures from early winter to spring and first flowering were calculated (section 5.8.1). Full bloom timing was significantly correlated to temperatures during August and September (section 5.8.2). End of bloom timing was similarly correlated to temperatures from June to October (section 5.8.3). Namaqualand flowering timing was also significantly correlated to precipitation events from April to October (section 5.8) and the onset of the rainy season was significantly correlated to first flowering and full bloom timing (section 5.10). A multiple regression analysis also proved that multiple climate variables at variable temporal periods can significantly influence flowering timing of the Namaqualand daisies (section 5.9). The relationships between flowering timing and different climate variables are mostly significant during the winter and spring months, which associate with the growing and flowering months of the Namaqualand daisies (section 6.1.3).

7.3 Significance of Study

As mentioned in section 3.5.3, ‘flower viewing tourism’ forms part of a niche market of tourism activities where people travel to specific destinations to view the floral majesty of a region (Turpie & Joubert, 2004; Andereck, 2009; Nagai *et al.,* 2019). Flower viewing tourism cannot take place in any region seeing that wildflowers and floral displays only occur in specific regional biomes at specific times during the year (Kruger *et al.,* 2013). This type of tourism activity is therefore regarded as a restricted tourism activity (Kruger *et al.,* 2013). Furthermore, tourism activities are largely impacted on by regional climatic conditions (Hernandez & Ryan, 2011; du Plessis *et al.,* 2012; Fitchett & Hoogendoorn, 2019). Due to the daisy flowering spectacle, the Namaqualand region can be regarded as a flower viewing hotspot.

Local and regional economic growth can come from tourism activities due to the indirect and direct money expenditure of people when they are visiting a region for flower viewing (James *et al.,* 2007; Wang *et al*., 2017). The Namaqualand region is very underdeveloped, and people can benefit greatly from increased tourism activities (Kruger *et al.,* 2013). It is therefore essential to assess and monitor the phenological shifts of the Namaqualand daisies caused by continuous climate change to understand regional phenological phase shifts (Kruger *et al.,* 2013; Wang *et al*., 2017). A better understanding of the drivers of the phenological advances of the Namaqualand daisies also allows people to be able to predict flowering timing to ensure that the tourist activities produced by the Namaqualand daisies can continue generating income for locals who are dependent on it (Retief, 2006; Kruger *et al.,* 2013; Wang *et al.*, 2017; Nagai *et al.,* 2019). Considering the current global pandemic (COVID-19) flower viewing tourism can still be promoted seeing as people can practice social distancing while traveling in their own cars and enjoying the beauty of Namaqualand.

Within global climate change studies, phenological analysis forms a critical part of ecosystem assessments seeing as phenological studies have the ability to demonstrate how plants and animals respond to changing climatic conditions (Kramer *et al.,* 2000; Amano *et al.,* 2010; Dawson *et al.,* 2011; Browning *et al.,* 2018). Phenological assessments that are related to changing climatic conditions can therefore contribute to global biodiversity indices which manage and monitor ecosystem health and function (Vina *et al.,* 2016; Ouchi-Melo *et al.,* 2018). Phenological shifts and changes over time are predominantly driven by changing climatic conditions but can also impact future climate changes through their atmospheric feedback responses (Czernecki *et al.,* 2018; Pearson, 2019). Phenological studies can therefore also be integrated into regional and global climate models (Chuine *et al.,* 2004; Richardson *et al.,* 2017).

Southern Hemisphere and South African phenological assessments are extremely limited (Grab & Craparo, 2011; Chambers *et al.,* 2017; Fitchett & Fani, 2018). Photographs, newspaper articles and recently social media are all documentary sources that can be used to demonstrate changes over time (Sparks, 2007). To assess the impacts of climate change in various regions across the planet, researchers must use the many sources of phenological information available even if it was not originally created for phenological or scientific studies (Sparks, 2007). This study utilised innovative methods to acquire high quality phenological information (section 4.2.2). Because of the lack of South African phenological records, the use of innovative data collection methods adds value to the field of phenology (Sparks, 2007; Chambers *et al.,* 2013). The acquired phenological dataset used in this study was correlated to regional climate datasets and therefore demonstrated that changing climatic conditions are causing the phenological flowering advances of the Namaqualand daisies. This study added to the field of South African, Southern Hemisphere and global phenological studies. The study further increases the understanding of the impacts of global warming on one plant species in the south western Cape.

7.4 Future Avenues of Study

The lack of South African phenological research is due to an absence of phenological records (Fitchett & Fani, 2018). To create a more complete picture of global phenological responses to climate change, more phenological research must be conducted within the Southern Hemisphere (Stöckli & Vidale, 2004; Chambers *et al.,* 2013; Fitchett *et al.,* 2015). Fitchett and Fani (2018) further mention that more unconventional methods of phenological data collection need to be utilised to create ground-breaking methods of phenological data collection and to increase the amount of phenological datasets and research in the Southern Hemisphere.

Future studies can aim to create a more complete phenological record for Namaqualand daisies and separate phenological flowering records for each of the different Namaqualand subregions, to increase the resolution of the study by comparing specific phenological datasets with site specific meteorological records. Further future phenological studies that can be conducted on the Namaqualand daisies include experimental studies where the impacts of different variables can be tested. Possible variables that can be tested against Namaqualand flowering phenology include the effects of water stress, photoperiod and increased atmospheric CO_2. Soil properties significantly influence a plant's root extent and flush timing (Noling, 2011). Root flush timing of a plant impacts the nutrient balance and uptake of a plant which ultimately influences the flowering timing of the plant (Fares & Alva, 2000; Noling, 2011). Different levels of soil moisture control a plant's moisture uptake and can therefore potentially drive flowering timing (Fares & Alva, 2000). Assessing the phenological flowering timing of Namaqualand daisies under variable soil moisture conditions can provide insight into how the daisies will respond to future decreased precipitation regimes. Pearson *et al.* (1995) also showed that the Cape daisy's flowering timing is advanced under increased photoperiod levels. Similar research can be done to assess how the Namaqualand daisies respond to different photoperiod levels. Studies related to Namaqualand daisy chilling requirements have not been done in the region. The observed trend of first flowering events occurring within four days of a frost event (section 5.13.2) leads one to consider the possibility of possible chilling requirements for the Namaqualand daisies. Another experimental study can therefore examine the effects of variable chilling regimes on the flowering timing of the Namaqualand daisies.

7.5 Recommendations

It is recommended that National parks in Namaqualand begin documenting the onset and end dates of the flowering period for the Namaqualand daisies. Through conducting more comprehensive and on site phenological research would make future Namaqualand daisy phenological studies more reliable and create a clearer understanding of the effects of climate change on specific species in their national parks. Additionally, increased phenological research on the Namaqualand daisies can help to predict the timing of future flowering events which will benefit the parks seeing as they can update and market the 'new' flower viewing tourism season. Tourist will be able to book flower viewing tours knowing that they will not miss the flowering spectacles. If one species' flowering phenology is studied the National parks should consider to start documenting the flowering phenology for other species in the parks, such as certain succulent species that flowering during winter which is also a great tourist attraction. This will add to the phenological record of South Africa and the southern hemisphere and once again help the parks to understand the effects of climate change in their own back yards and help them to prepare for 'new' tourism season.

It should further be suggested to tour guide operators that they and the people partaking in tours should make use of citizen science applications, which will help to document and georeference specific plants in specific phenological phases in Namaqualand. With the help of citizen science, a larger region can be assessed at an increased temporal resolution (Soroye *et al.,* 2018; Langvall & Löfvenius, 2019).

References

Abarca, M., Lill, J.T. and Frank-Bolton, P. (2018). Latitudinal variation in responses of a forest herbivore and its egg parasitoids to experimental warming. *Oecologia*, 186(3): 869-881.

Ahas, R., Aasa, A., Menzel, A., Fedotova, V.G. and Scheifinger, H. (2002). Changes in European spring phenology. *International Journal of Climatology*, 22(14): 1727-1738.

Ahmad, S., Abbas, G., Fatima, Z., Khan, R.J., Anjum, M.A., Ahmed, M., Khan, M.A., Porter, C.H. and Hoogenboom, G. (2017). Quantification of the impacts of climate warming and crop management on canola phenology in Punjab, Pakistan. *Journal of Agronomy and Crop Science*, 203(5): 442-452.

Alberton, B., Torres, R.D.S., Cancian, L.F., Borges, B.D., Almeida, J., Mariano, G.C., dos Santos, J. and Morellato, L.P.C. (2017). Introducing digital cameras to monitor plant phenology in the tropics: applications for conservation. *Perspectives in Ecology and Conservation*, 15(2): 82-90.

Allen, M.R., Dube, O.P., Solecki, W., Aragón-Durand, F., Cramer, W., Humphreys, S., Kainuma, M., Kala, J., Mahowald, N., Mulugetta, Y. Perez, R., Wairiu, M., and Zickfeld, K. (2018). Framing and context. In: Masson-Delmotte, V., P. Zhai, H.-O. Pörtner, D. Roberts, J. Skea, P.R. Shukla, A. Pirani, W. Moufouma-Okia, C. Péan, R. Pidcock, S. Connors, J.B.R. Matthews, Y. Chen, X. Zhou, M.I. Gomis, E. Lonnoy, T. Maycock, M. Tignor, and T. Waterfield (eds.) *Global Warming of 1.5°C. An IPCC Special Report on the impacts of global warming of 1.5°C above pre-industrial levels and related global greenhouse gas emission pathways, in the context of strengthening the global response to the threat of climate change, sustainable development, and efforts to eradicate* poverty, IPCC, Geneva: 49-91.

Allphin, L. and Harper, K.T. (1997). Demography and life history characteristics of the rare Kachina daisy (*Erigeron kachinensis*, Asteraceae). *American Midland Naturalist*, 138: 109-120.

Alo, C.A. and Wang, G. (2008). Potential future changes of the terrestrial ecosystem based on climate projections by eight general circulation models. *Journal of Geophysical Research: Biogeosciences*, 113(G1), DOI: 10.1029/2007JG000528.

Altwegg, R., Broms, K., Erni, B., Barnard, P., Midgley, G.F. and Underhill, L.G. (2012). Novel methods reveal shifts in migration phenology of barn swallows in South Africa. *Proceedings of the Royal Society B: Biological Sciences*, 279(1733): 1485-1490.

Amano, T., Smithers, R.J., Sparks, T.H. and Sutherland, W.J. (2010). A 250-year index of first flowering dates and its response to temperature changes. *Proceedings of the Royal Society B: Biological Sciences*, 277(1693): 2451-2457.

Amaral, F., Tiago, T. and Tiago, F. (2014). User-generated content: tourists' profiles on Tripadvisor. *International Journal of Strategic Innovative Marketing*, 1(3): 137-145.

Amekudzi, L.K., Yamba, E.I., Preko, K., Asare, E.O., Aryee, J., Baidu, M. and Codjoe, S.N.A. (2015). Variabilities in rainfall onset, cessation and length of the rainy season for the various agro-ecological zones of Ghana. *Climate*, 3: 416-434.

Andereck, K.L. (2009). Tourists' perceptions of environmentally responsible innovations at tourism businesses. *Journal of Sustainable Tourism*, 17(4): 489-499.

Anderson, J.T., Inouye, D.W., McKinney, A.M., Colautti, R.I. and Mitchell-Olds, T. (2012). Phenotypic plasticity and adaptive evolution contribute to advancing flowering phenology in response to climate change. *Proceedings of the Royal Society B: Biological Sciences*, 279(1743): 3843-3852.

Andersson, S. (2008). Pollinator and nonpollinator selection on ray morphology in *Leucanthemum vulgare* (Oxeye daisy, Asteraceae). *American Journal of Botany*, 95(9): 1072-1078.

Anwar, M.R., Li Liu, D., Farquharson, R., Macadam, I., Abadi, A., Finlayson, J., Wang, B. and Ramilan, T. (2015). Climate change impacts on phenology and yields of five broadacre crops at four climatologically distinct locations in Australia. *Agricultural Systems*, 132: 133-144.

Aono, Y. (2015). Cherry blossom phenological data since the seventeenth century for Edo (Tokyo), Japan, and their application to estimation of March temperatures. *International Journal of Biometeorology*, 59(4): 427-434.

Aono, Y. and Kazui, K. (2008). Phenological data series of cherry tree flowering in Kyoto, Japan, and its application to reconstruction of springtime temperatures since the 9th century. *International Journal of Climatology*, 28(7): 905-914.

Araujo, J.A., Abiodun, B.J. and Crespo, O. (2016). Impacts of drought on grape yields in Western Cape, South Africa. *Theoretical and Applied Climatology*, 123(1-2): 117-130.

Armbruster, W. S. (1995). The origins and detection of plant community structure: reproductive versus vegetative processes. *Folia geobotanica and phytotaxonomica*, 30: 483–497.

Arora, V.K. and Boer, G.J. (2005). A parameterization of leaf phenology for the terrestrial ecosystem component of climate models. *Global Change Biology*, 11(1): 39-59.

Badeck, F.W., Bondeau, A., Böttcher, K., Doktor, D., Lucht, W., Schaber, J. and Sitch, S. (2004). Responses of spring phenology to climate change. *New Phytologist*, 162(2): 295-309.

Bai, H., Xiao, D., Zhang, H., Tao, F. and Hu, Y. (2019). Impact of warming climate, sowing date, and cultivar shift on rice phenology across China during 1981–2010. *International Journal of Biometeorology*, 63(8): 1077-1089.

Bailey, P. and Kevan, P.G. (2017). Reproductive Strategies Matter for Rare Plant Conservation: Pollination, Phenology, and Mating in an Endemic Plant of the Sky Islands of Arizona, *Erigeron lemmonii* A. Gray (Lemmon's Fleabane) (Asteraceae). *Western North American Naturalist*, 77(3): 385-398.

Barnett, J.T. (2019). Irrational hope, phenological writing, and the prospects of earthly coexistence. *Communication and Critical/Cultural Studies*, 16(4): 382-391.

Bartomeus, I., Ascher, J.S., Wagner, D., Danforth, B.N., Colla, S., Kornbluth, S. and Winfree, R. (2011). Climate-associated phenological advances in bee pollinators and bee-pollinated plants. *Proceedings of the National Academy of Sciences*, 108(51): 20645-20649.

Beaubien, E. and Hamann, A. (2011). Spring flowering response to climate change between 1936 and 2006 in Alberta, Canada. *BioScience*, 61(7): 514-524.

Beaubien, E.G. and Freeland, H.J. (2000). Spring phenology trends in Alberta, Canada: links to ocean temperature. *International Journal of Biometeorology*, 44(2): 53-59.

Beaumont, L.J., McAllan, I.A. and Hughes, L. (2006). A matter of timing: changes in the first date of arrival and last date of departure of Australian migratory birds. *Global Change Biology*, 12(7): 1339-1354.

Bekele, F., Korecha, D. and Negatu, L. (2017). Demonstrating effect of rainfall characteristics on wheat yield: Case of Sinana District, south eastern Ethiopia. *Agricultural Sciences*, 8: 371-384.

Bendix, J., Homeier, J., Ortiz, E.C., Emck, P., Breckle, S.W., Richter, M. and Beck, E. (2006). Seasonality of weather and tree phenology in a tropical evergreen mountain rain forest. *International Journal of Biometeorology*, 50(6): 370-384.

Benjaminsen, T.A., Rohde, R., Sjaastad, E., Wisborg, P. and Lebert, T. (2006). Land reform, range ecology, and carrying capacities in Namaqualand, South Africa. *Annals of the Association of American Geographers*, 96(3): 524-540.

Benjaminsen, T.A., Kepe, T. and Bråthen, S. (2008). Between global interests and local needs: conservation and land reform in Namaqualand, South Africa. *Africa*, 78(2): 223-244.

Benmoussa, H., Mimoun, M.B., Ghrab, M. and Luedeling, E. (2018). Climate change threatens central Tunisian nut orchards. *International Journal of Biometeorology*, 62(12): 2245-2255.

Bertin, R.I. and Kerwin, M.A. (1998). Floral sex ratios and gynomonoecy in *Aster* (Asteraceae). *American Journal of Botany*, 85(2): 235-244.

Bertin, R.I. (2015). Climate change and flowering phenology in Worcester County, Massachusetts. *International Journal of Plant Sciences*, 176(2): 107-119.

Berzborn, S. (2007). The household economy of pastoralists and wage-labourers in the Richtersveld, South Africa. *Journal of Arid Environments*, 70(4): 672-685.

Binns, T. and Nel, E. (2002). Tourism as a local development strategy in South Africa. *Geographical Journal*, 168(3): 235-247.

Bison, M., Yoccoz, N.G., Carlson, B.Z. and Delestrade, A. (2019). Comparison of budburst phenology trends and precision among participants in a citizen science program. *International Journal of Biometeorology*, 63(1): 61-72.

Blamey, R.C. and Reason, C.J.C. (2009). Numerical simulation of a mesoscale convective system over the east coast of South Africa. *Tellus A: Dynamic Meteorology and Oceanography*, 61: 17-34.

Blanc, É. (2012). The impact of climate change on crop yields in Sub-Saharan Africa. *American Journal of Climate Change*, 1, DOI: 10.4236/ajcc.2012.11001.

Bock, A., Sparks, T.H., Estrella, N., Jee, N., Casebow, A., Schunk, C., Leuchner, M. and Menzel, A. (2014). Changes in first flowering dates and flowering duration of 232 plant species on the island of Guernsey. *Global Change Biology*, 20(11): 3508-3519.

Bock, A., Sparks, T.H., Estrella, N., Jee, N., Casebow, A., Leuchner, M. and Menzel, A. (2015). Climate sensitivity and variation in first flowering of 26 *Narcissus* cultivars. *International Journal of Biometeorology*, 59(4): 477-480.

Botai, C.M., Botai, J.O. and Adeola, A.M. (2018). Spatial distribution of temporal precipitation contrasts in South Africa. *South African Journal of Science*, 114(7-8): 70-78.

Bourne, A., Muller, H., de Villiers, A., Alam, M. and Hole, D. (2017). Assessing the efficiency and effectiveness of rangeland restoration in Namaqualand, South Africa. *Plant Ecology*, 218(1): 7-22.

Bolton, D.K. and Friedl, M.A. (2013). Forecasting crop yield using remotely sensed vegetation indices and crop phenology metrics. *Agricultural and Forest Meteorology*, 173: 74-84.

Bradley, N.L., Leopold, A.C., Ross, J. and Huffaker, W. (1999). Phenological changes reflect climate change in Wisconsin. *Proceedings of the National Academy of Sciences*, 96(17): 9701-9704.

Browning, D.M., Crimmins, T.M., James, D.K., Spiegal, S., Levi, M.R., Anderson, J.P. and Peters, D.P. (2018). Synchronous species responses reveal phenological guilds: implications for management. *Ecosphere*, 9(9), DOI.org/10.1002/ecs2.2395.

Buermann, W., Anderson, B., Tucker, C.J., Dickinson, R.E., Lucht, W., Potter, C.S. and Myneni, R.B. (2003). Interannual covariability in Northern Hemisphere air temperatures and greenness associated with El Niño-Southern Oscillation and the Arctic Oscillation. *Journal of Geophysical Research: Atmospheres*, *108(D13)*, DOI: 10.1029/2002JD002630.

Buitenwerf, R., Bond, W.J., Stevens, N. and Trollope, W.S.W. (2012). Increased tree densities in South African savannas: 50 years of data suggests CO_2 as a driver. *Global Change Biology*, 18(2): 675-684.

Bull, C.M. and Burzacott, D. (2002). Changes in climate and in the timing of pairing of the Australian lizard, *Tiliqua rugosa*: a 15-year study. *Journal of Zoology*, 256(3): 383-387.

Burge, D.O. (2013). Namaqualand Springtime. *Cactus and Succulent Journal*, 85(3): 88-96.

Burls, N.J., Blamey, R.C., Cash, B.A., Swenson, E.T., al Fahad, A., Bopape, M.M., Straus, D.M. and Reason, C.J.C. (2019). The Cape Town “Day Zero” drought and Hadley cell expansion. *Npj Climate and Atmospheric Sciences*, 2, DOI: 10.1038/s41612-019-0084-6.

Burt, J.E., Barber, G.M. and Rigby, D.L. (2009). Elementary statistics for geographers. Guilford Press: New York.

Bussière, E.M., Underhill, L.G. and Altwegg, R. (2015). Patterns of bird migration phenology in South Africa suggest northern hemisphere climate as the most consistent driver of change. *Global Change Biology*, 21(6): 2179-2190.

Butt, N., Seabrook, L., Maron, M., Law, B.S., Dawson, T.P., Syktus, J. and McAlpine, C.A. (2015). Cascading effects of climate extremes on vertebrate fauna through changes to low-latitude tree flowering and fruiting phenology. *Global Change Biology*, 21(9): 3267-3277.

Calinger, K.M., Queenborough, S. and Curtis, P.S. (2013). Herbarium specimens reveal the footprint of climate change on flowering trends across north-central North America. *Ecology Letters*, 16(8): 1037-1044.

Cannell, M.G.R. and Smith, R.I. (1986). Climatic warming, spring budburst and forest damage on trees. *Journal of Applied Ecology*, 23: 177-191.

Capinha, C. (2019). Predicting the timing of ecological phenomena using dates of species occurrence records: a methodological approach and test case with mushrooms. *International Journal of Biometeorology*, 63(8): 1015-1024.

CaraDonna, P.J., Iler, A.M. and Inouye, D.W. (2014). Shifts in flowering phenology reshape a subalpine plant community. *Proceedings of the National Academy of Sciences*, 111(13): 4916-4921.

CaraDonna, P.J. and Bain, J.A. (2016). Frost sensitivity of leaves and flowers of subalpine plants is related to tissue type and phenology. *Journal of Ecology*, 104(1): 55-64.

Carrick, P.J. and Krüger, R. (2007). Restoring degraded landscapes in lowland Namaqualand: Lessons from the mining experience and from regional ecological dynamics. *Journal of Arid Environments*, 70(4): 767-781.

Carrick, P.J., Erickson, T.E., Becker, C.H., Mayence, C.E. and Bourne, A.R. (2015). Comparing ecological restoration in South Africa and Western Australia: the benefits of a 'travelling workshop'. *Ecological Management and Restoration*, 16(2): 86-94.

Cayan, D.R., Kammerdiener, S.A., Dettinger, M.D., Caprio, J.M. and Peterson, D.H. (2001). Changes in the onset of spring in the western United States. *Bulletin of the American Meteorological Society*, 82(3): 399-416.

Chambers, L.E. (2004). Delayed breeding in Little Penguins–evidence of climate change? *Australian Meteorological Magazine*, 53(1): 13-19.

Chambers, L.E. (2005). Migration dates at Eyre Bird Observatory: links with climate change? *Climate Research*, 29(2): 157-165.

Chambers, L.E. (2009). *Evidence of climate related shifts in Australian phenology*. Proceedings of 18th World IMACS Congress and MODSIM09 International Congress on Modelling and Simulation, Australia, 13-17 July 2009.

Chambers, L.E., Atwegg, R., Barbraud, C., Barnard, P., Beaumont, L.J., Crawford, R.J.M., Durant, J.M., Hughes, L., Keatley, M.R., Low, M., Morellato, P.C., Poloczanska, E.S., Ruppolo, V., Vanstreels, R.E.T., Woehler, E.J. and Wolfaardt, A.C. (2013). Phenological changes in the southern Hemisphere. *Plos One,* 8(10), DOI: 10.1371/journal.pone.0075514.

Chambers, L.E., Barnard, P., Poloczanska, E.S., Hobday, A., Keatley, M.R., Allsopp, N. and Underhill, L.G. (2017). Southern hemisphere biodiversity and global change: data gaps and strategies. *Austral Ecology,* 42(1): 20-30.

Chandler, R. and Scott, E. (2011). *Statistical Methods for Trend Detection and Analysis.* Wiley, Chichester.

Chapman, C.A., Chapman, L.J., Struhsaker, T.T., Zanne, A.E., Clark, C.J. and Poulsen, J.R. (2005). A long-term evaluation of fruiting phenology: importance of climate change. *Journal of Tropical Ecology*, 21(1): 31-45.

Chen, X., Hu, B. and Yu, R. (2005). Spatial and temporal variation of phenological growing season and climate change impacts in temperate eastern China. *Global Change Biology*, 11(7): 1118-1130.

Chen, X. and Xu, L. (2012). Phenological responses of *Ulmus pumila* (Siberian Elm) to climate change in the temperate zone of China. *International Journal of Biometeorology*, 56(4): 695-706.

Chen, X., An, S., Inouye, D.W. and Schwartz, M.D. (2015). Temperature and snowfall trigger alpine vegetation green-up on the world's roof. *Global Change Biology*, 21(10): 3635-3646.

Chianucci, F. (2020). An overview of in situ digital canopy photography in forestry. *Canadian Journal of Forest Research*, 50(999): 227-242.

Chmielewski, F.M. and Rötzer, T. (2001). Response of tree phenology to climate change across Europe. *Agricultural and Forest Meteorology*, 108(2): 101-112.

Chmielewski, F.M. (2002). Climate variability and trends in plant phenology in Europe and in Germany. In: *15th conference on biometeorology and aerobiology joint with the 16th international congress on biometeorology*, Kansas City, Missouri: 373–374, 1 November 2002

Chmielewski, F.M. and Rötzer, T. (2002). Annual and spatial variability of the beginning of growing season in Europe in relation to air temperature changes. *Climate Research*, 19(3): 257-264.

Chmielewski, F.M., Müller, A. and Bruns, E. (2004). Climate changes and trends in phenology of fruit trees and field crops in Germany, 1961–2000. *Agricultural and Forest Meteorology*, 121(1-2): 69-78.

Chmielewski, F.M., Müller, A. and Küchler, W. (2005). Possible impacts of climate change on natural vegetation in Saxony (Germany). *International Journal of Biometeorology*, 50(2): 96-104.

Chuine, I., Yiou, P., Viovy, N., Seguin, B., Daux, V. and Ladurie, E.L.R. (2004). Historical phenology: grape ripening as a past climate indicator. *Nature*, 432(7015): 289-290.

Chuine, I. and Régnière, J. (2017). Process-based models of phenology for plants and animals. *Annual Review of Ecology, Evolution, and Systematics*, 48: 159-182.

Cleland, E.E., Chuine, I., Menzel, A., Mooney, H.A. and Schwartz, M.D. (2007). Shifting plant phenology in response to global change. *Trends in Ecology and Evolution*, 22(7): 357-365.

Cleland, E.E., Allen, J.M., Crimmins, T.M., Dunne, J.A., Pau, S., Travers, S.E., Zavaleta, E.S. and Wolkovich, E.M. (2012). Phenological tracking enables positive species responses to climate change. *Ecology*, 93(8): 1765-1771.

Cohen, J.M., Lajeunesse, M.J. and Rohr, J.R. (2018). A global synthesis of animal phenological responses to climate change. *Nature Climate Change*, 8(3), DOI: 10.1101/164806.

Colautti, R.I., Ågren, J. and Anderson, J.T. (2017). Phenological shifts of native and invasive species under climate change: insights from the Boechera–Lythrum model. *Philosophical Transactions of the Royal Society B: Biological Sciences*, 372(1712), DOI: 10.1098/rstb.2016.0032.

Collins, M., Minobe, S., Barreiro, M., Bordoni, S., Kaspi, Y., Kuwano-Yoshida, A., Keenlyside, N., Manzini, E., O'Reilly, C.H., Sutton, R. and Xie, S.P. (2018). Challenges and opportunities for improved understanding of regional climate dynamics. *Nature Climate Change*, 8(2): 101-108.

Conradie, W.J., Carey, V.A., Bonnardot, V., Saayman, D. and Van Schoor, L.H. (2002). Effect of different environmental factors on the performance of Sauvignon blanc grapevines in the

Stellenbosch/Durbanville districts of South Africa. I. Geology, soil, climate, phenology and grape composition. *South African Journal for Oenology and Viticulture*, 23(2): 78-91.

Cook, B.I., Wolkovich, E.M. and Parmesan, C. (2012). Divergent responses to spring and winter warming drive community level flowering trends. *Proceedings of the National Academy of Sciences*, 109(23): 9000-9005.

Corlett, R.T. and Lafrankie, J.V. (1998). Potential impacts of climate change on tropical Asian forests through an influence on phenology. *Climatic Change*, 39(2-3): 439-453.

Cortés-Flores, J., Hernández-Esquivel, K.B., González-Rodríguez, A. and Ibarra-Manríquez, G. (2017). Flowering phenology, growth forms, and pollination syndromes in tropical dry forest species: Influence of phylogeny and abiotic factors. *American Journal of Botany*, 104(1): 39-49.

Cossani, C.M., McMurray, L., Lake, L. and Sadras, V.O. (2017). Impact of sowing date on phenology and yield of lentil and faba bean. *"Doing More with Less", Proceedings of the 18th Australian Agronomy Conference 2017*, Ballarat, Victoria, Australia, 24-28 September 2017.

Cousins, B., Hoffman, M.T., Allsopp, N. and Rohde, R.F. (2007). A synthesis of sociological and biological perspectives on sustainable land use in Namaqualand. *Journal of Arid Environments*, 70(4): 834-846.

Cowling, R.M., Esler, K.J. and Rundel, P.W. (1999). Namaqualand, South Africa–an overview of a unique winter-rainfall desert ecosystem. *Plant Ecology*, 142(1-2): 3-21.

Cowling, R.M., Pressey, R.L., Rouget, M. and Lombard, A.T. (2003). A conservation plan for a global biodiversity hotspot—the Cape Floristic Region, South Africa. *Biological Conservation*, 112(1-2): 191-216.

Cowling, R.M. (2015). *Namaqualand: a succulent desert*. Penguin Random House, South Africa.

Craparo, A.C.W., Van Asten, P.J.A., Läderach, P., Jassogne, L.T.P. and Grab, S.W. (2015). *Coffea arabica* yields decline in Tanzania due to climate change: Global implications. *Agricultural and Forest Meteorology*, 207: 1-10.

Črepinšek, Z. and Kajfež-Bogataj, L. (2006). Phenology – indicator of plant response to climate regime [conference paper]. *BALWOIS Conference on Water Observation and Information System for Decision Support:* Ohrid: Macedonia, January 2006.

Crétat, J., Richard, Y., Pohl, B., Rouault, M., Reason, C. and Fauchereau, N. (2012). Recurrent daily rainfall patterns over South Africa and associated dynamics during the core of the austral summer. *International Journal of Climatology*, 32: 261-273.

Crétat, J., Pohl, B., Dieppois, B., Berthou, S. and Pergaud, J. (2019). The Angola Low: relationship with southern African rainfall and ENSO. *Climate Dynamics*, 52(3-4): 1783-1803.

Crimmins, T. M., M. A. Crimmins, and C. David Bertelsen. (2010). Complex responses to climate drivers in onset of spring flowering across a semi-arid elevation gradient. *Journal of Ecology*, 98:1042–1051.

Criscuola, L., Carrara, P., Oggioni, A., Pugnetti, A. and Antoninetti, M. (2018). Can VGI and mobile apps support long-term ecological research? A test in remote areas of the Alps, In: Bordogna, G. and Carrara, P. (eds.), *Mobile Information Systems Leveraging Volunteered Geographical Information for Earth Observation,* Springer, Cham: 53- 69.

Croitoru, A.E., Holobaca, I.H., Lazar, C., Moldovan, F. and Imbroane, A. (2012). Air temperature trend and the impact on winter wheat phenology in Romania. *Climatic Change*, 111(2): 393-410.

Cronje, R.B. and Ratlapane, I.M. (2016). Effect of various N application times on tree phenology and physiology of 'Mauritius' litchi in South Africa-preliminary results. In *V International Symposium on Lychee, Longan and Other Sapindaceae Fruits,* 1211: 7-14.

Czernecki, B., Nowosad, J. and Jabłońska, K. (2018). Machine learning modelling of plant phenology based on coupling satellite and gridded meteorological dataset. *International Journal of Biometeorology*, 62(7): 1297-1309.

da Silva Angelo, P.C., Ferreira, I.B., de Carvalho, C.H.S., Matiello, J.B. and Sera, G.H. (2019). Arabica coffee fruits phenology assessed through degree days, precipitation, and solar radiation exposure on a daily basis. *International Journal of Biometeorology*, 63(7): 831-843.

Dahlin, K.M., Fisher, R.A. and Lawrence, P.J. (2015). Environmental drivers of drought deciduous phenology in the Community Land Model. *Biogeosciences*, 12(16): 5061–5074.

Dalmolin, Â.C., de Almeida Lobo, F., Vourlitis, G., Silva, P.R., Dalmagro, H.J., Antunes, M.Z. and Ortíz, C.E.R. (2015). Is the dry season an important driver of phenology and growth for two Brazilian savanna tree species with contrasting leaf habits? *Plant Ecology*, 216(3): 407-417.

Darbyshire, R., Webb, L., Goodwin, I. and Barlow, E.W.R. (2013). Evaluation of recent trends in Australian pome fruit spring phenology. *International Journal of Biometeorology*, 57(3): 409-421.

Davies, S. J. J. F. (1976). Studies on the flowering season and fruit production of some arid zone shrubs and trees in Western Australia. *Journal of Ecology*, 64: 665-687.

Davis, C. (2010). *Climate change handbook for north-eastern South Africa*. Council for Scientific and Industrial Research (CSIR), Pretoria.

Davis, C.C., Willis, C.G., Primack, R.B. and Miller-Rushing, A.J. (2010). The importance of phylogeny to the study of phenological response to global climate change. *Philosophical Transactions of the Royal Society B: Biological Sciences*, 365(1555): 3201-3213.

Davis, C.C., Willis, C.G., Connolly, B., Kelly, C. and Ellison, A.M. (2015). Herbarium records are reliable sources of phenological change driven by climate and provide novel insights into species' phenological cueing mechanisms. *American Journal of Botany*, 102(10): 1599-1609.

Davis, C.L., Hoffman, M.T. and Roberts, W. (2016). Recent trends in the climate of Namaqualand, a megadiverse arid region of South Africa. *South African Journal of Science*, 112(3-4), DOI: 10.17159/sajs.2016/20150217.

Davis, C.L., Hoffman, M.T. and Roberts, W. (2017). Long-term trends in vegetation phenology and productivity over Namaqualand using the GIMMS AVHRR NDVI3g data from 1982 to 2011. *South African Journal of Botany*, 111: 76-85.

Dawson, T., Jackson, S., House, J., Prentice, I. and Mace, G. (2011). Beyond predictions: Biodiversity conservation in a changing climate. *Science,* 332(6025): 53-58.

De Melo-Abreu, J.P., Barranco, D., Cordeiro, A.M., Tous, J., Rogado, B.M. and Villalobos, F.J. (2004). Modelling olive flowering date using chilling for dormancy release and thermal time. *Agricultural and Forest Meteorology*, 125(1-2): 117-127.

De Villiers, M., Manrakhan, A., Addison, P. and Hattingh, V. (2013). The distribution, relative abundance, and seasonal phenology of *Ceratitis capitata*, *Ceratitis rosa*, and *Ceratitis cosyra* (Diptera: Tephritidae) in South Africa. *Environmental Entomology*, 42(5): 831-840.

de Waal, C., (2016). Rocking With Namaqualand's Daisies [image], SciBraai. Available from: https://scibraai.co.za/rocking-with-namaqualands-daisies/ (Accessed 5 November 2020)

de Waal, C., Rodger, J.G., Anderson, B. and Ellis, A.G. (2014). Selfing ability and dispersal are positively related, but not affected by range position: a multispecies study on southern African Asteraceae. *Journal of Evolutionary Biology*, 27(5): 950-959.

de Waal, C., Anderson, B. and Ellis, A.G. (2015). Relative density and dispersion pattern of two southern African Asteraceae affect fecundity through heterospecific interference and mate availability, not pollinator visitation rate. *Journal of Ecology*, 103(2): 513-525.

de Waal, C., Anderson, B., and Ellis, A.G. (2016). Dispersal, dormancy and life-history tradeoffs at the individual, population and species levels in southern African Asteraceae. *New Phytologist*, 210(1): 356-365.

DEA. (2013). Long-Term Adaptation Scenarios Flagship Research Programme (LTAS) for South Africa. Climate Trends and Scenarios for South Africa. Pretoria, South Africa. Accessed 24 May 2019: https://www.environment.gov.za/sites/default/files/docs/summary_policymakers_bookV3.pdf

Denny, E.G., Gerst, K.L., Miller-Rushing, A.J., Tierney, G.L., Crimmins, T.M., Enquist, C.A., Guertin, P., Rosemartin, A.H., Schwartz, M.D., Thomas, K.A. and Weltzin, J.F. (2014). Standardized phenology monitoring methods to track plant and animal activity for science and resource management applications. *International Journal of Biometeorology*, 58(4): 591-601.

Deressa, T., Hassan, R. and Poonyth, D. (2005). Measuring the impact of climate change on South African agriculture: The case of sugarcane growing regions. *Agrekon*, 44(4): 524-542.

Desmet, P.G. (2007). Namaqualand—a brief overview of the physical and floristic environment. *Journal of Arid environments*, 70(4): 570-587.

Dewar, G.I. (2007). *The archaeology of the coastal desert of Namaqualand, South Africa: a regional synthesis*. Doctoral dissertation submitted to the University of Cape Town.

Dieppois, B., Pohl, B., Rouault, M., New, M., Lawler, D. and Keenlyside, N. (2016). Interannual to interdecadal variability of winter and summer southern African rainfall, and their teleconnections. *Journal of Geophysical Research: Atmospheres*, 121(11): 6215-6239.

Diez, J.M., Ibáñez, I., Miller-Rushing, A.J., Mazer, S.J., Crimmins, T.M., Crimmins, M.A., Bertelsen, C.D. and Inouye, D.W. (2012). Forecasting phenology: from species variability to community patterns. *Ecology Letters*, 15(6): 545-553.

Doi, H. (2007). Winter flowering phenology of Japanese apricot *Prunus mume* reflects climate change across Japan. *Climate Research,* 34: 99-104.

Doi, H., Gordo, O., Mori, T. and Kubo, M.T. (2017). A macroecological perspective for phenological research under climate change. *Ecological Research*, 32(5): 633-641.

Donat, M.G., Alexander, L.V., Yang, H., Durre, I., Vose, R., Dunn, R.J.H., Willett, K.M., Aguilar, E., Brunet, M., Caesar, J. and Hewitson, B. (2013). Updated analyses of temperature and precipitation extreme indices since the beginning of the twentieth century: The HadEX2 dataset. *Journal of Geophysical Research: Atmospheres*, 118(5): 2098-2118.

Donnelly, A. and Yu, R. (2017). The rise of phenology with climate change: an evaluation of IJB publications. *International Journal of Biometeorology*, 61(1): 29-50.

Dore, M.H. (2005). Climate change and changes in global precipitation patterns: what do we know? *Environment International*, 31(8): 1167-1181.

Drake, A. and Martin, K. (2018). Local temperatures predict breeding phenology but do not result in breeding synchrony among a community of resident cavity-nesting birds. *Scientific Reports*, 8(1), DOI: 10.1038/s41598-018-20977-y.

Dreyer, L.L., Esler, K.J. and Zietsman, J. (2006). Flowering phenology of South African *Oxalis*—possible indicator of climate change? *South African Journal of Botany*, 72(1): 150-156.

Drkenda, P., Musić, O., Marić, S., Jevremović, D., Radičević, S., Hudina, M., Hodžić, S., Kunz, A. and Blanke, M.M. (2018). Comparison of Climate Change Effects on Pome and Stone Fruit Phenology Between Balkan Countries and Bonn/Germany. *Erwerbs-Obstbau*, 60(4): 295-304.

du Plessis, M.L., van der Merwe, P. and Saayman, M. (2012). Environmental factors affecting tourists experience in South African national parks. *African Journal of Business Management*, 6(8): 2911-2918.

Dunne, J., Harte, J. and Taylor, K. (2003). Subalpine meadow flowering phenology responses to climate change: integrating experimental and gradient methods. *Ecological Monographs,* 73(1): 69-86.

Dunning, C.M., Black, E.C. and Allan, R.P. (2016). The onset and cessation of seasonal rainfall over Africa. *Journal of Geophysical Research: Atmospheres*, 121(19): 11-405.

Durant, J.M., Hjermann, D.Ø., Ottersen, G. and Stenseth, N.C. (2007). Climate and the match or mismatch between predator requirements and resource availability. *Climate Research*, 33(3): 271-283.

Easterling, D.R., Horton, B., Jones, P.D., Peterson, T.C., Karl, T.R., Parker, D.E., Salinger, M.J., Razuvayev, V., Plummer, N., Jamason, P. and Folland, C.K. (1997). Maximum and minimum temperature trends for the globe. *Science*, 277(5324): 364-367.

Easterling, D.R., Evans, J.L., Groisman, P.Y., Karl, T.R., Kunkel, K.E. and Ambenje, P. (2000). Observed variability and trends in extreme climate events: a brief review. *Bulletin of the American Meteorological Society*, 81(3): 417-426.

Ellwood, E.R., Temple, S.A., Primack, R.B., Bradley, N.L. and Davis, C.C. (2013). Record-breaking early flowering in the eastern United States. *PloS one*, 8(1), DOI: 10.1371/journal.pone.0053788.

Ellwood, E.R., Playfair, S.R., Polgar, C.A. and Primack, R.B. (2014). Cranberry flowering times and climate change in southern Massachusetts. *International Journal of Biometeorology*, 58(7): 1693-1697.

Elzinga, J.A., Atlan, A., Biere, A., Gigord, L., Weis, A.E. and Bernasconi, G. (2007). Time after time: flowering phenology and biotic interactions. *Trends in Ecology and Evolution*, 22(8): 432-439.

Engelbrecht, C.J. and Engelbrecht, F.A. (2016). Shifts in Köppen-Geiger climate zones over southern Africa in relation to key global temperature goals. *Theoretical and applied Climatology*, 123(1-2): 247-261.

Engelbrecht, C.J., Engelbrecht, F.A. and Dyson, L.L. (2013). High-resolution model-projected changes in mid-tropospheric closed-lows and extreme rainfall events over southern Africa. *International Journal of Climatology*, 33(1): 173-187.

Engelbrecht, F., Adegoke, J., Bopape, M.J., Naidoo, M., Garland, R., Thatcher, M., McGregor, J., Katzfey, J., Werner, M., Ichoku, C. and Gatebe, C. (2015). Projections of rapidly rising surface temperatures over Africa under low mitigation. *Environmental Research Letters*, 10(8), DOI: 10.1088/1748-9326/10/8/085004.

Engelbrecht, F.A., Landman, W.A., Engelbrecht, C.J., Landman, S., Bopape, M.M., Roux, B., McGregor, J.L. and Thatcher, M. (2011). Multi-scale climate modelling over Southern Africa using a variable-resolution global model. *Water SA*, 37(5): 647-658.

Engelbrecht, F.A., McGregor, J.L. and Engelbrecht, C.J. (2009). Dynamics of the Conformal-Cubic Atmospheric Model projected climate-change signal over southern Africa. *International Journal of Climatology*, 29(7): 1013-1033.

Esler, K.J. and Rundel, P.W. (1999). Comparative patterns of phenology and growth form diversity in two winter rainfall deserts: The Succulent Karoo and Mojave Desert ecosystems. *Plant Ecology*, 142(1-2): 97-104.

Estrella, N., Sparks, T. and Menzel, A. (2007). Trends and temperature response in the phenology of crops in Germany. *Global Change Biology,* 13: 1737-1747.

Fadón, E., Herrero, M. and Rodrigo, J. (2015). Flower development in sweet cherry framed in the BBCH scale. *Scientia Horticulture*, 192: 141-147.

Faisal, A.M. (2008). Climate change and phenology. *New Age*, 3: 1-6.

Fares, A. and Alva, A.K. (2000). Evaluation of capacitance probes for optimal irrigation of citrus through soil moisture monitoring in an entisol profile. *Irrigation Science*, 19(2): 57-64.

Fauchereau, N., Trzaska, S., Rouault, M. and Richard, Y. (2003). Rainfall variability and changes in southern Africa during the 20th century in the global warming context. *Natural Hazards*, 29(2): 139-154.

Fauchereau, N., Pohl, B., Reason, C.J.C., Rouault, M. and Richard, Y. (2008). Recurrent Daily OLR Patterns in the Southern Africa/Southwest Indian Ocean Region: Implications for South African Rainfall and Teleconnections. *Climate Dynamics*, 32(4): 575–59.

Favre, A., Hewitson, B., Tadross, M., Lennard, C. and Cerezo-Mota, R. (2012). Relationships between cut-off lows and the semiannual and southern oscillations. *Climate Dynamics*, 38(7-8): 1473-1487.

Feldman, R.E., Žemaitė, I. and Miller-Rushing, A.J. (2018). How training citizen scientists affects the accuracy and precision of phenological data. *International Journal of Biometeorology*, 62(8): 1421-1435.

Fenech, A., MacIver, D. and Auld, H. (2005). The impact of climate on changes in the seasonal timing of life cycle events of eastern Canada from 1901 to 1924. *Integrated Mapping Assessment*, 4: 55-69.

Feng, S., and Q. Hu. (2007). Changes in winter snowfall/precipitation ratio in the contiguous United States. *Journal of Geophysical Research*, 112, DOI: 10.1029/2007JD008397.

Filippa, G., Cremonese, E., Galvagno, M., Migliavacca, M., Di Cella, U.M., Petey, M. and Siniscalco, C. (2015). Five years of phenological monitoring in a mountain grassland: inter-annual patterns and evaluation of the sampling protocol. *International Journal of Biometeorology*, 59(12): 1927-1937.

Firmat, C., Delzon, S., Louvet, J.M., Parmentier, J. and Kremer, A. (2017). Evolutionary dynamics of the leaf phenological cycle in an oak metapopulation along an elevation gradient. *Journal of Evolutionary Biology*, 30(12): 2116-2131.

Fitchett, J.M. (2013). Phenological Response of Citrus Flowering to Climate Variability and Change in Iran: 1960-2010. *Master of Science Dissertation submitted to the University of the Witwatersrand: Johannesburg*.

Fitchett, J.M., Grab, S.W., Thompson, D.I. and Roshan, G. (2014a). Spatio-temporal variation in phenological response of citrus to climate change in Iran: 1960-2010. *Agricultural and Forest Meteorology,* 198: 285-293.

Fitchett, J.M., Grab, S.W., Thompson, D.I. and Roshan, G. (2014b). Increasing frost risk associated with advanced citrus flowering dates in Kerman and Shiraz, Iran: 1960–2010. *International journal of biometeorology*, 58(8): 1811-1815.

Fitchett, J.M., Grab, S.W. and Thompson, D.I. (2015). Plant phenology and climate change: Progress in methodological approaches and application. *Progress in Physical Geography*, 39(4): 460-482.

Fitchett, J., Grab, S.W. and Thompson, D.I. (2016a). Temperature and tree age interact to increase mango yields in the Lowveld, South Africa. *South African Geographical Journal*, 98(1): 105-117.

Fitchett, J.M., Grant, B. and Hoogendoorn, G. (2016b). Climate change threats to two low-lying South African coastal towns: Risks and perceptions. *South African Journal of Science*, 112(5-6), DOI: 10.17159/sajs.2016/20150262.

Fitchett, J.M. and Ebhuoma, E. (2018). Phenological cues intrinsic in indigenous knowledge systems for forecasting seasonal climate in the Delta State of Nigeria. *International Journal of Biometeorology*, 62(6): 1115-1119.

Fitchett, J.M. and Fani, H.A. (2018). Advance in Jacaranda Blossom Phenology in the South African Highveld Interior: A Preliminary Analysis. *Proceedings of the Biennial Conference of the Society of South African Geographers. School of Geography, Archaeology and Environmental Studies*, University of the Free State, South Africa: 467-486, 1-5 October 2018.

Fitchett, J.M. and Hoogendoorn, G. (2019). Exploring the climate sensitivity of tourists to South Africa through TripAdvisor reviews. *South African Geographical Journal*, 101(1): 91-109.

Fitchett, J.M., Grab, S.W. and Portwig, H. (2019). Progressive delays in the timing of sardine migration in the southwest Indian Ocean. *South African Journal of Science*, 115(7-8): 1-6.

Fitter, A.H., Fitter, R.S.R., Harris, I.T.B. and Williamson, M.H. (1995). Relationships between first flowering date and temperature in the flora of a locality in central England. *Functional Ecology,* 9: 55-60.

Flemmer, A.C., Franchini, M.C. and Lindström, L.I. (2015). Description of safflower (*Carthamus tinctorius*) phenological growth stages according to the extended BBCH scale. *Annals of Applied Biology*, 166(2): 331-339.

Forrest, J.R. (2015). Plant–pollinator interactions and phenological change: what can we learn about climate impacts from experiments and observations? *Oikos*, 124(1): 4-13.

Forrest, J., Inouye, D.W. and Thomson, J.D. (2010). Flowering phenology in subalpine meadows: Does climate variation influence community co-flowering patterns? *Ecology*, 91(2): 431-440.

Fox, S.C., Hoffman, M.T. and Hoare, D. (2005). The phenological pattern of vegetation in Namaqualand, South Africa and its climatic correlates using NOAA-AVHRR NDVI data. *South African Geographical Journal*, 87(2): 85-94.

Franch, B., Vermote, E., Roger, J.C., Murphy, E., Becker-Reshef, I., Justice, C., Claverie, M., Nagol, J., Csiszar, I., Meyer, D. and Baret, F. (2017). A 30+ year AVHRR land surface reflectance climate data record and its application to wheat yield monitoring. *Remote Sensing*, 9(3): 296-310.

Francis, M.L., Fey, M.V., Prinsloo, H.P., Ellis, F., Mills, A.J. and Medinski, T.V. (2007). Soils of Namaqualand: compensations for aridity. *Journal of Arid Environments*, 70(4): 588-603.

Fu, Y.H., Piao, S., Vitasse, Y., Zhao, H., De Boeck, H.J., Liu, Q., Yang, H., Weber, U., Hänninen, H. and Janssens, I.A. (2015). Increased heat requirement for leaf flushing in temperate woody species over 1980–2012: effects of chilling, precipitation and insolation. *Global Change Biology*, 21(7): 2687-2697.

Fujisawa, M. and Kobayashi, K. (2010). Apple (*Malus pumila var. domestica*) phenology is advancing due to rising air temperature in northern Japan. *Global Change Biology*, 16(10): 2651-2660.

Futter, M.N. (2003). Patterns and trends in southern Ontario lake ice phenology. *Environmental*

Monitoring and Assessment, 88(1-3): 431-444.

Gallagher, R.V., Hughes, L. and Leishman, M.R. (2009). Phenological trends among Australian alpine species: using herbarium records to identify climate-change indicators. *Australian Journal of Botany*, 57(1), DOI: 10.1071/BT08051.

Gamon, J.A., Huemmrich, K.F., Wong, C.Y., Ensminger, I., Garrity, S., Hollinger, D.Y., Noormets, A. and Peñuelas, J. (2016). A remotely sensed pigment index reveals photosynthetic phenology in evergreen conifers. *Proceedings of the National Academy of Sciences*, 113(46): 13087-13092.

Ge, Q., Wang, H., Rutishauser, T. and Dai, J. (2015). Phenological response to climate change in China: a meta-analysis. *Global Change Biology*, 21(1): 265-274.

Gholipoor, M. and Sinclair, T. (2011). Historical changes of temperature and vapor pressure deficit during the crop growing season in Iran. *International Journal of Plant Production,* 5: 195-206.

Gibbs, J.P. and Breisch, A.R. (2001). Climate warming and calling phenology of frogs near Ithaca, New York, 1900–1999. *Conservation Biology*, 15(4): 1175-1178.

Gill, A.L., Gallinat, A.S., Sanders-DeMott, R., Rigden, A.J., Short Gianotti, D.J., Mantooth, J.A. and Templer, P.H. (2015). Changes in autumn senescence in northern hemisphere deciduous trees: a meta-analysis of autumn phenology studies. *Annals of Botany*, 116(6): 875-888.

Gillett, N.P., Kell, T.D. and Jones, P.D. (2006). Regional climate impacts of the Southern Annular Mode. *Geophysical Research Letters*, 33(23), DOI: 10.1029/2006GL027721.

Gordo, O. and Sanz, J.J. (2005). Phenology and climate change: a long-term study in a Mediterranean locality. *Oecologia*, 146(3): 484-495.

Gordo, O. and Sanz, J.J. (2009). Long-term temporal changes of plant phenology in the Western Mediterranean. *Global Change Biology*, 15(8): 1930-1948.

Gordo, O. and Sanz, J.J. (2010). Impact of climate change on plant phenology in Mediterranean ecosystems. *Global Change Biology*, 16(3): 1082-1106.

Gössling, S., Scott, D., Hall, C.M., Ceron, J.P. and Dubois, G. (2012). Consumer behaviour and demand response of tourists to climate change. *Annals of Tourism Research*, 39(1): 36-58.

Grab, S.W. and Craparo, A. (2011). Advance of apple and pear tree full bloom dates in response to climate change in the southwestern Cape, South Africa: 1973-2009. *Agricultural and Forest Meteorology*, 151: 406-413.

Grab, S.W. and Nash, D.J. (2010). Documentary evidence of climate variability during cold seasons in Lesotho, southern Africa, 1833–1900. *Climate Dynamics*, 34(4): 473-499.

Graham, E.A., Henderson, S. and Schloss, A. (2011). Using mobile phones to engage citizen scientists in research. *Eos, Transactions American Geophysical Union*, 92(38): 313-315.

Grewling, L., Jackowiak, B. and Smith, M. (2014). Variations in *Quercus* sp. Pollen seasons (1996-2011) in Poznan, Poland, in relation to meteorological parameters. *Aerobiologia*, 30(2): 149–159.

Groisman, P.Y., Knight, R.W., Easterling, D.R., Karl, T.R., Hegerl, G.C. and Razuvaev, V.N. (2005). Trends in intense precipitation in the climate record. *Journal of Climate*, 18(9): 1326-1350.

Guédon, Y. and Legave, J.M. (2008). Analyzing the time-course variation of apple and pear tree dates of flowering stages in the global warming context. *Ecological Modelling*, 219(1-2): 189-199.

Hack, H., Bleiholder, H., Buhr, L., Meier, U., Schnock-Fricke, U., Weber, E. and Witzenberger, A. (1992). Einheitliche codierung der phänologischen entwicklungsstadien mono-und dikotyler pflanzen–erweiterte BBCH-Skala, Allgemein. *Nachrichtenblatt des Deutschen Pflanzenschutzdienstes*, 44(12): 265-270.

Haggerty, B.P. and Mazer, S.J. (2008). *The phenology Handbook*. University of California, Santa Barbara: 2-24.

Hall, C.M., James, M. and Baird, T. (2011). Forests and trees as charismatic mega-flora: implications for heritage tourism and conservation. *Journal of Heritage Tourism*, 6(4): 309-323.

Hart, N.C.G., Reason, C.J.C. and Fauchereau, N. (2010). Tropical–extratropical interactions over southern Africa: Three cases of heavy summer season rainfall. *Monthly Weather Review*, 138(7): 2608-2623.

Haselhorst, D.S., Tcheng, D.K., Moreno, J.E. and Punyasena, S.W. (2017). The effects of seasonal and long-term climatic variability on neotropical flowering phenology: An ecoinformatic analysis of aerial pollen data. *Ecological Informatics*, 41: 54-63.

Hassall, C., Thompson, D., French, G. and Harvey, I. (2007). Historical changes in the phenology of British Odonata are related to climate. *Global Change Biology,* 13: 933-941.

Heberling, J.M., McDonough MacKenzie, C., Fridley, J.D., Kalisz, S. and Primack, R.B. (2019). Phenological mismatch with trees reduces wildflower carbon budgets. *Ecology Letters*, 22(4): 616-623.

Hegland, S.J., Nielsen, A., Lázaro, A., Bjerknes, A.L. and Totland, Ø. (2009). How does climate warming affect plant-pollinator interactions? *Ecology Letters*, 12(2): 184-195.

Heikinheimo, M. and Lappalainen, H. (1997). Dependence of the flower bud burst of some plant taxa in Finland on effective temperature sum: implications for climate warming. *Annales Botanici Fennici,* 34: 229-243.

Hernandez, A.B. and Ryan, G. (2011). Coping with climate change in the tourism industry: a review and agenda for future research. *Tourism and Hospitality Management*, 17(1): 79-90.

Hewitson, B.C. and Crane, R.G. (2006). Consensus between GCM climate change projections with empirical downscaling: precipitation downscaling over South Africa. *International Journal of Climatology*, 26(10): 1315-1337.

Heywood, V. H. (1993). *Flowering Plants of the World*, Oxford University Press, New York.

Hoare, D. and Frost, P. (2004). Phenological description of natural vegetation in southern Africa using remotely sensed vegetation data. *Applied Vegetation Science*, 7(1): 19-28.

Hoffman, M.T. (2014). Changing patterns of rural land use and land cover in South Africa and their implications for land reform. *Journal of Southern African Studies*, 40(4): 707-725.

Hoffman, M. and Cowling, R. (1987). Plant physiognomy, phenology and demography, In R.M. Cowling and P.W. Roux, (eds.), *The Karoo biome: a preliminary synthesis. Part 2, Vegetation and history,* South African National Scientific Programme Report 142, CSIR, Pretoria: 1-34.

Hoffman, M.T. and Rohde, R.F. (2007). From pastoralism to tourism: the historical impact of changing land use practices in Namaqualand. *Journal of Arid Environments*, 70(4): 641-658.

Hoffman, M.T. and Rohde, R.F. (2010). An analysis of 20th century vegetation change in Namaqualand using repeat photography. *Biodiversity in Southern Africa*, 2: 15-21.

Hoffman, M.T., Carrick, P.J., Gillson, L. and West, A.G. (2009). Drought, climate change and vegetation response in the succulent karoo, South Africa. *South African Journal of Science*, 105(1-2): 54-60.

Hogg, E., Price, D., and Black, T. (2000). Postulated feedbacks of deciduous forest phenology on seasonal climate patterns in the Western Canadian interior. *Journal of Climate,* 13: 4229-4243.

Hoogendoorn, G., Grant, B. and Fitchett, J. (2015). Towards green guest houses in South Africa: The case of Gauteng and KwaZulu-Natal. *South African Geographical Journal*, 97(2): 123-138.

Hoogendoorn, G., Grant, B. and Fitchett, J.M. (2016). Disjunct perceptions? Climate change threats in two-low lying South African coastal towns. *Bulletin of Geography. Socio-economic Series*, 31(31): 59-71.

Howard, A.F. (2018). *Asclepias Syriaca* (Common Milkweed) flowering date shift in response to climate change. *Scientific Reports*, 8(1): 17802.

Høye, T.T., Post, E., Meltofte, H., Schmidt, N.M. and Forchhammer, M.C. (2007). Rapid advancement of spring in the High Arctic. *Current Biology*, 17(12): 449-451.

Huang, J. and Hao, H. (2018). Detecting mismatches in the phenology of cotton bollworm larvae and cotton flowering in response to climate change. *International Journal of Biometeorology*, 62(8): 1507-1520.

Hubálek, Z. (2016). The North Atlantic Oscillation system and plant phenology. *International Journal of Biometeorology*, 60(5): 749-756.

Hulme, M., Doherty, R., Ngara, T., New, M. and Lister, D. (2001). African climate change: 1900-2100. *Climate Research*, 17(2): 145-168.

Hutchings, M.J., Robbirt, K.M., Roberts, D.L. and Davy, A.J. (2018). Vulnerability of a specialized pollination mechanism to climate change revealed by a 356-year analysis. *Botanical Journal of the Linnean Society*, 186(4): 498-509.

Iler, A.M., Inouye, D.W., Schmidt, N.M. and Høye, T.T. (2017). Detrending phenological time series improves climate–phenology analyses and reveals evidence of plasticity. *Ecology*, 98(3): 647-655.

Inouye, D.W. (2008). Effects of climate change on phenology, frost damage, and floral abundance of montane wildflowers. *Ecology*, 89(2): 353-362.

Inouye, D. W., M. A. Morales, and G. J. Dodge. (2002). Variation in timing and abundance of flowering by *Delphinium barbeyi* Huth (Ranunculaceae): the roles of snowpack, frost, and La Niña in the context of climate change. *Oecologia,* 130: 543–550.

IPCC. (2018). Summary for Policymakers. In: Masson-Delmotte, V., P. Zhai, H.-O. Pörtner, D. Roberts, J. Skea, P.R. Shukla, A. Pirani, W. Moufouma-Okia, C. Péan, R. Pidcock, S. Connors, J.B.R. Matthews, Y. Chen, X. Zhou, M.I. Gomis, E. Lonnoy, T. Maycock, M. Tignor, and T. Waterfield (eds.), *Global Warming of 1.5°C. An IPCC Special Report on the impacts of global warming of 1.5°C above pre-industrial levels and related global greenhouse gas emission pathways, in the context of strengthening the global response to the threat of climate change, sustainable development, and efforts to eradicate poverty*. Intergovernmental Panel on Climate Change, Geneva, Switzerland.

Irons, R.D., Harding Scurr, A., Rose, A.P., Hagelin, J.C., Blake, T. and Doak, D.F. (2017). Wind and rain are the primary climate factors driving changing phenology of an aerial insectivore. *Proceedings of the Royal Society B: Biological Sciences*, 284(1853). DOI: 10.1098/rspb.2017.0412.

Irvin, N.A., Wratten, S.D., Frampton, C.M., Bowie, M.H., Evans, A.M. and Moar, N.T. (1999). The phenology and pollen feeding of three hover fly (Diptera*: Syrphidae*) species in Canterbury, New Zealand. *New Zealand Journal of Zoology*, 26(2): 105-115.

Ise, T., Ikeda, S., Watanabe, S. and Ichii, K. (2018). Regional-scale data assimilation of a terrestrial ecosystem model: leaf phenology parameters are dependent on local climatic conditions. *Frontiers in Environmental Science*, 6, DOI: 10.3389/fenvs.2018.00095.

James, I., Hoffman, T., Munro, A., O'Farrell, P. and Smart, R. (2007). The value of flower tourism at the Namaqua National Park: environmental and ecological economics. *South African Journal of Economic and Management Sciences*, 10(4): 442-456.

Jeacle, I. and Carter, C. (2011). In TripAdvisor we trust: Rankings, calculative regimes and abstract systems. *Accounting, Organizations and Society*, 36(4-5): 293-309.

Jiang, L.L., Wang, S.P., Meng, F.D., Duan, J.C., Niu, H.S., Xu, G.P., Zhu, X.X., Zhang, Z.H., Luo, C.Y., Cui, S.J. and Li, Y.M. (2016). Relatively stable response of fruiting stage to warming and cooling relative to other phenological events. *Ecology*, 97(8): 1961-1969.

Jin, H., Jönsson, A.M., Olsson, C., Lindström, J., Jönsson, P. and Eklundh, L. (2019). New satellite-based estimates show significant trends in spring phenology and complex sensitivities to temperature and precipitation at northern European latitudes. *International Journal of Biometeorology*, 63(6): 763-775.

Johnson, S.D. (1992). Climatic and phylogenetic determinants of flowering seasonality in the Cape flora. *Journal of Ecology*, 81: 567-572.

Jolly, W.M. and Running, S.W. (2004). Effects of precipitation and soil water potential on drought deciduous phenology in the Kalahari. *Global Change Biology*, 10(3): 303-308.

Jones, J.M. and Widmann, M. (2004). Atmospheric science: Early peak in Antarctic oscillation index. *Nature*, 432: 290-291.

Kalbarczyk, R. (2009). Air temperature changes and phenological phases of field cucumber (*Cucumis sativus* L.) in Poland, 1966-2005. *Horticultural Science*, 36(2): 75-83.

Kaewthongrach, R., Vitasse, Y., Lamjiak, T. and Chidthaisong, A. (2019). Impact of Severe Drought during the Strong 2015/2016 El Nino on the Phenology and Survival of Secondary Dry Dipterocarp Species in Western Thailand. *Forests*, 10(11), DOI: 10.3390/f10110967.

Kassas, M. (1966). Plant life in deserts. *Arid Lands,* 1: 145-180.

Keatley, M.R. and Hudson, I.L. (2007). Shift in flowering dates of Australian plants related to climate: 1983-2006. In: Oxley, L. and Kulasiri, D. (eds.), M*ODSIM 2007 International Congress on Modelling and Simulation*. New Zealand: 504-510.

Keatley, M.R. and Hudson, I.L. (2012). Detecting change in an Australian flowering record: Comparisons of linear regression and cumulative sum analysis change point analysis. *Australian Ecology*, 37(7): 825-835.

Keatley, M.R., Chambers, L.E. and Phillips, R. (2013). Australia and New Zealand. In *Phenology: An Integrative Environmental Science*. Springer, Dordrecht: 23-52.

Keatley, M.R., Fletcher, T.D., Hudson, I.L. and Ades, P.K. (2002). Phenological studies in Australia: potential application in historical and future climate analysis. *International Journal of Climatology*, 22(14): 1769-1780.

Keenan, T.F., Gray, J., Friedl, M.A., Toomey, M., Bohrer, G., Hollinger, D.Y., Munger, J.W., O'Keefe, J., Schmid, H.P., Wing, I.S. and Yang, B. (2014). Net carbon uptake has increased through warming-induced changes in temperate forest phenology. *Nature Climate Change*, 4(7): 598-604.

Kelso, C. and Vogel, C. (2007). The climate of Namaqualand in the nineteenth century. *Climatic Change*, 83(3): 357-380.

Kemp, J.E., Bergh, N.G., Soares, M. and Ellis, A.G. (2018). Dominant pollinators drive non-random community assembly and shared flower colour patterns in daisy communities. *Annals of Botany*, 123(2): 277-288.

Kgope, B.S., Bond, W.J. and Midgley, G.F. (2010). Growth responses of African savanna trees implicate atmospheric [CO_2] as a driver of past and current changes in savanna tree cover. *Austral Ecology*, 35(4): 451-463.

Kharouba, H.M., Ehrlén, J., Gelman, A., Bolmgren, K., Allen, J.M., Travers, S.E. and Wolkovich, E.M. (2018). Global shifts in the phenological synchrony of species interactions over recent decades. *Proceedings of the National Academy of Sciences*, 115(20): 5211-5216.

Knevel, I.C. and Lubke, R.A. (2005). Reproductive phenology of *Scaevola plumieri*; a key coloniser of the coastal foredunes of South Africa. *Plant Ecology*, 175(1): 137-145.

Koenig, W.D., Funk, K.A., Kraft, T.S., Carmen, W.J., Barringer, B.C. and Knops, J.M. (2012). Stabilizing selection for within-season flowering phenology confirms pollen limitation in a wind-pollinated tree. *Journal of Ecology*, 100(3): 758-763.

König, P., Tautenhahn, S., Cornelissen, J.H.C., Kattge, J., Bönisch, G. and Römermann, C. (2018). Advances in flowering phenology across the Northern Hemisphere are explained by functional traits. *Global Ecology and Biogeography*, 27(3): 310-321.

Körner, C. and Basler, D. (2010). Phenology under global warming. *Science*, 327: 1461-1462.

Kraft, N.J., Adler, P.B., Godoy, O., James, E.C., Fuller, S. and Levine, J.M. (2015). Community assembly, coexistence and the environmental filtering metaphor. *Functional Ecology*, 29(5): 592-599.

Kramer, K. (1994). Selecting a model to predict the onset of growth of *Fagus sylvatica*. *Journal of Applied Ecology,* 31: 172-181.

Kramer, K., Leinonen, I. and Loustau, D. (2000). The importance of phenology for the evaluation of impact of climate change on growth of boreal, temperate and Mediterranean forests ecosystems: an overview. *International Journal of Biometeorology*, 44(2): 67-75.

Kruger, A.C. (1999). The Influence of the Decadal-Scale Variability of Summer Rainfall on the Impact of El Niño and La Niña Events in South Africa. *International Journal of Climatology*, 19(1): 59–68.

Kruger, A.C. (2006). Observed trends in daily precipitation indices in South Africa: 1910–2004. *International Journal of Climatology*, 26(15): 2275-2285.

Kruger, A.C. and Nxumalo, M.P. (2017). Historical rainfall trends in South Africa: 1921–2015. *Water SA*, 43(2): 285-297.

Kruger, A.C. and Sekele, S.S. (2013). Trends in extreme temperature indices in South Africa: 1962–2009. *International Journal of Climatology*, 33(3): 661-676.

Kruger, A.C. and Shongwe, S. (2004). Temperature trends in South Africa: 1960–2003. *International Journal of Climatology*, 24(15): 1929-1945.

Kruger, A.C., Rautenbach, H., Mbatha, S., Ngwenya, S. and Makgoale, T.E. (2019). Historical and projected trends in near-surface temperature indices for 22 locations in South Africa. *South African Journal of Science*, 115(5-6): 1-9.

Kruger, M., Viljoen, A. and Saayman, M. (2013). Who pays to view wildflowers in South Africa? *Journal of Ecotourism*, 12(3): 146-164.

Lambert, A.M., Miller-Rushing, A.J. and Inouye, D.W. (2010). Changes in snowmelt date and summer precipitation affect the flowering phenology of *Erythronium grandiflorum* (glacier lily; Liliaceae). *American Journal of Botany*, 97(9): 1431-1437.

Langowska, A., Zawilak, M., Sparks, T.H., Glazaczow, A., Tomkins, P.W. and Tryjanowski, P. (2017). Long-term effect of temperature on honey yield and honeybee phenology. *International Journal of Biometeorology*, 61(6): 1125-1132.

Langvall, O. and Löfvenius, M.O. (2019). Long-term standardized forest phenology in Sweden: a climate change indicator. *International Journal of Bometeorology*, DOI: 10.1007/s00484-019-01817-8.

Last, F. (2001). Keeping records. *The Horticulturist,* 10: 9–11.

Lavigne, H., Civitarese, G., Gačić, M. and D'Ortenzio, F. (2018). Impact of decadal reversals of the north Ionian circulation on phytoplankton phenology. *Biogeosciences*, 15(14): 4431–4445.

Le Roux, A. (2005). *Namaqualand: South African Wild Flower Guide 1.* Botanical Society of South Africa: Cape Town, 13-28.

Leech, N., Barrett, K. and Morgan, G. (2005). S*PSS for intermediate statistics: use and interpretation*. Lawrence Erlbaum Associates Inc Publishers: New Jersey: 90-109.

Ledneva, A., Miller-Rushing, A.J., Primack, R.B. and Imbres, C. (2004). Climate change as reflected in a naturalist's diary, Middleborough, Massachusetts. *The Wilson Journal of Ornithology*, 116(3): 224-232.

Lennard, C. and Hegerl, G. (2015). Relating changes in synoptic circulation to the surface rainfall response using self-organising maps. *Climate Dynamics*, 44(3-4): 861-879.

Leocadio, J., Veiga, A., Barbosa, M., Albertini, B., Lohmann, L., and Saraiva, A. (2018). A multi-platform mobile application to collect citizen science data for *Bignoniaceae* phenological research. *Biodiversity Information Science and Standards,* 2, DOI: 10.3897/biss.2.25582.

Lesica, P. and Kittelson, P.M. (2010). Precipitation and temperature are associated with advanced flowering phenology in a semi-arid grassland. *Journal of Arid Environments*, 74(9): 1013-1017.

Li, X., Jiang, L., Meng, F., Wang, S., Niu, H., Iler, A.M., Duan, J., Zhang, Z., Luo, C., Cui, S. and Zhang, L. (2016). Responses of sequential and hierarchical phenological events to warming and cooling in alpine meadows. *Nature Communications*, 7, DOI: 10.1038/ncomms12489.

Liebmann, B., Bladé, I., Kiladis, G.N., Carvalho, L.M., B. Senay, G., Allured, D., Leroux, S. and Funk, C. (2012). Seasonality of African precipitation from 1996 to 2009. *Journal of Climate,* 25: 4304-4322.

Lieth, H. (1974). Purposes of a phenology book. In H. Lieth (Ed.), *Phenology and Seasonality Modeling,* Springer-Verlag, New York: 3-19.

Lieth, H. (2013). *Phenology and Seasonality Modeling* (Vol. 8). Springer Science & Business Media, New York: 4-5.

Lindesay, J.A. (1988). South African rainfall, the Southern Oscillation and a Southern Hemisphere semi-annual cycle. *Journal of Climatology*, 8(1): 17-30.

Linkosalmi, M., Aurela, M., Tuovinen, J.P., Peltoniemi, M., Tanis, C.M., Arslan, A.N., Kolari, P., Böttcher, K., Aalto, T., Rainne, J. and Hatakka, J. (2016). Digital photography for assessing the link between vegetation phenology and CO_2 exchange in two contrasting northern ecosystems. *Geoscientific Instrumentation Methods and Data Systems*, 5: 417–426

Liu, L. and Hu, Y. (2012). Response of spring phenology to climate change across Tibetan Plateau. *In: The second international conference on remote sensing, environment and transportation engineering*, IEEE, Nanjing (China), DOI: 10.1109/RSETE.2012.6260713, 1-3 June 2012.

Liu, Y.Y., van Dijk, A.I., McCabe, M.F., Evans, J.P. and de Jeu, R.A. (2013). Global vegetation biomass change (1988–2008) and attribution to environmental and human drivers. *Global Ecology and Biogeography*, 22(6): 692-705.

Lomax, R. (2007). *An introduction to statistical concepts, second edition*, Lawrence Erlbaum Associates Inc Publishers*:* New Jersey: 33-34, 93-101, 361-415.

Lu, P., Yu, Q., Liu, J. and Lee, X. (2006). Advance of tree-flowering dates in response to urban climate change. *Agricultural and Forest Meteorology*, 138(1-4): 120-131.

Luedeling, E. and Gassner, A. (2012). Partial least squares regression for analyzing walnut phenology in California. *Agricultural and Forest Meteorology*, 158: 43-52.

Luo, Y., El-Madany, T., Filippa, G., Ma, X., Ahrens, B., Carrara, A., Gonzalez-Cascon, R., Cremonese, E., Galvagno, M., Hammer, T. and Pacheco-Labrador, J. (2018). Using Near-Infrared-Enabled Digital Repeat Photography to Track Structural and Physiological Phenology in Mediterranean Tree–Grass Ecosystems. *Remote Sensing*, 10(8): 1293, DOI: 10.3390/rs10081293.

Ma, Q., Huang, J.G., Hänninen, H. and Berninger, F. (2019). Divergent trends in the risk of spring frost damage to trees in Europe with recent warming. *Global Change Biology*, 25(1): 351-360.

Maan, I., Kaur, A., Singh, H.P., Batish, D.R. and Kohli, R.K. (2020). Evaluating the role of phenology in managing urban invasions: a case study of *Broussonetia papyrifera*. *Urban Forestry and Urban Greening*, 48, DOI: 10.1016/j.ufug.2020.126583.

MacKellar, N.C., Hewitson, B.C. and Tadross, M.A. (2007). Namaqualand's climate: recent historical changes and future scenarios. *Journal of Arid Environments*, 70(4): 604-614.

MacKellar, N., New, M. and Jack, C. (2014). Observed and modelled trends in rainfall and temperature for South Africa: 1960-2010. *South African Journal of Science*, 110(7-8): 1-13.

MacKenzie, C.M., Murray, G., Primack, R. and Weihrauch, D. (2017). Lessons from citizen science: assessing volunteer-collected plant phenology data with Mountain Watch. *Biological Conservation,* 208: 121-126.

Mahlangu, M.N. and Fitchett, J.M. (2019). Climate change threats to a floral wedding: Threats of shifting phenology to the emerging South African wedding industry. *Bulletin of Geography. Socio-economic Series*, 45(45): 7-23.

Mahlobo, D.D., Ndarana, T., Grab, S. and Engelbrecht, F. (2019). Integrated climatology and trends in the subtropical Hadley cell, sunshine duration and cloud cover over South Africa. *International Journal of Climatology*, 39(4): 1805-1821.

Malherbe, J., Dieppois, B., Maluleke, P., Van Staden, M. and Pillay, D.L. (2016). South African droughts and decadal variability. *Natural Hazards*, 80: 657-681.

Malherbe, J., Engelbrecht, F.A. and Landman, W.A. (2014). Response of the Southern Annular Mode to tidal forcing and the bidecadal rainfall cycle over subtropical southern Africa. *Journal of Geophysical Research: Atmospheres*, 119(5): 2032-2049.

Malo, A.R. and Nicholson, S.E. (1990). A study of rainfall and vegetation dynamics in the African Sahel using normalized difference vegetation index. *Journal of Arid Environments*, 19(1): 1-24, DOI: 10.1016/S0140-1963(18)30825-5.

Manly, B.F. (2008). *Statistics for environmental science and management*. Chapman and Hall/CRC, Florida: 68-74, 113, 182-184.

Manning, J. (2013). *Field guide to wild flowers of South Africa*. Penguin Random House, Cape Town.

Mason, S.J., Waylen, P.R., Mimmack, G.M., Rajaratnam, B. and Harrison, J.M. (1999). Changes in extreme rainfall events in South Africa. *Climatic Change*, 41(2): 249-257.

Massetti, L., Petralli, M. and Orlandini, S. (2015). The effect of urban morphology on *Tilia* x *europaea* flowering. *Urban Forestry & Urban Greening*, 14(1): 187-193.

McCormack, M.L., Adams, T.S., Smithwick, E.A. and Eissenstat, D.M. (2014). Variability in root production, phenology, and turnover rate among 12 temperate tree species. *Ecology*, 95(8): 2224-2235.

McKee, T.B., Doesken, N.J. and Kleist, J. (1993). The relationship of drought frequency and duration to time scales. In: *Proceedings of the 8th Conference on Applied Climatology,* Boston, MA: American Meteorological Society, 17(22): 179-183.

Meier, N., Rutishauser, T., Pfister, C., Wanner, H. and Luterbacher, J. (2007). Grape harvest dates as a proxy for Swiss April to August temperature reconstructions back to AD 1480. *Geophysical Research Letters*, 34(20): DOI: 10.1029/2007GL031381.

Meier, U. (2001). BBCH-monograph: growth stages of mono-and dicotyledonous plants. *Federal Biological Research Centre for Agriculture and Forestry*: 130-133.

Melaas, E.K., Sulla-Menashe, D. and Friedl, M.A. (2018). Multidecadal changes and interannual variation in springtime phenology of North American temperate and boreal deciduous forests. *Geophysical Research Letters*, 45(6): 2679-2687.

Mendivelso, H.A., Camarero, J.J., Gutiérrez, E. and Castaño-Naranjo, A. (2016). Climatic influences on leaf phenology, xylogenesis and radial stem changes at hourly to monthly scales in two tropical dry forests. *Agricultural and Forest Meteorology*, 216: 20-36.

Menzel, A. (2000). Trends in phenological phases in Europe between 1951 and 1996. *International Journal of Biometeorology*, 44(2): 76-81.

Menzel, A. (2002). Phenology: its importance to the global change community. *Climatic Change*, 54(4): 379-385.

Menzel, A. (2003). Plant phenological anomalies in Germany and their relation to air temperature and NAO, *Climate Change,* 57: 243–263.

Menzel, A. and Fabian, P. (1999). Growing season extended in Europe. *Nature*, 397(6721): 659.

Menzel, A., Sparks, T., Estrella, N., Koch, E., Aasa, A., Ahas., R, Alm-Kübler, A., Bissolli, P., Braslavská, O., Briede, A., Chmielewski, F., Črepinšek, Z., Curnel. Y., Dahl, Å., Defila, C., Donnelly, A., Filella, Y., Jatczak, K., Måge, F., Mestre, A., Nordli, Ø., Peñuelas, J., Pirinen, P., Remišová, V., Scheifinger, H., Striz, M., Susnik, A., Van Vliet, A., Wielgolaski, F., Zach, S. and Zust, A. (2006), European phenological response to climate change matches the warming pattern, *Global Change Biology,* 12: 1969-1976.

Menzel, A., Yuan, Y., Matiu, M., Sparks, T., Scheifinger, H., Gehrig, R. and Estrella, N. (2020). Climate change fingerprints in recent European plant phenology. *Global Change Biology*. 26(4): 2599-2612, DOI: 10.1111/gcb.15000.

Midgley, G.F., Chapman, R.A., Hewitson, B., Johnston, P., De Wit, M., Ziervogel, G., Mukheibir, P., Van Niekerk, L., Tadross, M., Van Wilgen, B.W. and Kgope, B. (2005). A status quo, vulnerability and adaptation assessment of the physical and socio-economic effects of climate change in the Western Cape. *Report to the Western Cape Government, Cape Town, South Africa*. CSIR Report No. ENV-S-C 2005-073, Stellenbosch.

Midgley, G., Makholela, T., Mantlana, B. (2016). South Africa's 1st Annual Climate Change Report: Climate Change Trends, Risks, Impacts and Vulnerabilities. *Department of Environmental Affairs*. Republic of South Africa. Pretoria.

Miguéns, J., Baggio, R. and Costa, C. (2008). Social media and tourism destinations: TripAdvisor case study. *Advances in Tourism Research*, 26(28): 1-6.

Miller-Rushing, A.J. and Inouye, D.W. (2009). Variation in the impact of climate change on flowering phenology and abundance: an examination of two pairs of closely related wildflower species. *American Journal of Botany*, 96(10): 1821-1829.

Miller-Rushing, A.J. and Primack, R.B. (2008a). Global warming and flowering times in Thoreau's Concord: a community perspective. *Ecology*, 89(2): 332-341.

Miller-Rushing, A.J. and Primack, R.B. (2008b). Effects of winter temperatures on two birch (*Betula*) species. *Tree Physiology*, 28(4): 659-664.

Miller-Rushing, A.J., Inouye, D.W. and Primack, R.B. (2008a). How well do first flowering dates measure plant responses to climate change? The effects of population size and sampling frequency. *Journal of Ecology*, 96(6): 1289-1296.

Miller-Rushing, A.J., Katsuki, T., Primack, R.B., Ishii, Y., Lee, S.D. and Higuchi, H. (2007). Impact of global warming on a group of related species and their hybrids: cherry tree (*Rosaceae*) flowering at Mt. Takao, Japan. *American Journal of Botany*, 94(9): 1470-1478.

Miller-Rushing, A., Lloyd-Evans, T., Primack, R. and Satzinger, P. (2008c). Bird migration times, climate change, and changing population sizes. *Global Change Biology,* 14: 1959-1972.

Miller-Rushing, A.J., Primack, R. and Stymeist, R. (2008b). Interpreting variation in bird migration times as observed by volunteers. *The Auk,* 125(3): 565-573.

Miller-Struttmann, N.E., Geib, J.C., Franklin, J.D., Kevan, P.G., Holdo, R.M., Ebert-May, D., Lynn, A.M., Kettenbach, J.A., Hedrick, E. and Galen, C. (2015). Functional mismatch in a bumble bee pollination mutualism under climate change. *Science*, 349(6255): 1541-1544.

Milton, S.J. (1987). Phenology of seven Acacia species in South Africa. *South African Journal of Wildlife Research-24-month delayed open access*, 17(1), DOI: 2410-7220E-ISSN: 2410-8200.

Milton, S.J. and Moll, E.J. (1982). Phenology of Australian acacias in the SW Cape, South Africa, and its implications for management. *Botanical Journal of the Linnean Society*, 84(4): 295-327.

Mitich, L.W. (2000). Oxeye Daisy (*Chrysanthemum leucanthemum L*.), the White-Flowered Gold Flower 1. *Weed Technology*, 14(3): 659-662.

Moeletsi, M.E. and Walker, S. (2012). Rainy season characteristics of the Free State Province of South Africa with reference to rain-fed maize production. *Water SA*, 38: 775-782.

Moeletsi, M.E., Moopisa, S.G., Walker, S. and Tsubo, M. (2013). Development of an agroclimatological risk tool for dryland maize production in the Free State Province of South Africa. *Computers and Electronics in Agriculture*, 95: 108-121.

Moore, C.E., Brown, T., Keenan, T.F., Duursma, R.A., Van Dijk, A., Beringer, J., Culvenor, D., Evans, B., Huete, A., Hutley, L. and Maier, S. (2016). Reviews and syntheses: Australian vegetation phenology: new insights from satellite remote sensing and digital repeat photography. *Biogeosciences*, 13: 5085–5102.

Morellato, L.P.C., Abernethy, K. and Mendoza, I. (2018). Rethinking tropical phenology: insights from long-term monitoring and novel analytical methods. *Biotropica*, 50(3): 371-373.

Morisette, J.T., Richardson, A.D., Knapp, A.K., Fisher, J.I., Graham, E.A., Abatzoglou, J., Wilson, B.E., Breshears, D.D., Henebry, G.M., Hanes, J.M. and Liang, L. (2009). Tracking the rhythm of the seasons in the face of global change: phenological research in the 21st century. *Frontiers in Ecology and the Environment*, 7(5): 253-260.

Mosiane, S.M., Villet, M.H. and Kfir, R. (2003). Seasonal phenology of the diamondback moth, *Plutella xylostella* (L.), (Lepidoptera: Plutellidae), and its parasitoids on canola, *Brassica napus* (L.), in Gauteng province, South Africa. *African Entomology*, 11(2): 277-285.

Mott, J.J. (1972). Germination studies on some annual species from an arid region in Western Australia. *Journal of Ecology*, 60: 293-304.

Mott, J.J. and McComb, A.J. (1975a). The role of photoperiod and temperature in controlling the phenology of three annual species from an arid region of Western Australia. *Journal of Ecology,* 63: 633-641.

Mott, J. J. and McComb, A.J. (1975b). Effects of moisture stress on the growth and reproduction of three annual species from an arid region of Western Australia. *Journal of Ecology*, 63: 825-834.

Motulsky, H. and Searle, P. (2003). The InStat guide to choosing and interpreting statistical tests. *GraphPad Software Inc*, San Diego: 12-100.

Mucina, L. and Rutherford, M.C. (2006). *The vegetation of South Africa, Lesotho and Swaziland*. South African National Biodiversity Institute, Pretoria: 221-299.

Munguía-Rosas, M.A., Ollerton, J., Parra-Tabla, V. and De-Nova, J.A. (2011). Meta-analysis of phenotypic selection on flowering phenology suggests that early flowering plants are favoured. *Ecology Letters*, 14(5): 511-521.

Munson, S.M. and Long, A.L. (2017). Climate drives shifts in grass reproductive phenology across the western USA. *New Phytologist*, 213(4): 1945-1955.

Myers, N., Mittermeier, R.A., Mittermeier, C.G., Da Fonseca, G.A. and Kent, J. (2000). Biodiversity hotspots for conservation priorities. *Nature*, 403(6772): 853-858.

Nagai, S., Saitoh, T.M. and Yoshitake, S. (2019). Cultural ecosystem services provided by flowering of cherry trees under climate change: a case study of the relationship between the periods of flowering and festivals. *International Journal of Biometeorology*, 63(8): 1051-1058.

Nandargi, S. and Mulye, S.S. (2012). Relationships between rainy days, mean daily intensity, and seasonal rainfall over the Koyna Catchment during 1961–2005. *The Scientific World Journal*, 2012: 1-10.

Nel, W. (2009). Rainfall trends in the KwaZulu-Natal Drakensberg region of South Africa during the twentieth century. *International Journal of Climatology*, 29: 1634-1641.

New, M., Hewitson, B., Stephenson, D.B., Tsiga, A., Kruger, A., Manhique, A., Gomez, B., Coelho, C.A., Masisi, D.N., Kululanga, E. and Mbambalala, E. (2006). Evidence of trends in daily climate extremes over southern and west Africa. *Journal of Geophysical Research: Atmospheres*, 111, DOI: 10.1029/2005JD006289.

Noling, J. (2011). Citrus root growth and soil pest management practises. *Institute of Food and Agricultural Sciences:* Florida, 1.

Nordli, Ø., Wielgolaski, F.E., Bakken, A.K., Hjeltnes, S.H., Måge, F., Sivle, A. and Skre, O. (2008). Regional trends for bud burst and flowering of woody plants in Norway as related to climate change. *International Journal of Biometeorology*, 52(7): 625-639.

Norman, S., Hargrove, W. and Christie, W. (2017). Spring and autumn phenological variability across environmental gradients of Great Smoky Mountains National Park, USA. *Remote Sensing*, 9(5): 407-425.

Ollerton, J., Winfree, R. and Tarrant, S. (2011). How many flowering plants are pollinated by animals? *Oikos*, 120(3): 321-326.

Ouchi-Melo, L.S., Meynard, C.N., Gonçalves-Souza, T. and de Cerqueira Rossa-Feres, D. (2018). Integrating phylogenetic and functional biodiversity facets to guide conservation: a case study using anurans in a global biodiversity hotspot. *Biodiversity and Conservation*, 27(12): 3247-3266.

Palmer, S.C., Odermatt, D., Hunter, P.D., Brockmann, C., Presing, M., Balzter, H. and Tóth, V.R. (2015). Satellite remote sensing of phytoplankton phenology in Lake Balaton using 10 years of MERIS observations. *Remote Sensing of Environment*, 158: 441-452.

Panchen, Z.A., Primack, R.B., Aniśko, T. and Lyons, R.E. (2012). Herbarium specimens, photographs, and field observations show Philadelphia area plants are responding to climate change. *American Journal of Botany*, 99(4): 751-756.

Pardee, G.L., Inouye, D.W. and Irwin, R.E. (2018). Direct and indirect effects of episodic frost on plant growth and reproduction in subalpine wildflowers. *Global Change Biology*, 24(2): 848-857.

Park, I.W. and Schwartz, M.D. (2015). Long-term herbarium records reveal temperature-dependent changes in flowering phenology in the southeastern USA. *International Journal of Biometeorology*, 59(3): 347-355.

Parmesan, C. (2007). Influences of species, latitudes and methodologies on estimates of phenological response to global warming. *Global Change Biology*, 13(9): 1860-1872.

Parmesan, C. and Yohe, G. (2003). A globally coherent fingerprint of climate change impacts across natural systems. *Nature*, 421(6918): 37-42.

Patterson-Jones, C. (1998). *Namaqualand, A Visual Souvenir*. Struik Publishers, Cape Town.

Pau, S., Wolkovich, E.M., Cook, B.I., Davies, T.J., Kraft, N.J., Bolmgren, K., Betancourt, J.L. and Cleland, E.E. (2011). Predicting phenology by integrating ecology, evolution and climate science. *Global Change Biology*, 17(12): 3633-3643.

Pearse, W.D., Davis, C.C., Inouye, D.W., Primack, R.B. and Davies, T.J. (2017). A statistical estimator for determining the limits of contemporary and historic phenology. *Nature Ecology & Evolution*, 1(12): 1876-1882.

Pearson, K.D. (2019). Spring-and fall-flowering species show diverging phenological responses to climate in the Southeast USA. *International Journal of Biometeorology*, 63(4): 481-492.

Pearson, S., Parker, A., Hadley, P. and Kitchener, H.M. (1995). The effect of photoperiod and temperature on reproductive development of cape daisy (*Osteospermum jucundum* cv.'Pink Whirls'). *Scientia Horticulturae*, 62(4): 225-235.

Pecl, G.T., Araújo, M.B., Bell, J.D., Blanchard, J., Bonebrake, T.C., Chen, I.C., Clark, T.D., Colwell, R.K., Danielsen, F., Evengård, B. and Falconi, L. (2017). Biodiversity redistribution under climate change: Impacts on ecosystems and human well-being. *Science*, 355(6332), DOI: 10.1126/science.aai9214.

Peichl, M., Sonnentag, O. and Nilsson, M.B. (2015). Bringing color into the picture: using digital repeat photography to investigate phenology controls of the carbon dioxide exchange in a boreal mire. *Ecosystems*, 18(1): 115-131.

Petrauski, L., Owen, S.F., Constantz, G.D. and Anderson, J.T. (2019). Changes in flowering phenology of *Cardamine concatenata* and *Erythronium americanum* over 111 years in the Central Appalachians. *Plant Ecology*, 220(9): 817-828.

Pettorelli, N., Vik, J.O., Mysterud, A., Gaillard, J.M., Tucker, C.J. and Stenseth, N.C. (2005). Using the satellite-derived NDVI to assess ecological responses to environmental change. *Trends in Ecology and Evolution*, 20(9): 503-510.

Philippon, N., Rouault, M., Richard, Y. and Favre, A. (2012). The influence of ENSO on winter rainfall in South Africa. *International Journal of Climatology*, 32: 2333-2347.

Piao, S., Liu, Q., Chen, A., Janssens, I.A., Fu, Y., Dai, J., Liu, L., Lian, X., Shen, M. and Zhu, X. (2019). Plant phenology and global climate change: Current progresses and challenges. *Global Change Biology*, 25(6): 1922-1940.

Pohl, B., Fauchereau, N., Reason, C.J.C. and Rouault, M. (2010). Relationships between the Antarctic Oscillation, the Madden–Julian Oscillation, and ENSO, and consequences for rainfall analysis. *Journal of Climate*, 23(2): 238-254.

Pohl, B., Richard, Y. and Fauchereau, N. (2007). Influence of the Madden–Julian oscillation on southern African summer rainfall. *Journal of Climate*, 20(16): 4227-4242.

Polgar, C.A. and Primack, R.B. (2011). Leaf-out phenology of temperate woody plants: from trees to ecosystems. *New Phytologist*, 191(4): 926-941.

Polgar, C.A. and Primack, R.B. (2013). Leaf out phenology in temperate forests. *Biodiversity Science*, 21(1): 111–116.

Polgar, C.A., Gallinat, A. and Primack, R.B. (2014). Drivers of leaf-out phenology and their implications for species invasions: insights from Thoreau's Concord. *New Phytologist*, 202(1): 106-115.

Post, E., Steinman, B.A. and Mann, M.E. (2018). Acceleration of phenological advance and warming with latitude over the past century. *Scientific Reports*, 8(1), DOI: 10.1038/s41598-018-22258-0.

Primack, R.B. (1980). Variation in the phenology of natural populations of montane shrubs in New Zealand. *The Journal of Ecology*, 68: 849-862.

Primack, R.B., Higuchi, H. and Miller-Rushing, A.J., (2009a). The impact of climate change on cherry trees and other species in Japan. *Biological Conservation*, 142(9): 1943-1949.

Primack, R.B., Ibáñez, I., Higuchi, H., Lee, S.D., Miller-Rushing, A.J., Wilson, A.M. and Silander Jr, J.A. (2009b). Spatial and interspecific variability in phenological responses to warming temperatures. *Biological Conservation*, 142(11): 2569-2577.

Rana, S., McGregor, J. and Renwick, J. (2015). Precipitation seasonality over the Indian subcontinent: An evaluation of gauge, reanalyses, and satellite retrievals. *Journal of Hydrometeorology*, 16: 631-651.

Reason, C.J.C., Allan, R.J., Lindesay, J.A. and Ansell, T.J. (2000). ENSO and climatic signals across the Indian Ocean basin in the global context: Part I, Interannual composite patterns. *International Journal of Climatology*, 20(11): 1285-1327.

Reason, C.J.C. and Rouault, M. (2002). ENSO-like decadal variability and South African rainfall. *Geophysical Research Letters*, 29(13), DOI: 10.1029/2002GL014663.

Reason, C.J.C. and Rouault, M. (2005). Links between the Antarctic Oscillation and winter rainfall over western South Africa. *Geophysical Research Letters*, 32(7), DOI: 10.1029/2005GL022419.

Renner, S.S. and Zohner, C.M. (2018). Climate change and phenological mismatch in trophic interactions among plants, insects, and vertebrates. *Annual Review of Ecology, Evolution, and Systematics*, 49: 165-182.

Retief, F. (2006). The quality and effectiveness of Strategic Environmental Assessment (SEA) as a decision-aiding tool for national park expansion—the greater Addo Elephant National Park case study. *Koedoe*, 49(2): 103-122.

Reyer, C.P., Leuzinger, S., Rammig, A., Wolf, A., Bartholomeus, R.P., Bonfante, A., De Lorenzi, F., Dury, M., Gloning, P., Abou Jaoudé, R. and Klein, T. (2013). A plant's perspective of extremes:

terrestrial plant responses to changing climatic variability. *Global Change Biology*, 19(1): 75-89.

Richardson, A.D., Anderson, R.S., Arain, M.A., Barr, A.G., Bohrer, G., Chen, G., Chen, J.M., Ciais, P., Davis, K.J., Desai, A.R. and Dietze, M.C. (2012). Terrestrial biosphere models need better representation of vegetation phenology: results from the North American Carbon Program Site Synthesis. *Global Change Biology*, 18(2): 566-584.

Richardson, B.A., Chaney, L., Shaw, N.L. and Still, S.M. (2017). Will phenotypic plasticity affecting flowering phenology keep pace with climate change? *Global Change Biology*, 23(6): 2499-2508.

Richardson, A.D., Hufkens, K., Milliman, T. and Frolking, S. (2018). Intercomparison of phenological transition dates derived from the PhenoCam Dataset V1.0 and MODIS satellite remote sensing. *Scientific Reports*, 8(1): 5679-5681.

Richardson, A.D., Keenan, T.F., Migliavacca, M., Ryu, Y., Sonnentag, O. and Toomey, M. (2013). Climate change, phenology, and phenological control of vegetation feedbacks to the climate system. *Agricultural and Forest Meteorology*, 169: 156-173.

Rigby, J. and Porporato, A. (2008). Spring frost risk in a changing climate. *Geophysical Research Letters,* 35: 12703-12707.

Rippke, U., Ramirez-Villegas, J., Jarvis, A., Vermeulen, S.J., Parker, L., Mer, F., Diekkrüger, B., Challinor, A.J. and Howden, M. (2016). Timescales of transformational climate change adaptation in sub-Saharan African agriculture. *Nature Climate Change*, 6(6): 605-609.

Roffe, S.J., Fitchett, J.M. and Curtis, C.J. (2019). Classifying and mapping rainfall seasonality in South Africa: A review. *South African Geographical Journal*, 101(2): 158-174.

Roffe, S.J., Fitchett, J.M. and Curtis, C.J. (2020). Determining the utility of a percentile-based wet-season start-and end-date metrics across South Africa. *Theoretical and Applied Climatology*, DOI: 10.1007/s00704-020-03162-y.

Rohde, R.F., Benjaminsen, T.A. and Hoffman, M.T. (2001). *Land reform in Namaqualand: poverty alleviation, stepping stones and economic units*. Institute for Poverty Land and Agrarian Studies (PLAAS), University of the Western Cape.

Root, T.L., Price, J.T., Hall, K.R., Schneider, S.H., Rosenzweig, C. and Pounds, J.A. (2003). Fingerprints of global warming on wild animals and plants. *Nature*, 421(6918): 57-60.

Rosbakh, S. and Poschlod, P. (2015). Initial temperature of seed germination as related to species occurrence along a temperature gradient. *Functional Ecology*, 29(1): 5-14.

Rötzer, T., Wittenzeller, M., Haeckel, H. and Nekovar, J. (2000). Phenology in central Europe – differences and trends of spring phenophases in urban and rural areas. *International Journal of Biometeorology* 44: 60-66.

Rudolf, V.H. (2019). The role of seasonal timing and phenological shifts for species coexistence. *Ecology Letters*, 22(8): 1324-1338.

Ruml, M., Vulić, T. and Đorđević, B. (2011). The effect of altitude and latitude on the phenology of the plum *cv. Pozegaca* in Serbia [conference paper]. *The 46th Croatian and 6th International Symposium on Agriculture,* Opatija, Croatia: 1052-1055, 14-18 February 2011.

Rundel, P.W., Cowling, R.M., Esler, K.J., Mustart, P.M., Van Jaarsveld, E. and Bezuidenhout, H. (1995). Winter growth phenology and leaf orientation in *Pachypodium namaquanum* (Apocynaceae) in the succulent karoo of the Richtersveld, South Africa. *Oecologia*, 101(4): 472-477.

Saarinen, J., Hambira, W.L., Atlhopheng, J. and Manwa, H. (2012). Tourism industry reaction to climate change in Kgalagadi South District, Botswana. *Development Southern Africa*, 29(2): 273-285.

Saayman, A. and Saayman, M. (2008). Determinants of inbound tourism to South Africa. *Tourism Economics*, 14(1): 81-96.

Sakai, S. and Kitajima, K. (2019). Tropical phenology: Recent advances and perspectives. *Ecological Research*, 34(1): 50-54.

SAWS. (2015). Summary of SAWS Research on Historical Climate Trends in South Africa: 1961-2014. CLS-CDAR- REPORT-2014-09. Available from: https://www.nda.agric.za/doaDev/sideMenu/forestry/docs/Booklet%203%20Agric%20Nat%20Cap%202%20Climate.pdf (Accessed on 3 June 2019).

SAWS. (2017). A Climate Change Reference Atlas. Based on CMIP5 – CORDEX downscaling. Available from: http://www.weathersa.co.za/climate/climate-change-reference-atlas (Accessed on 3 March 2020).

SAWS. (2019). *Our Climate Services.* Available from: http://www.weathersa.co.za/home/aboutclimateatsaws (Accessed on 29 April 2020).

Schmidt-Lebuhn, A.N., Knerr, N.J. and Kessler, M. (2013). Non-geographic collecting biases in herbarium specimens of Australian daisies (Asteraceae). *Biodiversity and Conservation*, 22(4): 905-919.

Schulze, R.E. (2007). South African Atlas of Climatology and Agrohydrology: Terminology. In*:* Schulze, R.E. (eds.), 2007. *South African Atlas of Climatology and Agrohydrology*, Water Research Commission, Pretoria.

Schwartz, M.D. and Reed, B.C. (1999). Surface phenology and satellite sensor-derived onset of greenness: an initial comparison. *International Journal of Remote Sensing*, 20(17): 3451-3457.

Schwartz, M.D. and Reiter, B.E. (2000). Changes in north American spring. *International Journal of Climatology*, 20(8): 929-932.

Schwartz, M.D., Ahas, R. and Aasa, A. (2006). Onset of spring starting earlier across the Northern Hemisphere. *Global Change Biology*, 12(2): 343-351.

Scott, L., Cadman, A. and McMillan, I. (2006). Early history of Cainozoic Asteraceae along the Southern African west coast. *Review of Palaeobotany and Palynology*, 142(1-2): 47-52.

Seiler, R.A., Hayes, M. and Bressan, L. (2002). Using the standardized precipitation index for flood risk monitoring. *International Journal of Climatology*, 22(11): 1365-1376.

Shackleton, C.M. (1999). Rainfall and topo-edaphic influences on woody community phenology in South African savannas. *Global Ecology and Biogeography*, 8(2): 125-136.

Shackleton, C.M. (2002). Growth patterns of *Pterocarpus angolensis* in savannas of the South African lowveld. *Forest Ecology and Management*, 166(1-3): 85-97.

Sheridan, J.A., Caruso, N.M., Apodaca, J.J. and Rissler, L.J. (2018). Shifts in frog size and phenology: Testing predictions of climate change on a widespread anuran using data from prior to rapid climate warming. *Ecology and Evolution*, 8(2): 1316-1327.

Shi, P., Chen, Z., Reddy, G.V., Hui, C., Huang, J. and Xiao, M. (2017). Timing of cherry tree blooming: Contrasting effects of rising winter low temperatures and early spring temperatures. *Agricultural and Forest Meteorology*, 240: 78-89.

Siebert, S. and Ewert, F. (2012). Spatio-temporal patterns of phenological development in Germany in relation to temperature and day length. *Agricultural and Forest Meteorology*, 152: 44-57.

Singh, R.K., Svystun, T., AlDahmash, B., Jönsson, A.M. and Bhalerao, R.P. (2017). Photoperiod-and temperature-mediated control of phenology in trees–a molecular perspective. *New Phytologist*, 213(2): 511-524.

Sloan, S., Jenkins, C.N., Joppa, L.N., Gaveau, D.L. and Laurance, W.F. (2014). Remaining natural vegetation in the global biodiversity hotspots. *Biological Conservation*, 177: 12-24.

Smith, A.M. and Ramsay, P.M. (2020). A comparison of ground-based methods for obtaining large-scale, high-resolution data on the spring leaf phenology of temperate tree species. *International Journal of Biometeorology*, 64(3): 521-531.

Sobey, J., (2018). Beginner botanising: a pilgrimage to Namaqualand [image], PlantLife SA, Volume 46:5. Available from: http://plantlifesouthafrica.blogspot.com/2019/01/plantlife-sa-volume-465-december-2018.html (Accessed 9 November 2020)

Soroye, P., Ahmed, N. and Kerr, J.T. (2018). Opportunistic citizen science data transform understanding of species distributions, phenology, and diversity gradients for global change research. *Global Change Biology*, 24(11): 5281-5291.

Souriau, A., and Yiou, P. (2012). Grape harvest dates for checking NAO paleoreconstructions. *Geophysical Research Letters*, 28(20): 3895–3896.

Sousa, P.M., Blamey, R.C., Reason, C.J., Ramos, A.M. and Trigo, R.M. (2018). The 'Day Zero' Cape Town drought and the poleward migration of moisture corridors. *Environmental Research Letters*, 13(12): 124025.

South African National Parks. (2012a). West Coast National Park management plan 2012. Available from: http://www.sanparks.org.za/assets/docs/conservation/park_man/west-coastdraft-plan.pdf (Assessed March 26, 2019).

South African National Parks. (2012b). Namaqua National Park management plan 2012. Available from: http://www.sanparks.org.za/assets/docs/conservation/park_man/namaquadraft-plan.pdf (Assessed March 26, 2019).

Souza, C.S., Maruyama, P.K., Aoki, C., Sigrist, M.R., Raizer, J., Gross, C.L. and de Araujo, A.C. (2018). Temporal variation in plant–pollinator networks from seasonal tropical environments: Higher specialization when resources are scarce. *Journal of Ecology*, 106(6): 2409-2420.

Sparks, T.H. and Carey, P.D. (1995). The responses of species to climate over two centuries: an analysis of the Marsham phenological record, 1736-1947. *Journal of Ecology*, 83: 321-329.

Sparks, T.H., Croxton, P.J., Collinson, N. and Taylor, P.W. (2005). Examples of phenological change, past and present, in UK farming. *Annals of Aapplied Biology*, 146(4): 531-537.

Sparks, T.H., Jeffree, E.P. and Jeffree, C.E. (2000). An examination of the relationship between flowering times and temperature at the national scale using long-term phenological records from the UK. *International Journal of Biometeorology*, 44(2): 82-87.

Steinke, T.D. (1988). Vegetative and floral phenology of three mangroves in Mgeni Estuary. *South African Journal of Botany*, 54(2): 97-102.

Steinke, T.D. and Charles, L.M. (1984). Productivity and phenology of *Avicennia marina* (Forsk.) Vierh. and *Bruguiera gymnorrhiza* (L.) Lam. in Mgeni estuary, South Africa. In: *Physiology and Management of Mangroves,* Springer: Dordrecht, 25-36.

Stenseth, N. and Mysterud, A. (2002). Climate, changing phenology, and other life history traits: non-linearity and match-mismatch to the environment, *PNAS,* 99(21): 13379-13381.

Stevenson, I. and Bryant, D. (2000). Avian phenology: Climate Change and Constraints on Breeding, *Nature,* 406: 366-367.

Steyn, H.M. (2004). Why the early bird won't see the daisies: feature. *Veld and Flora*, 90(3): 98-100.

Steyn, H.M., Van Rooyen, N., Van Rooyen, M.W. and Theron, G.K. (1996). The phenology of Namaqualand ephemeral species. The effect of water stress. *Journal of Arid Environments*, 33(1): 49-62.

Stockigt, L., Hoogendoorn, G., Fitchett, J.M. and Saarinen, J. (2018). Climatic Sensitivity and Snow-based Tourism in Africa: An Investigation of TripAdvisor reviews on Afriski, Lesotho. *Submitted for the Proceedings of the Society of South African Geographers Biennial Conference*: 207-224, 1-5 October 2018.

Stöckli, R. and Vidale, P.L. (2004). European plant phenology and climate as seen in a 20-year AVHRR land-surface parameter dataset. *International Journal of Remote Sensing*, 25(17): 3303-3330.

Struck, M. (1994). Flowering phenology in the arid winter rainfall region of southern Africa. *Bothalia*, 24(1): 77-90.

Studer, S., Appenzeller, C. and Defila, C. (2005). Inter-annual variability and decadal trends in alpine spring phenology: a multivariate analysis approach. *Climatic Change*, 73(3): 395-414.

Stutz, S., Mráz, P., Hinz, H.L., Müller-Schärer, H. and Schaffner, U. (2018). Biological invasion of oxeye daisy (*Leucanthemum vulgare*) in North America: Pre-adaptation, post-introduction evolution, or both? *PloS ONE*, 13(1), DOI: 10.1371/journal.pone.0190705.

Taljaard, J.J. (1996). Atmospheric Circulation Systems, Synoptic Climatology and Weather Systems of South Africa. Part 6. Rainfall in South Africa. *South African Weather Bureau Tech. Paper*, 32: 100.

Tao, F., Yokozawa, M., Xu, Y., Hayashi, Y. and Zhang, Z. (2006). Climate changes and trends in phenology and yields of field crops in China, 1981-2000. *Agricultural and Forest Meteorology,* 138: 82-92.

Thackeray, S.J., Sparks, T.H., Frederiksen, M., Burthe, S., Bacon, P.J., Bell, J.R., Botham, M.S., Brereton, T.M., Bright, P.W., Carvalho, L. and Clutton-Brock, T.I.M. (2010). Trophic level asynchrony in rates of phenological change for marine, freshwater and terrestrial environments. *Global Change Biology*, 16(12): 3304-3313.

Thackeray, S.J., Henrys, P.A., Hemming, D., Bell, J.R., Botham, M.S., Burthe, S., Helaouet, P., Johns, D.G., Jones, I.D., Leech, D.I. and Mackay, E.B. (2016). Phenological sensitivity to climate across taxa and trophic levels. *Nature*, 535(7611): 241-245.

Theobald, E.J., Breckheimer, I. and HilleRisLambers, J. (2017). Climate drives phenological reassembly of a mountain wildflower meadow community. *Ecology*, 98(11): 2799-2812.

Thomson, J.D. (2010). Flowering phenology, fruiting success and progressive deterioration of pollination in an early-flowering geophyte. *Philosophical Transactions of the Royal Society B: Biological Sciences*, 365(1555): 3187-3199.

Toda, M. and Richardson, A.D. (2018). Estimation of plant area index and phenological transition dates from digital repeat photography and radiometric approaches in a hardwood forest in the Northeastern United States. *Agricultural and Forest Meteorology*, 249: 457-466.

Tongwane, M.I. and Moeletsi, M.E. (2015). Intra-seasonal rainfall variability during the maize growing season in the northern lowlands of Lesotho. T*heoretical and Applied Climatology*, 120: 575-585.

Tooke, F. and Battey, N.H. (2010). Temperate flowering phenology. *Journal of Experimental Botany*, 61(11): 2853-2862.

Toomey, M., Friedl, M.A., Frolking, S., Hufkens, K., Klosterman, S., Sonnentag, O., Baldocchi, D.D., Bernacchi, C.J., Biraud, S.C., Bohrer, G. and Brzostek, E. (2015). Greenness indices from digital cameras predict the timing and seasonal dynamics of canopy-scale photosynthesis. *Ecological Applications*, 25(1): 99-115.

Torres, C. and Galetto, L. (2011). Flowering phenology of co-occurring Asteraceae: a matter of climate, ecological interactions, plant attributes or of evolutionary relationships among species? *Organisms Diversity and Evolution*, 11(1): 9-19.

Tribe, G.D. (1991). Phenology of Pinus radiata log colonization by the red-haired pine bark beetle *Hylurgus ligniperda* (Fabricius) (Coleoptera: Scolytidae) in the south-western Cape Province. *Journal of the Entomological Society of Southern Africa*, 54(1), DOI: 10520/AJA00128789_2658.

Turpie, J. and Joubert, A. (2004). The value of flower tourism on the Bokkeveld Plateau–a botanical hotspot. *Development Southern Africa*, 21(4): 645-662.

Tyson, P.D., Cooper, G. R. J. and McCarthy, T. S. (2002). Millennial to Multi-Decadal Variability in the Climate of Southern Africa. *International Journal of Climatology*, 22(9): 1105 –1117.

Underhill, L. and Bradfield, D. (2009). Introstat. *Juta and Co. Ltd*, Cape Town; 175, 299-353.

Usman, M.T. and Reason, C.J.C. (2004). Dry spell frequencies and their variability over southern Africa. *Climate Research*, *26*(3): 199-211.

Usui, T., Butchart, S.H. and Phillimore, A.B. (2017). Temporal shifts and temperature sensitivity of avian spring migratory phenology: A phylogenetic meta-analysis. *Journal of Animal Ecology*, 86(2): 250-261.

Valdivia-Mares, L.E., Zaragoza, F.A.R., González, J.J.S. and Vargas-Ponce, O. (2016). Phenology, agronomic and nutritional potential of three wild husk tomato species (*Physalis*, Solanaceae) from Mexico. *Scientia Horticulturae*, 200: 83-94.

Van Dijk, H. and Hautekeete, N. (2007). Long day plants and the response to global warming: rapid evolutionary change in day length sensitivity is possible in wild beet. *Journal of Evolutionary Biology,* 20: 349-357.

Van Rooyen, M.W., Grobbelaar, N., Theron, G.K. and Van Rooyen, N. (1991). The ephemerals of Namaqualand: effects of photoperiod, temperature and moisture stress on development and flowering of three species. *Journal of Arid Environments*, 20(1): 15-29.

Van Rooyen, M.W., Le Roux, A., Geldenhuys, C., Van Rooyen, N., Broodryk, N.L. and Van der Merwe, H. (2015). Long-term vegetation dynamics (40 yr) in the Succulent Karoo, South Africa: effects of rainfall and grazing. *Applied Vegetation Science*, 18(2): 311-322.

Van Rooyen, M.W., Theron, G.K. and Grobbelaar, N. (1979). Phenology of the vegetation in the Hester Malan Nature Reserve in the Namaqualand broken veld. I. General observations. *Journal of South African Botany*, 45: 279-293.

Van Rooyen, M.W., Theron, G.K. and Grobbelaar, N. (1990). Life form and dispersal spectra of the flora of Namaqualand, South Africa. *Journal of Arid Environments*, 19(2): 133-145.

Van Wilgen, N.J., Goodall, V., Holness, S., Chown, S.L. and McGeoch, M.A. (2016). Rising temperatures and changing rainfall patterns in South Africa's national parks. *International Journal of Climatology*, 36(2): 706-721.

Vander Mijnsbrugge, K. and Janssens, A. (2019). Differentiation and Non-Linear Responses in Temporal Phenotypic Plasticity of Seasonal Phenophases in a Common Garden of *Crataegus monogyna* Jacq. *Forests*, 10(4): 293-310

Ventura, F., Vignudelli, M., Poggi, G.M., Negri, L. and Dinelli, G. (2020). Phenological stages of Proso millet (*Panicum miliaceum* L.) encoded in BBCH scale. *International Journal of Biometeorology*, 64: 1167–1181.

Verghis, T.I., McKenzie, B.A. and Hill, G.D. (1999). Phenological development of chickpeas (*Cicer arietinum*) in Canterbury, New Zealand. *New Zealand Journal of Crop and Horticultural Science*, 27(3): 249-256.

Vilela, A.A., Del Claro, V.T.S., Torezan-Silingardi, H.M. and Del-Claro, K. (2018). Climate changes affecting biotic interactions, phenology, and reproductive success in a savanna community over a 10-year period. *Arthropod-plant Interactions*, 12(2): 215-227.

Villalobos-Jiménez, G. and Hassall, C. (2017). Effects of the urban heat island on the phenology of Odonata in London, UK. *International Journal of Biometeorology*, 61(7): 1337-1346.

Viña, A., Gitelson, A.A., Rundquist, D.C., Keydan, G., Leavitt, B. and Schepers, J. (2004). Monitoring maize (*Zea mays* L.) phenology with remote sensing. *Agronomy Journal*, 96(4): 1139-1147.

Viña, A., Liu, W., Zhou, S., Huang, J. and Liu, J. (2016). Land surface phenology as an indicator of biodiversity patterns. *Ecological Indicators*, 64: 281-288.

Viña, A., Tuanmu, M.N., Xu, W., Li, Y., Qi, J., Ouyang, Z. and Liu, J. (2012). Relationship between floristic similarity and vegetated land surface phenology: Implications for the synoptic monitoring of species diversity at broad geographic regions. *Remote Sensing of Environment*, 121: 488-496.

Visser, M.E. and Both, C. (2005). Shifts in phenology due to global climate change: The need for a yardstick. *Proceedings of the Royal Society of Biological Sciences,* 272(1581): 2561–2569.

Visser, M.E. and Holleman, L.J.M. (2001). Warmer springs disrupt the synchrony of oak and winter moth phenology. *Proceedings of the Royal Society of London*, 268(1464): 289–294.

Visser, M.E., Holleman, L. and Gienapp. P. (2006), Shifts in caterpillar biomass phenology due to climate change and its impact on the breeding biology of an insectivorous bird. *Oecologia,* 147: 164-172.

Vitasse, Y., Rebetez, M., Filippa, G., Cremonese, E., Klein, G. and Rixen, C. (2017). 'Hearing' alpine plants growing after snowmelt: ultrasonic snow sensors provide long-term series of alpine plant phenology. *International Journal of Biometeorology*, 61(2): 349-361.

Walck, J.L., Hidayati, S.N., Dixon, K.W., Thompson, K.E.N. and Poschlod, P. (2011). Climate change and plant regeneration from seed. *Global Change Biology*, 17(6): 2145-2161.

Walkovszky, A. (1998). Changes in phenology of the locust tree (*Robinia pseudoacacia* L.) in Hungary. *International Journal of Biometeorology*, 41(4): 155-160.

Walther, G.R., Post, E., Convey, P., Menzel, A., Parmesan, C., Beebee, T.J., Fromentin, J.M., Hoegh-Guldberg, O. and Bairlein, F. (2002). Ecological responses to recent climate change. *Nature*, 416: 389-395.

Wand, S.J.E., Steyn, W.J. and Theron, K.I. (2007). Vulnerability and impact of climate change on pear production in South Africa, In: *X International Pear Symposium 800*: 263-272, DOI: 10.17660/ActaHortic.2008.800.31.

Wang, H.L., Gan, Y.T., Wang, R.Y., Niu, J.Y., Zhao, H., Yang, Q.G. and Li, G.C. (2008). Phenological trends in winter wheat and spring cotton in response to climate changes in northwest China. *Agricultural and Forest Meteorology*, 148(8-9): 1242-1251.

Wang, L., Ning, Z., Wang, H. and Ge, Q. (2017). Impact of climate variability on flowering phenology and its implications for the schedule of blossom festivals. *Sustainability*, 9(7), DOI: 10.3390/su9071127.

Wang, T., Ottlé, C., Peng, S., Janssens, I.A., Lin, X., Poulter, B., Yue, C. and Ciais, P. (2014). The influence of local spring temperature variance on temperature sensitivity of spring phenology. *Global Change Biology*, 20(5): 1473-1480.

Wang, X., Wu, C., Peng, D., Gonsamo, A. and Liu, Z. (2018). Snow cover phenology affects alpine vegetation growth dynamics on the Tibetan Plateau: Satellite observed evidence, impacts of different biomes, and climate drivers. *Agricultural and Forest Meteorology*, 256: 61-74.

Wannenburgh, A. and Dickson, J.R. (1984). *The Natural Wonder of Southern Africa*. Struik Publishers, Cape Town.

Warburton, M.L. and Schulze, R.E. (2005). Historical Precipitation Trends over Southern Africa: A Hydrology Perspective. *Climate Change and Water Resources in Southern Africa: Studies on Scenarios, Impacts Vulnerabilities and Adaptation*. Water Research Commission Report, 1430(1), Pretoria, RSA: 325–338.

Warburton, M.L, Schulze, R.E. and Maharaj, M. (2005). Is South Africa’s Temperature Changing? An Analysis of Trends from Daily Records, 1950–2000. *Climate Change and Water Resources in Southern Africa: Studies on Scenarios, Impacts, Vulnerabilities and Adaptation*. Water Research Commission Report, 1430(1), Pretoria, RSA: 275–295.

Warren, R., Price, J., Graham, E., Forstenhaeusler, N. and VanDerWal, J. (2018). The projected effect on insects, vertebrates, and plants of limiting global warming to 1.5°C rather than 2°C. *Science*, 360(6390): 791-795.

Webb, L.B., Whetton, P.H. and Barlow, E.W.R. (2007). Modelled impact of future climate change on the phenology of winegrapes in Australia. *Australian Journal of Grape and Wine Research*, 13(3): 165-175.

Wessels, K., Steenkamp, K., Von Maltitz, G. and Archibald, S. (2011). Remotely sensed vegetation phenology for describing and predicting the biomes of South Africa. *Applied Vegetation Science*, 14(1): 49-66.

White, G.M. and Uller, T. (2014). Quo vadis amphibia? Global warming and breeding phenology in frogs, toads and salamanders. *Ecography*, 37(10): 921-929.

White, M.A., de Beurs, K.M., Didan, K., Inouye, D.W., Richardson, A.D., Jensen, O.P., O'Keefe, J.O.H.N., Zhang, G., Nemani, R.R., van Leeuwen, W.J. and Brown, J.F. (2009). Intercomparison, interpretation, and assessment of spring phenology in North America estimated from remote sensing for 1982–2006. *Global Change Biology*, 15(10): 2335-2359.

Whitecross, M.A., Witkowski, E.T.F. and Archibald, S. (2016). No two are the same: Assessing variability in broad-leaved savanna tree phenology, with watering, from 2012 to 2014 at Nylsvley, South Africa. *South African Journal of Botany*, 105: 123-132.

Whitecross, M.A., Witkowski, E.T. and Archibald, S. (2017a). Assessing the frequency and drivers of early-greening in broad-leaved woodlands along a latitudinal gradient in southern Africa. *Austral Ecology*, 42(3): 341-353.

Whitecross, M.A., Witkowski, E.T.F. and Archibald, S. (2017b). Savanna tree-grass interactions: A phenological investigation of green-up in relation to water availability over three seasons. *South African Journal of Botany*, 108: 29-40.

Whittington, H.R., Tilman, D., Wragg, P.D. and Powers, J.S. (2015). Phenological responses of prairie plants vary among species and year in a three-year experimental warming study. *Ecosphere*, 6(10), DOI: 10.1890/ES15-00070.1.

Wielgolaski, F.E. (2003). Climatic factors governing plant phenological phases along a Norwegian fjord. *International Journal of Biometeorology*, 47(4): 213-220.

Wiens, J.J. (2016). Climate-related local extinctions are already widespread among plant and animal species. *PLoS Biology*, 14(12), DOI: 10.1371/journal.pbio.2001104.

Williams, J.L., Jacquemyn, H., Ochocki, B.M., Brys, R. and Miller, T.E. (2015). Life history evolution under climate change and its influence on the population dynamics of a long-lived plant. *Journal of Ecology*, 103(4): 798-808.

Williams, S.E. and Middleton, J. (2008). Climatic seasonality, resource bottlenecks, and abundance of rainforest birds: implications for global climate change. *Diversity and Distributions*, 14(1): 69-77.

Wilson, A., Bacher, K., Breckheimer, I., Lundquist, J., Rochefort, R., Theobald, E., Whiteaker, L. and HilleRisLambers, J. (2017). Monitoring wildflower phenology using traditional science, citizen science, and crowd sourcing. *Park Science*, 33: 17-26.

Wipf, S., Stoeckli, V. and Bebi, P. (2009). Winter climate change in alpine tundra: plant responses to changes in snow depth and snowmelt timing. *Climatic Change*, 94(1-2): 105-121.

Wolf, A.A., Zavaleta, E.S. and Selmants, P.C. (2017). Flowering phenology shifts in response to biodiversity loss. *Proceedings of the National Academy of Sciences*, 114(13): 3463-3468.

Wolfe, D.W., Schwartz, M.D., Lakso, A.N., Otsuki, Y., Pool, R.M. and Shaulis, N.J. (2005). Climate change and shifts in spring phenology of three horticultural woody perennials in northeastern USA. *International Journal of Biometeorology*, 49(5): 303-309.

Wright, S.J. and Calderón, O. (2018). Solar irradiance as the proximate cue for flowering in a tropical moist forest. *Biotropica*, 50(3): 374-383.

Wright, S.J. and Van Schaik, C.P. (1994). Light and the phenology of tropical trees. *The American Naturalist*, 143(1): 192-199.

Wright, S.J., Calderón, O. and Muller-Landau, H.C. (2019). A phenology model for tropical species that flower multiple times each year. *Ecological Research*, 34(1): 20-29.

Wu, J., Albert, L.P., Lopes, A.P., Restrepo-Coupe, N., Hayek, M., Wiedemann, K.T., Guan, K., Stark, S.C., Christoffersen, B., Prohaska, N. and Tavares, J.V. (2016). Leaf development and demography explain photosynthetic seasonality in Amazon evergreen forests. *Science*, 351(6276): 972-976.

Xiao, D., Qi, Y., Shen, Y., Tao, F., Moiwo, J.P., Liu, J., Wang, R., Zhang, H. and Liu, F. (2016). Impact of warming climate and cultivar change on maize phenology in the last three decades in North China Plain. *Theoretical and Applied Climatology*, 124(3-4): 653-661.

Yun, J., Jeong, S.J., Ho, C.H., Park, C.E., Park, H. and Kim, J. (2018). Influence of winter precipitation on spring phenology in boreal forests. *Global Change Biology*, 24(11): 5176-5187.

Zhang, H., Yuan, W., Liu, S., Dong, W. and Fu, Y. (2015). Sensitivity of flowering phenology to changing temperature in China. *Journal of Geophysical Research: Biogeosciences*, 120(8): 1658-1665.

Zhang, J., Yi, Q., Xing, F., Tang, C., Wang, L., Ye, W., Ng, I.I., Chan, T.I., Chen, H. and Liu, D. (2018). Rapid Shifts of Peak Flowering Phenology in 12 Species under the Effects of Extreme Climate Events in Macao. *Scientific Reports*, 8(1): 13950.

Zhang, Q., Körnich, H. and Holmgren, K. (2013). How well do reanalyses represent the southern African precipitation? *Climate Dynamics*, 40(3-4): 951-962.

Zhang, X., Friedl, M.A., Schaaf, C.B., Strahler, A.H., Hodges, J.C., Gao, F., Reed, B.C. and Huete, A. (2003). Monitoring vegetation phenology using MODIS. *Remote Sensing of Environment*, 84(3): 471-475.

Zhu, L., Meng, J., Li, F. and You, N. (2019). Predicting the patterns of change in spring onset and false springs in China during the twenty-first century. *International Journal of Biometeorology*, 63(5): 591-606.

Zhu, Z., Piao, S., Myneni, R.B., Huang, M., Zeng, Z., Canadell, J.G., Ciais, P., Sitch, S., Friedlingstein, P., Arneth, A. and Cao, C. (2016). Greening of the Earth and its drivers. *Nature Climate Change*, 6(8): 791-795.

Ziello, C., Estrella, N., Kostova, M., Koch, E. and Menzel, A. (2009). Influence of altitude on phenology of selected plant species in the Alpine region (1971–2000). *Climate Research*, 39(3): 227-234.

Zipper, S.C., Schatz, J., Singh, A., Kucharik, C.J., Townsend, P.A. and Loheide II, S.P. (2016). Urban heat island impacts on plant phenology: intra-urban variability and response to land cover. *Environmental Research Letters*, 11(5): p.054023.

References for Chapter Cover Pages

[1] Craigcryptoking, (2020). Namaqualand Wild Flowers! Northern Cape! [image], PEAKD. Available from: https://peakd.com/nature/@craigcryptoking/namaqualand-wild-flowers-northern-cape (Accessed 9 November 2020)

[2] KDA Travel, (2017). Namaqualand Daisies in the Northern Cape, South Africa [image], DayTrips. Available from: http://www.daytrips.co.za/daisies.php#!prettyPhoto[gallery1]/2/ (Accessed 9 November 2020)

[3] Anne, (2017). Namaqualand Daisies [image], Something Over Tea. Available from: https://somethingovertea.wordpress.com/2017/10/16/namaqualand-daisies/ (Accessed 9 November 2020)

[4] Sobey, J., (2018). Beginner botanising: a pilgrimage to Namaqualand [image], PlantLife SA, Volume 46:5. Available from: http://plantlifesouthafrica.blogspot.com/2019/01/plantlife-sa-volume-465-december-2018.html (Accessed 9 November 2020)

[5] Stevewhysall, (2017). Oh no, Namaqualand has no flowers! This is a big disappointment [image], Steve Whysall. Available from: https://stevewhysall.net/oh-no-namaqualand-no-flowers-big-disappointment/ (Accessed 9 November 2020)

[6] Nortier, C., (2019). Namaqualand, One of Africa’s Best Natural Wonders [image], Getaway. Available from: https://www.getaway.co.za/inspiration/namaqualand-one-of-africas-best-natural-wonders/ (Accessed 9 November 2020)

[7] Bruns, T., (2019). Tips for Flower Viewing in Namaqualand, the Cederberg & West Coast [image], Cedarberg Africa – Personal Safari Planning. Available from: https://www.cedarberg-travel.com/africa-travel-tips/tips-for-flower-viewing-in-namaqualand-the-cederberg-west-coast/ (Accessed 9 November 2020)

Appendix A.1: Statistical Analysis of Climate Data. A linear regression analysis that was completed for the climate variables for all the weather stations after calculating the average temperatures and total precipitation values over the study period for each weather station.

Weather Stations	Climate Variable	Jan	Feb	Mar	Apr	May	Jun	Jul	Aug	Sept	Oct	Nov	Dec	Annual
Cape Columbine	T_{max}	r= 0,20 p= 0,1333 m= 0,01	r= 0,42 p= 0,0008 m= 0,02	r= 0,16 p= 0,2159 m= 0,01	r= 0,35 p= 0,0067 m= 0,02	r= 0,30 p= 0,0218 m= 0,02	r= 0,25 p= 0,0588 m= 0,01	r= 0,34 p= 0,0087 m= 0,02	r= 0,15 p= 0,2424 m= 0,01	r= 0,19 p= 0,1478 m= 0,01	r= 0,37 p= 0,0039 m= 0,02	r= 0,25 p= 0,0581 m= 0,01	r= 0,30 p= 0,0197 m= 0,02	r= 0,54 p= <0,0001 m= 0,01
	T_{min}	r= 0,34 p= 0,0083 m= 0,01	r= 0,34 p= 0,0074 m= 0,01	r= 0,28 p= 0,0347 m= 0,01	r= 0,27 p= 0,0356 m= 0,01	r= 0,41 p= 0,0011 m= 0,02	r= 0,20 p= 0,1244 m= 0,01	r= 0,35 p= 0,0057 m= 0,01	r= 0,24 p= 0,0732 m= 0,01	r= 0,29 p= 0,0263 m= 0,01	r= 0,40 p= 0,0013 m= 0,02	r= 0,35 p= 0,0056 m= 0,02	r= 0,37 p= 0,0038 m= 0,02	r= 0,50 p= <0,0001 m= 0,01
	T_{mean}	r= 0,28 p= 0,0311 m= 0,01	r= 0,41 p= 0,0011 m= 0,02	r= 0,23 p= 0,0739 m= 0,01	r= 0,34 p= 0,0071 m= 0,02	r= 0,37 p= 0,0035 m= 0,02	r= 0,12 p= 0,3671 m= 0,01	r= 0,37 p= 0,0038 m= 0,02	r= 0,21 p= 0,1160 m= 0,01	r= 0,21 p= 0,1132 m= 0,01	r= 0,41 p= 0,0010 m= 0,02	r=0 ,31 p= 0,0146 m= 0,01	r= 0,35 p= 0,0058 m= 0,02	r= 0,54 p= <0,0001 m= 0,01
	Precipitation	r= 0,02 p= 0,9097 m= 0,01	r= 0,05 p= 0,7137 m= 0,02	r= 0,06 p= 0,6499 m= -0,03	r= 0,04 p= 0,7632 m= -0,04	r= 0,15 p= 0,2487 m= -0,22	r= 0,04 p= 0,7840 m= -0,06	r= 0,17 p= 0,1818 m= 0,20	r= 0,05 p= 0,7229 m= -0,06	r= 0,13 p= 0,3319 m= 0,12	r= 0,22 p= 0,0846 m= -0,14	r= 0,04 p= 0,7821 m= 0,02	r= 0,03 p= 0,8358 m= -0,01	r= 0,06 p= 0,6541 m= -0,19
Vredendal	T_{max}	r= 0,67 p= <0,0001 m= 0,06	r= 0,58 p= <0,0001 m= 0,05	r= 0,53 p= <0,0001 m= 0,05	r= 0,64 p= <0,0001 m= 0,06	r= 0,50 p= <0,0001 m= 0,05	r= 0,32 p= 0,0139 m= 0,03	r= 0,39 p= 0,0022 m= 0,04	r= 0,34 p= 0,0018 m= 0,03	r= 0,34 p= 0,0079 m= 0,03	r= 0,62 p= <0,0001 m= 0,06	r= 0,32 p= 0,0137 m= 0,03	r= 0,52 p= <0,0001 m= 0,05	r= 0,84 p= <0,0001 m= 0,05
	T_{min}	r= 0,45 p= 0,0003 m= 0,03	r= 0,45 p= 0,0004 m= 0,03	r= 0,17 p= 0,1983 m= 0,01	r= 0,22 p= 0,0922 m= 0,01	r= 0,30 p= 0,0180 m= 0,02	r= 0,04 p= 0,7801 m<0.01	r= 0.08 p= 0.5428 m<0.01	r= 0.06 p= 0.6277 m<0.01	r= 0.21 p= 0.1030 m= 0.01	r= 0.27 p= 0.0341 m= 0.02	r= 0.13 p= 0.3175 m= 0.01	r= 0.39 p= 0.0021 m= 0.02	r= 0.51 p= <0,0001 m= 0.01
	T_{mean}	r= 0.62 p= <0,0001 m= 0.05	r= 0.57 p= <0,0001 m= 0.04	r= 0.43 p= 0.0006 m= 0.03	r= 0.56 p= <0,0001 m= 0.04	r= 0.56 p= <0,0001 m= 0.04	r= 0.22 p= 0.0859 m= 0.01	r= 0.34 p= 0.0075 m= 0.02	r= 0.32 p= 0.0114 m= 0.02	r= 0.34 p= 0.0078 m= 0.02	r= 0.54 p= <0,0001 m= 0.04	r= 0.28 p= 0.0304 m= 0.02	r= 0.52 p= <0,0001 m= 0.03	r= 0.82 p= <0,0001 m= 0.03
	Precipitation	r= 0.27 p= 0.0397 m= 0.06	r= 0.05 p= 0.6956 m= 0.01	r= 0.03 p= 0.8332 m= -0.01	r= 0.17 p= 0.2018 m= -0.15	r= 0.07 p= 0.5722 m= -0.08	r= 0.08 p= 0.5279 m= -0.11	r= 0.18 p= 0.1659 m= 0.19	r= 0.03 p= 0.8420 m= 0.02	r= 0.09 p= 0.5155 m= 0.05	r= 0.03 p= 0.8175 m= -0.02	r= 0.15 p= 0.2625 m= -0.10	r= 0.09 p= 0.4734 m= 0.09	r= 0.02 p= 0.8959 m= -0.05
Nieuwoudtville	T_{max}	r= 0.11 p= 0.6850 m= -0.04	r= 0.21 p= 0.4607 m= -0.06	r= 0.29 p= 0.3027 m= -0.10	r= 0.07 p= 0.8060 m= 0.02	r= 0.21 p= 0.4428 m= 0.11	r= 0.16 p= 0.5650 m= -0.04	r= 0.23 p= 0.3909 m= -0.08	r= 0.27 p= 0.3071 m= 0.14	r= 0.17 p= 0.6682 m= -0.05	r= 0.30 p= 0.2566 m= 0.12	r= 0.12 p= 0.6475 m= -0.03	r= 0.17 p= 0.5238 m= -0.05	r= 0.21 p= 0.4402 m= 0.04
	T_{min}	r= 0.15 p= 0.5836 m= -0.04	r= 0.35 p= 0.1967 m= -0.12	r= 0.48 p= 0.0716 m= -0.15	r= 0.50 p= 0.0494 m= -0.11	r= 0.43 p= 0.0985 m= -0.11	r= 0.42 p= 0.1099 m= -0.08	r= 0.56 p= 0.0226 m= -0.16	r= 0.41 p= 0.1114 m= -0.14	r= 0.61 p= 0.0126 m= -0.18	r= 0.42 p= 0.1027 m= -0.11	r= 0.55 p= 0.0266 m= -0.11	r= 0.12 p= 0.6660 m= -0.03	r= 0.46 p= 0.0753 m= -0.07
	T_{mean}	r= 0.15 p= 0.5899 m= -0.04	r= 0.31 p= 0.2556 m= -0.09	r= 0.42 p= 0.1172 m= -0.13	r= 0.21 p= 0.4246 m= -0.05	r= 0.01 p= 0.9582 m<0.01	r= 0.37 p= 0.1603 m= -0.06	r= 0.46 p= 0.0749 m= -0.12	r= 0.01 p= 0.9789 m<0.01	r= 0.38 p= 0.1440 m= -0.11	r= 0.02 p= 0.9281 m= 0.01	r= 0.35 p= 0.1788 m= -0.07	r= 0.18 p= 0.5040 m= -0.04	r= 0.12 p= 0.6525 m= -0.02
	Precipitation	r= 0.03 p= 0.9289 m= -0.09	r= 0.18 p= 0.5205 m= -0.81	r= 0.32 p= 0.2507 m= 0.75	r= 0.38 p= 0.1498 m= -1.82	r= 0.27 p= 0.3062 m= -2.62	r= 0.03 p= 0.8989 m= 0.36	r= 0.05 p= 0.8564 m= 0.47	r= 0.54 p= 0.0299 m= -5.77	r= 0.06 p= 0.8328 m= 0.21	r= 0.42 p= 0.1076 m= -0.98	r= 0.15 p= 0.5917 m= 0.49	r= 0.05 p= 0.8429 m= -0.26	r= 0.35 p= 0.1779 m= -9.32
Springbok	T_{max}	r= 0.18 p= 0.3350 m= 0.03	r= 0.40 p= 0.0265 m= 0.09	r= 0.14 p= 0.4588 m= 0.02	r= 0.14 p= 0.4509 m= 0.02	r= 0.08 p= 0.6594 m= 0.02	r= 0.16 p= 0.4012 m= 0.03	r= 0.08 p= 0.6669 m= 0.02	r= 0.01 p= 0.9772 m= -0.001	r= 0.15 p= 0.4443 m= -0.04	r= 0.35 p= 0.0582 m= 0.08	r= 0.10 p= 0.5829 m= 0.02	r= 0.16 p= 0.3865 m= 0.03	r= 0.15 p= 0.4207 m= 0.02
	T_{min}	r= 0.02 p= 0.9155 m<0.01	r= 0.07 p= 0.7033 m= -0.01	r= 0.15 p= 0.4412 m= -0.03	r= 0.04 p= 0.8307 m= 0.01	r= 0.20 p= 0.2717 m= -0.03	r= 0.09 p= 0.6345 m= -0.01	r= 0.07 p= 0.7124 m= 0.01	r= 0.23 p= 0.1534 m= -0.06	r= 0.47 p= 0.0093 m= -0.10	r= 0.03 p= 0.8785 m= 0.0 1	r= 0.17 p= 0.3603 m= -0.03	r= 0.05 p= 0.7790 m= -0.01	r= 0.36 p= 0.0447 m= -0.03

	T_{mean}	r= 0.11 p= 0.5669 m= 0.01	r= 0.25 p= 0.1826 m= 0.04	r= 0.01 p= 0.9446 m= -0.002	r= 0.10 p= 0.6061 m= 0.01	r= 0.04 p= 0.8478 m= -0.01	r= 0.06 p= 0.7637 m= 0.01	r= 0.09 p= 0.6376 m= -0.03	r= 0.13 p= 0.4953 m= -0.03	r= 0.30 p= 0.1109 m= -0.07	r= 0.22 p= 0.2538 m= 0.04	r= 0.02 p= 0.9083 m= -0.003	r= 0.06 p= 0.7618 m= 0.01	r= 0.10 p= 0.5941 m= -0.01
	Precipitation	r= 0.14 p= 0.5186 m= 0.29	r= 0.06 p= 0.7650 m= -0.11	r= 0.05 p= 0.8238 m= -0.12	r= 0.14 p= 0.4976 m= -0.26	r= 0.37 p= 0.0650 m= -1.47	r= 0.11 p= 0.6150 m= 0.44	r= 0.12 p= 0.5555 m= -0.48	r= 0.12 p= 0.5750 m= -0.34	r= 0.23 p= 0.2534 m= -0.57	r= 0.31 p= 0.1253 m= -0.43	r= 0.04 p= 0.8330 m= -0.08	r= 0.25 p= 0.2157 m= -0.18	r= 0.18 p= 0.3778 m= -1.91
Port Nolloth	T_{max}	r= 0.40 p= 0.0023 m= 0.02	r= 0.59 p= <0,0001 m= 0.04	r= 0.43 p= 0.0012 m= 0.03	r= 0.39 p= 0.0037 m= 0.04	r= 0.19 p= 0.1566 m= 0.02	r= 0.09 p= 0.5201 m= 0.01	r= 0.36 p= 0.0083 m= 0.04	r= 0.36 p= 0.0075 m= 0.03	r= 0.48 p= 0.0003 m= 0.03	r= 0.41 p= 0.0017 m= 0.03	r= 0.47 p= 0.0003 m= 0.03	r= 0.51 p= <0,0001 m= 0.04	r= 0.64 p= <0,0001 m= 0.03
	T_{min}	r= 0.36 p= 0.0081 m= 0.02	r= 0.19 p= 0.1602 m= 0.01	r= 0.24 p= 0.0727 m= 0.02	r= 0.19 p= 0.1648 m= 0.01	r= 0.31 p= 0.0236 m= 0.02	r= 0.10 p= 0.4524 m= -0.01	r= 0.12 p= 0.3708 m= 0.01	r= 0.06 p= 0.6845 m<0.01	r= 0.15 p= 0.2796 m= 0.01	r= 0.33 p= 0.0137 m= 0.02	r= 0.25 p= 0.0617 m= 0.01	r= 0.37 p= 0.0055 m= 0.03	r= 0.32 p= 0.0147 m= 0.01
	T_{mean}	r= 0.34 p= 0.0104 m= 0.02	r= 0.37 p= 0.0057 m= 0.02	r= 0.37 p= 0.0049 m= 0.02	r= 0.34 p= 0.0124 m= 0.02	r= 0.19 p= 0.1615 m= 0.01	r= 0.01 p= 0.9132 m= -0.001	r= 0.27 p= 0.0411 m= 0.02	r= 0.22 p= 0.1097 m= 0.01	r= 0.30 p= 0.0237 m= 0.02	r= 0.38 p= 0.0038 m= 0.02	r= 0.45 p= 0.0006 m= 0.02	r= 0.50 p= 0.0001 m= 0.03	r= 0.49 p= 0.0002 m= 0.02
	Precipitation	r= 0.26 p= 0.0510 m= 0.09	r= 0.01 p= 0.9248 m<0.01	r= 0.09 p= 0.5051 m= 0.02	r= 0.06 p= 0.6418 m= -0.04	r= 0.14 p= 0.3123 m= 0.05	r= 0.04 p= 0.7444 m= 0.03	r= 0.09 p= 0.5305 m= 0.04	r= 0.01 p= 0.9540 m<0.01	r= 0.06 p= 0.6642 m= 0.02	r= 0.04 p= 0.7891 m= -0.01	r= 0.15 p= 0.2772 m= 0.03	r= 0.03 p= 0.8015 m= -0.01	r= 0.20 p= 0.1256 m= 0.35
Lambertsbaai Nortier	T_{max}	r= 0.42 p= 0.0331 m= 0.05	r= 0.08 p= 0.7027 m= 0.01	r= 0.17 p= 0.3996 m= -0.04	r= 0.14 p= 0.5053 m= 0.02	r= 0.11 p= 0.5958 m= 0.02	r= 0.07 p= 0.7398 m= -0.02	r= 0.06 p= 0.7772 m= 0.01	r= 0.16 p= 0.4256 m= 0.03	r= 0.08 p= 0.7012 m= 0.01	r= 0.24 p= 0.2228 m= 0.05	r= 0.03 p= 0.8653 m= 0.01	r= 0.34 p= 0.0862 m= 0.05	r= 0.35 p= 0.0653 m= 0.04
	T_{min}	r= 0.32 p= 0.1114 m= 0.05	r= 0.17 p= 0.4049 m= -0.02	r= 0.10 p= 0.6181 m= -0.01	r= 0.01 p= 0.9695 m<-0.01	r= 0.08 p= 0.7073 m= 0.01	r= 0.08 p= 0.6862 m= -0.02	r= 0.08 p= 0.6890 m= -0.01	r= 0.10 p= 0.6313 m= -0.01	r= 0.16 p= 0.4260 m= -0.02	r= 0.11 p= 0.6013 m= 0.02	r= 0.01 p= 0.9570 m<-0.01	r= 0.10 p= 0.6032 m= -0.01	r= 0.16 p= 0.4070 m= 0.02
	T_{mean}	r= 0.39 p= 0.0517 m= 0.05	r= 0.03 p= 0.8753 m= -0.004	r= 0.17 p= 0.4161 m= -0.02	r= 0.09 p= 0.6825 m= 0.01	r= 0.10 p= 0.6350 m= 0.01	r= 0.08 p= 0.7094 m= -0.02	r= 0.003 p= 0.9847 m<-0.01	r= 0.05 p= 0.8180 m= 0.01	r= 0.04 p= 0.8387 m= -0.005	r= 0.18 p= 0.3575 m= 0.03	r= 0.03 p= 0.8983 m<0.01	r= 0.11 p= 0.5692 m= 0.02	r= 0.26 p= 0.1773 m= 0.03
	Precipitation	r= 0.02 p= 0.9445 m= 0.01	r= 0.32 p= 0.1248 m= -0.22	r= 0.01 p= 0.9617 m= -0.01	r= 0.08 p= 0.7231 m= 0.10	r= 0.22 p= 0.2911 m= -0.55	r= 0.38 p= 0.0703 m= 0.86	r= 0.08 p= 0.7110 m= -0.27	r= 0.15 p= 0.4705 m= -0.39	r= 0.01 p= 0.9719 m= 0.01	r= 0.21 p= 0.3275 m= -0.29	r= 0.07 p= 0.7437 m= 0.11	r= 0.08 p= 0.7185 m= -0.10	r= 0.11 p= 0.6022 m= -0.89
Clanwilliam	T_{max}	r= 0.28 p= 0.2677 m= 0.07	r= 0.32 p= 0.1961 m= -0.09	r= 0.30 p= 0.2340 m= -0.09	r= 0.17 p= 0.5058 m= 0.04	r= 0.01 p= 0.6824 m= 0.03	r= 0.35 p= 0.1562 m= -0.12	r= 0.13 p= 0.6162 m= -0.04	r= 0.21 p= 0.4133 m= 0.07	r= 0.22 p= 0.3815 m= -0.08	r= 0.21 p= 0.4073 m= 0.05	r= 0.23 p= 0.3339 m= -0.05	r= 0.05 p= 0.8352 m= 0.01	r= 0.40 p= 0.0888 m= -0.07
	T_{min}	r= 0.48 p= 0.0441 m= 0.10	r= 0.18 p= 0.4734 m= -0.04	r= 0.18 p= 0.4700 m= -0.04	r= 0.02 p= 0.9385 m<0.01	r= 0.12 p= 0.6325 m= 0.02	r= 0.32 p= 0.1917 m= 0.08	r= 0.003 p= 0.9890 m<0.01	r= 0.13 p= 0.6202 m= -0.02	r= 0.48 p= 0.0456 m= -0.07	r= 0.16 p= 0.5182 m= 0.03	r= 0.10 p= 0.6977 m= -0.01	r= 0.20 p= 0.4181 m= 0.04	r= 0.27 p= 0.2681 m= -0.03
	T_{mean}	r= 0.38 p= 0.1163 m= 0.09	r= 0.27 p= 0.2707 m= -0.06	r= 0.26 p= 0.2941 m= -0.06	r= 0.12 p= 0.6322 m= 0.02	r= 0.17 p= 0.5118 m= 0.03	r= 0.16 p= 0.5182 m= -0.02	r= 0.10 p= 0.7041 m= -0.02	r= 0.11 p= 0.6520 m= 0.02	r= 0.33 p= 0.1879 m= -0.07	r= 0.21 p= 0.4057 m= 0.04	r= 0.20 p= 0.4146 m= -0.03	r= 0.12 p= 0.6124 m= 0.03	r= 0.38 p= 0.1120 m= -0.05
	Precipitation	r= 0.29 p= 0.2480 m= 0.54	r= 0.14 p= 0.5907 m= 0.12	r= 0.24 p= 0.3283 m= 0.30	r= 0.20 p= 0.4162 m= -0.35	r= 0.22 p= 0.3728 m= -0.77	r= 0.59 p= 0.0100 m= 2.67	r= 0.30 p= 0.2203 m= -1.84	r= 0.25 p= 0.3235 m= -0.95	r= 0.27 p= 0.2763 m= -0.46	r= 0.09 p= 0.7268 m= -0.11	r= 0.13 p= 0.5937 m= 0.20	r= 0.14 p= 0.5770 m= 0.20	r= 0.20 p= 0.4106 m= 2.45